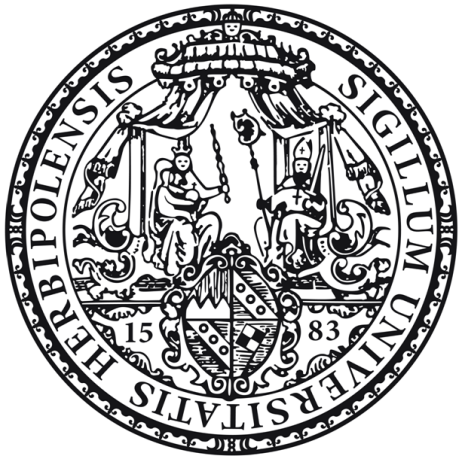

Novel mechanisms underlying arterial thrombus formation: *in vivo* studies in (genetically modified) mice

~~~

Neue Mechanismen der arteriellen Thrombusbildung: *in vivo*-Studien in (genetisch veränderten) Mäusen

Doctoral thesis for a doctoral degree
at the Graduate School of Life Sciences,
Bayerische Julius-Maximilians-Universität Würzburg,
Section Biomedicine

submitted by

Ina Hagedorn
from
Northeim

Würzburg, 2011
~~~

Submitted on:

Members of the *Promotionskomitee*:

Chairperson:	**Prof. Dr. Manfred Gessler**
Primary Supervisor:	**Prof. Dr. Bernhard Nieswandt**
Supervisor (Second):	**Prof. Dr. Utz Fischer**
Supervisor (Third):	**Prof. Dr. Johan W. M. Heemskerk**

Date of Public Defense:

Date of Receipt of Certificate:

This thesis is dedicated to Uli, who always supports me.

SUMMARY

Thrombus formation at sites of vascular lesions is a dynamic process that requires a defined series of molecular events including the action of platelet adhesion/activation receptors, intracellular signal transduction, cytoskeletal rearrangements and activation of plasma coagulation factors. This process is essential to limit post-traumatic blood loss but may also contribute to acute thrombotic diseases such as myocardial infarction and stroke. With the help of genetically modified mice and the use of specific protein inhibitors and receptor-depleting antibodies, the work presented in this thesis identified novel mechanisms underlying thrombus formation in hemostasis and thrombosis.

In the first part of the study, it was shown that von Willebrand Factor (vWF) binding to glycoprotein (GP)Ibα is critical for the formation of stable pathological thrombi at high shear rates, suggesting GPIbα as an attractive pharmacological target for antithrombotic therapy. The subsequent analysis of recently generated phospholipase (PL)D1-deficient mice identified this enzyme, whose role in platelet function had been largely unknown, as a potential target protein downstream of GPIbα. This was based on the finding that PLD1-deficient mice displayed severely defective GPIbα-dependent thrombus stabilization under high shear conditions *in vitro* and *in vivo* without affecting normal hemostasis.

The second part of the thesis characterizes the functional relevance of the immunoreceptor tyrosine-based activation motif (ITAM)-bearing collagen receptor GPVI and the recently identified hemITAM-coupled C-type lectin-like receptor 2 (CLEC-2) for *in vivo* thrombus formation. Genetic- and antibody-induced GPVI deficiency was found to similarly protect mice from arterial vessel occlusion in three different thrombosis models. These results confirmed GPVI as a promising antithrombotic target and revealed that antibody-treatment had no obvious off-target effects on platelet function. Similarly, immunodepletion of CLEC-2 by treating mice with the specific antibody INU1 resulted in markedly impaired thrombus growth and stabilization under flow *in vitro* and *in vivo*. Furthermore, it could be demonstrated that double-immunodepletion of GPVI and CLEC-2 resulted in severely decreased arterial thrombus formation accompanied by dramatically prolonged bleeding times. These data revealed an unexpected redundant function of the two receptors for *in vivo* thrombus formation and might have important implications for the potential development of anti-GPVI and anti-CLEC-2 antithrombotic agents.

The third part of the thesis provides the first functional analysis of megakaryocyte- and platelet-specific RhoA knockout mice. RhoA-deficient mice displayed a defined signaling defect in platelet activation, leading to a profound protection from arterial thrombosis and ischemic brain infarction, but at the same time also strongly increased bleeding times. These

findings identified the GTPase as an important player for thrombus formation in hemostasis and thrombosis.

Based on the previous proposal that the coagulation factor (F)XII might represent an ideal target for safe antithrombotic therapy without causing bleeding side effects, the last part of this thesis assesses the antithrombotic potential of the newly generated FXIIa inhibitor rHA-Infestin-4. It was found that rHA-Infestin-4 injection into mice resulted in virtually abolished arterial thrombus formation but no change in bleeding times. Moreover, rHA-Infestin-4 was similarly efficient in a murine model of ischemic stroke, suggesting that the inhibitor might be a promising agent for effective and safe therapy of cardio- and cerebrovascular diseases.

ZUSAMMENFASSUNG

Thrombusbildung an einer verletzten Gefäßstelle ist ein dynamischer Prozess, der ein definiertes Zusammenspiel von Thrombozytenadhäsions-/aktivierungsrezeptoren, intrazellulären Signalen, Zytoskelettumstrukturierungen sowie die Aktivierung von Plasma Koagulationsfaktoren benötigt. Dieser Prozess ist essenziell um Blutungen nach einer Gefäßverletzung zu stoppen, kann aber auch zu akuten thrombotischen Erkrankungen wie Herzinfarkt und Schlaganfall führen. Mit Hilfe von genetisch veränderten Mäusen und der Verwendung von spezifischen Proteininhibitoren und Rezeptor-depletierenden Antikörpern wurden in der hier vorliegenden Dissertation neue Mechanismen der Thrombusbildung in Hämostase und Thrombose identifiziert.

In dem ersten Teil der Studie konnte gezeigt werden, dass die Interaktion zwischen von Willebrand Faktor (vWF) und Glykoprotein (GP)Ibα entscheidend für die Bildung von pathologischen Thromben bei hohen Scherraten ist, was auf die Eignung von GPIbα als eine attraktive pharmakologische Zielstruktur (Target) für eine antithrombotische Therapie hindeutet. Die anschließende Analyse von vor kurzem generierten Phospholipase (PL)D1-defizienten Mäusen identifizierte dieses Enzym, dessen Rolle in der Thrombozytenfunktion bislang unbekannt war, als eine mögliches Targetprotein im Signalweg von GPIbα. Dies basierte vor allem auf der Erkenntnis, dass PLD1-defiziente Mäuse eine stark gestörte GPIbα-abhängige Thrombusstabilisierung unter hohen Scherbedingungen aufwiesen, ohne jedoch dabei die normale Hämostase zu beeinflussen.

Im zweiten Teil der Arbeit wurde die funktionelle Relevanz des *immunoreceptor tyrosine-based activation motif* (ITAM)-gekoppelten Kollagenrezeptors GPVI und des vor kurzem entdeckten hemITAM-gekoppelten *C-type lectin-like receptor 2* (CLEC-2) für die *in vivo* Thrombusbildung charakterisiert. Es wurde gezeigt, dass genetisch- und durch Antikörper-induzierte GPVI-Defizienz Mäuse gleichermaßen vor arteriellem Gefäßverschluss in drei verschiedenen Thrombosemodellen schützt. Diese Ergebnisse bestätigten GPVI als ein viel versprechendes antithrombotisches Target und zeigten, dass eine Antikörperbehandlung in Mäusen keine offensichtlichen unspezifischen Effekte auf die Thrombozytenfunktion hatte. Eine gleichermaßen induzierte Immunodepletion von CLEC-2 durch die Behandlung von Mäusen mit dem spezifischen Antikörper INU1 führte zu deutlich vermindertem Thrombuswachstum und reduzierter Thrombusstabilisierung unter Flussbedingungen *in vitro* und *in vivo*. Darüber hinaus konnte gezeigt werden, dass eine Doppel-Immunodepletion von GPVI und CLEC-2 zu einer stark reduzierten arteriellen Thrombusbildung führte, die mit dramatisch verlängerten Blutungszeiten einherging. Diese Ergebnisse machten eine unerwartete funktionelle Redundanz der beiden Rezeptoren deutlich und könnten

möglicherweise einen wichtigen Einfluss auf eine eventuelle Entwicklung von anti-GPVI und anti-CLEC-2 antithrombotischen Wirkstoffen haben.

Der dritte Teil der Arbeit liefert die erste funktionelle Analyse von Megakaryozyten- und Thrombozyten-spezifischen RhoA-Knockout Mäusen. RhoA-defiziente Mäuse zeigten einen definierten Signaldefekt in der Thrombozytenaktivierung, der zu einem deutlichen Schutz vor arterieller Thrombose und ischämischen Hirninfarkt aber gleichzeitig auch zu stark erhöhten Blutungszeiten führte. Dieses Ergebnis identifizierte die GTPase als einen wichtigen Spieler für die Thrombusbildung in Hämostase und Thrombose.

Basierend auf dem vorausgegangenen Vorschlag, dass der Koagulationsfaktor XII (FXII) ein ideales Target für eine sichere antithrombotische Therapie darstellen könnte, ohne Blutungsnebenwirkungen zu verursachen, untersucht der letzte Teil der Arbeit das antithrombotische Potential des neu generierten FXIIa Inhibitors rHA-Infestin-4. Es konnte gezeigt werden, dass eine Injektion von rHA-Infestin-4 in Mäuse die arterielle Thrombusbildung nahezu aufhob aber Blutungszeiten nicht veränderte. Außerdem war rHA-Infestin-4 gleichermaßen effizient in einem Mausmodell des ischämischen Schlaganfalls, was darauf schließen lässt, dass der Inhibitor ein vielversprechender Wirkstoff für eine effektive und sichere Therapie von kardio- und zerebrovaskulären Erkrankungen sein könnte.

TABLE OF CONTENTS

1 INTRODUCTION 1
1.1 Platelets 1
1.2 Platelet activation and thrombus formation 2
1.3 The GPIb-V-IX complex 5
1.4 Phospholipase D1 6
1.5 GPVI 7
1.6 CLEC-2 8
1.7 Small GTPases of the Rho family 9
1.7.1 RhoA 10
1.8 Blood coagulation 12
1.9 Murine arterial thrombosis models 15
2 AIM OF THE STUDY 17
3 MATERIALS AND METHODS 18
3.1 Materials 18
3.1.1 Chemicals and kits 18
3.1.2 Antibodies 20
3.1.2.1 Purchased primary and secondary antibodies 20
3.1.2.2 Monoclonal Antibodies (mAbs) 20
3.1.3 Human serine proteases 21
3.1.4 Buffers 21
3.1.5 Animals 24
3.2 Methods 26
3.2.1 Mouse genotyping 26
3.2.1.1 Isolation of genomic DNA from mouse ears 26
3.2.1.2 Detection of the *RhoA* floxed allele by PCR 26
3.2.1.3 Detection of the PF4-Cre transgene by PCR 27
3.2.2 *In vitro* analysis of platelet function 27
3.2.2.1 Platelet isolation and washing 27
3.2.2.2 Platelet counting 28
3.2.2.3 Western blotting 28
3.2.2.4 Flow cytometric analysis 28
3.2.2.5 Aggregation 29
3.2.2.6 Aggregation + ATP release 30
3.2.2.7 Intracellular Calcium-measurements 30
3.2.2.8 Determination of platelet filamentous (F)-actin content 30
3.2.2.9 Clot retraction 31

3.2.2.10 Static adhesion on human fibrinogen 31
3.2.2.11 Adhesion under flow conditions 31
3.2.3 Coagulation and fibrinolysis assays 32
3.2.3.1 Preparation of mouse plasma 32
3.2.3.2 Determination of aPTT and PT 32
3.2.3.3 Chromogenic assays 32
3.2.3.4 D-Dimer concentration measurements 33
3.2.4 *In vivo* murine models 33
3.2.4.1 Determination of platelet life span 33
3.2.4.2 $FeCl_3$-induced thrombus formation in small mesenteric arterioles 33
3.2.4.3 Mechanical injury of the abdominal aorta 33
3.2.4.4 Carotid artery thrombosis model 34
3.2.4.5 Bleeding time assays 34
3.2.4.6 Transient occlusion model of the middle cerebral artery 34
3.2.5 Statistics 34
3.2.6 Electron microscopy 35
3.2.6.1 Transmission electron microscopy (TEM) of platelets in suspension 35
3.2.6.2 Scanning electron microscopy (SEM) of platelets 35
3.2.7 Fluorescence microscopy of platelets 36
3.2.7.1 Staining of spread platelets for confocal microscopy 36
3.2.7.2 Stimulated Emmision Depletion (STED) microscopy of spread platelets 36
3.2.8 Histology 36
3.2.8.1 Preparation of paraffin sections 36
3.2.8.2 Hematoxylin/eosin staining of paraffin sections 37
4 RESULTS 38
4.1 Relevance of the GPIbα-vWF interaction and downstream signaling in thrombus formation 38
4.1.1 Targeting of GPIbα protects mice from arterial thrombosis, but causes a hemostatic defect 38
4.1.2 Phospholipase D1 is a critical mediator of shear-dependent thrombus formation downstream of GPIb 40
4.1.2.1 *Pld1*$^{-/-}$ platelets fail to form stable aggregates on collagen under flow conditions 41
4.1.2.2 PLD1-deficient platelets display defective adhesion on vWF under flow conditions 42
4.1.2.3 PLD1-deficient mice are protected from occlusive arterial thrombus formation 43

4.2 Genetic and antibody-induced GPVI deficiency similarly protects mice from $FeCl_3$- and mechanically induced thrombosis 45
4.3 The platelet activating receptor CLEC-2 is essentially involved in thrombosis and hemostasis 48
4.3.1 CLEC-2 can specifically be downregulated from circulating platelets by the monoclonal antibody INU1 48
4.3.2 CLEC-2 deficiency leads to the formation of unstable thrombi under flow 49
4.3.3 CLEC-2-deficient mice display defective thrombus formation in a $FeCl_3$-injury model and prolonged bleeding times 51
4.4 Severely defective arterial thrombus formation in mice lacking GPVI and CLEC-2 54
4.5 The small GTPase RhoA is a crucial mediator of platelet activation in hemostasis and thrombosis 58
4.5.1 *RhoA*$^{-/-}$ mice display a marked thrombocytopenia 58
4.5.2 *RhoA*$^{-/-}$ mice display a reduced platelet life span 59
4.5.3 Reduced integrin activation and release of α granules in *RhoA*$^{-/-}$ platelets upon G_{13}- and G_q-stimulation 60
4.5.4 Defective shape change of *RhoA*$^{-/-}$ platelets after low agonist stimulation 62
4.5.5 RhoA is dispensable for agonist-induced Ca^{2+} mobilization in platelets 65
4.5.6 *RhoA*$^{-/-}$ platelets spread normally on fibrinogen but exhibit abolished integrin-dependent clot-retraction 66
4.5.7 *RhoA*$^{-/-}$ platelets show slightly reduced aggregate formation on collagen and adhesion on vWF under high shear flow 70
4.5.8 RhoA is critical for thrombus stabilization *in vivo* 71
4.5.9 *RhoA*$^{-/-}$ mice are protected from ischemic brain infarction 73
4.6 FXIIa inhibitor rHA-Infestin-4 abolishes occlusive arterial thrombus formation without affecting bleeding 75
4.6.1 rHA-Infestin-4 specifically inhibits the coagulation factor XIIa 75
4.6.2 rHA-Infestin-4 displays a significant impact on fibrinolysis 77
4.6.3 Prevention of arterial thrombosis in rHA-Infestin-4 treated mice 77
4.6.4 rHA-Infestin-4 does not reduce residual thrombus formation in *F12*$^{-/-}$ mice 80
4.6.5 rHA-Infestin-4 protects mice from ischemic brain infarction 81
5 DISCUSSION 83
5.1 Studies on the functional role of the GPIbα-vWF interaction and downstream signaling in shear-dependent thrombus formation 84
5.1.1 The GPIbα-vWF interaction is essential for *in vivo* thrombus stabilization at high shear 84

5.1.2 PLD1 mediates αIIbβ3 integrin activation under high shear and is critical for pathological thrombus formation but dispensable for hemostasis 87
5.2 Studies on the functional role of the (hem)ITAM-coupled receptors GPVI and CLEC-2 in hemostasis and thrombosis 90
5.2.1 GPVI is a critical mediator of arterial thrombosis upon $FeCl_3$- and mechanically induced vascular injury 90
5.2.2 CLEC-2 is important for thrombus stabilization in hemostasis and thrombosis 94
5.2.3 Functionally redundancy of GPVI and CLEC-2 during *in vivo* thrombus formation 99
5.3 RhoA is involved in G_{13}-and G_q-mediated platelet activation and essential for *in vivo* thrombus formation 101
5.4 The FXIIa inhibitor rHA-Infestin-4 is a potent antithrombotic agent without causing bleeding side effects 107
5.5 Concluding remarks and future plans 112
6 REFERENCES 114
7 APPENDIX 134

1 INTRODUCTION

1.1 Platelets

Platelets are discoid-shaped anucleate cell fragments that originate from megakaryocytes residing in the bone marrow. The exact mechanism how platelet production occurs *in vivo* is still controversially discussed. According to a recently emerged hypothesis, mature megakaryocytes expand pseudopodial protrusions, so-called proplatelets, into sinusoids in the bone marrow where the tip of these structures become continuously shed and further fragmented into platelets by shear forces present in the blood stream[1,2]. Platelets are only found in mammals and represent the smallest cells of the blood system with a diameter of 2-4 µm in humans and 1-2 µm in mice. They normally circulate in an inactive or resting state for 7-10 days in humans and approximately 5 days in mice at a relatively high concentration of ~250,000/µl and 1,000,000/µl, respectively. Most of the platelets never undergo activation during their life time and are then constantly removed from the circulation by the reticulo-endothelial system in the spleen and liver. However, platelets have the capacity to rapidly respond at any time to disruption in the endothelial layers of the vessel wall. Under these conditions, exposed components of the *extracellular matrix* (ECM) trigger initial platelet adhesion and activation. Soluble mediators which are released from activated platelets further amplify this event and lead, together with locally produced thrombin, to the activation and recruitment of further platelets from the circulation resulting in aggregate and finally thrombus formation. This process is essential for normal hemostasis by preserving the vascular integrity after tissue trauma and limiting excessive blood loss. Under pathological conditions, however, such as after rupture of an atherosclerotic plaque in stenosed vessels, thrombus formation may cause complete vessel occlusion leading to ischemia in the distal tissue[3]. This results, if occurring in coronary arteries or in the brain, in myocardial infarction or stroke, respectively, which are among the most common causes of death in the developed world[4]. Therefore, antithrombotic treatment is the prime therapeutic option in the prophylaxis and treatment of ischemic cardio- and cerebrovascular diseases.

The dual function of platelets indicates that their activation requires a very defined and tight regulation to guarantee on the one hand efficient sealing of a wound site while at the same time uncontrolled platelet adhesion and excessive platelet activation has to be limited to avoid undesired vessel occlusion. To achieve this tightrope walk under physiological conditions, platelets exhibit various adhesion/activation and inhibition receptors combined with a complex signaling machinery.

It should be noted that beyond their function in hemostasis and thrombosis, platelets also play important roles in wound healing, inflammatory processes, angiogenesis and tumor metastasis.

1.2 Platelet activation and thrombus formation

Platelet activation and thrombus formation at sites of vascular injury require a series of well coordinated signaling events which can be divided into three major steps: (1) Platelet tethering, (2) activation and (3) firm adhesion/aggregation (Figure 1). The first step of initial platelet adhesion involves sequential interactions of platelet surface receptors with numerous macromolecules of the exposed subendothelial ECM such as collagens, laminin and fibronectin. In general, the adhesion mechanisms are largely dependent on the predominant rheological conditions present in the vasculature. Assuming blood flow as laminar, the velocity of the fluid is greater in the center than near the wall, thereby causing shear forces between adjacent layers. Consequently, platelets are exposed to the maximal hemodynamic forces at the vessel wall[5]. The distinct wall shear rates, however, which trigger certain platelet adhesion mechanisms depend on the vascular bed. Under high shear flow conditions, such as found in arterioles or stenosed arteries, the initial platelet contact, also called “tethering”, with the ECM is mediated by the platelet receptor *glycoprotein* (GP)Ib and *von Willebrand Factor* (vWF) immobilized on exposed collagen[6]. This interaction is not stable enough to mediate firm platelet adhesion to the wound site but rather induces a rapid deceleration and “rolling” of the cells thereby facilitating the binding of other platelet receptors to ECM components. Among them, the interaction of the immunoglobulin family receptor GPVI with collagen is the most important event leading to platelet activation.

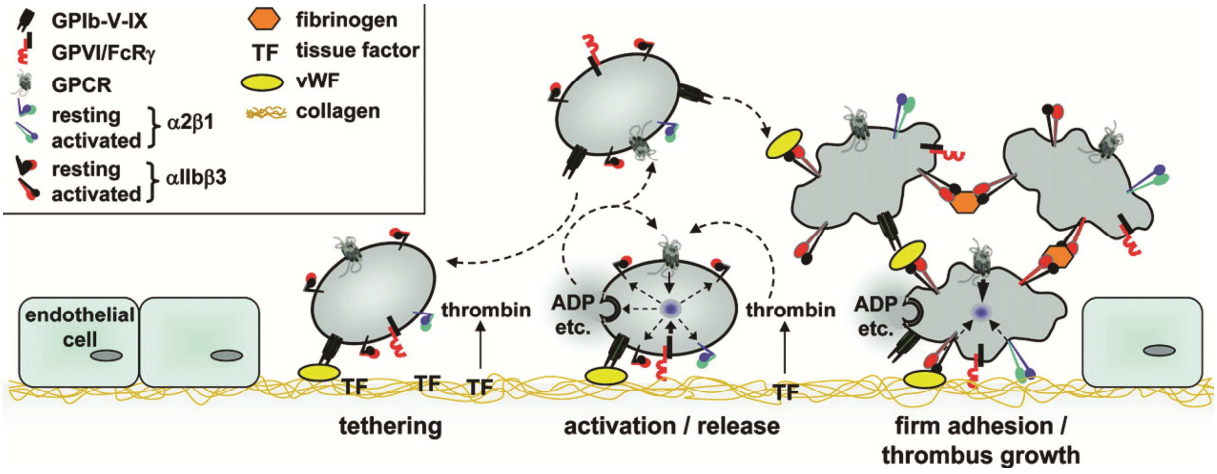

Figure 1. Multistep model of platelet adhesion/activation and thrombus formation at sites of vascular injury. The GPIbα-vWF interaction mediates platelet deceleration and tethering on the exposed ECM thereby allowing the interaction of GPVI with collagen. This in turn leads to platelet activation by triggering the release of secondary mediators such as ADP and TXA_2 and inducing a shift of integrins (most notably α2β1 and αIIbβ3 integrins) from a low to a high affinity state. Together with locally tissue factor (TF)-induced thrombin formation, soluble mediators enhance platelet activation and contribute to the recruitment of platelets into a growing thrombus. Activated integrins mediate firm adhesion of platelets to the ECM and stabilize the platelet thrombus by connecting platelets via αIIbβ3-bound fibrinogen or vWF. (Taken from: Varga-Szabo *et al., Arterioscler Thromb Vasc Biol*, 2008)[7].

Platelets have evolved multiple activation receptors that can be classified according to their signal transduction into two major receptor groups which converge into common activation processes[7].

GPVI belongs to one class of platelet-activating receptors and signals upon binding to collagen via the *immunoreceptor tyrosine-based activation motif* (ITAM)-bearing *Fc receptor* (FcR) γ chain[8]. The related C-type lecitin-like receptor CLEC-2 is a type II transmembrane receptor that initiates activation via a single YXXL-motif and shares many similarities to GPVI-induced signaling with both culminating in the stimulation of the key effector molecule *phospholipase* (PL) Cγ2[9,10] (Figure 2). PLCs cleave the membrane phospholipid *phosphatidylinositol-4,5-bisphosphate* (PIP_2) to the second messengers *inositol-1,4,5-trisphosphate* (IP_3) and *diacylglycerol* (DAG). While the latter activates *protein kinase* (PK)C, IP_3 can liberate Ca^{2+} from intracellular stores which then opens calcium channels in the plasma membrane leading to a transient but massive influx of extracellular Ca^{2+} via a process termed *store operated Ca^{2+} entry* (SOCE)[11]. The increases in cytosolic Ca^{2+} concentration ($[Ca^{2+}]_i$) is a central step for platelet activation and required for proper platelet adhesion, secretion and aggregation.

The release and secretion of soluble mediators by activated platelets is a crucial step for the amplification of the initial signal and the activation and recruitment of further platelets from the circulation[12]. Platelets exhibit three different types of granules: α granules, dense granules and lysosomes. α granules contain adhesive molecules like vWF, fibrinogen and thrombospondin but also growth and coagulation factors whereas dense granules contain small molecules like *adenosine diphosphate* (ADP), *adenosine triphosphate* (ATP) and serotonin. Among the released molecules, ADP and ATP together with intracellularly produced and released *thromboxane A_2* (TXA_2) are the most important secondary mediators for autocrine and paracrine platelet activation (Figure 2).

Upon vascular injury, platelet activation is also locally coordinated with the induction of the coagulation system, leading to thrombin generation. This is partially initiated by the exposure of *tissue factor* (TF) to *coagulation factor* (F)VII circulating in the blood (see also section 1.8) but also by the exposure of negatively charged *phosphatidylserine* (PS) on the surface of activated platelets, that provides a platform for the assembly of the prothrombinase[13] and tenase[14] complexes. These two coagulation enzyme-cofactor complexes are essential for effective propagation of coagulation.

The above mentioned secondary mediators as well as thrombin act via specific receptors coupled to heterotrimeric G proteins (GPCRs) which represent the second largest group of activating receptors[15] and induce different signaling pathways (Figure 2). $G_{12/13}$ stimulation results in a Rho/Rho kinase-mediated regulation of *myosin light chain* (MLC) phosphorylation and consequently induction of platelet shape change[16]. G_q-induced signaling, in contrast,

leads to the activation of PLCβ[17], followed by Ca^{2+} mobilization as well as PKC stimulation (see above), G_i proteins trigger subunit-specific *adenylyl cyclase* (AC) inhibition and *phosphatidylinositol 3-kinase* (PI3K) activation[18]

These platelet signaling events converge in the "final common pathway" of platelet activation, the functional up-regulation of heterodimeric transmembrane adhesion receptors of the integrin family leading to firm platelet adhesion and aggregation[7]. The shift from a low to a high affinity state enables platelet adhesion to collagen (via α2β1), fibronectin (via α5β1) and laminin (via α6β1) present in the ECM[19]. The main platelet integrin αIIbβ3 is predominantly involved in the adhesion process by binding to collagen-bound vWF as well as fibronectin and it is a critical mediator of platelet aggregation by linking platelets via fibrinogen and vWF.

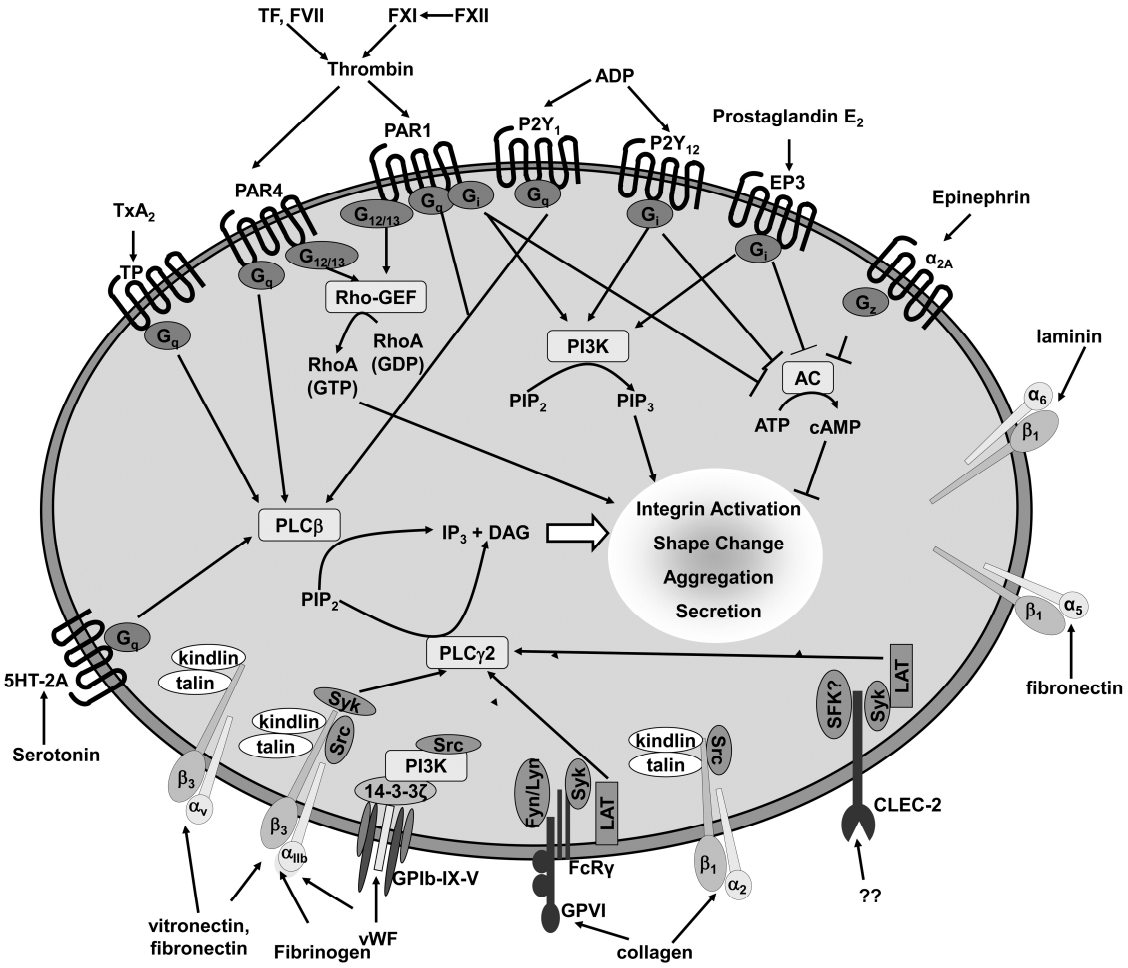

Figure 2. Scheme of platelet receptors and main signaling pathways. Receptor stimulation leads to activation of different intracellular signaling molecules. Soluble agonists such as ADP, TXA_2, thrombin, serotonin and epinephrine act via specific G protein-coupled receptors (GPCRs) involving $G_{12/13}$, G_q and $G_{i/z}$ activation. $G_{12/13}$ stimulation leads to Rho/Rho kinase-mediated cytoskeleton rearrangements, G_q activates phospholipase (PL)Cβ and $G_{i/z}$ induces inhibition of the adenylyl cyclase (AC). Adhesion receptor signaling induced by GPVI and CLEC-2, but also GPIb and integrins results in PLCγ2 activation. PLCs generate inositol-1,4,5-trisphosphate (IP_3) and diacylglycerol (DAG) from phosphatidylinositol-4,5-bisphosphate (PIP_2). IP_3 then mediates elevation of intracellular Ca^{2+} concentration $[Ca^{2+}]_i$, a process that is crucial for full platelet activation. Abbreviations: TXA_2, thromboxane A2; PAR, protease activated receptor; Rho-GEF, Rho-specific guanine nucleotide exchange factor; PI-3-K, phosphatidylinositol 3-kinase; PIP_3, phosphatidylinositol-3,4,5-trisphosphate; Fg, fibrinogen. (Taken from: Stegner *et al., J Mol Med*, 2011)[20].

1.3 The GPIb-V-IX complex

At high shear rates, the rapid interaction between GPIb of the GPIb-V-IX complex and vWF immobilized on collagen is essential for the initial recruitment of flowing platelets to the ECM at sites of vascular injury[6]. As described above, this contact has a high "off-rate" and only mediates deceleration of platelets to enable the interaction of other surface receptors with their respective ligands exposed at the wound site. Recent findings proposed an additional role for GPIb at extremely high shear rates (>10.000 sec^{-1}), such as found in stenosed arteries. Under these conditions, shear-microgradients guide initial adhesion and aggregation of discoid platelets and thereby constitute the driving force of thrombus formation, most likely through a GPIb-dependent mechanism but independently of integrin αIIbβ3 activation[21-23].

The GPIb-V-IX complex is a highly abundant receptor complex exclusively expressed in platelets and megakaryocytes that functions independently of the activation state of the cell. It is encoded by four different genes, the α- and β-subunit of GPIb, GPV and GPIX which all belong to the leucine-rich repeat proteins superfamily[24,25]. Lack or dysfunction of the GPIb-V-IX complex in humans causes the *Bernard-Soulier syndrome* (BSS), a congenital bleeding disorder associated with mild thrombocytopenia and giant platelets[26]. Gene deletion of Gp1ba[27] or Gp1bb[28] in mice leads to a deficiency of the entire complex and resembles the human BSS, as the mice suffer from a severe bleeding phenotype and macrothrombocytopenia. Whereas lack of GPIX similarly results in BSS, GPV deficiency in humans has not been described to date[26] and mice lacking the receptor show unaltered platelet counts and rather normal hemostasis[29,30].

GPIbα represents the main functional subunit of the receptor complex and bears multiple binding domains in its N-terminal extracellular part for different interaction molecules most notably vWF, which is the major and best characterized binding partner, Mac-1, P-selectin, thrombospondin-I, thrombin, high molecular weight kininogen and coagulation factors XI and XII[25,31]. Besides the pivotal role of GPIb-V-IX as adhesion receptor there is growing evidence that ligand-binding to the receptor complex generates transmembrane signals leading to intracellular Ca^{2+} mobilization, cytoskeletal rearrangements, granule release and integrin αIIbβ3 activation[32,33]. However, GPIb-V-IX signaling is generally considered to induce only weak platelet activation compared to GPVI or GPCR-dependent signaling pathways. Several molecules have been proposed to mediate GPIb-V-IX signaling via association with GPIbα such as 14-3-3ζ, Src kinases, calmodulin and PI3K[34-36]. Some reports indicated a role for GPIb-V-IX in ITAM signaling of FcγRIIA[37] or the FcRγ chain[38] by binding to GPVI[39], whereas other studies could not confirm these observations[40]. Recently, the *adhesion and degranulation promoting adaptor protein* (ADAP) was shown to be involved in integrin αIIbβ3 activation downstream of GPIb-V-IX upon vWF binding[41].

The essential role for GPIbα in the process of arterial thrombus formation has been demonstrated in mice where the vWF binding site of GPIbα was blocked by Fab fragments of the inhibitory antibody p0p/B[42] and in mice expressing GPIbα with a mutated extracellular domain[43,44]. Platelet tethering to the injured vessel wall and subsequent thrombus formation was abrogated in both mice. In addition, GPIbα and its interaction with vWF appears to be a major pathophysiological mechanism underlying ischemic brain infarction as administration of anti-GPIb Fab fragments or vWF deficiency profoundly protected mice from lesion progression in an experimental stroke model[45,46]. This absolute requirement for GPIbα in thrombosis makes this receptor and possibly also its downstream signaling machinery an attractive pharmacological target for antithrombotic therapy.

1.4 Phospholipase D1

Phospholipase C isoforms have been well characterized as major effector molecules required for intracellular signal transduction during platelet activation[7]. In contrast, the role of PLDs in platelet function is less clear and all findings so far have been obtained from either indirect inhibition studies of PLD activity or correlation studies, which consign the knowledge about PLD from other cells to platelets.

Two isoforms of PLD, PLD1[47] and PLD2, which share a 50% sequence identity[48], have been described to be ubiquitously expressed in mammalian cells[49]. PLDs comprise a phosphodiesterase activity and hydrolyze *phosphatidylcholine* (PC) to *phosphatidic acid* (PA) and choline. PA in turn is the major effector downstream of PLD and probably acts as a second messenger for direct enzyme activation, most notably *phosphatidylinositol-4-phosphate 5-kinase* (PI4P5 kinase), but can also be further metabolized into DAG and lyso-PA[50]. The regulation of PLD activity is still not fully understood, however, multiple candidate molecules/mechanisms have already been proposed. Among them, phospholipids, such as PIP_2 and *phosphatidylinositol-3,4,5-triphosphate* (PIP_3), have been shown to directly interact with specific binding sites of PLD and thus stimulating its enzymatic activity[51]. Furthermore, PKC and small GTPases of the ARF and Rho families have been reported to directly activate PLD[52].

According to the large number of downstream targets which have been proposed for PLD and PA, the protein is also supposed to mediate diverse cellular processes such as signal transduction, cytoskeletal reorganizations, vesicle trafficking, as well as endo- and exocytosis[49,53-56].

As mentioned above, only a limited number of studies addressed the role for PLD in platelet activation. Thrombin, U46619 and collagen, but not ADP alone have been shown to induce PLD activation in human platelets and thereby its translocation to the plasma membrane[57-60].

Fibrinogen binding to integrin αIIbβ3 has been suggested to mediate similar events[61]. Other reports indicated that PLD modulates dense granule release[60,62] but is required for lysosomal secretion in response to *protease activated receptors* (PAR) signaling[63]. Moreover, PLD is supposed to be involved in PAR1-mediated platelet aggregation via Rap1[63,64]. However, the specific function of PLD in platelet activation and aggregation has not been definitively determined and hence its role in thrombosis and hemostasis was unclear when this project was started.

1.5 GPVI

Subendothelial fibrillar collagens represent the most potent thrombogenic substrates at the wound site which trigger platelet adhesion, activation and ultimately aggregation. Besides GPIb and integrin αIIbβ3, which indirectly interact with collagen via vWF[6], platelets express several direct collagen receptors[65], most importantly integrin α2β1 and GPVI. Whereas integrin α2β1 contributes to platelet adhesion on collagen, but plays only a subordinated role in platelet activation, GPVI has meanwhile been established as the main activatory receptor for collagen[8].

GPVI is a 62 kDa type I transmembrane receptor that is exclusively expressed in platelets and megakaryocytes[66]. It belongs to the immunoglobulin superfamily and is constitutively associated with ITAM-containing FcRγ-chain dimers which act as the signal-transducing subunit of the receptor complex[67,68]. Upon crosslinking of GPVI by ligand-binding, the Src family tyrosine kinases Fyn and Lyn, bound to the cytoplasmatic tail of GPVI, come into contact with the FcRγ-chain and mediate tyrosine phosphorylation of the ITAM[69,70]. As a consequence, Syk kinase can bind and becomes autophosphorylated thereby initiating a complex downstream signaling cascade via the phosphorylation of the adaptors *linker for activated T cells* (LAT) and *Src homology 2 domain-containing leukocyte phosphoprotein of 76-kDa* (SLP-76), which leads to the activation of the central effector molecule PLCγ2[71]. This signaling process results in Ca^{2+} mobilization, granule release, integrin activation and PS exposure[8] (see also section 1.2). Moreover, recently laminin, a major component of the basal lamina in the basement membrane has been identified as a new endogenous ligand for GPVI[72], however, its relative significance for platelet activation remains elusive. Laminin has a ten-fold lower affinity for GPVI as compared to collagen, probably because it requires initial interaction with its main receptor integrin α6β1 before enabling GPVI binding[73].

For a detailed investigation of GPVI-induced platelet activation events *in vitro*, different experimental tools are available. Besides special forms of collagen, also synthetically generated *collagen-related peptide* (CRP) is used to induce GPVI signaling. CRP is a powerful platelet agonist consisting of repeated GPO (G=glycine, P=proline,

O=hydroxyproline) motifs, a typical amino acid sequence found in native collagen I and III, which are cross-linked to achieve a fibrillar structure[74]. Furthermore, numerous snake venom peptides have been demonstrated to act on GPVI, most notably the C-type lectin convulxin which induces platelet activation by clustering of the collagen receptor[75,76].

During the last years, major advances have been made in the understanding of GPVI-dependent platelet activation and aggregation as well as its particular role in thrombus formation *in vivo* by the generation and analysis of mice lacking the receptor[77-81]. The first *in vivo* study showed that injection of the anti-GPVI antibody JAQ1 into mice induces an irreversible downregulation of the receptor from the surface of circulating platelets, resulting in a transient "GPVI knockout-like" phenotype for at least two weeks. These mice exhibit a long-term antithrombotic protection in experimental thrombosis models but display overall normal tail bleeding times[42,77,82,83], an observation which could later be confirmed in *FcRg*$^{-/-}$ and *Gp6*$^{-/-}$mice[44,78,81,84]. In addition, antibody-induced GPVI-depletion also effectively protected mice from ischemic brain infarction in a model of *transient middle cerebral occlusion* (tMCAO) without increasing bleeding complications[45]. Based on these results, GPVI has been proposed as an attractive antithrombotic target for the therapy of cardio- and cerebrovascular diseases. However, some studies with GPVI-deficient mice provided contradictory results on the relative importance of GPVI in different experimental thrombosis models[78,79,85,86].

So far, also two GPVI-deficient patients have been reported with high levels of anti-GPVI autoantibodies in their blood[87,88]. These patients showed a mild bleeding syndrome and their platelets were refractory to collagen stimulation. As mentioned above, this observation could later be explained by the phenomenon of antibody-induced GPVI-depletion in mouse platelets[77]. Furthermore, two patients have been described which bear a compound heterozygous mutation in GPVI[89,90]. One of the mutations prevents expression of GPVI and the other causes impaired receptor function, resulting in both cases in a mild bleeding disorder.

1.6 CLEC-2

The 32 kDa *C-type lectin-like receptor 2* (CLEC-2) was initially identified on a transcript level in immune cells such as monocytes, dendritic cells and granulocytes[91,92] and later found at a low level on peripheral blood mouse neutrophils[93]. Only recently, CLEC-2 has been discovered to be expressed primarily on the surface of platelets where it can mediate potent platelet activation and aggregation by the snake venom protein rhodocytin, isolated from the Malayan pit viper *Calloselasma rhodostoma*[9]. CLEC-2 is a type II transmembrane receptor and contains, in contrast to the GPVI/FcRγ-chain complex, only one single YxxL sequence which forms together with three upstream amino acid residues a novel signaling motif

referred to as hemITAM[9,10]. Ligand-binding to the extracellular domain of CLEC-2 induces Src kinase-dependent tyrosine phosphorylation of the YxxL sequence followed by Syk kinase binding that is suggested to trigger a successional activation pathway by linking two phosphorylated hemITAMs of dimerized CLEC-2 receptors[9,94]. This Syk-regulated signaling involves activation of similar effector molecules to those stimulated by signaling of the GPVI/FcRγ-chain complex such as LAT, SLP-76, Gads and PLCγ2[9,10].

The physiological role of CLEC-2 is only partially known to date but represents a very dynamic and rapidly proceeding research field. First evidence for a specific function of CLEC-2 came from a study where platelets were identified to facilitate the transport of the *human immunodeficiency virus type I* (HIV-1). CLEC-2 is suggested to act as a binding partner for the virus on the platelet surface, whereby it probably enables virus-spread in infected humans[95]. Recent studies also reported important roles for CLEC-2 in phagocytic activity and release of proinflammatory cytokines of neutrophils[93], and in hematogenous tumor metastasis by binding to podoplanin, a type I transmembrane sialomucin-like glycoprotein expressed on the tumor surface[96]. Podoplanin has been described as the only established endogenous ligand for CLEC-2 so far and displays a wide tissue distribution with high expression levels in lung type I alveolar cells, kidney podocytes, distinct tumor cells and lymphatic endothelial cells[97]. CLEC-2 induced platelet activation by endothelial podoplanin from the lymphatic sac has recently been shown to be essential for the separation of the lymphatic from the blood vascular system during embryonic development[98-100]. According to the remarkable platelet activatory potential of CLEC-2, it was early speculated that the receptor might become a valuable antithrombotic target; however, a direct proof for a role of CLEC-2 in hemostasis and in the setting of thrombotic events was lacking.

1.7 Small GTPases of the Rho family

Mammalian Rho GTPases comprise a subfamily of 20 small Ras-related proteins that are best known for their important roles in regulating the actin cytoskeleton[101]. Among them, the best documented family members are the highly conserved GTPases RhoA, Rac1 and Cdc42. A common feature of many Rho GTPases is the molecular switch between an inactive *guanosine diphosphate* (GDP)-bound form and an active *guanosine triphosphate* (GTP)-bound status which is catalyzed by upstream *guanine nucleotide exchange factors* (GEFs). Conversely, *GTPase-activating proteins* (GAPs) initiate the hydrolysis of GTP to GDP, thereby inactivating the Rho GTPase. *Guanine nucleotide-dissociation inhibitors* (GDIs) reduce the dissociation rate of GDP from the Rho protein and prevent its activation. The capacity of Rho GTPases to cycle between these two states enables a spatially and temporally controlled activation of effector molecules initiating a variety of processes,

including cell migration, adhesion and division. Moreover, Rho GTPases are implicated in vesicle trafficking, microtubule dynamics, cell-cycle progression and gene transcription[102].

The specific role of Rho GTPase-mediated signaling in platelet function has been intensively studied during the last years as cytoskeleton reorganizations are crucial to mediate proper platelet activation responses at sites of vascular injury. This involves change of the discoid to a spherical shape of the platelets (so-called: shape change), as well as adhesion and spreading on the exposed components of the ECM such as collagen, fibronectin and laminin. Stimulation of Cdc42 and Rac1 has been suggested to induce formation of filopodia and lamellipodia, respectively[103,104], whereas RhoA has been proposed to mediate shape change and stress fiber formation upon platelet activation[105,106]. The major findings, however, about the functional role of Rho GTPase were yielded by overexpression studies in cell lines with dominant negative and constitutively active Rho proteins or in the case of platelet analysis mainly from pharmacological inhibition studies. These approaches often provide conflicting results probably caused by additional uncontrolled side effects or unspecific protein inhibition in the manipulated cells. The recent development of platelet and MK-specific knockout mice for several Rho GTPases could provide more reliable conclusions about their role in platelet function and moreover their contribution to thrombus formation under *in vivo* conditions. MK and platelet-specific Cdc42-deficent mice, for example, showed that the protein is not per se required for filopodia formation upon platelet activation[107]. Furthermore, these platelets displayed, in contrast to previous indications, increased granule release after activation that even translated into accelerated thrombus formation *in vivo.* Conditional Rac1 knockout mice could clearly confirm that this GTPase is essential for platelet lamellipodia formation and for PLCγ2 activation downstream of the platelet collagen receptor GPVI[108]. These signaling defects protected Rac1-deficient mice from arterial thrombosis.

In this thesis, the relevance of RhoA for platelet function was addressed in detail using a conditional knockout approach.

1.7.1 RhoA

RhoA is ubiquitously expressed and implicated in many cellular functions most notably cell contraction, adhesion, migration and cytokinesis[109]. Activation of RhoA has been demonstrated to be crucial for the organization of cytoplasmatic stress fiber assembly and maturation of focal adhesions in multiple cell types[110-112]. Further studies indicated an important role of the GTPase in vascular smooth muscle cell contractility[113,114] and destabilization of endothelial cell-cell junctions[115], thereby regulating blood pressure[116] and vascular membrane permeability, respectively. In the hematopoietic system, overexpression studies revealed that RhoA inhibition leads to increased hematopoietic stem and progenitor cell proliferation[117] and enhanced T cell polarization and survival[118,119]. Other studies reported

a role for RhoA in neutrophil chemotaxis[120] and phagocytic activity of macrophages[121]. The first cell type-specific conditional knockout mouse for RhoA was recently published by Jackson *et al.*. This study described mice with a keratinocyte-restricted loss of RhoA which displayed normal skin development but reduced keratinocyte contraction and migration[122].

The functional role of RhoA in platelet activation has also been assessed in numerous pharmacological inhibition studies using either botulinum C3 ADP ribosyltransferase to inactivate RhoA[123] or inhibitors for specific RhoA downstream effectors. The GTPase was shown to be activated by GPCR-induced signaling most notably downstream of $G\alpha_{12/13}$ by specific RhoGEFs (Figure 3)[124]. Some studies also indicated that RhoA can be stimulated via G_q-mediated activation processes, particularly at high agonist concentrations[125,126]. RhoA in turn mediates activation of *RhoA-kinase* (ROCK)[127], which is the best characterized RhoA effector molecule, and mDia1 (first identified mammalian homologue of *Drosophila* diaphanous)[128]. Consequently, RhoA-kinase inhibits *myosin light chain phosphatase* (MLCP) which regulates together with the Ca^{2+}/calmodulin-dependent *myosin light chain kinase* (MLCK) phosphorylation of the *myosin light chain* (MLC; Figure 3)[129]. The RhoA/RhoA-kinase-mediated MLC phosphorylation results in actomyosin assembly and contraction which is thought to be crucial for shape change and stress fiber formation during platelet activation[105,130-134]. Furthermore, RhoA is suggested to be involved in dense granule release and integrin αIIbβ3 activation[135-137] as well as in sustained αIIbβ3-dependent platelet adhesion on ECM proteins at high shear[138]. In a recent study, Gong *et al.* reported a defined regulation of RhoA activity during integrin αIIbβ3-induced intracellular signaling events[139]. They suggested that $G\alpha_{13}$, bound to the cytoplasmatic tail of the activated β3 domain, triggers a transient inhibition of RhoA during the early phase of platelet spreading which is finally terminated by calpain leading to the reactivation of RhoA to mediate clot retraction[139]. This is in line with a previous report by Leng *et al.* showing that RhoA is dispensable for platelet spreading on fibrinogen but contradicts with the finding that the protein is also not required for clot retraction[140]. In contrast, Gao *et al.* implicated a role for RhoA in mDia1-dependent spreading of thrombin-stimulated platelets[141]. Moreover, one study on cultured human MKs indicated that the RhoA/ROCK signaling pathway may negatively regulate proplatelet formation[142].

Although multiple studies have already investigated the function of RhoA in platelets, it has not been addressed in detail yet, particularly not in a knockout approach. Furthermore, the role of RhoA-mediated signaling in physiological and pathological thrombus formation is entirely unclear.

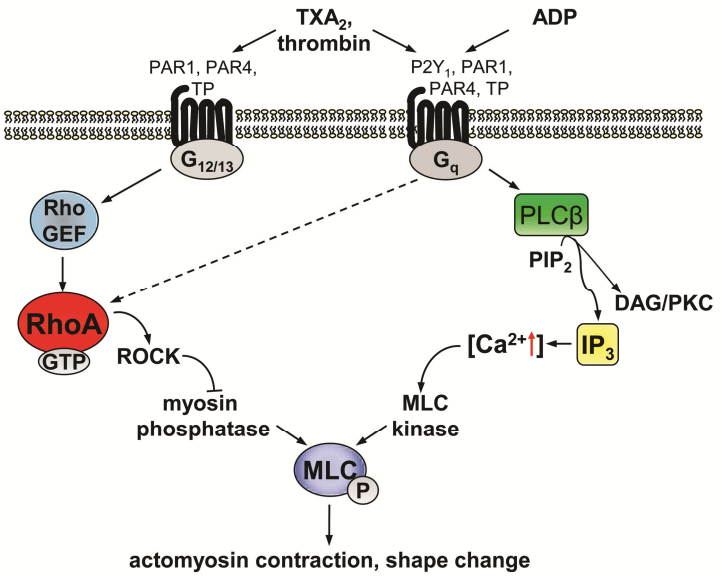

Figure 3. Scheme of RhoA-dependent signaling in platelets. RhoA becomes activated upon $G\alpha_{12/13}$ protein-coupled receptor stimulation by RhoGEFs or downstream of $G\alpha_q$ protein-coupled receptors via so far unknown mechanisms. GTP-bound RhoA stabilizes MLC phosphorylation through inhibition of myosin phosphatase by ROCK. MLC phosphorylation is initially induced by a Ca^{2+}/calmodulin-dependent activation of MLC kinase. These platelet signaling pathways result in actomyosin contraction and shape change.

1.8 Blood coagulation

Vascular injury also triggers rapid activation of the plasma coagulation system that acts in concert with activated platelets to induce the formation of a fibrin- and platelet-rich clot. In the classical cascade or waterfall model, blood coagulation is described as a process which can be initiated by two distinct pathways, the extrinsic and the intrinsic pathway. These cascades involve a tightly regulated sequential activation of plasma serine proteases and cofactors culminating in the formation of thrombin. This in turn enhances platelet stimulation via cleavage of PARs (see section 1.2) and converts fibrinogen into fibrin[143,144], thereby stabilizing the growing thrombus. Clot formation through the extrinsic pathway occurs when the transmembrane glycoprotein TF, expressed by cells within the vessel wall and adjacent tissue or on cell-derived microparticles, comes into contact with *activated coagulation factor* VII (FVIIa) leading to concomitant activation of FX and FIX[145] (Figure 4). FXa and FIXa then amplify TF-bound FVII activation in a feedback signal and efficiently propagate coagulation by activating prothrombin and FX, respectively, when assembled in enzyme-cofactor complexes on the platelet surface[13,14] (see also section 1.2). According to the original assumption, the intrinsic pathway is initiated when FXII (Hageman factor) becomes autoactivated on a negatively charged surface (contact activation) and forms the enzyme αFXIIa comprising a 50 kD heavy and a 30 kDa catalytic domain-bearing light chain linked by a disulfide bond[146]. Surface-bound αFXIIa is capable of activating FXI followed by successive activation of FIX and FX[147] (Figure 4). Furthermore, it converts *prekallikrein* (PK) into plasma kallikrein and initiates the classical complement cascade by activation of C1 esterases. Kallikrein in turn reciprocally activates more FXII and liberates the vasoactive peptide *bradikinin* (BK) from *high molecular weight kininogen* (HK)[148]. Further αFXIIa cleavage by kallikrein leads to formation of a soluble 28 kDa catalytic domain fragment βFXIIa that can

activate PK and the complement system but lacks the catalytic activity for FXI[149,150]. FXII has also been shown to promote fibrinolysis directly by activation of plasminogen[151] or the inhibition of the *plasminogen activator inhibitor-I* (PAI-1)[152] and indirectly by kallikrein which can activate *tissue plasminogen activator* (tPA) and *urokinase plasminogen activator* (uPA)[153], however the relevance of each function *in vivo* has yet to be determined.

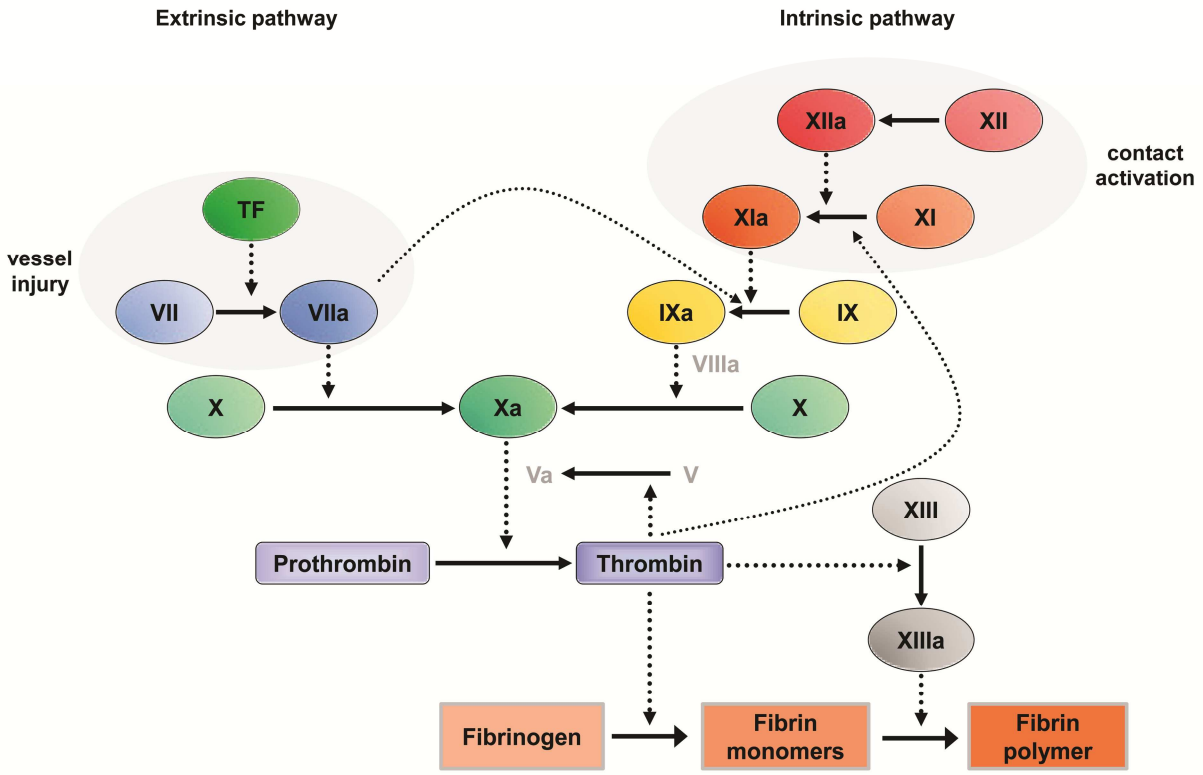

Figure 4. Scheme of the classical coagulation cascade. The extrinsic pathway is initiated by the tissue factor (TF): factor (F)VII complex at sites of vascular injury followed by the activation of FX and FIX. FXII, the starting point of the intrinsic pathway, is activated via contact activation and triggers sequential activation of FXI, FIX and X. Both pathways culminate in the prothrombinase (FX:FV complex)-induced activation of prothrombin. The resulting thrombin is the key protease of the coagulation system and activates multiple proteases and cofactors. Thrombin can also cleave fibrinogen into soluble fibrin monomers which are consequently cross-linked by the action of the activated FVIII, leading to clot-stabilizing fibrin polymers.

Although negatively charged material, such as glass, kaolin, silicone rubber and various polymers are well known to initiate contact activation *in vitro*, the mechanisms and substances supporting FXII autoactivation under physiological conditions are still a matter of intensive debate. A number of biologic candidates have already been suggested to promote FXII activation, including fatty acids, sulfatides, glycosaminoglycans, cholesterol sulfate as well as phosphatidic acid[154]. Recent studies identified novel interesting procoagulant mediators such as extracellular RNA[155], misfolded or aggregated proteins[156], inorganic polyphosphates released from dense granules of activated platelets[157] and exposed collagen[158] and laminin[159] at sites of vascular injury. However, the (patho-) physiological

relevance of these mediators as well as the relative contribution of each substance to FXII activation remains to be elucidated.

In order to prevent uncontrolled protease activation and limit excessive blood clotting, the coagulation system is also tightly linked to endogenous anticoagulatory pathways. This is primarily done by the *tissue factor pathway inhibitor* (TFPI) limiting TF-FVIIa complex activity[160], the protease inhibitor antithrombin and the FVa-FVIIIa specific Protein C inhibitor pathway[161]. Until recently, *C1 esterase inhibitor* (C1 inhibitor) was considered the best known physiological inhibitor of FXIIa[162], however, new *in vitro* studies suggested that platelet-induced FXII activation is dominantly regulated by antithrombin[163] and that *Histidine-rich glycoprotein* (HRG) is involved in the inhibition of FXIIa-mediated coagulation[164].

The two classical pathways of coagulation also serve as the basis of the widely used standard methods to determine overall plasma coagulation in clinical practice: the *prothrombin time* (PT) by TF-FVIIa-initiated coagulation and the *activated partial thromboplastin time* (aPTT) by FXII-mediated clotting. The relevance of the intrinsic pathway for blood coagulation *in vitro*, as aforementioned, has been obvious for decades now, whereas its importance for physiological clot formation remained elusive. A long-standing model suggested that fibrin formation is mainly, if not exclusively, mediated by the TF-FVIIa pathway, whereas FXII-induced processes were considered not to be relevant for blood clotting *in vivo*. This hypothesis was mainly based on the observation that hereditary deficiency of FXII is not associated with hemorrhages[165] contrary to deficiencies of components of the extrinsic cascade. TF-deficient humans have not been described and severe FVII deficiency was only found at a low frequency[166] which could be reproduced in mice lacking either of the proteases and die during embryonic development or perinatally due to massive vascular and hemostatic defects[167,168].

This original view was recently challenged by studies showing that FXII-deficient mice are profoundly protected from pathological thrombus formation in different models of arterial thrombosis and ischemic stroke but do, like FXII-deficient humans, not display any detectable alteration of hemostasis[169,170]. These surprising observations not only changed the long-standing paradigm that hemostasis and thrombosis involve the same mechanisms but also led to the intriguing hypothesis that inhibitors of FXII-dependent coagulation might represent powerful antithrombotic agents that do not induce an increased bleeding risk, the major clinical complication associated with current anticoagulative therapies, most notably heparins and vitamin K antagonists.

1.9 Murine arterial thrombosis models

Arterial thrombus formation is a complex process involving a well-coordinated action and a defined interplay of numerous platelet adhesion/activation receptors, intracellular signaling molecules, subcellular structures and plasma coagulation factors. The generation of genetically modified mouse strains during the last decade has provided a powerful tool to elaborate the functional significance of a certain protein or signaling pathway for platelet physiology. In this context, *in vitro* experiments are indispensable for a detailed analysis of the individual roles and the interactions of defined proteins during platelet adhesion, activation and aggregation processes. However, these findings are partially difficult to correlate with their true *in vivo* relevance for thrombosis and hemostasis, as *in vitro* conditions cannot resemble the innumerable hemodynamic changes and spatiotemporal cellular and molecular interactions that are present during the initiation and propagation of thrombi at sites of vascular lesions.

Therefore, multiple mouse models of thrombotic disease have been developed during recent years to assess the molecular mechanisms underlying arterial thrombus formation *in vivo*. These models differ in the type of vessel injury, the severity of injury, the targeted vascular bed and consequently the signaling pathways that are predominantly triggered[171]. The combination of thrombosis models with *in vivo* fluorescence microscopy, e.g. of fluorescently labeled platelets, allows direct real-time visualization and quantification of dynamics during the thrombotic process.

The most commonly used method to induce vascular injury is the topical application of *Ferric(III)chloride* ($FeCl_3$) on a macro- or microvessel (carotid artery or mesenteric arterioles), which typically results in formation of platelet-rich occlusive thrombi[172,173] that are morphologically similar to those found in humans[174]. The mechanisms underlying $FeCl_3$-induced thrombosis are still controversially discussed. While it was widely accepted until now that $FeCl_3$ treatment leads to vascular endothelial denudation and exposure of the ECM through production of reactive oxygen species[172,175], a recent study suggested alternative mechanisms[86]. In that study, Eckly *et al.* showed that $FeCl_3$ diffuses through the vessel wall resulting on the one hand only in the exposure of endothelial basement membrane components and on the other hand in the development of $FeCl_3$-filled spherical bodies on the endothelium which carry large amounts of TF on the surface[86]. Another, less commonly applied chemical injury model involves a systemic injection of the photoreactive reagent Rose Bengal followed by exposure of a vessel segment to epi-illumination at 540 nm[176]. The endothelial damage is caused by the generation of free radicals that leads to formation of occlusive thrombi. A laser-induced vascular injury in the microcirculation is another frequently used technique to trigger thrombus formation[177]. In this model, the intensity of the laser-beam and the exposure time can be tightly controlled to produce different types of lesions ranging

from mild endothelial injury or activation to denudation of the endothelium. It has been proposed that the consequently activated signaling events that drive thrombus formation depend on the severity of the laser-induced injury[78,85,178]. Whereas, a severe injury is suggested to trigger thrombus growth predominantly by TF-dependent thrombin generation, a superficial injury has been shown to also involve collagen-mediated platelet activation. A third principle to experimentally achieve a vascular damage is the mechanical injury of a macrovessel (abdominal aorta, carotid artery or femoral artery) either by compression or ligation of the vessel using a forceps[169] or a filament[42] or by direct injury of the luminal side of the artery with a flexible wire[179]. This model is characterized by occlusive thrombus formation within a few minutes after massive endothelial denudation.

As the mentioned murine thrombosis models differ in their experimental procedures and may accordingly induce different signaling pathways that predominately drive thrombus formation, mutant mice should be ideally analyzed in different injury models. Thereby, more reliable conclusions can ultimately been drawn about the relevance of the particular targeted protein in arterial thrombosis.

All thrombosis models have in common that the vascular damage is induced in healthy blood vessels instead of diseased, atherosclerotic vessels where atherothrombotic events normally occur in humans. To replicate the thrombogenic conditions of a ruptured atherosclerotic plaque in mice two groups have developed a special thrombosis model using *Apoe*$^{-/-}$ mice. Thrombus formation in this model was provoked by acute plaque rupture in the carotid artery using either an ultrasound treatment[180] or a suture needle technique[181]. However, the results obtained in this model were largely variable, indicating that further studies are required to improve the reproducibility of thrombus formation upon plaque rupture.

Although murine thrombosis models are artificial and have many limitations, they have already provided enormous insights into the molecular mechanisms of platelet function and thrombus formation *in vivo* during the last years and they will also be a promising tool in the future to improve the understanding of arterial thrombosis and as a consequence to propose new antithrombotic therapies in humans.

In this thesis, different *in vivo* thrombosis models were utilized where arterial thrombus formation was initiated by either $FeCl_3$-induced injury of small mesenteric arterioles or the carotid artery or mechanically induced vascular damage in the abdominal aorta. A severe laser-induced injury model was also established in our laboratory under supervision by the master student Marianne Frings. This technique was, however, not used for the analyses in the present study.

2 AIM OF THE STUDY

Thrombus formation during hemostasis and thrombosis is a multistep process that involves the sequential interplay of platelet adhesion and activation receptors, intracellular signal transduction, cytoskeletal reorganizations, granule release, integrin activation and initiation of coagulation. However, the respective key proteins and signaling mechanisms underlying these processes are still not fully identified or understood.

The aim of this thesis was (I) to analyze the function of different platelet signaling proteins and receptors during the distinct steps of platelet adhesion/activation, aggregation and consequently thrombus formation and thereby (II) to identify novel pharmacological target candidates or pathways for a possible antithrombotic therapy. The focus of this thesis was on the relevance of the GPIbα-vWF interaction for arterial thrombus formation, the functional significance of the collagen receptor GPVI in different murine thrombosis models, the role of the recently identified platelet activating receptor CLEC-2 for hemostasis and thrombosis as well as on the effect of GPVI/CLEC-2 double deficiency on *in vivo* thrombus formation. Furthermore, this study intended to assess the function of the intracellular signaling protein PLD1 particularly during platelet aggregation and thrombus formation and the role of the small GTPase RhoA in platelet function and signaling. For this purpose, different strategies of specific protein blockage or deficiency in mice were used. The vWF binding site of GPIbα was inhibited in mice by injecting Fab fragments of the GPIbα blocking antibody p0p/B. GPVI and CLEC-2 deficient mice were generated by immunodepletion of the respective receptors after antibody injection. Furthermore, constitutive *Gp6* and *Pld1* as well as conditional *RhoA* knockout mice were analyzed.

The (III) aim of the study was to determine the suitability of a newly generated anti-FXIIa inhibitor as potential antithrombotic agent.

3 MATERIALS AND METHODS

3.1 Materials

3.1.1 Chemicals and kits

2-methyl-2-butanol	Sigma (Deisenhofen, Germany)
6x Loading Dye Solution	Fermentas (St. Leon-Rot, Germany)
acetic acid	Roth (Karlsruhe, Germany)
ADP	Sigma (Deisenhofen, Germany)
agarose	Roth (Karlsruhe, Germany)
agarose, low melting	Euromedex (France)
ammonium peroxodisulphat (APS)	Roth (Karlsruhe, Germany)
apyrase (grade III)	Sigma (Deisenhofen, Germany)
Avertin® (2,2,2-tribromoethanol)	Sigma (Deisenhofen, Germany)
beta-mercaptoethanol	Roth (Karlsruhe, Germany)
bovine serum albumin (BSA)	AppliChem (Darmstadt, Germany)
calcium chloride	Roth (Karlsruhe, Germany)
Chrono-Lume® (d-luciferase/luciferin reagent +ATP standard)	Probe & go (Osburg, Germany)
convulxin	Axxora (Lörrach, Germany)
D-Dimer ELISA kit, Asserachrom	Roche (Basel, Switzerland)
dNTP mix	Fermentas (St. Leon-Rot, Germany)
Dylight-488™	Pierce (Rockford, IL,USA)
eosin	Roth (Karlsruhe, Germany)
Epinephrine	Sigma (Deisenhofen, Germany)
epon 812	Roth (Karlsruhe, Germany)
ethanol	Roth (Karlsruhe, Germany)
ethidium bromide	Roth (Karlsruhe, Germany)
Eukitt mounting medium	Sigma (Deisenhofen, Germany)
fat-free dry milk	AppliChem (Darmstadt, Germany)
fentanyl	Janssen-Cilag GmbH, (Neuss, Germany)
fibrilar type I collagen (Horm)	Nycomed (Munich, Germany)
flumazenil	Delta Select GmbH (Dreieich, Germany)
fluorescein-isothiocyanate (FITC)	Molecular Probes (Oregon, USA)
Forene® (isoflurane)	Abott (Wiesbaden, Germany)
Fura-2 acetoxymethyl ester	Molecular Probes (Oregon, USA)

Gelatine capsules	Agar scientific (Stansted, England)
GeneRuler 1kb DNA Ladder	Fermentas (St. Leon-Rot, Germany)
glucose	Roth (Karlsruhe, Germany)
glutaraldehyde	Roth (Karlsruhe, Germany)
hematoxylin	Sigma (Deisenhofen, Germany
Hexomethyldizilasin (HMDS)	Merck (Darmstadt, Germany)
high molecular weight heparin	Sigma (Deisenhofen, Germany)
human fibrinogen	Sigma (Deisenhofen, Germany)
iron-III-chloride hexahydrate ($FeCl_3\,6H_2O$)	Roth (Karlsruhe, Germany)
isopropanol	Roth (Karlsruhe, Germany)
magnesium cloride	Roth (Karlsruhe, Germany)
medetomidine	Pfizer (Karlsruhe, Germany)
midazolam	Roche Pharma AG (Grenzach- Wyhlen, Germany)
naloxon	Delta Select GmbH (Dreieich, Germany)
NP40	Sigma (Deisenhofen, Germany)
paraformaldehyde	Roth (Karlsruhe, Germany)
phenol/chloroform/isoamylalcohol	AppliChem (Darmstadt, Germany)
Pluronic F-127	Invitrogen (Karlsruhe, Germany)
poly L-lysin	Sigma (Deisenhofen, Germany)
propyleneoxide	Sigma (Deisenhofen, Germany)
prostacyclin	Calbiochem (Bad Soden, Germany)
R-phycoerythrin (PE)	EUROPA (Cambridge, UK)
sodium cacodylate	Roth (Karlsruhe, Germany)
sodium chloride	AppliChem (Darmstadt, Germany)
Taq polymerase buffer (10x)	Fermentas (St. Leon-Rot, Germany)
Taq polymerase	Fermentas (St. Leon-Rot, Germany)
thrombin	Roche Diagnostics (Mannheim, Germany)
Triton X-100	AppliChem (Darmstadt, Germany
U46619	Alexis Biochemicals (San Diego, USA)
uranylacetate	Electron Microscopical Sciences (Hatfield, USA)
Vectashield hardset mounting medium	Vector Laboratories (Burlingame, USA)

Chromogenic substrates were purchased from Chromogenix (Lexington, USA) or Hyphen Biomed (Neuville sur Oise, France). All enzymes were obtained from Invitrogen (Karlsruhe, Germany). Collagen related peptide (CRP) was kindly provided by Paul Bray (Baylor College, USA). Rhodocytin was a generous gift from Johannes Eble (University Hospital Frankfurt, Germany). All other chemicals were obtained from Sigma (Deisenhofen, Germany) or Roth (Karlsruhe, Germany).

3.1.2 Antibodies

3.1.2.1 Purchased primary and secondary antibodies

hvWF antibody	DAKO (Hamburg, Germany
myosin light chain antibody	Cell Signaling Technologies (Danvers, USA)
phalloidin-atto647N	Sigma (Deisenhofen, Germany)
phalloidin-FITC	Sigma (Deisenhofen, Germany)
phospho-myosin light chain antibody	Cell Signaling Technologies (Danvers, USA)
rat anti-mouse IgG-HRP	DAKO (Hamburg, Germany)
RhoA antibody	Cytoskeleton (Denver, USA)
α-tubulin antibody-Alexa 488	Invitrogen (Karlsruhe, Germany)

3.1.2.2 Monoclonal Antibodies (mAbs)

mAbs generated and modified in our laboratory

antibody	isotype	antigen	described in
JAQ1	IgG2a	GPVI	[77]
INU1	IgG1	CLEC-2	[182]
p0p4	IgG2b	GPIbα	[183]
p0p/B	IgG2b	GPIbα	[42]
DOM2	IgG2a	GPV	[183]
p0p6	IgG2b	GPIX	[183]
JON/A	IgG2b	GPIIbIIIa	[184]
JON1	IgG2b	GPIIbIIIa	[183]
ULF1	IgG2a	CD9	[183]
12C6	IgG2b	α2 integrin	unpublished
WUG1.9	IgG1	P-selectin	unpublished

3.1.3 Human serine proteases

coagulation factor XIIaα	Kordia (Leiden, Netherlands)
coagulation factor XIIaβ	Kordia (Leiden, Netherlands)
coagulation factor XIa	Kordia (Leiden, Netherlands)
coagulation factor IXa	Kordia (Leiden, Netherlands)
coagulation factor Xa	Kordia (Leiden, Netherlands)
coagulation factor VIIa	Kordia (Leiden, Netherlands)
thrombin	Kordia (Leiden, Netherlands)
kallikrein	Kordia (Leiden, Netherlands)
plasmin	Kordia (Leiden, Netherlands)
tissue plasminogen activator	Kordia (Leiden, Netherlands)
urokinase plasminogen activator	Kordia (Leiden, Netherlands)
Thromborel S	Dade Behring (Marburg, Germany)

3.1.4 Buffers

All buffers were prepared and diluted in double distilled water (ddH_2O).

- Acid-citrate-dextrose buffer (ACD), pH 4.5

Trisodium citrate dehydrate	85 mM
Citric acid anhydrous	65 mM
Glucose anhydrous	110 mM

- Cacodylate buffer (electron microscopy)

sodium cacodylate (pH 7.2)	50 mM

- Citrate buffer, pH 7.0

Sodium citrate	0.129 M
add H_2O	

- Fixation buffer I (electron microscopy)

Sodium cacodylate, pH 7.2	0.1 M
Glutaraldehyde	2.5%
Formaldehyde	2%

- Fixation buffer II (electron microscopy)

Sodium cacodylate, pH 7.2	50 mM
Osmium tretroxid	2%

- Lysis buffer (DNA isolation)

TRIS base	100 mM
EDTA	5 mM
NaCl	200 mM
SDS	0.2%
add Proteinase K (20 mg/ ml)	100 µg/ml

- Phosphate buffered saline (PBS), pH 7.14

NaCl	137 mM (0.9%)
KCl	2.7 mM
KH2PO4	1.5 mM
Na2HPO4	8 mM

- 50x TAE buffer

TRIS base	0.2 M
Acetic acid	5.7 %
EDTA (0.5 M, pH 8)	10 %

- TE buffer

TRIS base	10 mM
EDTA	1 mM

- Tris-buffered saline (TBS), pH 7.3

NaCl	137 mM (0.9%)
Tris/HCl	20 mM

- Tris-HCl buffer, pH 7.8

Tris-HCl	200 mM
BSA	1%

- Tyrode-HEPES buffer, pH 7.3

NaCl	137 mM (0.9%)
KCl	2.7 mM
$NaHCO_3$	12 mM
NaH_2PO_4	0.43 mM
$CaCl_2$	2 mM
$MgCl_2$	1 mM

HEPES	5 mM
BSA	0.35%
Glucose	0.1%

- Blocking solution for immunoblotting

BSA or fat-free dry milk	5%
in PBS or washing buffer	

- Blotting buffer A for immunoblotting

TRIS, pH 10.4	0.3 M
Methanol	20%

- Blotting buffer B for immunoblotting

TRIS, pH 10.4	25 mM
Methanol	20 %

- Blotting buffer C for immunoblotting

ε-amino-n-caproic acid, pH 7.6	4 mM
Methanol	20%

- Coomassie staining solution

Acetic acid	10%
Methanol	40%
Coomassie Brilliant blue	1 g

- Coomassie destaining solution

Acetic acid	10%
Methanol	40%

- IP buffer

TRIS HCl, pH 8.0	15 mM
NaCl	155 mM
EDTA	1 mM
NaN_3	0.005%

- Laemmli buffer for SDS-PAGE

TRIS	40 mM
Glycine	0.95 M
SDS	0.5%

- PHEM buffer, pH 6.8

PIPES	100 mM
HEPES	5.25 mM
EGTA	10 mM
$MgCl_2$	20 mM

- SDS sample buffer, 2x

β-mercaptoethanol (for reduced conditions)	10%
TRIS buffer (1.25 M), pH 6.8	10%
Glycerine	20%
SDS	4%
Bromophenolblue	0.02%

- Separating gel buffer

TRIS HCl, pH 8.8	1.5 M
add H_2O	

- Stacking gel buffer

TRIS/ HCl, pH 6.8	0.5 M
add H_2O	

- Washing buffer (western blot)

Tween 20	0.1 %
in PBS	

3.1.5 Animals

Specific pathogen free NMRI and C57Bl6/J mice were purchased from Harlan Winkelmann GmbH (Borchen, Germany). Mice with floxed genes of RhoA were kindly provided by Cord Brakebusch (University of Copenhagen, Denmark) and transgenic mice carrying the Cre recombinase under the PF4 promoter (PF4-cre+) were from Radek Skoda (Basel, Switzerland). For the PF4-Cre strategy, these two mice were crossed to receive *RhoA*$^{fl/fl}$/PF4-cre+ mice where gene deletion occurred intrinsically upon activation of the PF4 promoter

during megakaryopoiesis. Littermates (*RhoA*$^{fl/fl}$/PF4-cre- mice) served as controls. The *Gp6*$^{-/-}$ and the *Pld1*$^{-/-}$ mice were generated in our laboratory by Markus Bender and Attila Braun, respectively. For GPVI and CLEC-2 receptor depletion in platelets, NMRI or C57Bl6/J mice were intravenously or intraperitoneally injected with 100 µg of JAQ1 and 200 µg of INU1, respectively. Mice were used for experiments 5 to 6 days after antibody injection.

Animal studies were approved by the district government of Lower Frankonia (Bezirksgerierung Unterfranken).

3.2 Methods

3.2.1 Mouse genotyping

3.2.1.1 Isolation of genomic DNA from mouse ears

An approximately 5 mm^2 piece of the mouse ear was cut and dissolved in 500 µl lysis buffer by overnight incubation at 56℃ under shaking conditions (~900 rpm). 500 µl of a phenol/chloroform mixture were added to the samples which were then vortexed and centrifuged at 14,000 rpm for 10 min at room temperature (RT). 450 µl supernatant were transferred into a new tube containing 500 µl isopropanol. After vigorous shaking, samples were centrifuged at 14,000 rpm for 10 min at 4℃. The resulting DNA pellet was washed twice with ice cold 70% ethanol and centrifuged at 14,000 rpm for 5 min at RT. Finally, the DNA pellet was left to dry and resuspended in 50 µl TE buffer. The genotyping PCR was performed using 1 µl DNA solution.

3.2.1.2 Detection of the *RhoA* floxed allele by PCR

- **Composition of the sample**

1 µl	DNA
2 µl	10x Taq polymerase buffer
0.6 µl	$MgCl_2$ (50 mM)
0.4 µl	dNTPs (10 µM)
0.2 µl	Primer 1 1:10 (stock: 1 µg/µl)
0.2 µl	Primer 2 1:10 (stock: 1 µg/µl)
0.2 µl	Taq polymerase (0.5 U/ml)
14.4 µl	H_2O

- **Primers**

RhoA_for AGC CAG CCT CTT GAC CGA TTT A
RhoA_rev TGT GGG ATA CCG TTT GAG CAT

- **PCR program**

94℃	2:00 min	
94℃	0:30 min	35x
55℃	0:30 min	
72℃	0:30 min	
72℃	10:00 min	
4℃	∞	

- **Band sizes**

  wt: 297 bp

  floxed: 393 bp

3.2.1.3 Detection of the PF4-Cre transgene by PCR

- **Composition of the sample**

1 µl	DNA
2.5 µl	10x Taq polymerase buffer
2.5 µl	$MgCl_2$ (25 mM)
1 µl	dNTPs (10 µM)
1 µl	Primer 1 1:10 (stock: 1 µg/µl)
1 µl	Primer 2 1:10 (stock: 1 µg/µl)
0.5 µl	Taq-Polymerase (0.5 U/ml)
15.5 µl	H_2O

- **Primers**

  PF4-Cre_for CCC ATA CAG CAC ACC TTT TG

  PF4-Cre_rev TGC ACA GTC AGC AGG TT

- **PCR program**

95℃	5:00 min	
95℃	0:30 min	35x
58℃	0:30 min	
72℃	0:45 min	
72℃	5 min	
4℃	∞	

- **Band sizes**

  wt: no PCR product

  PF4-cre+ 450 bp

3.2.2 *In vitro* analysis of platelet function

3.2.2.1 Platelet isolation and washing

Mice were bled under isofluran anesthesia from the retroorbital plexus. 700 µl blood were collected into a 1.5 ml tube containing either 300 µl heparin in TBS (20 U/ml, pH 7.3) or ACD buffer (pH 4.5). Blood was centrifuged at 1,800 rpm (Eppendorf 5415C) for 5 min at RT.

Supernatant and buffy coat were transferred into a new tube and centrifuged at 800 rpm for 6 min at RT to obtain platelet rich plasma (prp). To prepare washed platelets, prp was centrifuged at 2,500 rpm for 5 min at RT in the presence of prostacyclin (PGI_2) (0.1 µg/ml) and apyrase (0.02 U/ml). The resulting pellet was resuspended in 1 ml Ca^{2+}-free Tyrode's buffer, containing PGI_2 (0.1 µg/ml) and apyrase (0.02 U/ml) and left to incubate at 37℃ for 10 min. After a second washing step, the platelet pellet was resuspended in Tyrode's buffer containing apyrase (0.02 U/ml) and left to incubate for at least 30 min at 37℃ before analysis.

3.2.2.2 Platelet counting

For determination of platelet counts and size, 50 µl blood were drawn from the retroorbital plexus of anesthetized mice using siliconized microcapillaries and collected in a 1.5 ml tube containing 300 µl heparin in TBS (20 U/ml, pH 7.3). Platelet counts and size were determined using a Sysmex KX-21N automated hematology analyzer (Sysmex Corp., Kobe, Japan).

3.2.2.3 Western blotting

For western blot analysis, prp was prepared as described in section 3.2.2.1. Prp was centrifuged at 1500 rpm for 5 min and platelets were washed twice in PBS + 5 mM EDTA. The final platelet pellet was resuspended in IP buffer containing protease inhibitors and 1% NP40 to a final concentration of at least $0.5x10^6$ platelets/µl. After an incubation step of 20 min at 4℃ and centrifugation at 14,000 rpm for 5 min, the supernatant was mixed with an equal amount of 2x SDS sample buffer and boiled at 95℃ for 5 min. Samples were separated by 12 or 15% SDS-PAGE and transferred onto a polyvinylidene difluoride (PVDF) membrane. To prevent non-specific antibody binding, membranes were blocked in 5% fat-free milk or 5% BSA dissolved in washing buffer for 2 h at RT or over night (o/n) at 4℃. Membranes were incubated with the required primary antibody (5 µg/ml) o/n at 4℃ by gentle shaking. Afterwards membranes were washed three times with washing buffer for 15 min at RT under shaking conditions. Then, membranes were incubated with appropriate HRP-labeled secondary antibodies for 1 h at RT. After three washing steps, proteins were visualized by ECL.

3.2.2.4 Flow cytometric analysis

To determine glycoprotein expression levels, platelets ($1x10^6$) were stained for 15 min at RT with saturating amounts of fluorophore-conjugated antibodies described in section 3.1.2.2, and analyzed directly after addition of 500 µl PBS. For activation measurements, platelets were stimulated with different agonists in the presence of saturating amounts of the

phycoerythrin (PE)-coupled JON/A and the fluorescein isothiocyanate (FITC)-coupled anti-P-selectin antibody for 5 min at 37℃ and additional 5 min at RT. The reaction was stopped by addition of 500 µl PBS and the samples were analyzed on a FACSCalibur (Becton Dickinson, Heidelberg, Germany). For a two-colour staining, the following settings were used:

Detectors/Amps:

Parameter	Detector	Voltage
P1	FSC	E01
P2	SSC	380
P3	Fl1	650
P4	Fl2	580
P5	Fl3	150

Threshold:

Value	Parameter
253	FSC-H
52	SSC-H
52	Fl1-H
52	Fl2-H
52	Fl3-H

Compensation:

Fl1	2.4% of Fl2
Fl2	7.0% of Fl1
Fl2	0% of Fl3
Fl3	0% of Fl2

3.2.2.5 Aggregation

For aggregation studies, washed platelets were adjusted to a concentration of 1.5×10^8 platelets/ml with Tyrode's buffer. Alternatively, prp from heparinized blood was diluted 1:3 in Tyrode's buffer. Agonists were added (100-fold concentrated) and light transmission was recorded over 10 min on an Apact 4-channel optical aggregation system (APACT, Hamburg, Germany). As calibration before each measurement, Tyrode's buffer (for washed platelets) or 1:3 diluted plasma (for prp) was set as 100% aggregation and washed platelet suspension or prp was set as 0% aggregation. Measurements with washed platelets (except for thrombin-induced aggregation) were performed in the presence of Tyrode's buffer containing 100 µg/ml fibrinogen.

3.2.2.6 Aggregation + ATP release

Washed platelets were adjusted to a concentration of 5 x 10^8 platelets/ml with Tyrode's buffer and further diluted 1:3 in Tyrode's buffer containing 100 µg/ml fibrinogen (except for measurements with thrombin). For ATP release measurements, 25 µl Chrono-Lume reagent was added to the platelet suspension and incubated for 2 min at 37°C before addition of agonists (50-fold concentrated). Subsequent ATP release and increase in light transmission was recorded using a Chrono-Log 4-channel aggregation system (Probe & go, Osburg, Germany). Calibration for the aggregation measurement was performed as mentioned above (section 3.2.2.5). An ATP-standard solution was used as calibrator to determine the concentration of agonist-induced ATP release.

3.2.2.7 Intracellular Calcium-measurements

Washed platelets at a concentration of approximately 5x10^8 platelets/ml in Ca^{2+}-free Tyrode's buffer were loaded with fura-2 AM (5 µM) in the presence of Pluronic F-127 (0.2 µg/ml) for 30 min at 37°C. After labeling, platelets were washed once and resuspended in Tyrode's buffer without Ca^{2+} (for measurement of store release). Stirred platelets were activated with different agonists and fluorescence was measured with a PerkinElmer LS 55 fluorimeter (Massachusetts, USA). Excitation was alternated between 340 and 380 nm, and emission was measured at 509 nm. Each measurement was calibrated using 1% Triton X-100 and EGTA.

3.2.2.8 Determination of platelet filamentous (F)-actin content

Washed platelets were prepared and the platelet count was adjusted to approximately 2x10^5 platelets/µl in Tyrode's buffer without Ca^{2+}. Platelets were diluted 1:10 in Tyrode's buffer in a final volume of 50 µl per sample and incubated for 3 min at 37°C after addition of 5 µl Dylight 649-conjugated anti-GPIX Ig derivative. Then, platelets were stimulated with 1 U/ml thrombin (final concentration) for 2 min at 37°C (400 rpm) and fixed for 10 min by addition of 0.55% volume 10% PFA in PBS. Samples were finally centrifuged for 5 min at 2500 rpm, the pellet was resuspended in 55 ml Tyrode´s buffer containing 0.1 volume % Triton-X 100 and 50 µl were mixed with phalloidin-FITC at a final concentration of 10 µM. Samples were incubated 30 min at RT in the dark and the reaction was stopped by addition of 500 µl PBS. After centrifugation for 5 min at 2500 rpm and the pellet was resuspended again in 500 µl PBS. Samples were immediately analyzed on a FACSCalibur.

3.2.2.9 Clot retraction

For Clot retraction studies, platelets were adjusted to a concentration of $3x10^8$ platelets/ml in platelet poor plasma (ppp). 250 µl of the platelet suspension was mixed with 1.5 µl erythrocyte suspension (to contrast the clot), obtained during platelet isolation from whole blood, and 20 mM $CaCl_2$. Clotting was induced by addition of high thrombin concentrations (3 U/ml). Subsequent clot retraction was monitored at 37℃ under non-stirring conditions and recorded with a digital camera over time.

3.2.2.10 Static adhesion on human fibrinogen

Rectangular glass coverslips (Roth, Karlsruhe, Germany) were coated with 100 µg human fibrinogen (diluted in PBS) overnight at 4℃ under humid conditions and blocked for 2 h at RT with 1% BSA in PBS. The coverslips were rinsed with Tyrode´s buffer and 100 µl thrombin-stimulated (0.001 U/ml) washed platelets (0.03×10^6 platelets/µl) were immediately added and incubated at RT for the indicated time periods. The coverslips were rinsed again with Tyrode´s buffer and platelets were visualized with an Axiovert 200M inverted microscope (Zeiss, Göttingen, Germany) at 100x magnification using differential interference contrast (DIC) microscopy. Representative images were taken and evaluated according to different platelet spreading stages.

3.2.2.11 Adhesion under flow conditions

3.2.2.11.1 Flow adhesion assay on collagen

Coverslips (24 x 60 mm) were coated with 200 µg/ml fibrilar type-I collagen (Horm) overnight at 37℃ and blocked for 1 h with 1% BSA. Blood (700 µl) was collected into 300 µl heparin (20 U/ml in TBS, pH 7.3) and diluted 2:1 with Tyrode´s buffer. For flow adhesion studies under non-coagulated conditions, blood was taken 1:10 into citrate buffer (129 mM; pH 7.0). Platelets were labeled with a Dylight-488 conjugated anti-GPIX Ig derivative (0.2 µg/ml) for 5 min at 37℃ and blood was finally filled into a 1 ml syringe. Perfusion studies were performed as follows. Transparent flow chambers with a slit depth of 50 µm, equipped with the coated coverslips, were connected to the syringe filled with the diluted whole blood. Perfusion was performed using a pulse-free pump under high shear stress equivalent to a wall shear rate of 1000 sec^{-1}, 1700 sec^{-1} or 7700 sec^{-1} (5 min, 4 min or 2 min, respectively). Thereafter, coverslips were washed by a 1 to 4 min perfusion with Tyrode's buffer at the same shear stress and phase-contrast and fluorescent images were recorded from at least five different microscope fields (40x objective). Image analysis was performed off-line using MetaMorph® software (Visitron, Munich, Germany). Thrombus formation was expressed as

the mean percentage of total area covered by thrombi, and as the mean integrated fluorescence intensity per mm^2.

3.2.2.11.2 Flow adhesion assay on vWF

Coverslips were coated with 200 µl rabbit anti-human vWF antibody (1:500, diluted) over night at 37°C and rinsed with Tyrode`s buffer. After blocking with 1% BSA for 1 h at 37°C, coverslips were rinsed again and incubated with 200 µl mouse plasma for 2 h at 37°C. Blood preparation and subsequent perfusion studies were performed as described in section 3.2.2.11.1. Platelet adhesion on vWF was determined by counting the platelet number per visual field.

3.2.3 Coagulation and fibrinolysis assays

3.2.3.1 Preparation of mouse plasma

Anesthetized mice were bled and 720 µl blood were collected into a 1.5 ml tube containing 80 µl citrate buffer. Blood was centrifuged at 2500 rpm for 5 min at RT and supernatant was transferred into a new tube. After a second centrifugation step at 10,000 rpm for 5 min at RT, supernatant containing pure plasma was used for experiments.

3.2.3.2 Determination of aPTT and PT

Activated partial thromboplastin time (aPTT) and prothrombin time (PT) of standard human plasma (SHP), mouse and rat plasma was determined using standard methods according to the manufacturer´s protocol. (Siemens Healthcare, Erlangen, Germany). These assays have been performed in the laboratory of Stefan Schmidbauer, CSL Behring Marburg, Germany).

3.2.3.3 Chromogenic assays

rHA-Infestin-4 was incubated at different concentrations with pure human serine proteases (FXIIaα, FXIIaβ, FXIa, FIXa, FVIIa, FXa, thrombin, kallikrein, plasmin, tPA and urokinase, respectively) for 10 min at 37°C in a 96-well plate (total volume 160 µl). Tris-HCl buffer, pH 7.8 was used for all required dilutions. A specific chromogenic substrate (40 µl, 2-4 mM) for the respective protease was added and incubated for a defined time period according to the protease activity. The reaction was stopped by acetic acid (20%) and absorption was measured at 405 nm on an ELISA reader a Multiskan EX (Thermo Scientific, Waltham, USA). Additionally, different concentrations of rHA-Infestin-4 were incubated with FXIIaα and FXIa, respectively, for 3 h at 37°C in the presence of the macromolecular chromogenic substrate Casein-Resorufin. The reaction was stopped by trichloroacetic acid and absorption

was measured at 574 nm. The amount of active protease was calculated against a standard curve.

3.2.3.4 D-Dimer concentration measurements

Pooled mouse plasma (100 µl) was incubated with vehicle (PBS) or rHA-Infestin-4 (0.1/1/10 mg/ml) for 2 min at 37℃. Clot formation was induced using Thromborel S (200 µl) according to the manufacturer's instructions and samples were left for 1 h at 37℃. Fibrinolysis was stopped by addition of 4.5 µl HCl (1:1) and samples were neutralized by 25 µl NaOH (1 M) and centrifuged at 14,000 rpm for 5 min at RT. D-Dimer concentration in the supernatant was finally determined with an ELISA kit (Asserachrom, Roche) according to the manufacturer's instructions.

3.2.4 *In vivo* murine models

3.2.4.1 Determination of platelet life span

Mice were injected intravenously with a Dylight-488 conjugated anti-GPIX Ig derivative (0.5 µg/g body weight). 1 h after injection (day 0), as well as at the other indicated time points, 50 µl blood were collected and the percentage of GPIX-positive platelets was determined by flow cytometry.

3.2.4.2 $FeCl_3$-induced thrombus formation in small mesenteric arterioles

3- to 4-wk-old mice were anesthetized with 2,2,2-tribromoethanol (450 µg/g body weight). After a midline abdominal incision, 35-60-µm-diameter arterioles were gently exteriorized and visualized at 10x magnification with an inverted microscope (Axiovert 200; Zeiss, Göttingen, Germany) equipped with a 100-W mercury lamp (HBO) and a CoolSNAP-EZ camera (Visitron, Munich, Germany). Endothelial damage was induced by topical application of a 3 mm^2 filter paper saturated with 20% $FeCl_3$. Digital images were recorded and analyzed offline using MetaMorph® software. Adhesion and thrombus formation of fluorescently labeled platelets (DyLight 488-conjugated anti-GPIX Ig derivate) were recorded for 40 min or until complete occlusion of the vessel (blood flow stopped for >1 min) occurred.

3.2.4.3 Mechanical injury of the abdominal aorta

The abdominal cavity of anesthetized mice was opened with a longitudinal incision to expose the abdominal aorta. An ultrasonic flowprobe (0.5PSB699, Transonic Systems, New York, USA) was placed around the vessel and thrombus formation was induced by a single firm compression with a forceps upstream of the flowprobe. Blood flow was monitored for 30 min.

3.2.4.4 Carotid artery thrombosis model

Mice were anesthetized and the left carotid artery was exposed through a vertical midline incision in the neck. Thrombus formation was induced by a filter paper saturated with a $FeCl_3$ solution at the indicated concentration and placed on the carotid artery for a defined period. Blood flow was monitored using an ultrasonic flow probe (Transonic System, New York, USA) until complete vessel occlusion occurred or for 30/60 min.

3.2.4.5 Bleeding time assays

Mice were anesthetized with a triple anesthesia (medetomidine 0.5 µg/g, midazolam 5 µg/g and fentanyl 0.05 µg/g body weight) and a 2 mm segment of the tail tip was removed with a scalpel. Tail bleeding was monitored by gently absorbing blood with filter paper at 20 second intervals, without directly contacting the wound site. When no blood was observed on the paper, bleeding was determined to have ceased. Alternatively, the tail was immediately immersed in 0.9% isotonic saline at 37°C and the bleeding time was defined as time until cessation of blood flow. Experiments were stopped in each case after 20 min.

3.2.4.6 Transient occlusion model of the middle cerebral artery

Analyses were conducted according to the published recommendations for research in mechanism-driven basic stroke studies[185]. Transient middle cerebral artery occlusion (tMCAO) was induced under inhalation anesthesia using the intraluminal filament (6021PK10; Doccol Company) technique[186]. After 60 min, the filament was withdrawn to allow reperfusion. For determination of ischemic brain volume, mice were sacrificed 24 h after induction of tMCAO and brain sections were stained with 2% 2,3,5-triphenyltetrazolium chloride (TTC; Sigma-Aldrich). Brain infarct volume was calculated and corrected for edema as described 24 h after tMCAO Neurological function was analyzed by two independent and blinded investigators. Global neurological status was scored according to Bederson *et al.*[187]. Motor function and coordination were graded using the grip test[188]. This model was performed by Christoph Kleinschnitz in the group of Prof. Guido Stoll, Department of Neurology, University Clinic, Würzburg, Germany.

3.2.5 Statistics

Statistical evaluation was performed using the Welch's test. Results are indicated as mean ± SD of at least three individual experiments. If appropriate, the Fisher`s exact test was used. Data of Bederson score and grip test in the rHA-Infestin-4 study were analyzed with the Mann-Whitney U test. P-values <0.05 were considered statistically significant.

3.2.6 Electron microscopy

3.2.6.1 Transmission electron microscopy (TEM) of platelets in suspension

Washed platelets were adjusted to a concentration of $3x10^8$ platelets/ml in Tyrode's buffer. Platelets in a resting state or activated with 0.01 µM U46619 were fixed by addition of an equal amount of cacodylate buffer containing 5% glutaraldehyde for 10 min at 37°C without stirring. For complete fixation, samples were incubated for 1 h at RT and afterwards stored at 4°C until further processing. A small amount of the sample was further diluted to 1:10 in cacodylate buffer and washed three times by addition of 1 ml cacodylate buffer and subsequent centrifugation for 5 min at 1,000 x g (RT). Platelets were then left to adhere for 1 h on poly-lysine-coated coverslips and processed for scanning electron microscopy (see 3.2.6.2). The remaining samples were washed three times for 5 min by addition of 1 ml cacodylate buffer and subsequent centrifugation for 5 min at 1,500 x g (37°C). A 2% low melting agarose solution in cacodylate buffer was prepared and kept at 45°C. After the final washing step, platelets were resuspended carefully in 1 ml agarose solution and immediately centrifuged for 5 min at 14,000 rpm (37°C). The agarose solution was discarded except 100 µl and samples were incubated on ice for 10 min. The hardened agarose pellets were cut out of the tubes and the platelet pellets were cut into approximately 1 mm^2 pieces and stored in cacodylate buffer. Samples were fixed in cacodylate buffer containing 1% OsO_4 for 45 min - 1 h at RT, washed twice with ddH_2O and incubated for 1 h at 4°C in 2% uranylacetate in ddH_2O. After three washing steps with ddH_2O, samples were dehydrated in 70% (4x5 min), 95% (3x15 min) and 100% (3x15 min) ethanol. Next, samples were incubated in 100% propylenoxyde (2x10 min) and then in a 1:1 mixture of propylenoxyde and epon for 1 h under rotating conditions. After 2 further incubations in epon at RT (first step: o/n, second step: 2-3 h) samples were embedded in gelatine capsules and left to dry for 48 h at 60%. 50 nm thin sections were cut using a Leica Ultracut microtom UCT (Leica Microsystems, Wetzlar, Germany), contrasted and analyzed on an FEI electron microscope (Phillips, Hillsboro, USA). This method was performed by Irina Pleines in the group of Prof. Bernhard Nieswandt.

3.2.6.2 Scanning electron microscopy (SEM) of platelets

For immobilization and visualization of platelets fixed in suspension, coverslips were coated with 0.01% poly-lysine for 15 min at RT and left to dry o/n at RT. Fixed platelets (see 3.2.6.1) were left to adhere for 20 min - 1h and further processed as described below.

For static adhesion, roundish coverslips (12 mm diameter) were coated with 100 µg/ml human fibrinogen in PBS for 2 h at RT, blocked for 1 h with 1% BSA in PBS and shortly washed with PBS. Washed platelets were adjusted to a concentration of $3x10^4$ platelets/µl

and activated with 0.01 U/ml thrombin. 100 µl of this suspension were immediately added to the coverslips and incubated at 37℃ for the indicated time points. Samples were fixed by addition of 300 µl cacodylate buffer containing 2.5% glutaraldehyde for 1 h at 37℃, 1 h at RT and kept at 4℃ until further processing. Coverslips were washed twice with 200 µl cacodylate buffer and dehydrated in 70% (4x5 min), 80% (1x5 min), 95% (1x5 min) and 100% (2x30 min) ethanol. The coverslips were then incubated with increasing concentrations of hexomethyldizilasin (HMDS) in 100% ethanol (25%: 1x 5 min; 50%: 1x5 min; 75%: 1x5 min and 100%: 2x5 min). Samples were left to dry, sputtered with gold using a Cressington Sputter Coater 108 Auto and a 0.2 µm thin gold foil (both from Cressington, Chalk Hill, England) and analyzed using a FEI electron microscope (Phillips, Hillsboro, USA). This method was performed by Irina Pleines in the group of Prof. Bernhard Nieswandt.

3.2.7 Fluorescence microscopy of platelets

3.2.7.1 Staining of spread platelets for confocal microscopy

Washed platelets were activated with 0.01 U/ml and immediately put on a fibrinogen-coated coverslip as described in section 3.2.2.10. After 40 min, fully spread platelets were fixed in PHEM buffer containing 4% PFA and 10% NP40 for 20 min at 4℃ and blocked with 5% BSA in PBS for 2 h at 37℃. Samples were washed with PBS and stained with mouse anti α-tubulin-Alexa 488 antibody (1:100) and phalloidin-atto647N (1:300) for 1 h in the dark at 37℃. Then, samples were washed again with PBS, mounted using Vectashield mounting medium and finally left to dry o/n at 4℃. Samples were visualized on a Leica SP5 confocal microscope with a 100x oil objective (Leica Microsystems, Mannheim, Germany).

3.2.7.2 Stimulated Emmision Depletion (STED) microscopy of spread platelets

Spread platelets were prepared and stained as described in sections 3.2.2.10 and 3.2.7.1. Samples were analyzed on a STED-Leica SP5 microscope (Leica Microsystems, Mannheim, Germany). This method was performed by Shuchi Gupta in the group of Prof. Bernhard Nieswandt.

3.2.8 Histology

3.2.8.1 Preparation of paraffin sections

A piece of the abdominal aorta was cut around the injury site at the end of the perfomed thrombosis model (see 3.2.4.3) and immediately fixed in PBS 4% PFA o/n. Afterwards, organs were washed 3 times with PBS and directly dehydrated and embedded in paraffin. Organs were cut using a Microm Cool Cut microtom (Thermo Scientific, Braunschweig, Germany) to prepare 5 µm thin sections.

3.2.8.2 Hematoxylin/eosin staining of paraffin sections

Sections were deparaffinated by two incubation steps in Xylol (3 min each). Rehydration was carried out using decreasing ethanol concentrations (100, 96, 90, 80 and 70%) with 2 incubation steps in each solution and a final incubation of 2 min in ddH_2O. Sections were then stained for 2 min with hematoxylin, followed by a 10 min washing step using running tab water and 2 min staining with 0.05% Eosin G. The sections were washed shortly and dehydration was carried out using the same ethanol concentrations and incubation times as described above in reversed order. Finally, sections were incubated twice in Xylol for 3 min each, dried and mounted onto an object plate with Eukitt mounting medium. Samples were analyzed using a Leica DHI 4000B inverse microscope equipped with a Leica digital camera (Leica Microsystems, Wetzlar, Germany).

4 RESULTS

4.1 Relevance of the GPIbα-vWF interaction and downstream signaling in thrombus formation

Initiation of thrombus formation at sites of vascular damage involves platelet recruitment to the exposed ECM, a process that is mediated by the platelet receptor GPIb-V-IX complex. Its essential role for arterial thrombus formation has been impressively demonstrated using $FeCl_3$-induced injury models in mice lacking the functional extracellular domain of GPIbα or a binding site for the signaling molecule 14-3-3ξ in the C-terminus of the molecule[43,44,189]. In contrast, vWF, the main ligand of GPIbα, has been shown to be less but still significantly important for arterial thrombosis in the same injury model[173,175], however essential for platelet tethering after mechanical injury of the carotid artery[42]. Interestingly, the use of *vWF*$^{-/-}$ mice and Fab fragments of the GPIbα blocking antibody p0p/B revealed that the interaction of GPIbα and vWF is a major pathophysiological mechanism underlying stroke development[45,46].

Since the role of GPIbα and vWF in thrombus formation has previously been analyzed, this part of the present study assessed the effect of p0p/B Fab fragments in commonly used $FeCl_3$- and mechanically induced thrombosis models to initially characterize the reliability and comparability of these *in vivo* models when performed in our laboratory.

4.1.1 Targeting of GPIbα protects mice from arterial thrombosis, but causes a hemostatic defect

Wild-type mice were intravenously injected with 100 µg p0p/B Fab fragments 30 min prior to vascular injury to specifically block the vWF-binding site on GPIbα. These mice were first challenged in a model of $FeCl_3$-induced endothelial damage in small mesenteric arterioles and intravital microscopy of fluorescently labeled platelets was used to visualize subsequent platelet adhesion and aggregation. In all wild-type mice, first thrombi >10 µm in diameter formed within 6.4 ± 1.6 min after injury and expanded to full vessel occlusion in 8 out of 9 arterioles (mean time to occlusion 16.7 ± 4.4 min; Figure 5A,B). In line with data obtained in *vWF*$^{-/-}$ mice[173], beginning of thrombus formation was significantly delayed in p0p/B Fab fragment-treated mice (10.6 ± 2.0 min; $p<0.05$) and further thrombus growth was clearly decelerated and finally arrested leaving a small open channel in 8 out of 9 vessels (Figure 5A,B). This defect could be ascribed to the permanent release of single platelets from the thrombus surface which became maximal when the thrombus reached ~50 to 90% of the vessel diameter (mean vessel stenosis 77.6 ± 16.5% for p0p/B Fab fragment-treated mice and 97.3 ± 8.6% for wild-type mice; $p<0.01$; Figure 5C). These data clearly confirmed that in

this experimental setting the GPIbα-vWF interaction only partially contributes to the adhesion of platelets to the injury site but is essential for platelet incorporation into a growing thrombus, particularly under conditions of very high-shear.

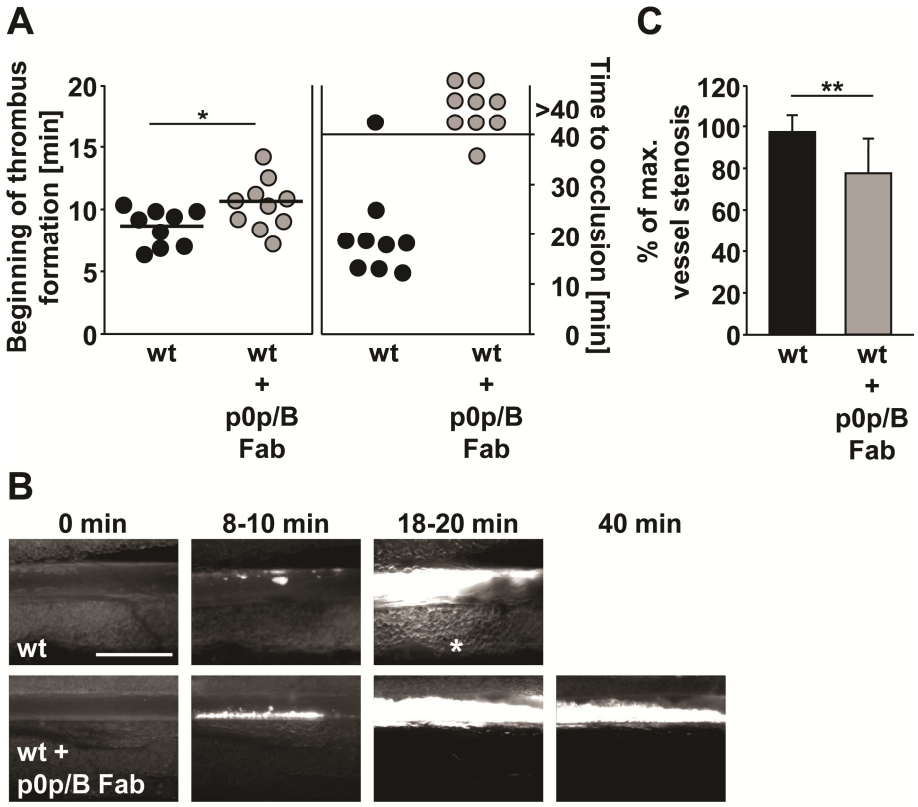

Figure 5. Defective $FeCl_3$-induced thrombus formation in mice treated with Fab fragments of a GPIbα blocking antibody. Mesenteric arterioles were injured by application of $FeCl_3$ and thrombus formation was monitored using intravital fluorescence microscopy. Mice were i.v. injected with vehicle or 100 µg p0p/B Fab fragments 30 min prior to injury. A, Time to beginning of thrombus formation (left) and to stable vessel occlusion (right) are shown. Horizontal lines indicate mean values. Each symbol represents one arteriole. B, Representative pictures acquired at the indicated time points/intervals. Bar, 50 µm. Asterisk indicates vessel occlusion. C, Percentage of maximal thrombus-caused vessel stenosis is illustrated. *, $p<0.05$; **, $p<0.01$. p0p/B Fab indicates p0p/B Fab fragments.

Additionally, mice injected with 100 µg p0p/B Fab fragments were analyzed in an arterial thrombosis model where the abdominal aorta was injured by a single tight compression with a forceps. An ultrasonic perivascular Doppler flowprobe was used to monitor thrombus formation. Under these conditions, all wild-type vessels irreversibly occluded (7/7) after 280 ± 107 sec. However, although blood flow initially declined in most of the p0p/B Fab fragment-treated mice similar to wild-type, indicating beginning of thrombus formation, it remained rather constant at this level for the rest of the observation period (Figure 6A,B). Consequently, none of these vessels occluded, demonstrating that functional GPIbα is crucial for occlusive arterial thrombus formation also under these experimental conditions.

To test whether GPIbα blockage also impairs hemostasis, a tail bleeding time assay was performed. The tail tip of anesthetized mice was removed 30 min after injection of 100 µg

p0p/B Fab fragments and time until cessation of blood loss was determined using the filter paper method. Whereas bleeding stopped in 11 out of 12 (92%) wild-type mice within 12 min (mean bleeding time 436 ± 178 sec; Figure 6C), only 5 out of 15 (33%) of the p0p/B Fab fragment-treated mice could arrest bleeding while the rest bled for >20 min ($p<0.01$; Figure 6C). All together, these findings support previously published data and emphasize the importance of the GPIbα-vWF interaction in thrombosis and hemostasis.

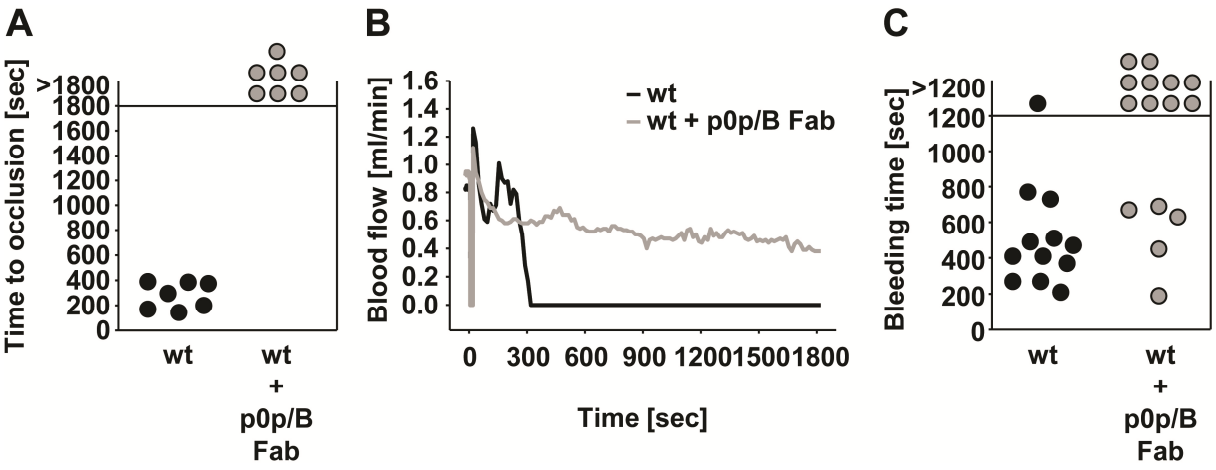

Figure 6. Blockage of GPIbα results in protection from mechanically induced thrombosis and in prolonged bleeding times. The abdominal aorta was injured by one firm compression with a forceps 30 min after injection of either vehicle or p0p/B Fab fragments (100 µg i.v.). Thrombus formation was monitored by blood flow measurements. A, Time to vessel occlusion and B. representative curves of the blood flow after injury are shown. C, Tail bleeding times of vehicle-treated and p0p/B Fab fragment-injected wt mice. Each symbol represents one individual. p0p/B Fab indicates p0p/B Fab fragments.

4.1.2 Phospholipase D1 is a critical mediator of shear-dependent thrombus formation downstream of GPIb

The role of PLC isoforms as essential intracellular signaling proteins during platelet activation is well established. In contrast, the specific function of PLD in platelets has been elusive. Platelets express two PLD isoforms, PLD1 and PLD2 which are known to produce PA and translocate to the plasma membrane upon platelet activation[58]. To elucidate the relevance of the PLD1 isoform for platelet physiology and thrombus formation, constitutive knockout mice for PLD1 were generated and analyzed in our laboratory. *In vitro* studies with these mice were mainly performed by Margitta Elvers and David Stegner in our group.

Pld1$^{-/-}$ mice displayed normal platelet counts and only slightly increased platelet size which was accompanied with a small increase in the expression levels of some prominent surface receptors, indicating that PLD1 is dispensable for megakaryopoiesis and platelet production[190]. The ability of these platelets to become activated in response to agonists was determined by flow cytometric measurements of fibrinogen-binding to the activated integrin αIIbβ3 and α-degranulation-dependent P-selectin exposure. Binding of fibrinogen

after stimulation with low doses of CRP or PAR-4 activating peptide was significantly reduced in *Pld1*$^{-/-}$ platelets compared to wild-type but unaltered when high agonist concentrations were used. Moreover, this activation defect could be ascribed to the lack of PLD1-generated PA[190]. Interestingly, and contrary to a previous hypothesis[191], agonist-induced dense-granule release, and also α granule release was not affected[190]. These findings suggested that PLD1 acts as a signaling mediator contributing to integrin αIIbβ3 activation downstream of G protein and ITAM-coupled receptors after submaximal stimulation.

4.1.2.1 *Pld1*$^{-/-}$ platelets fail to form stable aggregates on collagen under flow conditions

Under physiological conditions, platelet adhesion and aggregation occur in the flowing blood where shear forces strongly influence platelet functions. To analyze the functional consequence of the aforementioned impaired integrin activation in this setting, the ability of *Pld1*$^{-/-}$ platelets to form thrombi on a collagen-coated surface at different shear rates was tested in a whole-blood perfusion system. At low (150 sec^{-1}) and intermediate (1000 sec^{-1}) shear rates, which resemble venous or arterial flow conditions, respectively, no alterations in initial platelet adhesion or in aggregate formation on collagen were detectable between *Pld*$^{-/-}$ and wild-type platelets (Figure 7A). Remarkably, however, *Pld1*$^{-/-}$ platelets displayed strongly reduced thrombus stability under high shear rates (1700 sec^{-1}) which mimics flow conditions in small arterioles. Although, *Pld1*$^{-/-}$ platelets normally adhered to the collagen fibers and formed large thrombi covering a comparable surface area as wild-type platelets during the perfusion time (mean surface coverage 48.2 ± 15.8% for *Pld1*$^{-/}$ mice and 56.8 ± 9.7% for wild-type mice, p=0.77; Figure 7A, bottom left), all thrombi of *Pld1*$^{-/-}$ platelets disintegrated during the following washing period. Consequently, virtually no aggregates remained on the surface and only a monolayer of adherent platelets was detectable at the end of the perfusion experiment (relative thrombus volume 0.9 ± 0.6 for *Pld1*$^{-/}$ mice and 3.7 ± 1.3 for wild-type mice; p<0.01; Figure 7A, bottom right). These results demonstrated that PLD1 is required for thrombus stabilization at high, but not at intermediate and low shear rates, suggesting defective shear-dependent GPIb-mediated signaling in *Pld1*$^{-/-}$ platelets.

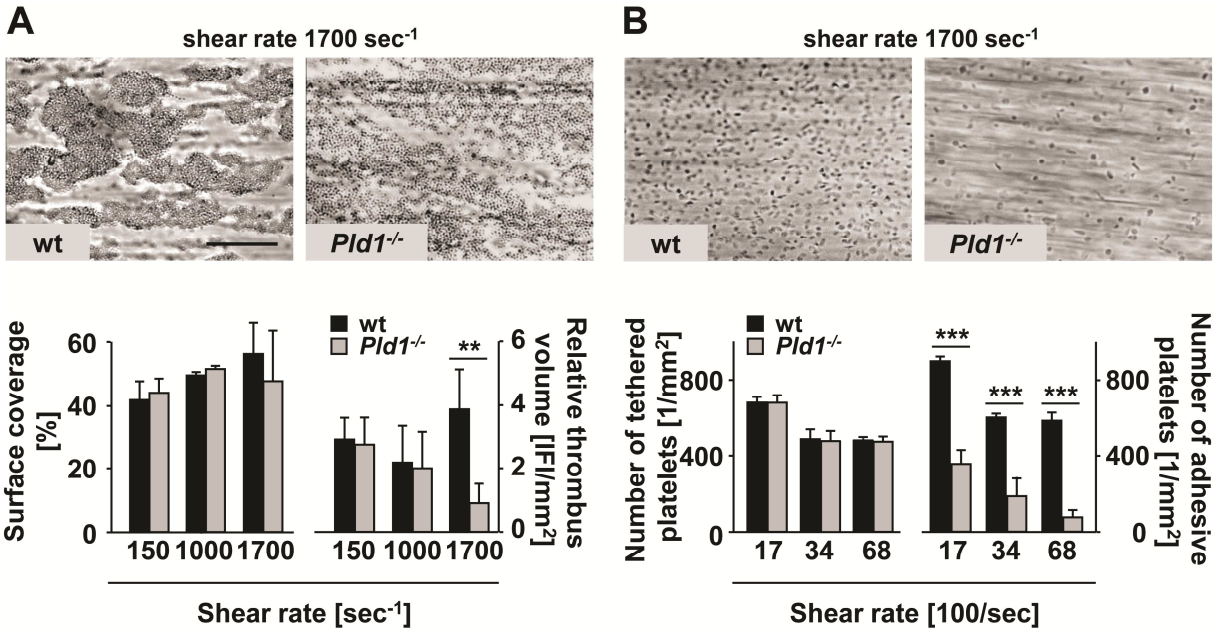

Figure 7. *Pld1*$^{-/-}$ platelets fail to form stable aggregates on collagen and to adhere on vWF under high shear conditions. Whole blood of wt and *Pld1*$^{-/-}$ mice was perfused over a collagen-coated (A) and a vWF-coated (B) surface at the indicated shear rates and then washed with Tyrode`s buffer for a period equal to the perfusion time. A, Representative phase contrast images at the end of the perfusion and washing period (top). Bar, 100 µm. Mean surface coverage (bottom, left) and relative thrombus volume expressed as integrated fluorescence intensity (IFI) per mm^2 (bottom, right) ± SD of 6 mice per group are shown. B, Representative phase contrast images at the end of the washing period (top). Number of platelets were counted 100 sec after beginning of blood perfusion (bottom, left) and at the end of the washing period (bottom, right). Values are mean ± SD of 6 mice per group. **, p<0.01; ***, p<0.001. (Elvers. *et al.*, *Sci.Signal.,*2010)[190].

4.1.2.2 PLD1-deficient platelets display defective adhesion on vWF under flow conditions

To directly investigate a possible role of PLD1 in GPIb-dependent interaction of platelets with vWF, adhesion of *Pld1*$^{-/-}$ platelets on immobilized vWF under high shear conditions was analyzed in a flow chamber system. In this experimental setting, thrombogenic collagen which drives platelet activation is absent and thus a shift from transient to stable platelet adhesion is exclusively dependent on integrin αIIbβ3 activation triggered by vWF-occupied GPIb[192]. At all tested shear rates, wild-type platelets rapidly attached to the immobilized murine vWF and in part firmly adhered to the surface (Figure 7B). In contrast, whereas the initial tethering of *Pld1*$^{-/-}$ platelets was unaltered compared to wild-type platelets, transition to firm adhesion was defective, resulting in strongly reduced numbers of *Pld1*$^{-/-}$ platelets detectable on the surface at the end of the experiment (Figure 7B). This defect could be observed at all tested shear rates but was most profound at very high shear rates (3400 and 6800 sec^{-1}), resembling flow conditions in small arterioles and stenosed arteries. These results indicated that PLD1 might be involved in GPIb-mediated integrin αIIbβ3 activation under flow.

4.1.2.3 PLD1-deficient mice are protected from occlusive arterial thrombus formation

In a next step, the relevance of the so far described functional defects in *Pld1*$^{-/-}$ platelets for *in vivo* thrombus formation was assessed in two different arterial thrombosis models. In the first model, thrombosis was induced by mechanical injury of the abdominal aorta and blood flow was subsequently monitored using an ultrasonic flow probe. In all wild-type vessels blood flow progressively decreased to complete and irreversible vessel occlusion within 12 min after injury (mean time to occlusion 444 ± 174 sec; Figure 8A,B). In contrast, blood flow irreversibly stopped in only 20% (2/10) of *Pld1*$^{-/-}$ mice during the observation period of 30 min ($p<0.001$; Figure 8A,B). In 30% of *Pld1*$^{-/-}$ mice no vessel occlusion occurred, and although in 50% of *Pld1*$^{-/-}$ mice blood flow declined similar to wild-type, vessels were only occluded for <1 min and then completely recanalized (Figure 8A,B).

To confirm these findings, mice were challenged in a second arterial thrombosis model in which the right carotid artery was injured by topically applied $FeCl_3$ (15%). Blood flow was again monitored with an ultrasonic flow probe. Whereas in all wild-type vessels (8/8) full occlusion occurred within 14 min (mean time to occlusion 538.9 ± 255.6 sec) and persisted in all animals except one (87.5%) for the rest of the observation period, vessel occlusion occurred in only 2 out of 7 *Pld1*$^{-/-}$ mice (28.6%). However, this occlusion was only transient and consequently all vessels of *Pld1*$^{-/-}$ mice remained open until the end of the experiment (Figure 8C). These data show that PLD1 plays an important role for occlusive thrombus formation *in vivo*.

To determine the effect of PLD1-deficiency on normal hemostasis, a tail bleeding time assay was performed. Interestingly, no differences in the bleeding times of *Pld1*$^{-/-}$ mice compared to wild-type mice were detectable (mean bleeding time 337 ± 242 sec for *Pld1*$^{-/-}$ mice and 367 ± 282 sec for wild-type mice; $p=0.76$; Figure 8D), demonstrating that PLD1 is not required for hemostasis.

Since ischemic stroke development has previously been described to be largely dependent on vWF/GPIbα interactions[45,46], wild-type and *Pld1*$^{-/-}$ mice were analyzed in a stroke model of transient middle cerebral artery occlusion (tMCAO). Remarkably, also *Pld1*$^{-/-}$ mice displayed markedly reduced brain infarction areas and a better neurological outcome than wild-type mice in this model that was not associated with an increased risk of intracranial hemorrhage[190]. These data were also confirmed by bone marrow transplantation experiments where lethally irradiated wild-type mice were reconstituted with *Pld1*$^{-/-}$ bone marrow and vice versa[190], indicating that the observed protection of *Pld1*$^{-/-}$ mice resulted from the lack of PLD1 in the hematopoietic system.

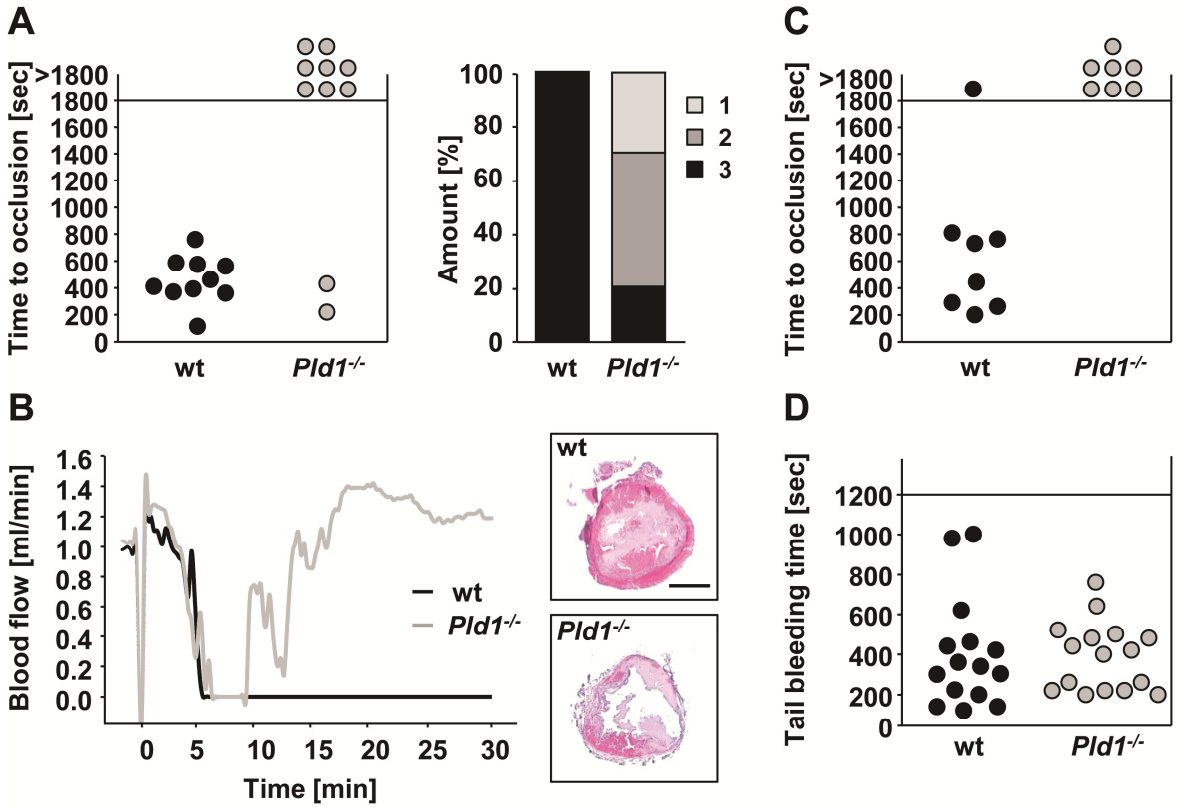

Figure 8. *Pld1*$^{-/-}$ mice show reduced thrombus stability in arterial thrombosis models but unaltered bleeding times. The abdominal aorta of wt and *Pld1*$^{-/-}$ mice was injured by a single firm compression with a forceps and thrombus formation was monitored using an ultrasonic flow probe. A, Time to stable vessel occlusion (left) and amount of (1) non-occluded, (2) recanalized and (3) stably occluded vessels after injury of wt and *Pld1*$^{-/-}$ mice (right) are shown. Each symbol represents one individual. B, Representative blood flow curves after injury (left) and cross sections of the aorta taken 30 min after injury (right). Bar, 200 µm. C, The carotid artery of wt and *Pld1*$^{-/-}$ mice was injured by 15% $FeCl_3$ and time to stable vessel occlusion was determined using blood flow measurements. Each symbol represents one individual. D, Tail bleeding times of wt and *Pld1*$^{-/-}$ mice are depicted. Each symbol represents one individual. (Elvers *et al.*, *Sci.Signal.,*2010)[190].

4.2 Genetic and antibody-induced GPVI deficiency similarly protects mice from $FeCl_3$- and mechanically induced thrombosis

GPVI is the major receptor for platelet adhesion and activation on exposed collagen at the wound site. Different mouse models of GPVI deficiency (GPVI-immunodepleted[77], *FcRg*$^{-/-}$ [79] and *Gp6*$^{-/-}$ mice[80,81]) have been used to determine the functional relevance of the receptor in arterial thrombus formation in diverse models of chemically, mechanically or laser-induced vascular injury. Although GPVI is generally considered as a critical mediator of pathological thrombus formation, the relative significance of GPVI-dependent platelet activation in some of these models, particularly $FeCl_3$-induced injury models, is still controversially discussed[42,44,78,86]. To systematically assess the relevance of GPVI-mediated platelet adhesion/activation at sites of $FeCl_3$- and mechanically injured vessel walls, *Gp6*$^{-/-}$ and GPVI-immunodepleted mice were analyzed in three different thrombosis models. For immunodepletion of GPVI from the surface of circulating platelets, wild-type C57Bl/6 mice received 100 µg of the anti-GPVI antibody, JAQ1, i.p. 6 days before the experiment and loss of GPVI was confirmed by flow cytometric measurements at the day of the experiment. In the first model, endothelial damage was induced by topical application of a drop of 20% $FeCl_3$ solution on small mesenteric arterioles and subsequent thrombus formation of fluorescently labeled platelets was monitored using intravital microscopy for 40 min or until complete occlusion of the vessel had occurred. Kinetics of initial platelet adhesion (data not shown) and beginning of first thrombus formation were comparable between control and *Gp6*$^{-/-}$ mice and only slightly delayed in some of the GPVI-immunodepleted mice (7.5 ± 1.5 min for control, 7.5 ± 1.4 min for *Gp6*$^{-/-}$ mice; p=0.99; and 9.5 ± 2.7 min for GPVI-immunodepleted mice; p=0.08; Figure 9A). In all control mice, thrombi grew progressively finally resulting in stable vessel occlusion (mean time to occlusion 17.9 ± 3.2 min, Figure 9A,B), whereas both groups of GPVI-deficient mice displayed reduced thrombus stability evident by permanent embolization of differently sized thrombus fragments during the propagation phase. Consequently, most vessels of *Gp6*$^{-/-}$ (8/10) and GPVI-immunodepleted mice (6/11) remained open during the entire observation period or occlusion occured significantly delayed compared to control mice (mean time to occlusion 30.8 ± 8.1 for GPVI-immunodepleted; p<0.05, Figure 9A,B).

Similar results were obtained in the second model where the carotid artery of mice was injured by topical application of a filter paper saturated with 10% $FeCl_3$ for 1.5 min and blood flow was monitored with an ultrasonic flow probe. Whereas 11 out of 12 vessels in control mice rapidly occluded within 589 ± 295 sec after injury, initial reduction of blood flow was observed in both *Gp6*$^{-/-}$ and GPVI-immunodepleted mice but permanent embolization in most vessels prevented or delayed stable vessel occlusion (7/9 *Gp6*$^{-/-}$ and 6/9 GPVI-immunodepleted mice; Figure 9C).

These data demonstrated that GPVI plays a significant role for $FeCl_3$-induced thrombus formation and that this is independent of the studied vascular bed.

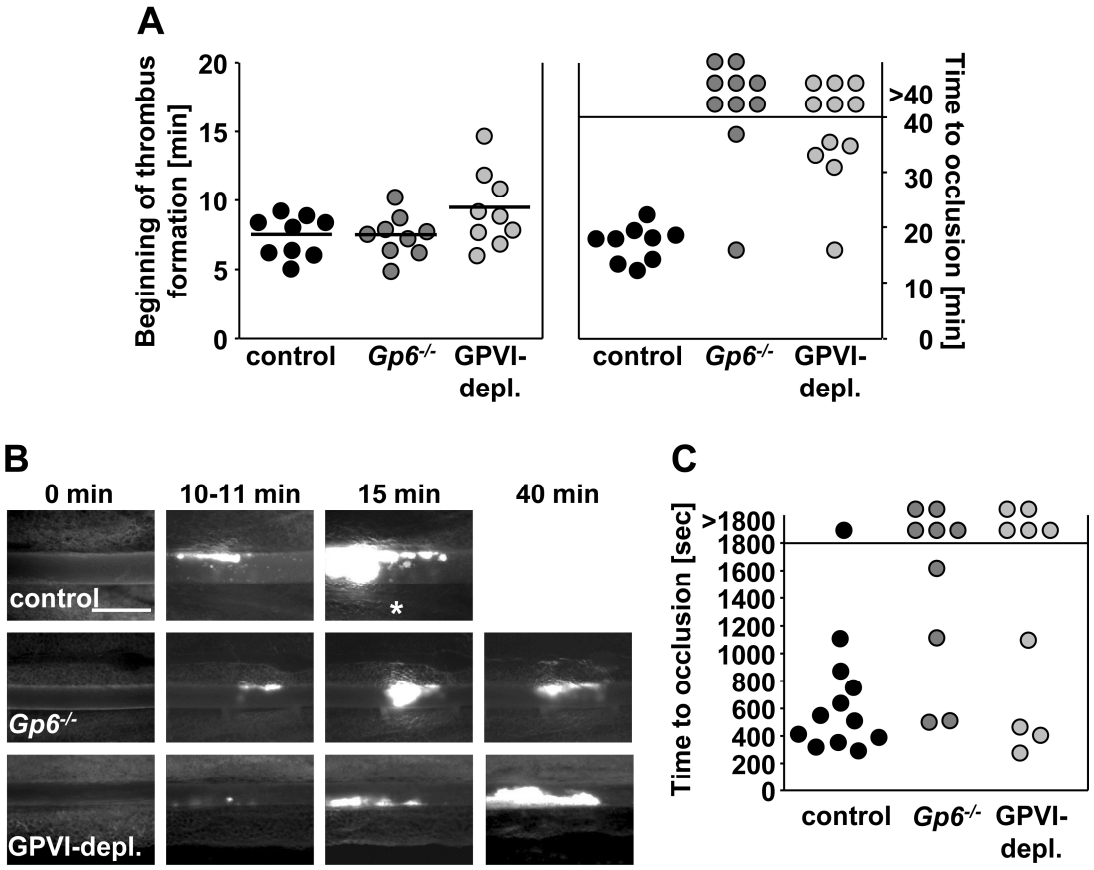

Figure 9. GPVI-deficient mice display defective thrombus formation in $FeCl_3$-induced thrombosis models. Mesenteric arterioles of control, *Gp6*$^{-/-}$ and GPVI-immunodepleted mice were injured with 20% $FeCl_3$ and adhesion and thrombus formation of fluorescently labeled platelets was monitored by *in vivo* microscopy. A, Beginning of first thrombus formation (left) and time to occlusion (right) are shown. Horizontal lines indicate mean values. Each symbol represents one arteriole. B, Representative images at the indicated time points after injury are depicted. Bar, 100 µm. Asterisk indicates vessel occlusion. C, Carotid arteries were topically injured with 10% $FeCl_3$ and time to occlusion was determined. Each symbol represents one individual. Depl.=depleted. (Bender*, Hagedorn* *et al. J Thromb Haemost.* 2011)[193].

Furthermore, mice were subjected to a mechanical injury model in which the abdominal aorta was compressed for 15 sec with a forceps and thrombus formation was monitored by blood flow measurements. In line with findings from the previous two thrombosis models, GPVI deficiency resulted in profound protection from occlusive thrombosis. Remarkably, the thrombus formation defect in this model was even more pronounced than that observed in GPVI-deficient mice after $FeCl_3$-induced vascular injuries. All *Gp6*$^{-/-}$ (6/6) and 6 out of 7 GPVI-immunodepleted mice indeed displayed initial reduction of the blood flow and in some cases also minimal embolization was detected; however, the blood flow remained rather constant throughout the observation period of 30 min, (Figure 10A,B). In comparison, all

control mice exhibited irreversible vessel occlusion within 272 ± 98 sec. This demonstrated that GPVI deficiency results in severely reduced thrombus growth after mechanical vessel injury. Furthermore, the data suggested that genetic- and antibody-induced loss of GPVI lead to comparable defects in arterial thrombus formation.

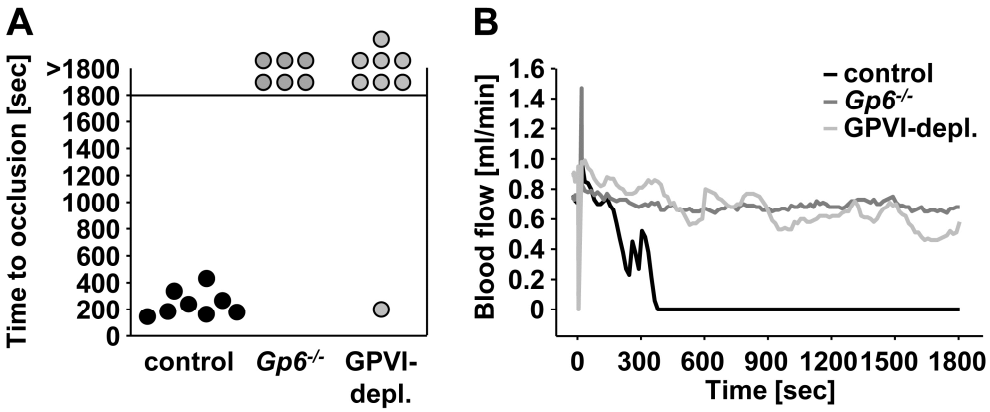

Figure 10. GPVI-deficient mice are protected from mechanically induced arterial thrombosis. The abdominal aorta was injured by tight compression with a forceps and blood flow was monitored for 30 min. A, Time to stable vessel occlusion and B, representative blood flow curves are shown. Each symbol represents one individual. Depl.=depleted. (Bender*, Hagedorn* *et al*. *J Thromb Haemost*. 2011)[193].

4.3 The platelet activating receptor CLEC-2 is essentially involved in thrombosis and hemostasis

The recently identified platelet activating receptor CLEC-2 has been shown to use a similar intracellular signaling pathway as GPVI[73]. However, the functional role of CLEC-2 for platelet activation during hemostasis or thrombosis has not been determined. The following study was conducted together with Frauke May, who mainly performed the *in vitro* analyses on the function of CLEC-2 in platelets.

4.3.1 CLEC-2 can specifically be downregulated from circulating platelets by the monoclonal antibody INU1

To analyze the effect of CLEC-2 deficiency in platelets, an approach of antibody-induced depletion of the receptor from the platelet surface, similar to the previously described GPVI-immuodepletion (see[77] and section 4.2), was used.

A novel rat monoclonal antibody against murine CLEC-2, termed INU1 (rat IgG1), was generated by Frauke May in our laboratory[182]. Intravenous injection of INU1 (8 µg/g body weight) into NMRI mice resulted in a rapid but transient thrombocytopenia with a maximal reduction of platelet counts of more than 85% on day 1[182]. Platelet counts returned to normal or in some mice slightly increased levels on day 5 (Figure 11A, left) where they remained for at least 6 more days. Platelet size was also slightly increased in these animals, most probably due to increased production of new platelets to overcome the induced thrombocytopenia (Figure 11A, right). Interestingly, platelets of INU1-teated mice completely lacked CLEC-2 on the surface from day 1 to 5 and even for up to 7 days post injection as determined with INU1-FITC by flow cytometry, whereas expression levels of other prominent surface receptors such as GPIb-V-IX, GPVI, CD9 and integrins αIIbβ3 and α2β1 were unaltered (Figure 11B). Blockage of the CLEC-2 receptor *in vivo* by INU1 could be excluded as the injected antibody was not detectable by a FITC-conjugated anti-rat IgG antibody on the surface of the platelets[182]. To test the physiological relevance of CLEC-2 deficiency in more detail, flow cytometric analysis of integrin αIIbβ3 activation and α granule release-dependent P-selectin exposure in response to different platelet agonists was performed. Platelets from mice on day 5 after INU1 injection were completely resistant to activation with rhodocytin but displayed normal activation responses to ADP, U46619 (a TxA_2 analogue), thrombin and convulxin (Figure 11C,D). These findings were confirmed by aggregation studies[182]. These results demonstrated that INU1-treatment specifically abolished CLEC-2 signaling in platelets while leaving other activation pathways fully intact.

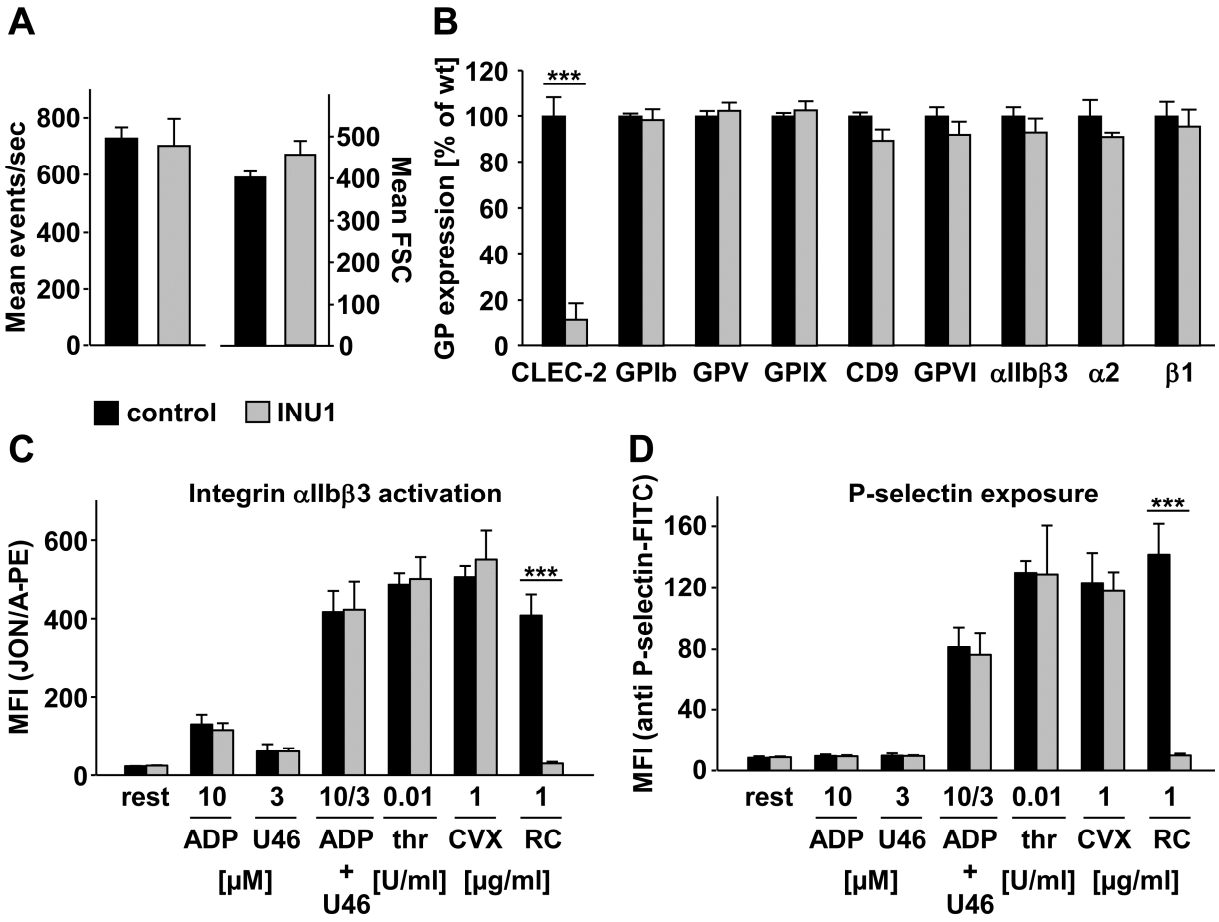

Figure 11. INU1-treatment induces specific loss of the CLEC-2 receptor and abolishes CLEC-2 signaling in circulating platelets. Mice were injected with either vehicle or 8 µg/g b.w. INU1 and platelets were analyzed on day 5 on a FACSCalibur. A, Mean platelet count expressed as mean events/sec (left) and mean platelet size (right) determined by FSC characteristics. B, Relative expression of glycoproteins and integrins on the platelet surface. Diluted whole blood of the indicated mice was incubated with the respective FITC-labeled antibodies and analyzed directly. Values are means ± SD of 5 mice per group. C, Flow cytometric analyses of αIIbβ3 integrin activation (binding of JON/A-PE) and D, degranulation-dependent P-selectin exposure in response to the indicated agonists. Values are mean fluorescence intensity (MFI) ± SD of 5 mice per group. U46=U46619, thr=thrombin, CVX=convulxin, RC=rhodocytin. ***, p<0.001. (May, Hagedorn *et al*., *Blood*, 2009)[182].

The following experiments were performed with mice 5 days after INU1-treatment to ensure normal platelet counts but complete CLEC-2 deficiency in these animals.

4.3.2 CLEC-2 deficiency leads to the formation of unstable thrombi under flow

Since platelet activation at sites of vascular injury involves a complex interplay of various receptors to enable thrombus formation under flow conditions, the importance of CLEC-2 in this process was assessed in a whole blood perfusion assay. Thus, anticoagulated blood from control and INU1-treated mice was perfused over a collagen-coated surface at an arterial shear rate of 1700 sec^{-1}. Control platelets rapidly adhered to collagen within 2 min and formed small aggregates that constantly grew into big thrombi covering 51 ± 5.7% of the surface area at the end of the 4 min perfusion period. In sharp contrast, although CLEC-2

deficient platelets normally adhered to collagen (Figure 12A), they failed to subsequently build stable thrombi. During the entire perfusion time, adherent platelets recruited numerous platelets from the blood flow but many of these were unable to firmly attach and were released after a few seconds. Consequently, only small aggregates formed and the overall surface coverage was reduced by 36% (31 ± 12.1%; $p<0.01$, Figure 12B). The thrombus formation defect became even more evident by assessing the relative thrombus volume, determined as the integrated intensity of fluorescently labeled platelets per mm^2, which was reduced by ~82% compared to control mice (0.3 ± 0.2 for CLEC-2 deficient mice, 1.4 ± 0.2 for control mice; $p<0.01$; Figure 12B). Similar results were obtained in studies using a higher shear rate of 3400 sec^{-1} (data not shown). This indicates that CLEC-2 is dispensable for the initial adhesion of platelets on collagen but essential for stable aggregate formation.

To test whether the observed aggregate instability was based on altered platelet activation, the same perfusion study was performed with non-anticoagulated blood to allow thrombin generation. To do so, blood was drawn from mice into citrate buffer instead of heparin, coinfused with a $CaCl_2/MgCl_2$ buffer and then perfused over a collagen surface in the flow chamber system. Under these conditions, both control and CLEC-2 deficient platelets formed stable thrombi covering equal surface areas (Figure 12C). This was also true when anticoagulated blood was coinfused with ADP (10 µM) and U46619 (1 µM) into the flow chamber system (data not shown). CLEC-2 deficient platelets displayed similarly sized thrombi as compared to control platelets, demonstrating that CLEC-2 is a platelet activating receptor that is critically involved in thrombus stabilization under conditions where other platelet agonists are limited and unable to provide full platelet activation.

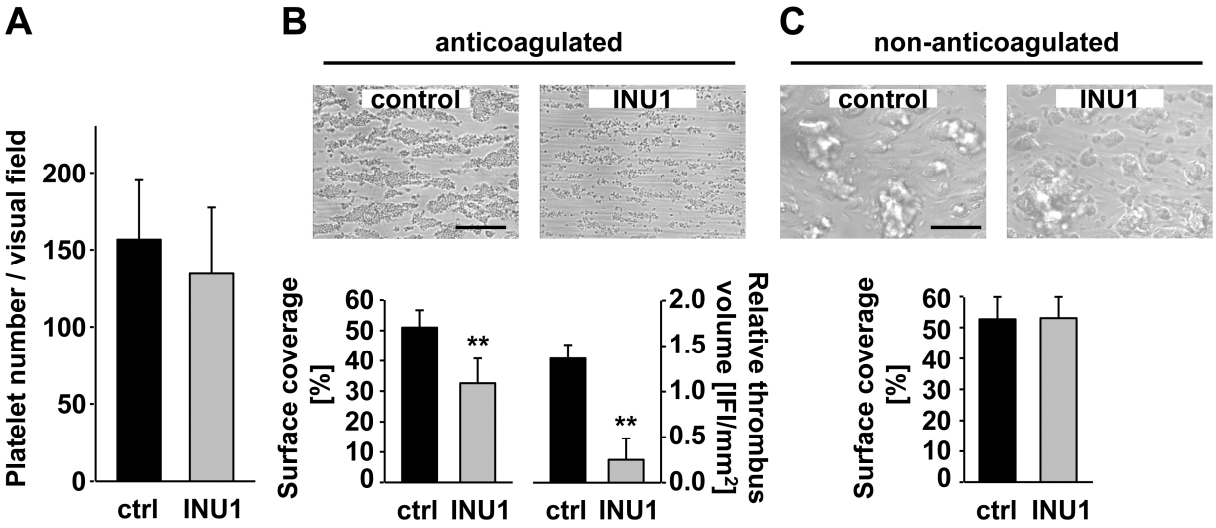

Figure 12. CLEC-2-deficient platelets fail to form stable thrombi under flow conditions. Whole blood from the indicated mice was perfused over a collagen-coated surface at a shear rate of 1,700 sec^{-1}. A, Platelet adhesion on collagen after 30 sec, indicated as number of platelets per visual field. Values are mean ± SD. B, Aggregate formation on collagen after 4 min perfusion time under anticoagulated conditions. Top, representative phase contrast images. Bottom, mean surface coverage (left) and relative thrombus volume expressed as integrated fluorescence intensity (IFI) per mm^2 (right) ± SD of 6 mice per group, **, $p<0.01$. C, Aggregate formation on collagen after 4 min perfusion time under non-anticoagulated conditions. Top, representative phase contrast images. Bottom, mean surface coverage ± SD of 6 mice per group. Bar, 100 µm. Ctrl=control. (May, Hagedorn *et al*., *Blood*, 2009)[182].

4.3.3 CLEC-2-deficient mice display defective thrombus formation in a $FeCl_3$-injury model and prolonged bleeding times

Based on the previous results, it was important to assess the relevance of CLEC-2-mediated platelet activation in thrombus formation *in vivo* after vascular injury. Thus, INU1-treated mice were analyzed in a thrombosis model where endothelial damage was induced by $FeCl_3$ on mesenteric arterioles and subsequent thrombus formation was monitored by intravital fluorescence microscopy. In all control mice, appearance of first thrombi >10 µm in diameter was observed 5 to 8 min after injury with progression to complete and stable occlusion of the vessel within 20 min (mean time to occlusion 16.4 ± 2.2 min; Figure 13). Remarkably, whereas the initial adhesion and formation of small aggregates occurred with similar kinetics in CLEC-2 deficient mice compared to control (6.9 ± 1.5 min for CLEC-2 deficient mice and 6.5 ± 1.5 min for control mice; $p=0.7$), progression to occlusive thrombi was virtually abrogated (Figure 13). This defect was mainly caused by the release of individual platelets from the thrombus surface, but also to a certain extent by embolization of small fragments during thrombus growth leading to maintenance of the blood flow during the entire observation period of 40 min. This observation revealed a crucial role for CLEC-2 for pathological thrombus formation.

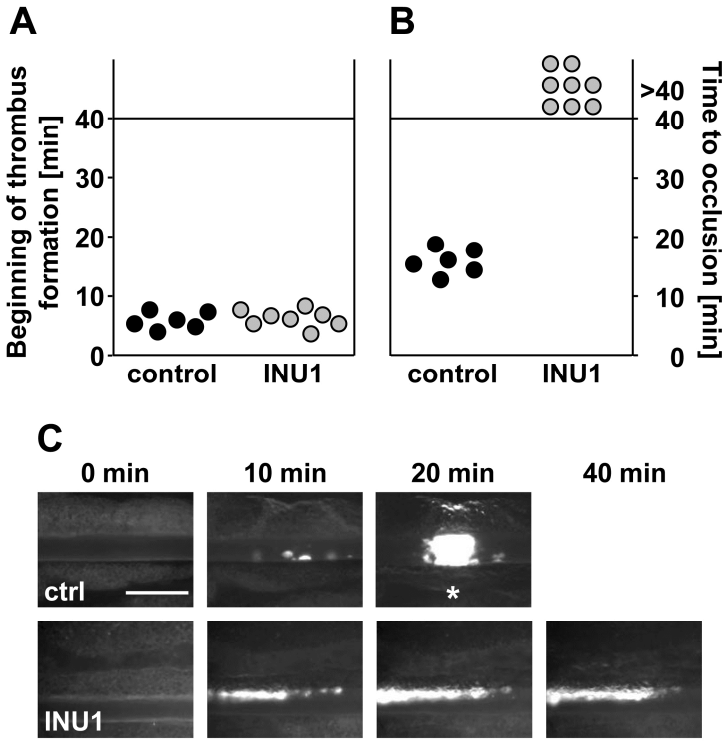

Figure 13. Defective thrombus formation in CLEC-2-deficient mice. Thrombus formation in mesenteric arterioles was induced by $FeCl_3$ and monitored using intravital fluorescence microscopy. A, Beginning of first thrombus formation and B, time to stable vessel occlusion are shown. Each symbol represents one arteriole. Data are representative of 2 individual stets of experiments. C, Representative fluorescence microscopical images at the indicated time points. Bar, 100 µm. Asterisk indicates occlusion of the vessel. Ctrl=control. (May, Hagedorn *et al*., *Blood*, 2009)[182].

To further assess whether CLEC-2 deficient mice are similarly protected from thrombus formation after mechanically induced vascular injury, these animals were challenged in a model where the abdominal aorta was injured by a single firm compression with a forceps and thrombus formation was monitored by blood flow measurements. Interestingly, and in contrast to the findings of the $FeCl_3$-injury model, CLEC-2 deficient mice displayed largely unaltered thrombus formation as compared to control mice (Figure 14). Only 3 out of 7 CLEC-2 deficient mice displayed slightly but not significantly delayed vessel occlusion (mean time to occlusion 425.9 ± 179.1 sec for CLEC-2 deficient and 275.9 ± 69.2 sec for control mice; p=0.07, Figure 14). To clarify whether this observed tendency has a considerable statistical relevance, the number of animals subjected to this injury model has to be further increased. So far, these findings indicated that CLEC-2 is of minor importance for arterial thrombus formation in the mechanically injured aorta in mice.

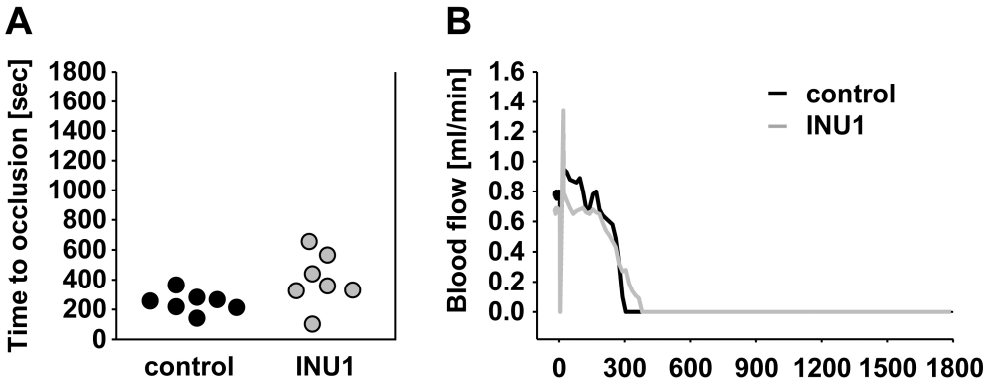

Figure 14. CLEC-2 deficient mice are not protected from mechanically induced thrombosis. Thrombus formation was induced in control and INU1-injected mice by a single firm compression of the abdominal aorta with a forceps. A, Time to vessel occlusion and B, representative blood flow curves are shown. Each symbol represents one individual.

Next, a tail bleeding assay was performed to study the impact of CLEC-2 deficiency on physiological thrombus formation. To do so, 2 mm of the mouse tail tip were removed and time to cessation of bleeding was determined using the filter paper method. Whereas all tested control mice (22/22) were able to arrest bleeding during the 20 min observation time (mean bleeding time 6.1 ± 3.9 min), bleeding times of CLEC-2 deficient mice were highly variable. While 33.3% (8/24) of these mice stopped bleeding within the same time frame as control mice, 33.3% had a prolonged bleeding time (10.8 ± 6.0 min in total, $p<0.05$) and the remaining 33.3% of the mice bled for more than 20 min, indicating an important, but not essential role for CLEC-2 in hemostasis (Figure 15).

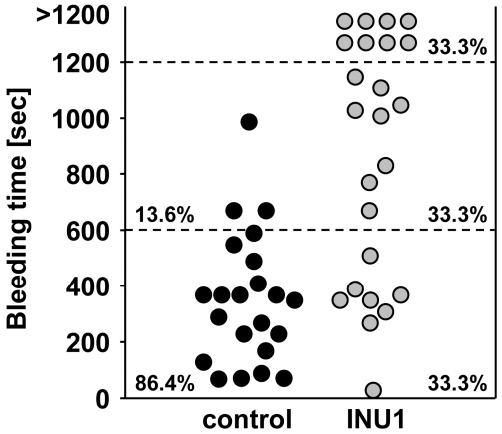

Figure 15. Prolonged bleeding times in CLEC-2 deficient mice. Bleeding times after tail tip cut of control and CLEC-2 deficient mice. Each symbol represents one individual. (May, Hagedorn *et al*., *Blood*, 2009)[182].

4.4 Severely defective arterial thrombus formation in mice lacking GPVI and CLEC-2

As described in sections 4.2 and 4.3, the (hem)ITAM receptors GPVI and CLEC-2 can be specifically targeted and immunodepleted from the platelet surface which results in a clear protection from arterial thrombosis but only mildly[77] prolonged or variably increased bleeding times, respectively. Since both receptors involve similar downstream effector proteins, most notably LAT, SLP76 and PLCγ2[73], the question raised whether both receptors have redundant functions in platelet activation *in vivo.* To address this issue, NMRI mice were intravenously injected with INU1 (200 µg) and JAQ1 (100 µg) to concomitantly deplete GPVI and CLEC-2. The *in vitro* characterization of these mice in comparison to the respective single deficient mice was performed by Markus Bender and Frauke May in our group.

Mice subjected to the combined antibody treatment (JAQ1+INU1) displayed a transient thrombocytopenia with a recovery of platelet counts after 5 to 6 days, similar to the observations in INU1-treated mice[182]. Flow cytometric analyses of the platelets showed that JAQ1 + INU1 treatment induced the specific loss of the respective receptor without significantly influencing the expression levels of other platelet surface proteins. Accordingly, these platelets were unresponsive to collagen-related-peptide (CRP), convulxin and rhodocytin but activation with other classical platelet agonists was fully functional (Bender, May *et al.,* in revision). Only P-selectin exposure upon thrombin stimulation was slightly reduced at early time points after antibody injection but completely restored on day 6, which is in line with observations made in JAQ1-injected mice[82]. These findings revealed that GPVI and CLEC-2 can be simultaneously downregulated from circulating platelets without interfering with other platelet activation pathways.

Hence, the following experiments on single- and double-deficient mice were conducted on day 5 or 6 after antibody treatment and loss of the appropriate platelet receptor(s) was each time confirmed by flow cytometry.

To study the functional effect of GPVI/CLEC-2 double deficiency on occlusive thrombus formation, JAQ1-, INU1- and JAQ1 + INU1-injected mice were subjected to the $FeCl_3$-induced thrombosis model in small mesenteric arterioles. In all control mice, small aggregates formed at 7.8 ± 1.2 min after injury (Figure 16A,C) and continuously grew to large thrombi which completely occluded the vessel within 20 min (mean time to occlusion 16.4 ± 2.2 min; Figure 16B,C). In line with the previously described results (section 4.2 and 4.3), GPVI and CLEC-2 single-deficient mice showed similar kinetics of small aggregate formation compared to control mice but exhibited, as expected, reduced thrombus stability preventing in most cases firm vessel occlusion during the observation period (8/12 of GPVI-depleted and 7/10 of CLEC-2 depleted mice). Remarkably, already the onset of small aggregate formation was significantly delayed in GPVI/CLEC-2-depleted mice compared to

control and single-deficient mice (11.4 ± 3.0 min, p<0.01; Figure 16A,C) and following propagation of thrombi was dramatically reduced as indicated by the strongly decreased ratio of thrombi size to vessel diameter (44 ± 19% for GPVI/CLEC-2 double-deficient mice, p<0.001, 80 ± 18% for GPVI-deficient mice, 81 ± 20% for CLEC-2 deficient mice and 100 ± 0% for control mice, Figure 16D). As a consequence, blood flow was maintained in all vessels (12/12; Figure 16B,C) of double-deficient mice.

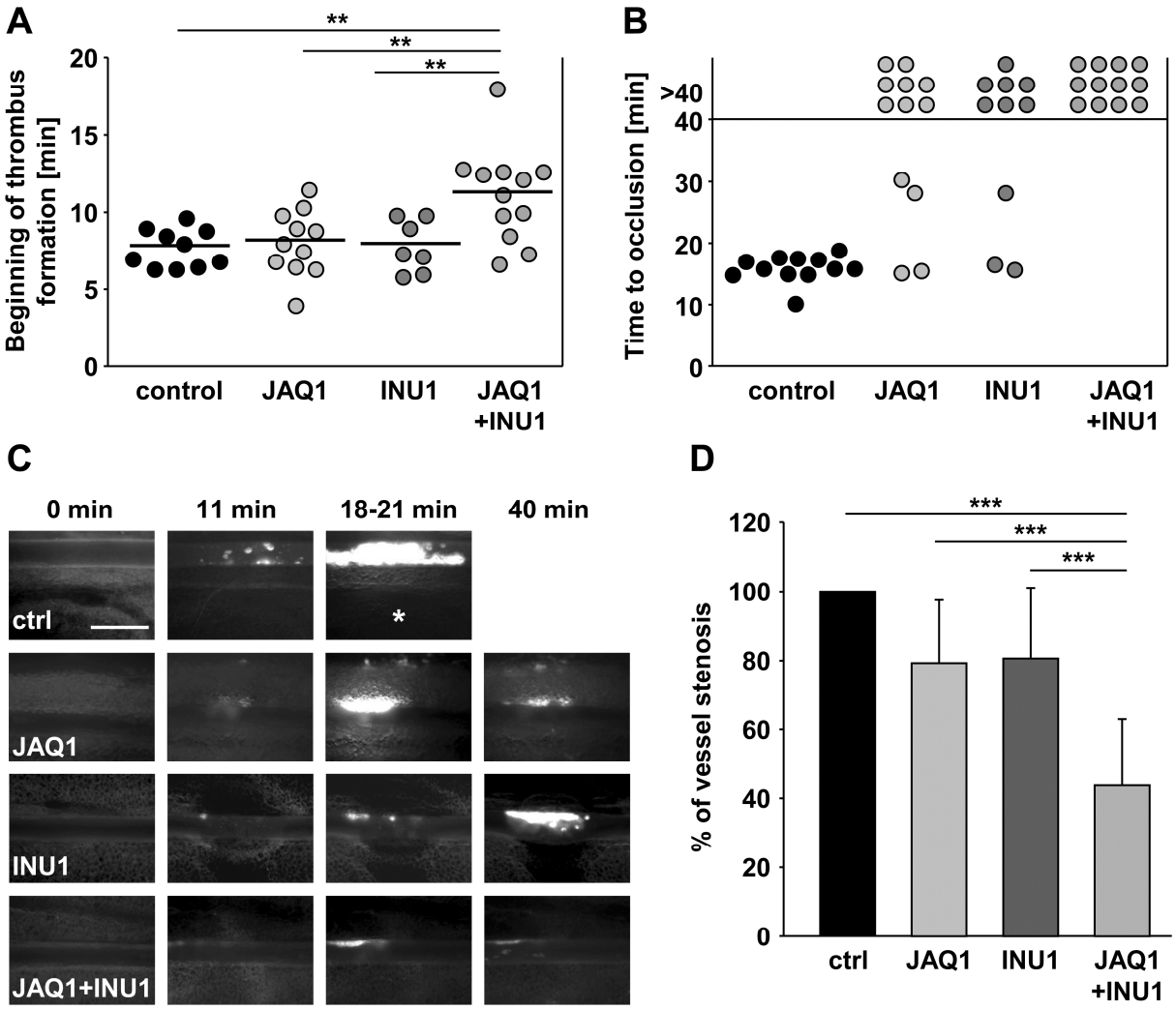

Figure 16. Arterial thrombus formation in mice lacking GPVI and CLEC-2 is virtually abrogated in contrast to the respective single-deficient mice. Small mesenteric arterioles of the indicated mice were injured by $FeCl_3$ on day 5 after antibody injection and thrombus formation was analyzed using intravital fluorescence microscopy. A, Beginning of thrombus formation and B, time to stable vessel occlusion are shown. Horizontal lines indicate mean values. Each symbol represents one arteriole C, Representative pictures of thrombus formation at the indicated time points after injury. Bar, 100 µm. Asterisk indicates stable vessel occlusion. D, Percentage of maximal thrombus-caused vessel stenosis is illustrated. **, p<0.01; ***, p<0.001. Ctrl=control.

The consequence of GPVI/CLEC-2 double-depletion on hemostasis was assessed by Markus Bender and Frauke May in a tail bleeding assay. Whereas the phenotype of GPVI and CLEC-2 single-deficient mice could be reproduced in this model, mice lacking both

receptors displayed virtually abrogated hemostatic function, as bleeding did not stop and even the drop size remained constant during the 20 min observation period (Bender, May *et al.*, in revision). Taken together, these data demonstrate that, in contrast to the respective single-deficient mice, the lack of both receptors, GPVI and CLEC-2, results in almost completely abolished thrombus formation and thereby suggest partially redundant functions of the two platelet receptors *in vivo*.

To at least partially exclude that the profound defect in thrombus growth and stability observed in GPVI/CLEC-2 depleted mice was based on possible side effects of the antibody treatment, *Gp6*$^{-/-}$ mice were injected with INU1 (200 µg) and analyzed on day 6 post injection in the $FeCl_3$-injury model. *Gp6*$^{-/-}$ and wild-type C57Bl6/J mice injected with INU1 were analyzed in parallel as controls. These single-deficient mice showed the expected phenotypes in this model as described before and are therefore not depicted again. However, before comparing GPVI/CLEC-2 double-depleted mice with *Gp6*$^{-/-}$/CLEC-2 depleted mice, it is important to note, that CLEC-2 deficient mice in a C57Bl6/J genetic background displayed a less severe defect in pathological thrombus formation compared to CLEC-2 deficient NMRI mice, evident in a small subpopulation of vessels where thrombi finally occurred which, albeit delayed, occluded the vessel. This was probably due to a different genetically determined thickness of the tissue surrounding the vessel or the vessel wall itself which influenced the diffusion of $FeCl_3$ and thereby the severity of the injury (Hagedorn *et al.* unpublished).

Similar to the aforementioned observations in GPVI/CLEC-2 depleted mice, small aggregate formation in *Gp6*$^{-/-}$/CLEC-2 depleted mice was significantly delayed compared to wild-type mice (8.3 ± 1.8 min for *Gp6*$^{-/-}$/CLEC-2 depleted mice and 6.4 ± 0.9 min for wild-type mice, $p<0.01$, Figure 17A,C) and consequent thrombus growth was severely reduced which resulted in no occlusion in 7 out of 11 vessels and significantly delayed occlusion times for the rest of the arterioles (mean time to occlusion 27.5 ± 4.6 min for *Gp6*$^{-/-}$/CLEC-2 depleted mice and 16.2 ± 2.0 min for wild-type mice; $p<0.05$, Figure 17B,C). This defect also clearly exceeded the thrombus instability observed in the respective single-deficient mice (data not shown).

Additionally, in the bleeding time assay, *Gp6*$^{-/-}$/CLEC-2 depleted mice showed the same hemostatic defect as seen in the double-depleted mice (Bender, May *et al.*, in revision). These data confirmed that the profound thrombotic defects in GPVI/CLEC-2 deficient mice were most probably exclusively related to the functional consequences of the receptor deficiencies and not to unspecific effects of the antibody treatment, although genetic double-deficient mice would be necessary to completely exclude this possibility.

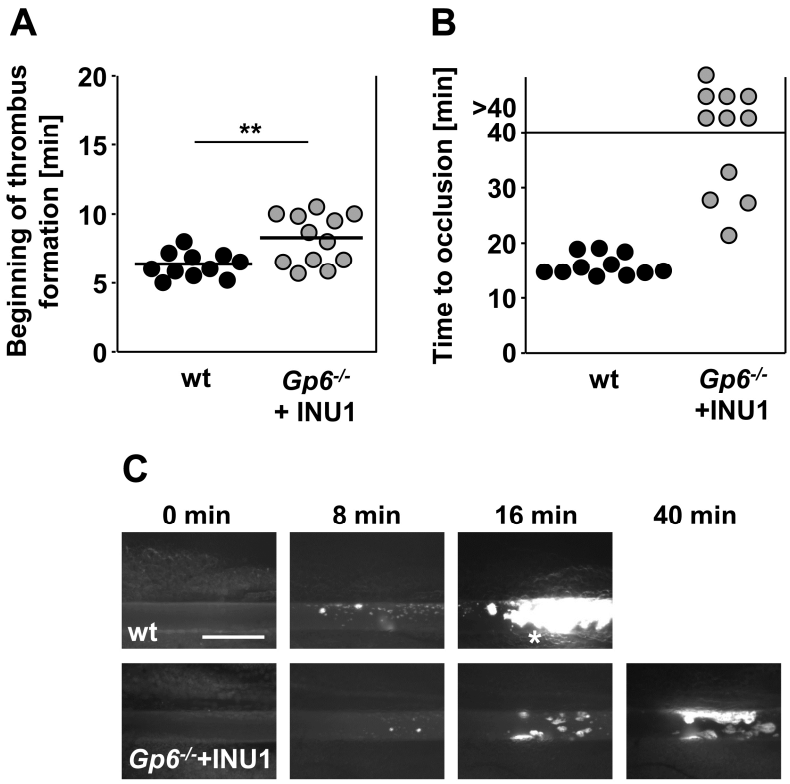

Figure 17. Arterial thrombus formation in INU1-treated *Gp6*$^{-/-}$ mice. Small mesenteric arterioles were injured by $FeCl_3$ on day 5 after antibody injection and thrombus formation was analyzed using intravital fluorescence microscopy. A, Time to beginning of thrombus formation and B, time to stable vessel occlusion are shown. Horizontal lines indicate mean values. Each symbol represents one arteriole. C, Representative pictures at the indicated time points. Bar, 100 µm. Asterisk indicates occlusion of the vessel.

4.5 The small GTPase RhoA is a crucial mediator of platelet activation in hemostasis and thrombosis

To investigate the specific function of RhoA in platelets, a conditional knockout approach was used. Mice carrying the *RhoA* gene flanked by loxP sites[122] were crossed with transgenic mice expressing the Cre recombinase under the control of the megakaryocyte- and platelet-specific platelet factor (PF) 4 promoter[194]. Gene deletion was intrinsically induced in RhoA (fl/fl, cre+, in the following referred to as *RhoA*$^{-/-}$) mice upon induction of the PF4 promoter activity during megakaryopoiesis. Littermate RhoA (fl/fl, cre-, in the following referred to as wild-type) mice served as control animals.

4.5.1 *RhoA*$^{-/-}$ mice display a marked thrombocytopenia

The absence of RhoA protein in *RhoA*$^{-/-}$ platelets was confirmed by western blot analysis using GPIIIa protein expression as loading control (Figure 18A). Specific deletion of RhoA in megakaryocytes and platelets led to a pronounced macrothrombocytopenia apparent as an approximately 50% reduction of peripheral platelet counts ($p<0.001$; Figure 18B) and a 25% increased platelet volume when compared to wild-type mice ($p<0.001$; Figure 18C), suggesting a critical role of RhoA in megakaryocyte maturation and/or platelet production. The increased platelet size in *RhoA*$^{-/-}$ mice was also visualized by *transmission electron microscopy* (TEM; Figure 18D).

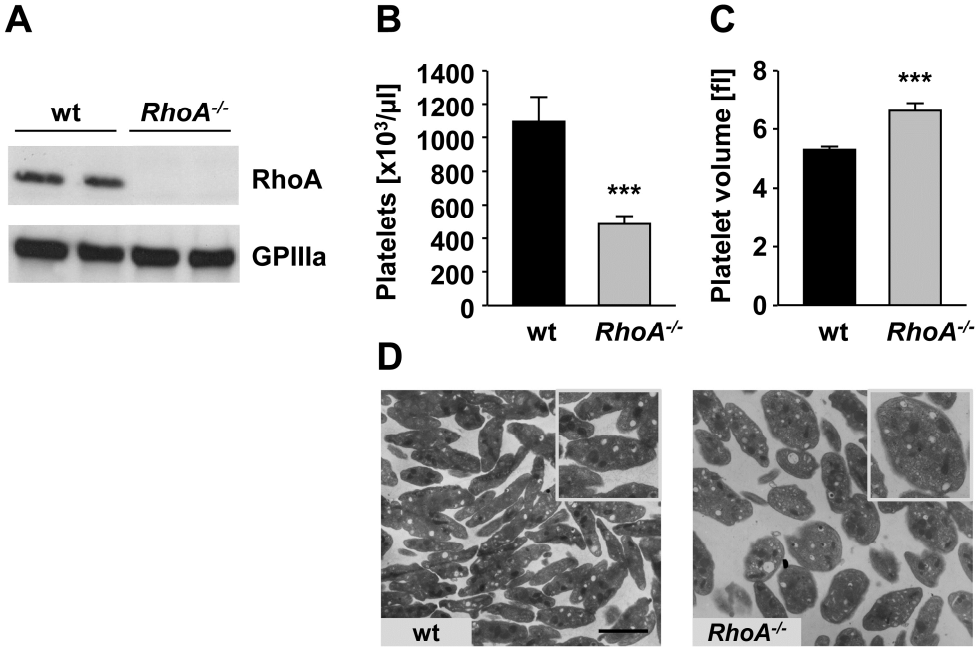

Figure 18. *RhoA*$^{-/-}$ mice display a macrothrombocytopenia. A, Western blot analysis of platelet lysates from the indicated mice; α-GPIIIa antibody was used as control. B, Peripheral platelet counts and C, platelet volume of wt and *RhoA*$^{-/-}$ mice measured with a blood cell counter are depicted. Values are mean ± SD of 8 mice per group and representative of 3 individual measurements. D, Representative transmission electron microscopy (TEM) pictures of resting platelets from wt and *RhoA*$^{-/-}$ mice. Bar, 2 µm.***, $p<0.001$.

Resting RhoA-deficient platelets displayed a roundish shape in contrast to the normal discoid-shaped wild-type platelets. However, the overall ultrastructure of *RhoA*$^{-/-}$ platelets, as well as the numbers and distribution of granules appeared normal when compared to wild-type platelets (Figure 18D).

The abundance of major platelet surface receptors was unaltered in the mutant mice except for CLEC-2 and the integrins β1 and αIIbβ3 where expression levels were significantly increased compared to wild-type (Table 1). This can probably be ascribed to the increased size of *RhoA*$^{-/-}$ platelets

	wild-type	*RhoA*$^{-/-}$	significance
GPIb	353±22	349±14	n.s.
GPV	302±8	329±25	n.s.
GPIX	503±16	530±31	n.s.
CD9	1433±42	1441±36	n.s.
GPVI	48±5	56±5	n.s.
α2 integrin	61±3	62±1	n.s.
β1 integrin	163±4	183±3	***
αIIbβ3	457±10	590±39	**
CLEC-2	155±5	180±12	*

Table 1. Platelet glycoprotein expression in wild-type and *RhoA*$^{-/-}$ mice. Expression of glycoproteins on the platelet surface was determined by flow cytometry. Diluted whole blood from the indicated mice was incubated with the respective FITC-labeled antibody at saturating conditions for 15 min at RT and platelets were analyzed directly. Results are expressed as mean fluorescence intensity ± SD for 4 mice per group. Values are representative of 3 individual experiments. n.s.=not significant. *, p<0.05; ** p<0.01; ***, p<0.001.

4.5.2 *RhoA*$^{-/-}$ mice display a reduced platelet life span

Continuous and rapid clearance of non-functional, structurally altered or hyperactive platelets by the reticulo-endothelial system can lead to a sustained thrombocytopenia. Hence, the platelet life span in *RhoA*$^{-/-}$ and wild-type mice was determined *in vivo*. To do so, circulating platelets were labeled with a fluorescent non-cytotoxic anti GPIX antibody derivative injected into mice and the labeled platelet population was monitored by flow cytometry over time. One hour after antibody treatment, >90% of circulating platelets were labeled in both wild-type and *RhoA*$^{-/-}$ mice and this platelet population constantly declined over 5 days in wild-type mice which is in accordance with the reported life span of mouse platelets (Figure 19). In contrast, the platelet life span was slightly reduced in *RhoA*$^{-/-}$ mice with a significant decrease of 30% on day 2 compared to wild-type mice and almost complete absence of labeled platelets on day 4 (3.8 ± 1.8% vs. 10.5 ± 1.7%; p<0.001; Figure 19). This finding demonstrated that RhoA-deficiency causes a moderately increased platelet turnover *in vivo* which may partially explain the observed thrombocytopenia in these mice. Consequently, the degree of the thrombocytopenia in *RhoA*$^{-/-}$ mice rather points to impaired platelet production from megakaryocytes.

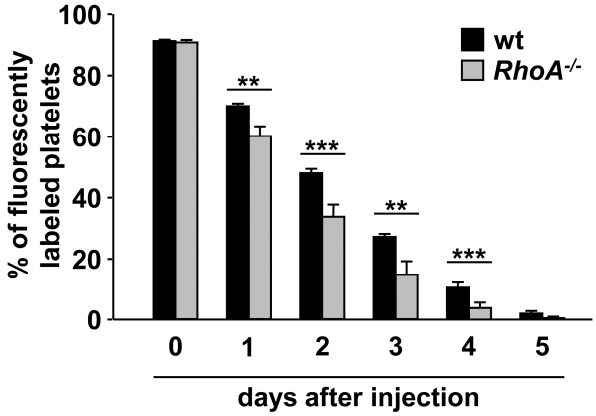

Figure 19. *RhoA*$^{-/-}$ mice display a moderately reduced platelet life span. Wt and *RhoA*$^{-/-}$ mice were injected with a DyLight 488-conjugated anti-GPIX Ig derivate to label platelets *in vivo*. Percentage of fluorescently labeled platelets determined by flow cytometry at the indicated days after injection is illustrated. Values are mean ± SD of 5 mice per group. **, p<0.01; ***, p<0.001.

4.5.3 Reduced integrin activation and release of α granules in *RhoA*$^{-/-}$ platelets upon G_{13}- and G_q-stimulation

RhoA has been shown, albeit indirectly, to act downstream of G_{13} coupled receptors[124,125] and suggested to be involved in PAR-mediated platelet granule release and integrin activation[136,195]. To address the functional role of RhoA in these processes directly, integrin αIIbβ3 activation and exposure of P-selectin, a commonly used marker for α granule release, were analyzed upon agonist stimulation of wild-type and *RhoA*$^{-/-}$ platelets by flow cytometry. The use of a highly diluted platelet suspension in this experimental setting largely excludes the accumulation of released secondary mediators and thereby allows conclusions about the primary platelet signaling response. Interestingly, and contrary to the observations from $G\alpha_{13}$-deficient mice, *RhoA*$^{-/-}$ platelets displayed significantly reduced integrin activation compared to wild-type platelets when stimulated with thrombin at high or intermediate concentrations (Figure 20A). This result was also confirmed by platelet stimulation with the PAR-4 activating peptide, activating the main thrombin receptor in mouse platelets (PAR4; data not shown). Responses to the weak agonists U46619 and ADP were similar in wild-type and *RhoA*$^{-/-}$ platelets, whereas the combination of both agonists resulted in profound integrin activation in wild-type but slightly reduced responses in *RhoA*$^{-/-}$ platelets. Interestingly, although *RhoA*$^{-/-}$ platelets reacted normally upon GPVI/ITAM-coupled receptor stimulation by CRP and convulxin, they showed decreased integrin activation levels in response to activation with rhodocytin (Figure 20A). *RhoA*$^{-/-}$ platelets also displayed specific defects in α granule release. U46619 alone is not able to mediate significant release of platelet α granules, unless costimulation with ADP occurs. Upon activation with both agonists, *RhoA*$^{-/-}$ platelets showed dramatically reduced P-selectin exposure as compared to wild-type platelets. Similarly, thrombin-induced degranulation was significantly reduced in *RhoA*$^{-/-}$ platelets at high agonist concentrations and this effect was even more pronounced at intermediate thrombin concentrations (Figure 20B). A remarkable reduction in P-selectin exposure of *RhoA*$^{-/-}$ platelets was also seen after stimulation with PAR-4 activating peptide

(data not shown). Responses to all other tested agonists were indistinguishable between wild-type and *RhoA*$^{-/-}$ platelets. These data indicate that RhoA is involved in integrin αIIbβ3 activation and critical for α granule release upon $G\alpha_{13}$- and $G\alpha_q$-mediated signaling in platelets.

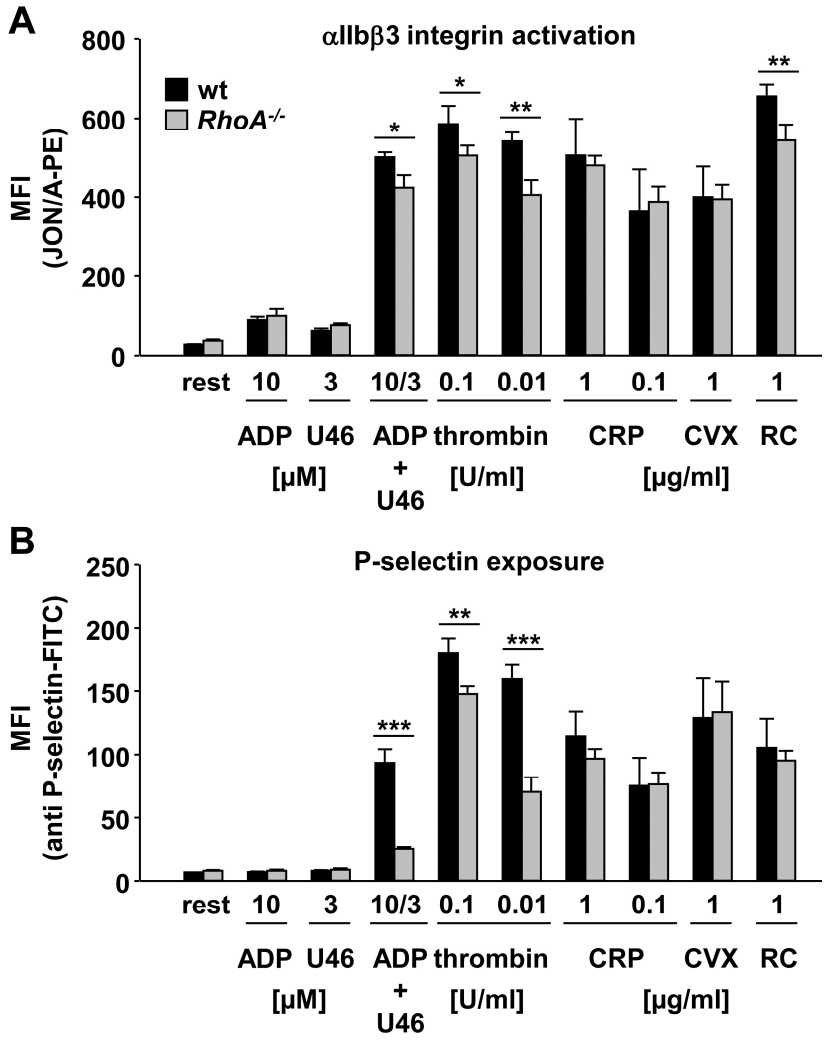

Figure 20. Reduced integrin activation and α granule release in *RhoA*$^{-/-}$ platelets upon $G\alpha_{13}$- and $G\alpha_q$-stimulation. A, Flow cytometric analysis of αIIbβ3 integrin activation (binding of JON/A-PE) and B, degranulation-dependent P-selectin exposure in response to the indicated agonists from wt and *RhoA*$^{-/-}$ mice. Results are mean fluorescence intensities (MFI) ± SD of 4 mice per group and representative of 4 individual measurements. Abbreviations: U46=U46619, CVX=convulxin, RC=rhodocytin. *, p<0.05; ** p<0.01; ***, p<0.001.

Previous studies with inhibitors indicated a specific role for RhoA in dense granule release[136]. To assess whether dense granule release was also affected by RhoA deficiency, release of ATP, which is stored in dense granules, was measured upon agonist stimulation. At high and intermediate concentrations of U46619 and PAR-4 activating peptide, ATP release was clearly reduced in *RhoA*$^{-/-}$ platelets as compared to wild-type, whereas, interestingly, thrombin-induced ATP release was not significantly different between both groups. In line with data from α granule release, collagen stimulation lead to comparable ATP releases at

the tested concentrations in *RhoA*$^{-/-}$ and wild-type platelets (Figure 21). These observations demonstrated that RhoA-deficient platelets are principally able to release their granule content but rather display a defined defect in signaling via G_{13} and G_q.

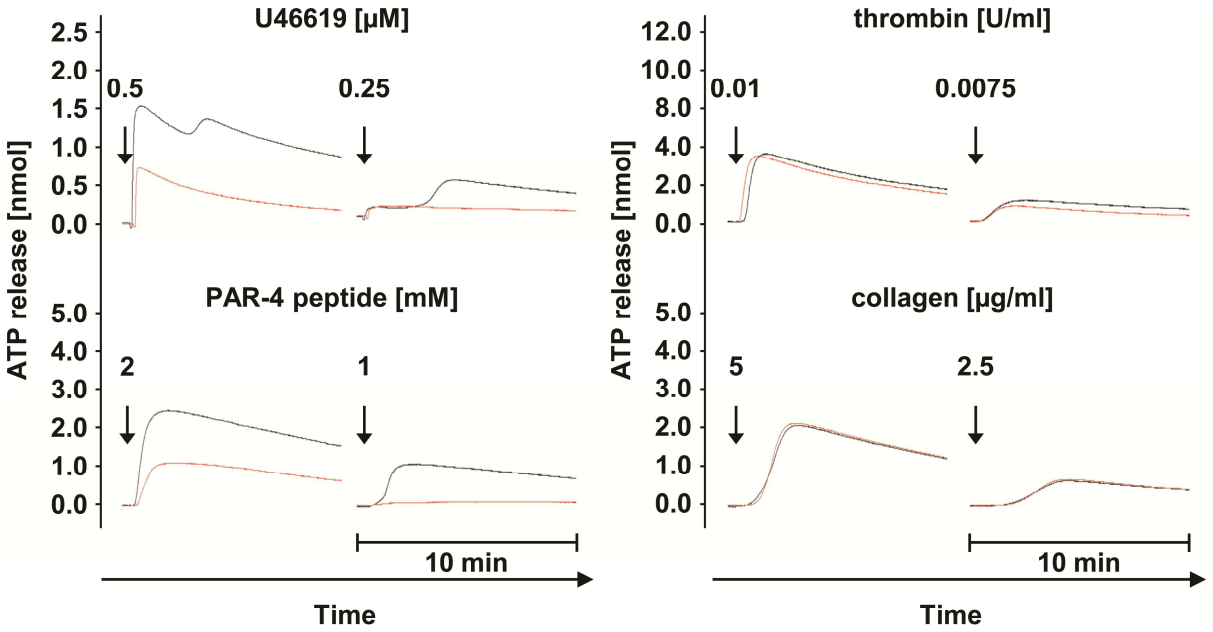

Figure 21. Decreased ATP release in *RhoA*$^{-/-}$ platelets after G_{13} and G_q-stimulation. Washed wt (black line) and *RhoA*$^{-/-}$ platelets (red line) were incubated with Luciferase-Luciferin reagent and ATP release was measured in a Chrono Log aggregometer after stimulation with the indicated agonists. Representative curves of 2 individual experiments of n=2 are shown.

4.5.4 Defective shape change of *RhoA*$^{-/-}$ platelets after low agonist stimulation

Previous studies have suggested that RhoA-mediated inhibition of the myosin light chain (MLC) phosphatase downstream of G_{13} activation is essential for stabilizing MLC phosphorylation and subsequently for platelet shape change[105,130-134]; however all these results were obtained in studies using isolated cell systems and/or pharmacological inhibitors of RhoA. To investigate the role of RhoA in platelet shape change in a more specific approach and to define the functional consequences of the reduced granule release and integrin αIIbβ3 activation in *RhoA*$^{-/-}$ platelets at the same time, aggregation studies were performed. At low concentrations of U46619, signaling is supposed to be dominantly mediated via G_{13}. Under these conditions, shape change of *RhoA*$^{-/-}$ platelets was abolished. In line with this, shape change in response to low doses of thrombin was also affected in *RhoA*$^{-/-}$ platelets. The inability of *RhoA*$^{-/-}$ platelets to mediate platelet shape change at low U46619 concentrations could be clearly visualized by *scanning electron microscopy* (SEM; Figure 22A right). Whereas wild-type platelets showed a spherical shape and typically extended filopodia, *RhoA*$^{-/-}$ platelets maintained their roundish morphology and displayed only minimal protrusions. Notably, however, the shape change defect of RhoA-deficient

platelets was overcome when using higher concentrations of U46619 or thrombin, which involve also G_q-mediated signaling (Figure 22A).

Remarkably, U46619-induced aggregation was significantly reduced in *RhoA*$^{-/-}$ platelets at intermediate concentrations, whereas it was completely restored at high agonist concentrations (Figure 22A left, C). Similar results were obtained when platelets were stimulated with PAR-4 activating peptide. A possible explanation for these findings may be that due to the high platelet concentration used in platelet aggregation measurements, released secondary mediators accumulate and influence the degree of maximal aggregation. Thus, the reduced granule release observed in *RhoA*$^{-/-}$ platelets upon U46619 and PAR-4 activating peptide stimulation could account for the decreased aggregation response at threshold agonist concentrations. In contrast, thrombin induced similar aggregation in *RhoA*$^{-/-}$ and wild-type platelets irrespectively of the used concentration, suggesting that the reduced thrombin-dependent integrin activation and α degranulation, detected by flow cytometric analysis, did not translate into an altered aggregation response (Figure 22A,C). Stimulation with the weak agonist ADP, which signals via G_q and G_i proteins and does not trigger granule release by itself, caused normal aggregation, but interestingly failed to mediate shape change in *RhoA*$^{-/-}$ platelets at low concentrations, indicating that the GTPase may also be involved in $G\alpha_q$-induced shape change (Figure 22B,C). Surprisingly, whereas the aggregation responses to high concentrations of the GPVI/ITAM agonists CRP and collagen were comparable between *RhoA*$^{-/-}$ and wild-type platelets, aggregation was clearly enhanced in RhoA-deficient platelets when stimulated with intermediate or low concentrations of the respective agonist (Figure 22B,C). Furthermore, shape change in response to CRP and collagen was also reduced in *RhoA*$^{-/-}$ platelets compared to wild-type platelets, irrespective of the used agonist concentration; particularly pronounced after activation with collagen. Taken together, these findings demonstrate that RhoA plays a central role for platelet shape change and is critical for platelet aggregation downstream of G_{13} and G_q protein-coupled receptor activation.

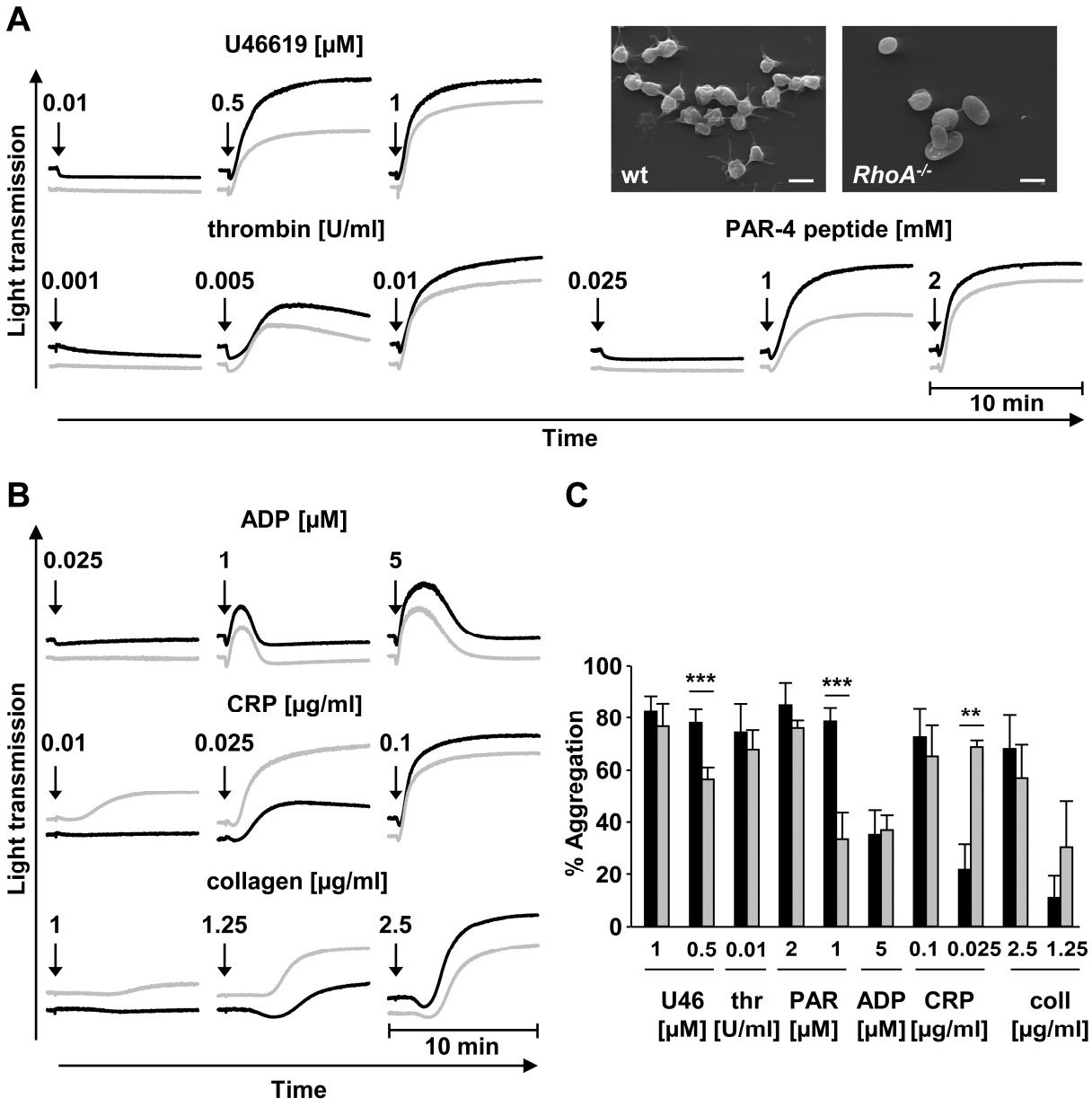

Figure 22. Defective shape change of *RhoA*$^{-/-}$ platelets after agonist stimulation at low concentrations. Washed platelets were stimulated with the indicated agonists and light transmission was recorded on a Fibrintimer 4-channel aggregometer. ADP measurements were performed in prp. A,B Representative aggregation curves of wt (black line) and *RhoA*$^{-/-}$ platelets (grey line) of 3 individual measurements with n=2 are depicted. Representative scanning electron microscopy pictures of platelets after stimulation with 0.01 µM U46619 (right) are shown. Bar, 2 µm. C, Mean maximal % aggregation ± SD of each group. **,p<0.01; ***,p<0.001. Abbreviations: U46=U46619, thr=thrombin, PAR=PAR-4 peptide, coll=collagen.

To analyze whether the observed platelet shape change defect was directly associated with decreased phosphorylation of MLC, the main effector molecule downstream of RhoA, (semi-) quantitative western blot analysis of MLC and phosphorylated MLC (MLC-P) upon agonist stimulation was performed (Figure 23). As expected, MLC-P was detectable after activation of wild-type platelets with all tested agonists. In contrast, *RhoA*$^{-/-}$ platelets showed virtually no MLC-P upon U46619, PAR-4 activating peptide and thrombin stimulation. Only MLC-P in response to CRP was similar to wild-type platelets.

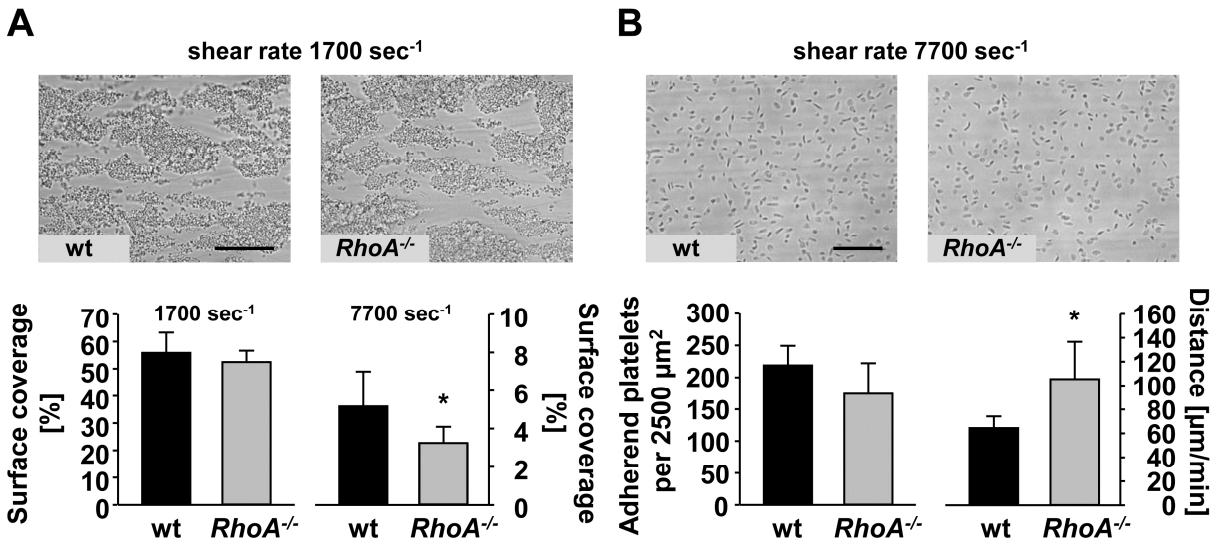

Figure 23. Myosin light chain phosphorylation of wt and *RhoA*$^{-/-}$ platelets after activation. Western blot analysis of platelet lysates from wt and *RhoA*$^{-/-}$ platelets after stimulation with the indicated agonists. Expression levels of myosin light chain (MLC) and phosphorylated MLC (MLC-P) was assessed using appropriate antibodies. An α-GPIIIa antibody served as control. Data are representative of 2 individual experiments. Abbreviations: U46=U46619, thr=thrombin.

4.5.5 RhoA is dispensable for agonist-induced Ca^{2+} mobilization in platelets

Since *RhoA*$^{-/-}$ platelets displayed clearly reduced thrombin- and PAR-4 peptide-triggered integrin activation and α degranulation as well as impaired shape change response upon ADP stimulation, one may speculate that RhoA also signals downstream of G_q. To test whether RhoA is involved in the respective classical signaling cascade leading to PLCβ activation and subsequent Ca^{2+} mobilization, changes in intracellular calcium concentrations ($[Ca^{2+}]_i$) in response to U466619 and thrombin were assessed (Figure 24). In addition, platelets were stimulated with CRP to determine whether an altered Ca^{2+} mobilization possibly accounts for the increased aggregation of *RhoA*$^{-/-}$ platelets in response to ITAM-coupled agonists. However, notably, Ca^{2+} release from intracellular stores was similar between *RhoA*$^{-/-}$ and wild-type platelets for all tested agonists (Figure 24).

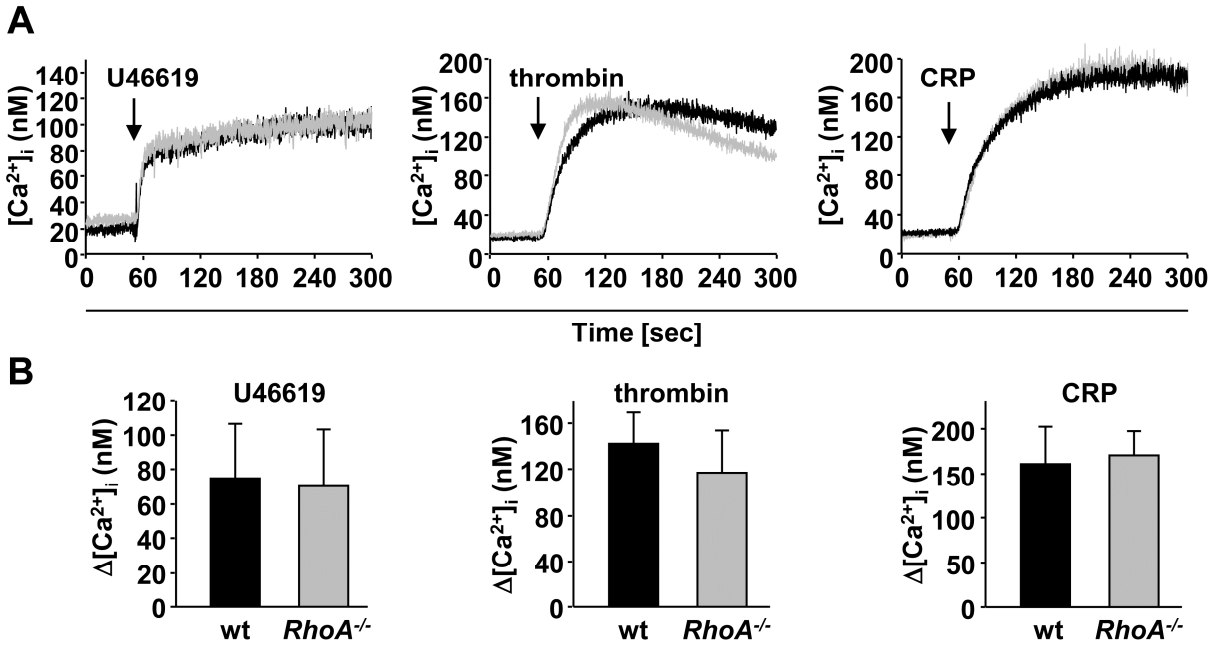

Figure 24. *RhoA*$^{-/-}$ platelets show normal Ca^{2+} responses upon activation. Fura-2-loaded wt and *RhoA*$^{-/-}$ platelets were stimulated with 3 µM U46619, 0.005 U/ml thrombin or 10 µg/ml CRP in the absence of Ca^{2+} and intracellular Ca^{2+} mobilization ($[Ca^{2+}]_i$) was monitored. A, Representative measurements of wt (black line) and *RhoA*$^{-/-}$ platelets (gray line) and B, maximal increase in intracellular Ca^{2+} concentration compared with baseline levels before stimulus ($\Delta[Ca^{2+}]_i$) ± SD of at least 10 mice per group are shown.

4.5.6 *RhoA*$^{-/-}$ platelets spread normally on fibrinogen but exhibit abolished integrin-dependent clot-retraction

Platelet spreading requires integrin αIIbβ3 signaling-dependent cytoskeletal reorganizations leading to the development of F-actin bundles and focal adhesion-like structures, processes which have been ascribed to the function of RhoA[106,112,196]. However, previous studies suggested that RhoA is either not required[140] or has to be inhibited[139] for proper platelet spreading. To clarify this issue, wild-type and *RhoA*$^{-/-}$ platelets were allowed to spread on a fibrinogen-coated surface in the presence of thrombin (0.01 U/ml final concentration; Figure 25A). Interestingly, *RhoA*$^{-/-}$ platelets were able to form filopodia and lamellipodia to the same extent and with similar kinetics as wild-type platelets, resulting in fully spread platelets after 20 min in both groups. The overall morphological structure of spread *RhoA*$^{-/-}$ platelets seemed to be unchanged compared to wild-type platelets, however, the inner cell body appeared less condensed, indicating reduced granule centralization. A more detailed analysis of the morphology of both wild-type and *RhoA*$^{-/-}$ platelets by SEM studies confirmed these observations (Figure 25B).

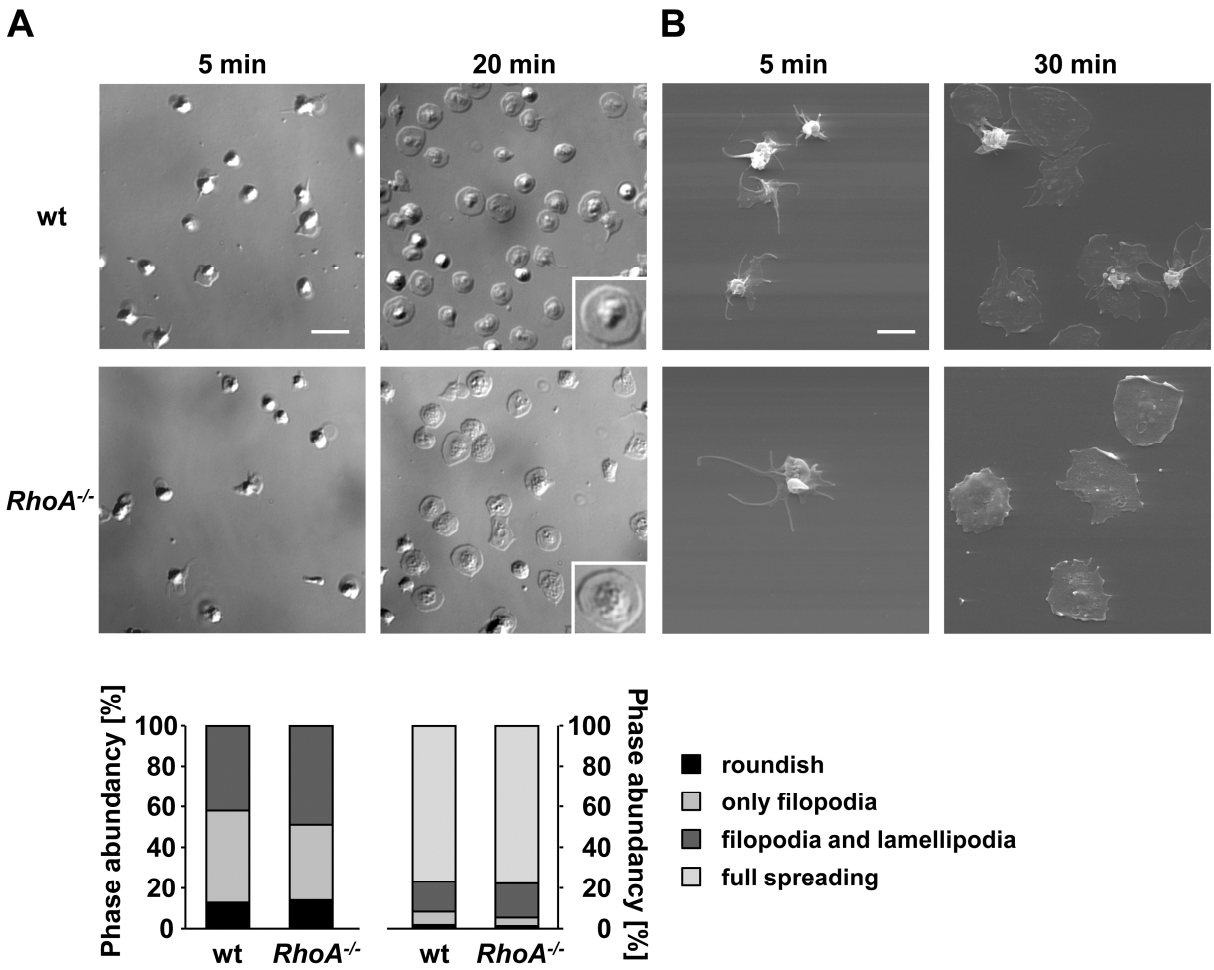

Figure 25. *RhoA*$^{-/-}$ platelets normally spread on fibrinogen. Washed platelets of wt and *RhoA*$^{-/-}$ mice were allowed to spread on fibrinogen (100 µg/ml) after stimulation with 0.001 U/ml thrombin. A, Representative DIC images of 3 individual experiments were taken at the indicated time points (top) and statistical evaluation of the percentage of spread platelets at different spreading stages at the respective time point (bottom). Bar, 5 µm. B, Scanning electron microscopy (SEM) pictures of spread wt and *RhoA*$^{-/-}$ platelets. Bar, 2.5 µm.

Furthermore, to assess whether the cytoskeletal ultrastructure was influenced by the RhoA deficiency although the spreading process of these platelets was entirely normal, the actin structures were visualized in more detail by *Stimulated Emission Depletion* (STED) microscopy in collaboration with Shuchi Gupta in our group (Figure 26A). Interestingly, spread wild-type platelets displayed a typical condensed F-actin ring structure and marked stress fiber formation, whereas in contrast, these structures were only partially formed and appeared more diffuse in fully spread *RhoA*$^{-/-}$ platelets. To determine whether *RhoA*$^{-/-}$ platelets generally have the capacity to assemble actin filaments, flow cytometric analyses were performed to measure F-actin assembly after agonist stimulation (Figure 26B). In these measurements, no differences in the F-actin content of resting platelets and thrombin-induced F-actin assembly could be detected between the two groups. These data indicated that, although RhoA is suggested to be essential for F-actin bundling and stress fiber

formation in numerous cell types, RhoA-deficiency only moderately influenced actin cytoskeletal structures in activated platelets.

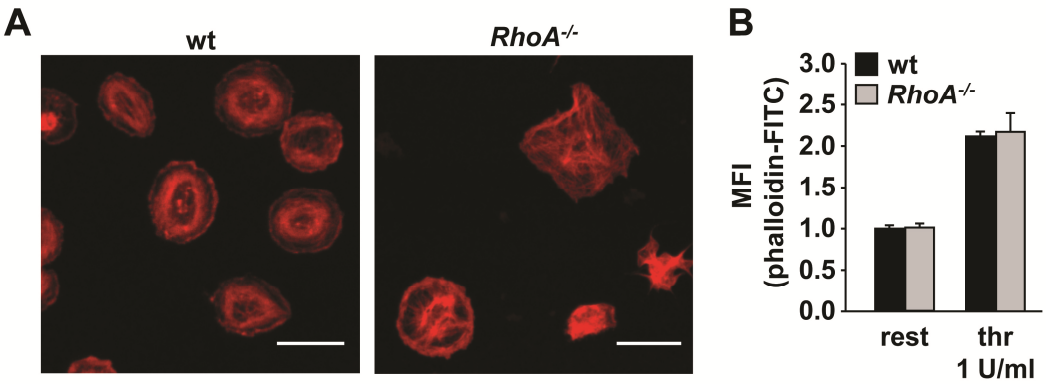

Figure 26 *RhoA*$^{-/-}$ platelets show moderately altered actin cytoskeletal structures but unaltered F-actin assembly after activation. Washed wt and *RhoA*$^{-/-}$ platelets were allowed to spread on a fibrinogen-coated surface and analyzed with STED microscopy. A, Representative pictures taken after 40 min of spreading are depicted. Bars, 5 µm. B, Resting and activated platelets of the indicated genotype were fixed, permeabilized, stained with phalloidin-FITC and directly analyzed using flow cytometry. Values are mean ± SD of at least 4 mice per group. Abbreviations: thr= thrombin.

Moreover, additional detailed confocal microscopy studies were performed to visualize on the one hand tubulin structures and on the other hand the distribution of α granules in spread *RhoA*$^{-/-}$ platelets as the aforementioned DIC and SEM pictures indicated a less condensed cell body in these platelets. The microtubules formed a nearly two-ring structure with an outer and inner ring in wild-type platelets after spreading, whereas, in contrast the microtubule coil seemed rather disassembled and more branched in *RhoA*$^{-/-}$ platelets (Figure 27A). VWF–staining of spread *RhoA*$^{-/-}$ platelets showed a broader distribution of granules by confocal microscopic analysis as compared to wild-type platelets, which confirmed the previous assumption that granules are less centralized in spread *RhoA*$^{-/-}$ platelets (Figure 27B).
Together, these findings strongly suggest that RhoA deficiency affects to a certain extent the actin and tubulin cytoskeletal reorganization which, however, does not result in altered spreading of these platelets.

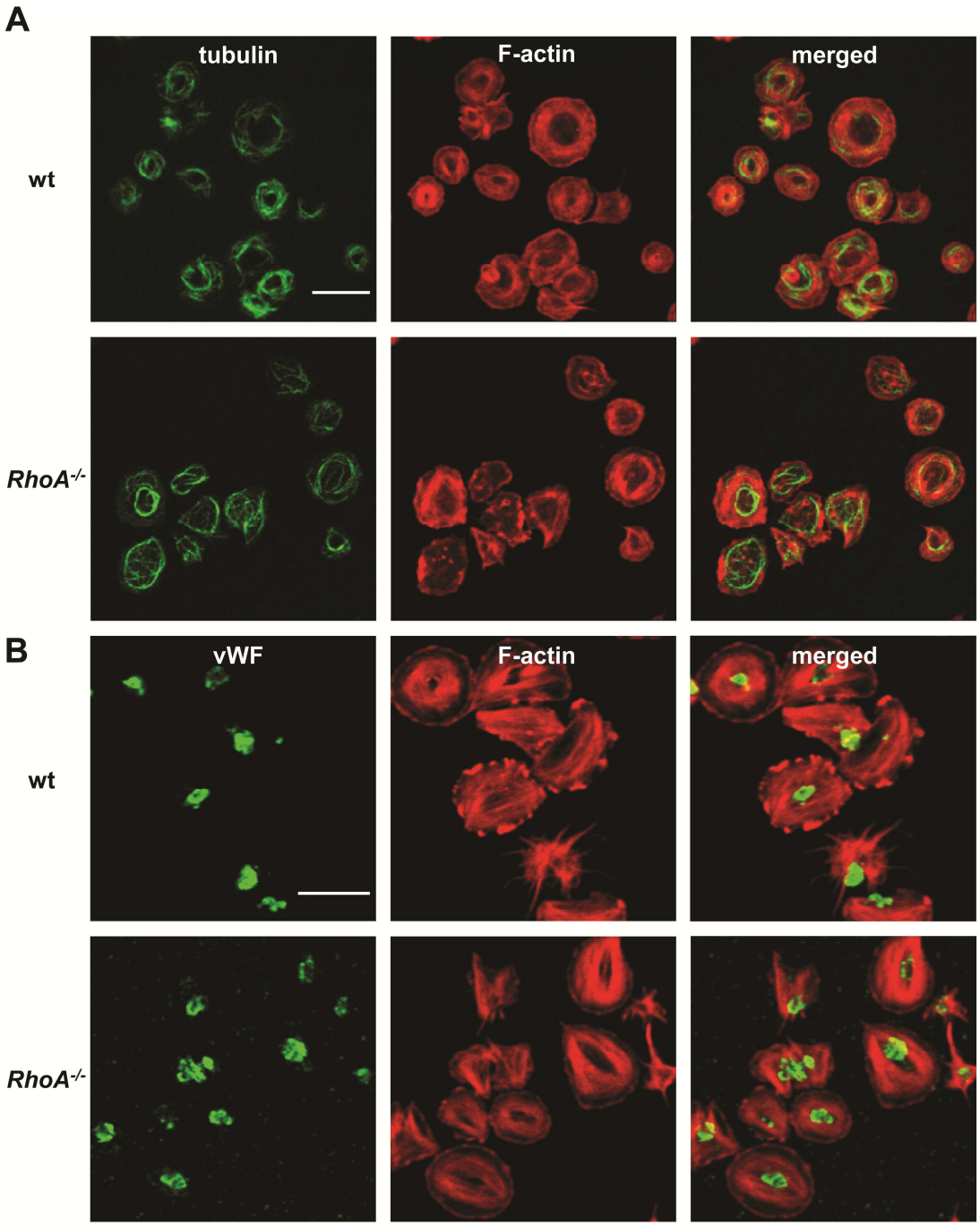

Figure 27. Moderately altered tubulin structures and less centralized α granules in spread *RhoA*$^{-/-}$ platelets. Washed wt and *RhoA*$^{-/-}$ platelets were allowed to spread on a fibrinogen-coated surface and analyzed with confocal microscopy after A, staining for tubulin (green) and actin (red) and B, vWF (green) and actin (red; acquired with STED technique). Representative pictures taken after 40 min of spreading are depicted. Bars, 5 µm.

Upon ligand binding integrin αIIbβ3 can also mediate clot retraction which is highly dependent on the cytoskeletal contractility of platelets[197]. The role of RhoA in this signaling process is, however, controversially discussed[139,140]. Therefore, clot formation in prp of wild-type and *RhoA*$^{-/-}$ mice was induced by high dose thrombin (5 U/ml) in the presence of high Ca^{2+} concentrations (20 mM) and clot retraction was monitored under non-stirring conditions over time (Figure 28). While, clot retraction started already 30 min after activation of wild-type

prp and proceeded to the maximum after 4 h, it was nearly abolished in *RhoA*-deficient prp showing only moderately retraction within the same time period.

These data revealed that RhoA is essential for integrin-mediated clot retraction, but dispensable for spreading of activated platelets on fibrinogen.

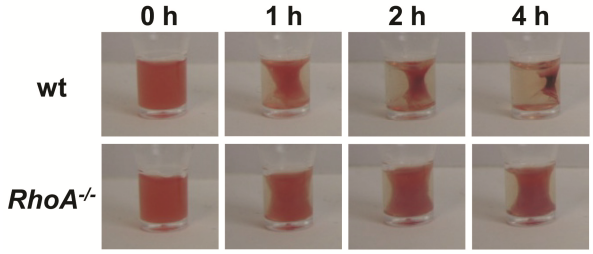

Figure 28. *RhoA*$^{-/-}$ platelets fail to support integrin-dependent clot retraction. Clot retraction of wt and RhoA-deficient prp upon activation with 5 U/ml thrombin and 20 mM $CaCl_2$ at the indicated time points is depicted.

4.5.7 *RhoA*$^{-/-}$ platelets show slightly reduced aggregate formation on collagen and adhesion on vWF under high shear flow

Thrombus formation at the wound site is initiated by platelet adhesion and activation on the extracellular matrix and promoted by the action of locally released secondary mediators which become, however, rapidly cleared in the flowing blood. Under these conditions, reduced platelet degranulation may limit thrombus formation, particularly at high shear rates. Therefore, the ability of *RhoA*$^{-/-}$ platelets to form platelet aggregates on a collagen-coated surface was analyzed in a whole blood perfusion system. To avoid differences in thrombus size due to the reduced platelet count in *RhoA*$^{-/-}$ mice, blood from RhoA-deficient mice was reconstituted with isolated *RhoA*$^{-/-}$ platelets to adjust the platelet count comparable to that of wild-type mice. At a shear rate of 1700 sec^{-1}, mimicking flow conditions in arterioles, wild-type and *RhoA*$^{-/-}$ platelets formed large three-dimensional aggregates which covered similar surface areas at the end of the perfusion time (52.3 ± 4.3% for *RhoA*$^{-/-}$ platelets and 53.7 ± 6.0% for wild-type platelets; p=0.68; Figure 29A). The relative thrombus volume was also indistinguishable between wild-type and *RhoA*$^{-/-}$ platelets (data not shown). Remarkably, however, under higher shear rates (7700 sec^{-1}), resembling flow conditions in small arterioles or stenosed arteries, aggregate formation of *RhoA*$^{-/-}$ platelets was moderately, but significantly reduced as compared to wild-type platelets (mean surface coverage 3.2 ± 0.9% for *RhoA*$^{-/-}$ platelets and 5.2 ± 1.8% for wild-type platelets, $p<0.05$; Figure 29A) indicating that RhoA is relevant for thrombus formation only under high shear conditions. These findings pointed to an impaired interaction between GPIb and collagen-bound vWF in the absence of RhoA.

To directly test whether the reduced shear-dependent aggregate formation in RhoA-deficient blood was caused by an altered GPIb-vWF interaction, platelet adhesion to immobilized murine vWF was analyzed at a shear rate of 7700 sec^{-1} in the same flow chamber system.

Although the initial adhesion of *RhoA*$^{-/-}$ platelets and also the number of platelets adherent after 1 min of the washing period was comparable to wild-type platelets (Figure 29B), the distance which could be covered by rolling platelets within 1 min of the washing period on the vWF surface was significantly increased for *RhoA*$^{-/-}$ platelets in contrast to wild-type platelets (mean distance 26.4 ± 7.8 µm for *RhoA*$^{-/-}$ and 16.1 ± 2.3 µm for wild-type platelets; $p<0.05$; Figure 29B), suggesting a reduced ability of RhoA-deficient platelets to interact with vWF.

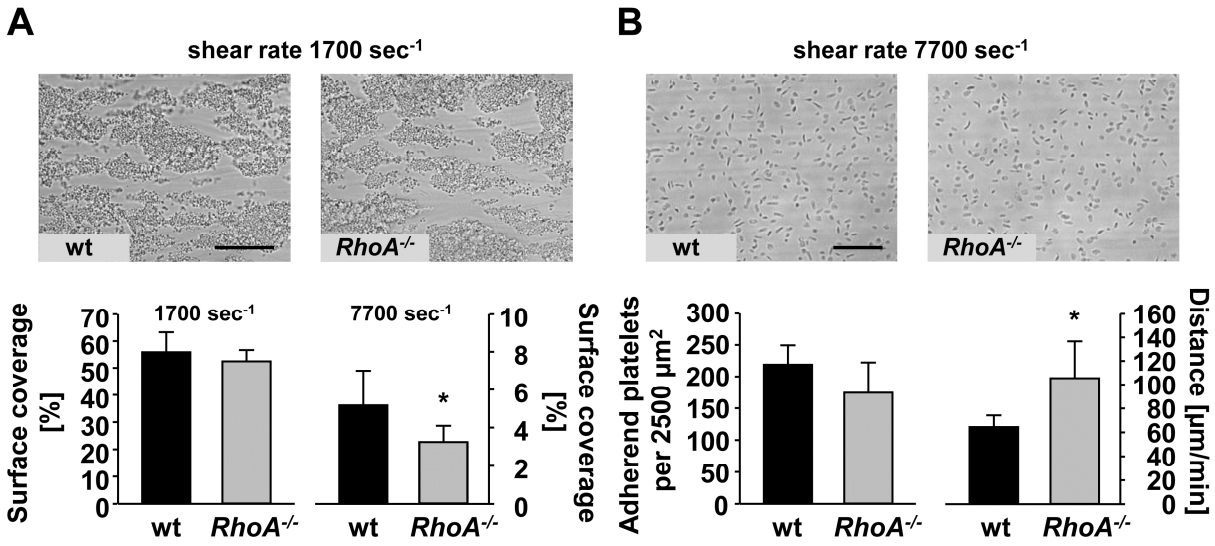

Figure 29. Aggregate formation on collagen and adhesion on vWF of *RhoA*$^{-/-}$ platelets under flow conditions. Whole blood was perfused over a collagen-coated surface at the indicated shear rates. A, Representative phase contrast images at the end of the perfusion time are illustrated (top) and mean surface coverage ± SD of at least 5 mice is shown (bottom). Bar, 100 µm. B, Blood was perfused over immobilized murine vWF at a shear rate of 7700 sec^{-1} and representative pictures after 1 min of the washing period are shown (top). The number of adherent platelets after 1 min of the washing period (bottom, left) and distance covered by wt and *RhoA*$^{-/-}$ platelets within 1 min under flow is depicted (bottom, right). *, $p<0.05$.

4.5.8 RhoA is critical for thrombus stabilization *in vivo*

To examine to which extent the observed *in vitro* defects of *RhoA*$^{-/-}$ platelets influence thrombus formation *in vivo*, intravital fluorescence microscopy after $FeCl_3$-induced vascular injury of small mesenteric arterioles was performed. Although the kinetics of first thrombus formation were comparable between wild-type and *RhoA*$^{-/-}$ mice (data not shown), subsequent stable and occlusive thrombus formation was strongly impaired in RhoA-deficient mice as compared to wild-type. Whereas thrombi progressed to complete vessel occlusion in 8 out of 9 wild-type arterioles (89%) (mean time to occlusion 16.9 ± 2.9 min; Figure 30A-C), only 21.5% of *RhoA*$^{-/-}$ vessels occluded irreversibly within the observation period of 40 min ($p<0.01$). In 57% arterioles of *RhoA*$^{-/-}$mice no occlusion occurred at all and further 21.5% of the vessels were transiently occluded for <2 min but then completely recanalized (Figure 30A-C). This defect was mainly based on embolization of thrombus fragments from the thrombus surface, after reaching a considerable size in the vessel whereby shear forces

probably passed a threshold at which the RhoA-dependent platelet activation defect became evident.

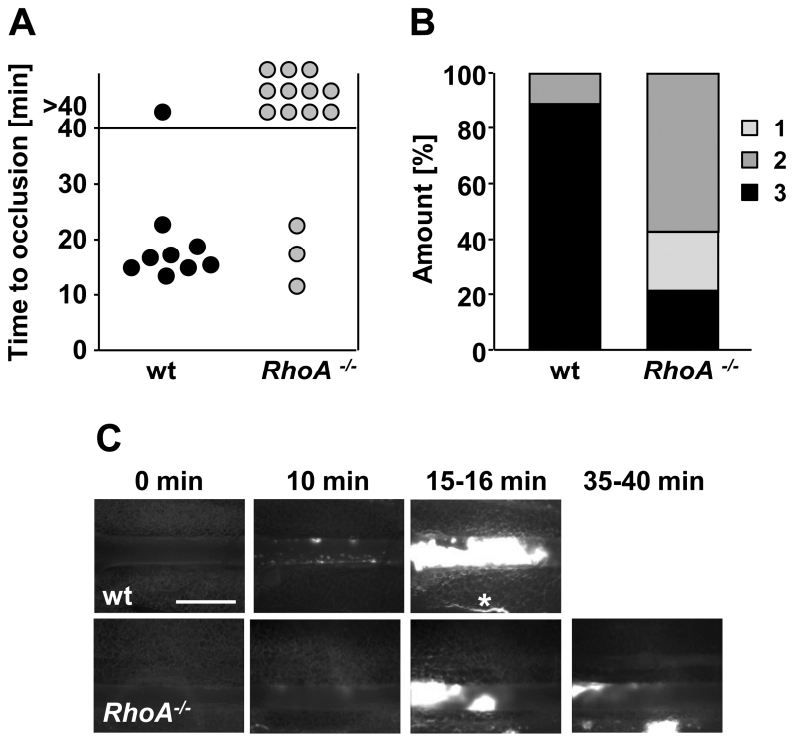

Figure 30. *RhoA*$^{-/-}$ mice display unstable thrombus formation after $FeCl_3$-induced vascular injury. Small mesenteric arterioles were injured by topical application of $FeCl_3$ and thrombus formation of fluorescently labeled platelets was monitored using intravital microscopy. A, Time to stable vessel occlusion and B, amount of (1) non-occluded, (2) recanalized and (3) stably occluded vessels after injury of wt and *RhoA*$^{-/-}$ mice are shown. Each symbol represents one arteriole. C, Representative pictures at the indicated time point. Bar, 100 µm. Asterisk indicates stable occlusion of the vessel.

In a second arterial thrombosis model, thrombus formation was induced by mechanical injury of the abdominal aorta and monitored by blood flow measurements using an ultrasonic flow probe. Although full and stable occlusion occurred in 9 out of 10 wild-type mice within 8 min (mean time to occlusion 384 ±79 sec; Figure 31A-C), blood flow only decelerated on average to 50% of the initial value after injury in *RhoA*$^{-/-}$ mice and remained rather constant with some fluctuations, indicating thrombus embolization, until the end of the observation period ($p<0.001$; Figure 31A-C). Consequently, none of the *RhoA*$^{-/-}$ mice displayed vessel occlusion. These results demonstrate that RhoA is required for final thrombus propagation and stabilization in small as well in large arteries.

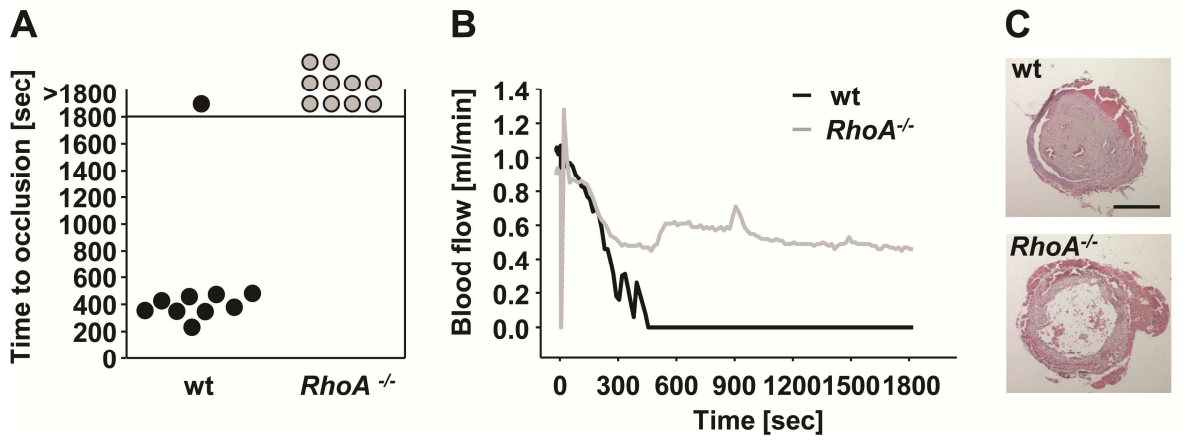

Figure 31. Defective thrombus formation in *RhoA*$^{-/-}$ mice after mechanical injury. The abdominal aorta of wt and *RhoA*$^{-/-}$ mice was injured by tight compression with a forceps and blood flow was monitored for 30 min. A, Time to stable vessel occlusion and B, Representative blood flow curves are shown. Each symbol represents one individual. C, Representative cross sections of the abdominal aorta of wt and *RhoA*$^{-/-}$ mice 30 min after injury. Bar, 200 µm.

In line with the above described observations, RhoA-deficient mice also exhibited a profound hemostatic defect as assessed in a tail bleeding assay where mouse tails were immediately immerged into saline at 37°C after tail tip cut. Whereas bleeding stopped in 15 out of 16 (94%) wild-type mice (mean bleeding time 179 ± 196 sec; Figure 32), bleeding was markedly increased in *RhoA*$^{-/-}$ mice with 13 out of 18 (72%) mice which bled for more than 20 min ($p<0.001$; Figure 32). Interestingly, in many of the *RhoA*$^{-/-}$ mice blood loss, determined by visual inspection, temporarily decreased or even transiently stopped for <1 min during the observation period, indicating that RhoA deficiency also destabilizes clots during normal hemostasis.

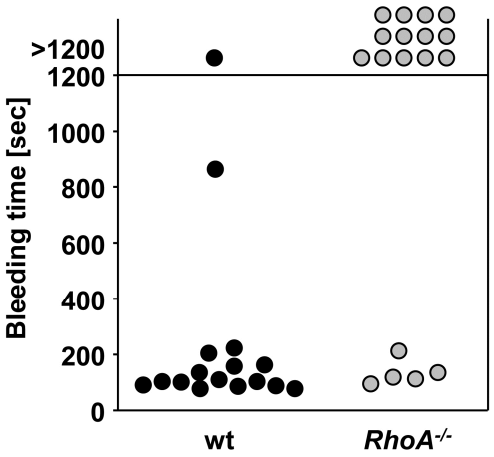

Figure 32. Impaired hemostasis in *RhoA*$^{-/-}$ mice. Tail bleeding times determined in saline at 37°C of wt and *RhoA*$^{-/-}$ mice. Each symbol represents one individual.

4.5.9 *RhoA*$^{-/-}$ mice are protected from ischemic brain infarction

Cerebral ischemia has been proposed to be a complex thrombo-inflammatory disease[198] in which the microvascular integrity is disturbed[199]. However the signaling events leading to intravascular thrombus formation in the ischemic brain are only partially understood. To test

whether the observed thrombus instability of *RhoA*$^{-/-}$ mice in arterial thrombosis also affects the outcome in this setting, mice were challenged in a tMCAO model, performed in collaboration with Christoph Kleinschnitz, Department of Neurology, University Clinic, Würzburg, Germany. Therefore, a thread was advanced through the carotid artery into the middle cerebral artery to reduce cerebral blood flow and removed after 1 h to allow reperfusion. The extent of infarction was quantitatively assessed 24 h after reperfusion on 2,3,5-triphenyltetrazolium chloride (TTC)-stained brain slices. In *RhoA*$^{-/-}$ mice, brain infarct volumes were reduced to ~50% of the infarct volumes in wild-type mice (43.7 ± 30.5 mm^3 for *RhoA*$^{-/-}$ and 80.1 ± 28.8 mm^3 for wild-type mice, $p<0.01$; Figure 33A). This reduction in ischemic lesions of *RhoA*$^{-/-}$ mice also resulted in significantly fewer neurological deficits compared to wild-type, determined as Bederson score assessing global neurological function (1.2 ± 1.3 vs. 2.9 ± 1.6, $p<0.05$; Figure 33B) and grip test which indicates motor function and coordination of the mice (3.7 ± 0.7 vs. 2.6 ± 1.0; $p<0.01$; Figure 33C). These data also established an important role for RhoA-dependent platelet signaling in the pathomechansim of ischemic stroke.

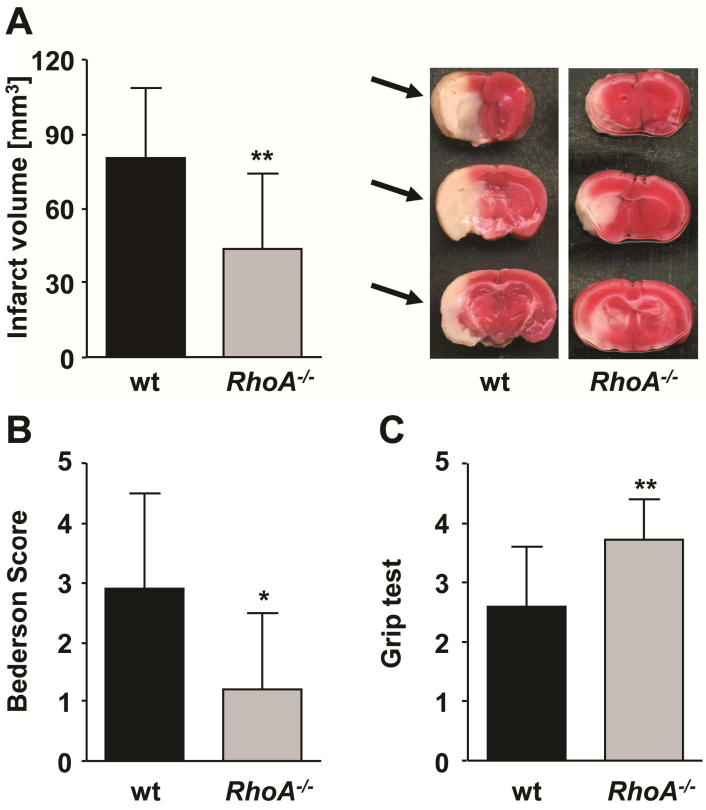

Figure 33. *RhoA*$^{-/-}$ mice are protected from cerebral ischemia. Formation of cerebral brain infarction and consequential neurological defects were investigated in a murine stroke model. A, Brain infarct volumes in wt (n=24) and *RhoA*$^{-/-}$ mice (n=14) presented as mean ± SD; (left). Representative images of three corresponding coronal sections from wt and *RhoA*$^{-/-}$ mice stained with TTC 24 h after tMCAO. Infarct areas are marked with arrows (right). Bederson score B, and grip test C, determined 24 h after tMCAO. *, $p<0.05$; **, $p<0.01$.

4.6 FXIIa inhibitor rHA-Infestin-4 abolishes occlusive arterial thrombus formation without affecting bleeding

Previous studies with FXII deficient mice revealed that this coagulation factor is essential for arterial thrombus formation but dispensable for normal hemostasis[169,170]. Accordingly, FXII was proposed as a very promising target candidate for effective antithrombotic therapy that may not be accompanied by bleeding side effects. Based on this proposal, it was aspired to generate a new antithrombotic agent that targets FXII and concurrently exhibits clinically suitable pharmacokinetics. One possible approach for the identification of new inhibitors of the plasma coagulation system is the search for examples in nature and thus most promising anticoagulant proteins produced by blood-feeders. These animals have developed efficient mechanisms to overcome the host's hemostatic barrier and to keep blood in a fluid state during acquisition and digestion. In 2002, Campos *et al*. isolated a specific thrombin inhibitor, named Infestin, from the midgut of the hematophagus insect *Triatoma infestans*[200]. Infestin belongs to the non-classical Kazal-type serine protease inhibitor family and is composed of two non-classical Kazal-type domains, although its gene encodes four domains, most probably due to unknown post-transcriptional mechanisms. Subsequent analysis of recombinant proteins expressing different non-classical Kazal-type domains of the Infestin gene revealed that domains 1-2 show strong thrombin inhibition whereas the fourth domain encodes a protein (Infestin-4) that exhibits a strong inhibitory potential against FXIIa[201].
According to these findings, CSL Behring (Marburg, Germany) generated a 73 kDa fusion protein consisting of recombinant human albumin (rHA) and Infestin-4 with the intention to develop a specific FXIIa inhibitor suitable for antithrombotic therapy. The protein was found to display a high recovery of ~92% and a half-life of 4.6 h after i. v. injection into mice[202]. The effect of rHA-Infestin-4 on the integrity of plasma coagulation *in vitro* was initially assessed by determining the clinical parameters activated partial thromboplastin time (aPTT) and prothrombin time (PT). rHA-Infestin-4 was shown to prolong aPTT in a dose-dependent manner without affecting PT in standard human plasma (SHP), in mouse as well as in rat plasma[202]. Similar results were obtained *ex vivo* when mice were treated with 200 mg/kg rHA-Infestin-4[202]. The following functional characterization of rHA-Infestin-4 was performed in collaboration with CSL Behring.

4.6.1 rHA-Infestin-4 specifically inhibits the coagulation factor XIIa

The initial analyses by CSL Behring indicated that rHA-Infestin-4 specifically inhibits the intrinsic coagulation pathway. To test this in more detail, the specificity of the protein for different human serine proteases of the intrinsic (αFXIIa, βFXIIa, FXIa and FIXa), the extrinsic (FVIIa) and the common (FXa and thrombin) pathway was analyzed using

chromogenic assays. After incubation of rHA-Infestin-4 with the respective protease in the presence of a specific chromogenic substrate, the remaining protease activity was determined based on absorption measurements at 405 nm. Interestingly, a 1:1 molar ratio of fully enzymatically active αFXIIa and rHA-Infestin-4 resulted in efficient FXIIa inhibition of >90%, equal to the inhibitory efficiency of rHA-Infestin-4 towards the small βFXIIa fragment, indicating that the inhibitor most probably interferes with the catalytic domain of FXIIa (Table 2). In contrast, even a molar ratio of 1:90 of FXIa and rHA-Infestin-4 showed no effect on FXIa activity. To relate this inhibitory potential of rHA-Infestin-4 to the activity of the physiological inhibitor of contact activation, the plasmatic C1 inhibitor was used under the same conditions as control. Only a 16-fold molar excess of C1 inhibitor resulted in an approximate but not full inhibition of FXIIa, and a 1:90 molar ratio already inhibits 60% of FXIa activity. Since the used specific chromogenic substrates are small peptides which do not completely resemble the steric conditions during proteolysis present *in vivo*, a more physiologically structured macromolecule (Casein-Resorufin) was used by Stefan Schmidbauer (CSL Behring, Marburg, Germany) as chromogenic substrate for FXIIa and FXIa. Under these conditions, similar to results obtained with peptide substrates, a 1:1 ratio of FXIIa and rHA-Infestin-4 lead to a remarkable protease inhibition of ~85%, whereas it did not affect FXIa activity.

Inhibitor	Molar ratio	Inhibition [%]
rHA-Infestin-4	1:1, αFXIIa:inhibitor	>90
C1 inhibitor	1:16, αFXIIa:inhibitor	85
rHA-Infestin-4	1:90, FXIa:inhibitor	0
C1 inhibitor	1:90, FXIa:inhibitor	60
rHA-Infestin-4	1:1, βFXIIa:inhibitor	>90
rHA-Infestin-4	1:100, FIXa:inhibitor	0
rHA-Infestin-4	1:100, FXa:inhibitor	8
rHA-Infestin-4	1:100, FVIIa:inhibitor	0
rHA-Infestin-4	1:100, thrombin:inhibitor	0
rHA-Infestin-4	1:100, kallikrein:inhibitor	7

Table 2. Protease specificity of rHA-Infestin-4. Inhibition of the indicated proteases by rHA-Infestin-4 was assessed in a chromogenic assay. The inhibitor was incubated with the respective protease at the indicated molar ratio in presence of a specific protease substrate. The resulting protease activity was determined at 405 nm. The percentage of protease inhibition was calculated according to a standard curve. Results were obtained from 4 independent experiments. C1 inhibitor (plasmatic FXIIa inhibitor, CSL Behring) served as control inhibitor. (Hagedorn *et al*., *Circulation*, 2010)[202].

Furthermore, rHA-Infestin-4 did not inhibit FIXa, FVIIa or thrombin activity and only mildly influenced (8% inhibition) FXa activity when tested in a 100-fold molar excess (Table 2).

Since FXIIa can also activate the kallikrein/kinin system, the direct effect of rHA-Infestin-4 on plasma kallikrein was determined, though, rHA-Infestin-4 only slightly inhibited (7% inhibition) the activity of the protease at a 1:100 molar ratio (Table 2). Taken together, these results clearly confirmed that rHA-Infestin-4 is a highly selective inhibitor of FXIIa.

4.6.2 rHA-Infestin-4 displays a significant impact on fibrinolysis

FXIIa has also been shown to be involved in the initiation of fibrinolytic processes[151-153]. Hence, to test a possible effect of rHA-Infestin-4 on fibrinolysis, pooled mouse plasma was incubated with either vehicle or different concentrations of rHA-Infestin-4 before clotting was triggered by thromboplastin (activation of the extrinsic pathway). The degree of subsequent clot lysis was determined as D-Dimer concentration assessed by an ELISA system 1 h after starting the reaction. A rHA-Infestin-4 concentration of 0.1 mg/ml had no influence on D-Dimer concentration, whereas 1 mg/ml, which approximately mimics the inhibitor concentration used for the following *in vivo* experiments, moderately decreased D-Dimer concentration compared to control by 23% (158.8 ± 16.6 ng/ml for rHA-Infestin-4 and 205.5 ± 21.0 ng/ml for control; p=0.04). However, this reduction never exceeded 38% even when a tenfold higher concentration of rHA-Infestin-4 (10 mg/ml) was used. These results showed that rHA-Infestin-4 exerts a moderate inhibitory effect on fibrinolysis.

To determine whether this effect of rHA-Infestin-4 is indirectly mediated via FXIIa inhibition or directly by blockage of proteases of the fibrinolytic cascade, the potency of rHA-Infestin-4 to inhibit plasmin, tPA and uPA was analyzed using chromogenic assays. Interestingly, whereas rHA-Infestin-4 did not influence tPA and uPA activity, it efficiently inhibited 95% of the plasmin activity in a molar ratio of 1:0.8 (Table 3). These data suggested that rHA-Infestin-4 affects fibrinolysis most probably by inhibiting plasmin.

Inhibitor	Molar ratio	Inhibition [%]
rHA-Infestin-4	1:0.8, plasmin	95
rHA-Infestin-4	1:100, tPA	0
rHA-Infestin-4	1:100, uPA	0

Table 3. Inhibition of serine proteases of the fibrinolytic cascade by rHA-Infestin-4. Inhibition of the indicated proteases by rHA-Infestin-4 was assessed in a chromogenic assay. The inhibitor was incubated with the respective protease at the indicated molar ratio in presence of a specific protease substrate. The resulting protease activity was determined at 405 nm. The percentage of protease inhibition was calculated according to a standard curve. Results were obtained from 4 independent experiments. tPA=tissue plasminogen activator, uPA= urokinase plasminogen activator.

4.6.3 Prevention of arterial thrombosis in rHA-Infestin-4 treated mice

At sites of atherosclerotic plaque rupture, platelets and the plasma coagulation system become activated and lead to arterial thrombosis. Therefore, it was important to determine

the inhibitory effect of rHA-Infestin-4 on thrombus formation *in vivo* using a model of occlusive arterial thrombosis. The injury was induced on small mesenteric arterioles by topical application of 20% $FeCl_3$. Based on results of previous dose-finding studies, one consistent and potent concentration of rHA-Infestin-4 was chosen for the *in vivo* experiments (200 mg/kg body weight). It is important to note that only approximately 10% of the molecular mass of rHA-Infestin-4 corresponds to the active inhibitor, Infestin-4 (~7 kDa), whereas albumin (~66 kDa) accounts for the rest. To additionally assess the time course of the effect of rHA-Infestin-4, arterioles of mice treated i.v. with the recombinant fusion protein or PBS as control were injured at different time points after the treatment and monitored by intravital fluorescence microscopy. In the first group of mice, vessels were subjected to injury 10 min after the injection of rHA-Infestin-4. In all animals, platelets rapidly adhered to the injured vessel wall, however, whereas in control mice formation of thrombi and finally full occlusion of the vessel occurred in all cases (mean time to occlusion 16.9 ± 2.2 min), only platelet adhesion was detectable in all (7/7) of the rHA-Infestin-4 injected mice throughout the observation period of 40 min (Figure 34A,C). A similar inhibitory potency of the fusion protein was detectable when injury was induced 60 min after injection (data not shown). When the lesion was induced in vessels ~105 min after the application of rHA-Infestin-4, small platelet aggregates formed but this was delayed in 71% of the arterioles (20.0 ± 3.7 min for rHA-Infestin-4 treated mice and 6.3 ± 0.7 min for control; $p<0.001$; Figure 34B). Furthermore, all formed thrombi were unstable and in no case reached the size necessary for vessel occlusion. This was mainly due to the permanent detachment of single platelets from the surface of the thrombi. Similar findings were made when the mice were challenged in a second *in vivo* model, where the carotid artery was injured by 10% $FeCl_3$ and blood flow was monitored by an ultrasonic flow probe to assess thrombus formation. In all control animals (10/10) irreversible vessel occlusion occurred within 14 min (mean time to occlusion 8.6 ± 2.2 min) after injury, whereas in 90% of the rHA-Infestin-4 injected (189 mg/kg body weight) mice blood flow remained unaltered throughout the observation period of 60 min (Figure 34D).

In addition, to exclude that the observed inhibitory potency of rHA-Infestin-4 was only restricted to mice, CSL Behring (Marburg, Germany) also analyzed the effect of the inhibitor on arterial thrombosis in rats. Injection of rHA-Infestin-4 (100 mg/kg body weight) efficiently prolonged aPTT in these animals as compared to controls without affecting PT and as a consequence profoundly protected rats from occlusive thrombus formation in a $FeCl_3$-induced injury model of the carotid artery[202].

Together, these results demonstrated that rHA-Infestin-4 is a strong inhibitor of arterial thrombus formation in mice as well as in rats.

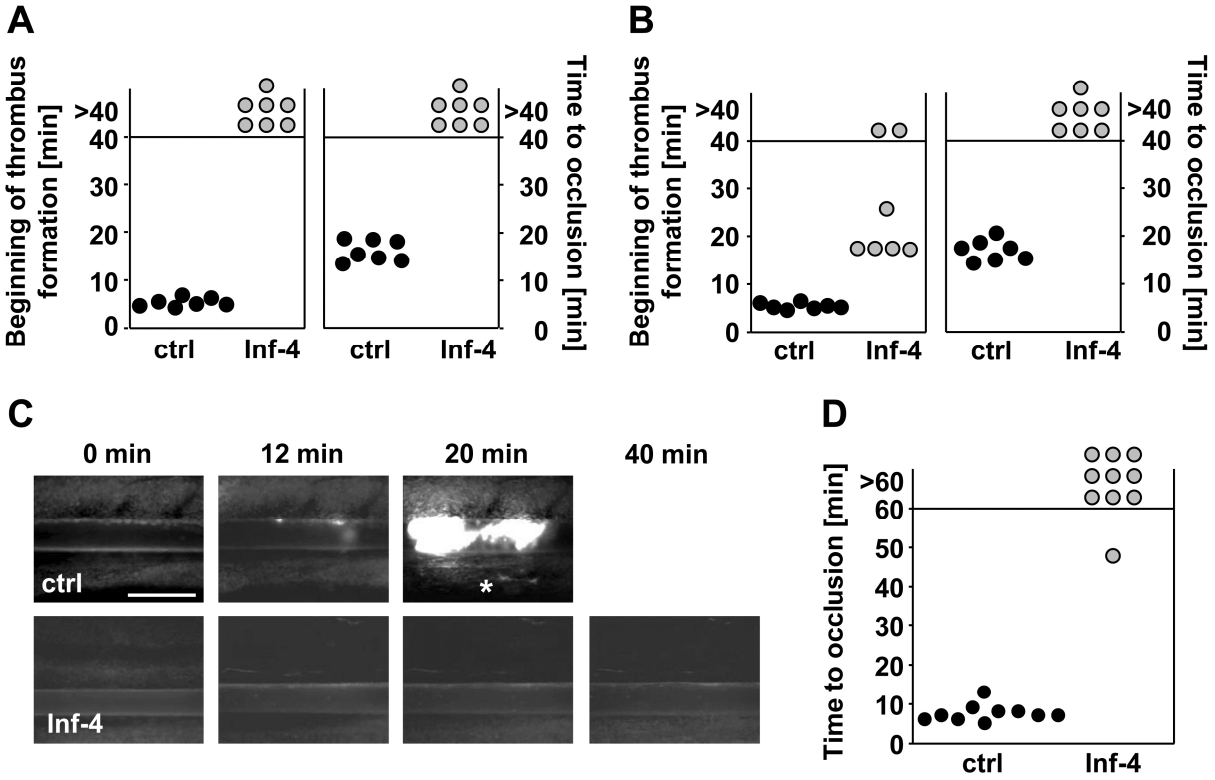

Figure 34. rHA-Infestin-4 blocks arterial thrombus formation in mice. Thrombus formation after $FeCl_3$-induced injury of mesenteric arterioles was monitored using intravital fluorescence microscopy. Beginning of first thrombus formation >10 µm and time to full vessel occlusion after injury, A, 10 min and B, 105 min, prior to i.v. injection of rHA-Infestin-4 (n=7) and PBS (n=7), respectively, are illustrated. Each symbol represents one arteriole. C, Representative images taken at the indicated time points. Bar, 100 µm. The asterisk indicates complete vessel occlusion. D Time to occlusion after $FeCl_3$-induced thrombosis in the carotid artery is depicted (n=10). Each symbol represents one individual. Ctrl = control and Inf-4 = recombinant human albumin-Infestin-4 fusion protein. (Hagedorn *et al*., *Circulation*, 2010)[202].

During the operations to gain access to the respective vessels, small lesions of the circumjacent tissue could not be avoided. However, similar to the observations in FXII-deficient mice[169], rHA-Infestin-4 injected animals showed no alterations in surgery-caused bleeding compared to controls. To corroborate this observation, the effect of rHA-Infestin-4 on hemostasis was studied in a tail bleeding model (Figure 35). All rHA-Infestin-4 treated mice (10/10) were able to arrest bleeding within the same time frame as the control animals, even when injected with an extremely high dose (400 mg/kg of body weight), (114 ± 77 sec for rHA-Infestin-4 treated mice, 190 mg/kg; p=0.38; 115 ± 35 sec for rHA-Infestin-4 treated mice, 400 mg/kg; p=0.34; 153 ± 146 sec for control). In line with this, also the blood loss during the period of bleeding was comparable between rHA-Infestin-4 treated and control mice (data not shown). Similarly, also rHA-Infestin-4 treated rats displayed normal bleeding times as assessed in a tail bleeding assay by CSL Behring (Marburg, Germany)[202]. These results indicate that rHA-Infestin-4 treatment does not interfere with normal hemostasis.

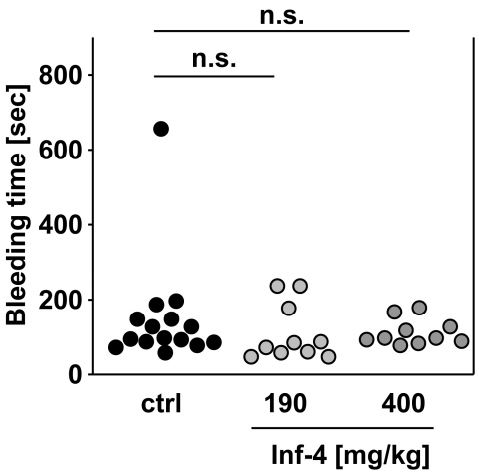

Figure 35. Tail bleeding assay of control and rHA-Infestin-4 treated mice. Tail tip was removed 10 min after i.v. injection of PBS (n=15) or rHA-Infestin-4 (n=10). Each symbol represents one individual. Ctrl = control and Inf-4 = recombinant human albumin-Infestin-4 fusion protein. (Hagedorn *et al*., *Circulation*, 2010)[202].

4.6.4 rHA-Infestin-4 does not reduce residual thrombus formation in *F12*$^{-/-}$ mice

Previous studies on FXII-deficient mice revealed that they are markedly protected from arterial thrombosis, but the formation of microaggregates and unstable thrombi was still observed after endothelial damage in those animals[169]. In contrast, FXIIa inhibition in wild-type mice by rHA-Infestin-4 resulted in completely abolished thrombus formation raising the question whether the inhibitor, in addition to FXIIa, interfered with other components of the coagulation system. To test this directly, we compared thrombus formation in the mesenteric arteriole thrombosis model between wild-type and *F12*$^{-/-}$ mice, in each case untreated or treated with 200 mg/kg of rHA-Infestin-4 (Figure 36A,B). In all control animals (6/6) $FeCl_3$-induced injury lead to initial thrombus formation within 7.3 ± 0.9 min resulting in complete vessel occlusion during the 40 min observation period (mean time to occlusion 17.7 ± 3.0 min). As previously reported[169], beginning of thrombus formation in *F12*$^{-/-}$ mice was delayed (18.4 ± 9.3 min; p=0.02) compared to control mice and all formed thrombi were consistently unstable, degraded and frequently detached from the vessel wall and, consequently, never occluded the vessel. Remarkably, virtually the same result was obtained when *F12*$^{-/-}$ mice had been treated with rHA-Infestin-4 10 min prior to injury. In these animals, platelets rapidly adhered to the vessel wall and also formed little thrombi within a time frame similar to untreated *F12*$^{-/-}$ mice (18.1 ± 3.0 min; p=0.95). These thrombi were similarly unstable as those observed in untreated *F12*$^{-/-}$ mice and never reached vessel occlusion (Figure 36A,B). Importantly, in wild-type mice injected with rHA-Infestin-4 no aggregates formed and the vessel did not occlude during the observation period (data not shown). These observations demonstrated that rHA-Infestin-4 had no detectable effect on thrombus formation in FXII-deficient mice.

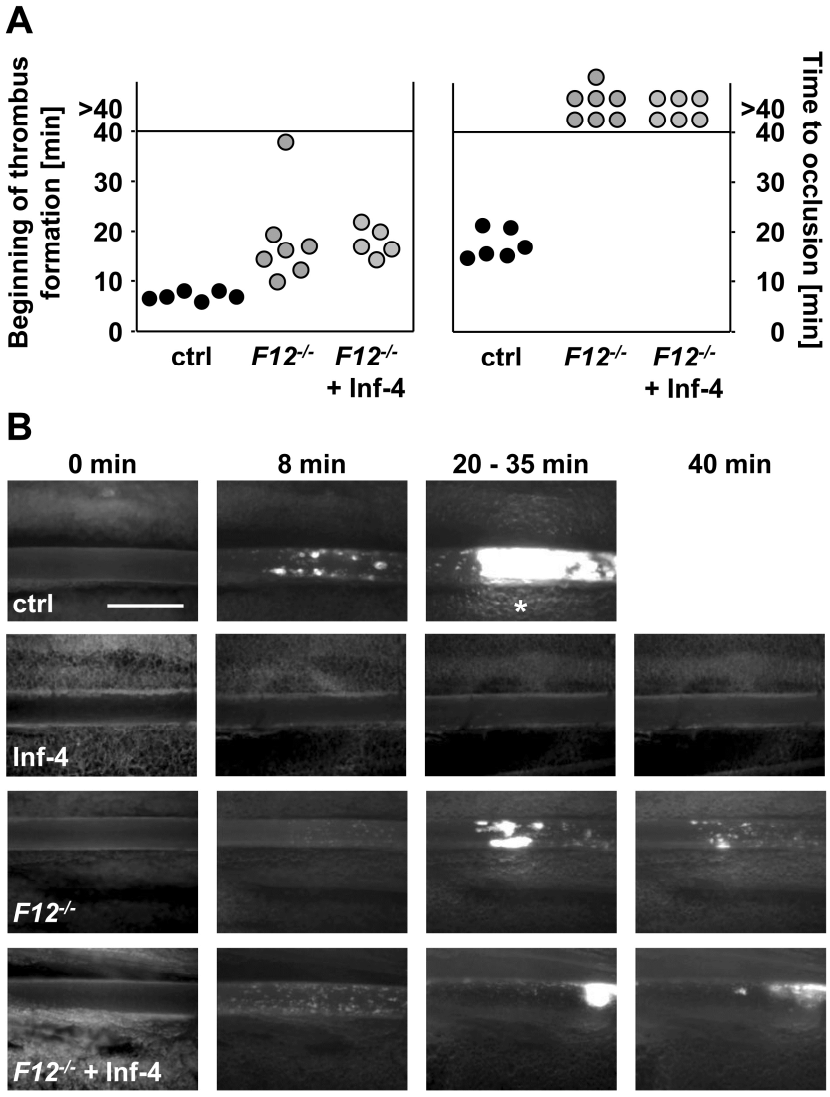

Figure 36. Arterial thrombosis in *F12*$^{-/-}$ mice injected with rHA-Infestin-4. *F12*$^{-/-}$ mice received rHA-Infestin-4 10 min before $FeCl_3$-induced endothelial injury. A, Time to first thrombus formation and B, time to complete vessel occlusion are shown. Each symbol represents one arteriole (n=6 for control and rHA-Infestin-4 inj. *F12*$^{-/-}$ mice, n=7 for *F12*$^{-/-}$ mice). C, Representative images acquired at the indicated time points/interval. Ctrl = control and Inf-4 = recombinant human albumin-Infestin-4 fusion protein. (Hagedorn *et al*., *Circulation*, 2010)[202].

4.6.5 rHA-Infestin-4 protects mice from ischemic brain infarction

Ischemic brain infarction is a thromboembolic disease that is frequently associated with death and severe disability. As recently shown on knockout mice, FXII is an important player in the development of experimental ischemic stroke making it a promising target for effective and safe therapy[170,203]. To test this hypothesis directly, the protective potency of rHA-Infestin-4 was assessed in a murine model of ischemic stroke together with Christoph Kleinschnitz, Department of Neurology, University Hospital, Würzburg, Germany. To initiate transient cerebral ischemia, a thread was advanced through the carotid artery into the middle cerebral artery (MCA) and allowed to remain for 1 h (transient MCA occlusion - tMCAO), reducing regional cerebral flow by >90%[204]. In rHA-Infestin-4 treated animals, infarct volumes

24 h after reperfusion, as assessed by 2,3,5-triphenyltetrazolium chloride (TTC) staining, were reduced to less than 17% of the infarct volumes in untreated animals (69.5 ± 33.7 mm^3 vs. 11.2 ± 5.3 mm^3; p<0.001; Figure 37A). Importantly, the observed protective effect of rHA-Infestin-4 was functionally relevant, as the Bederson score assessing global neurological function (1.2 ± 0.9 vs. 3.7 ± 0.7; p<0.001; Figure 37B) and the grip test, which specifically measures motor function and coordination (3.8 ± 0.8 vs. 1.9 ± 1.4; p=0.003; Figure 37C) were both significantly better in rHA-Infestin-4 treated mice as compared to control. These findings strongly indicate that inhibition of FXIIa by rHA-Infestin-4 could be a promising strategy to prevent ischemic brain infarction.

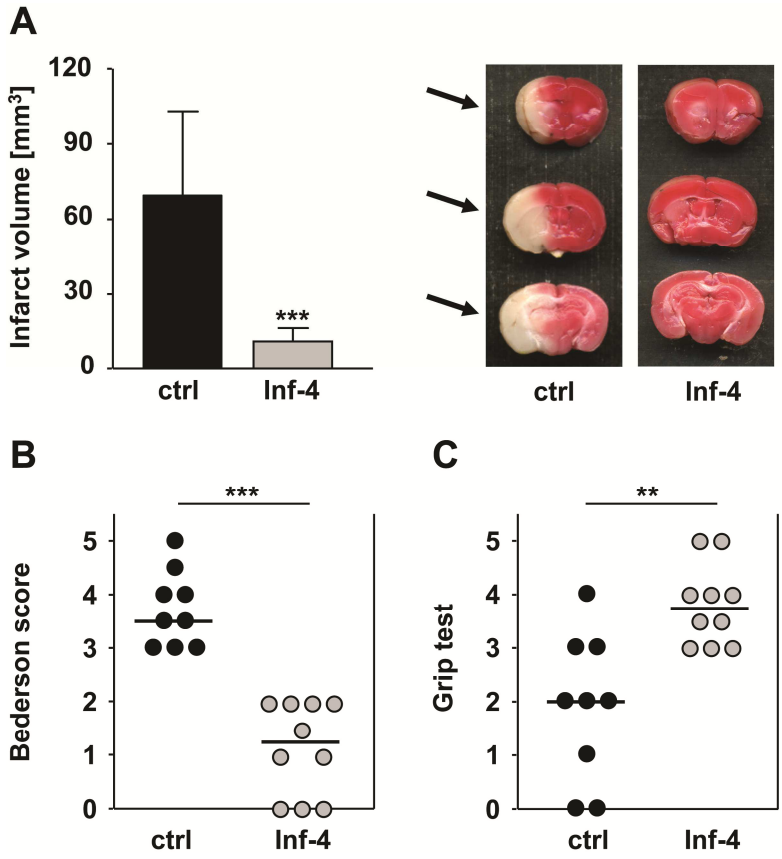

Figure 37. rHA-Infestin-4 injected mice are protected from ischemic stroke. Formation of cerebral ischemia and consequential neurological defects were investigated in a murine stroke model. A, Brain infarct volumes in controls (n=13) and rHA-Infestin-4 treated mice (n=10) presented as mean ± SD (left). Representative images of three corresponding coronal sections from control and rHA-Infestin-4-treated mice stained with TTC 24 h after tMCAO. Infarct areas are marked with arrows (right). Bederson score B, and grip test C, determined 24 h after tMCAO of control (n=9) and rHA-Infestin-4 treated mice (n=10); horizontal bar indicates the median. The experiment was started 10 min after i.v. injection of PBS and rHA-Infestin-4, respectively; **, p<0.01; ***, p<0.001. Ctrl = control and Inf-4 = recombinant human albumin-Infestin-4 fusion protein. (Hagedorn *et al*., *Circulation*, 2010)[202].

5 DISCUSSION

Platelet activation and aggregation together with the initiation of the coagulation system are critical steps during thrombus formation to limit post-traumatic blood loss at sites of vascular injury. However, under pathological conditions, these processes may also lead to full vessel occlusion causing myocardial infarction or stroke. Therefore, antiplatelet agents such as aspirin, clopidogrel and integrin αIIbβ3 antagonists that act by the inhibition of platelet function have been beneficial in the prophylaxis and treatment of cardio-and cerebrovascular diseases[205]. Similarly, anticoagulation with vitamin K antagonists, heparins and direct inhibitors of thrombin and FXa has provided an efficient therapeutic option against thromboembolic events[206]. However, reduced pathological thrombus formation by the application of the currently available antithrombotic agents is often associated with an increase in bleeding complications, which can possibly either aggravate the clinical outcome of the thrombotic disease or even be life-threatening. Hence, the detailed analysis of platelet activation and the respective signaling pathways as well as activation mechanisms of plasma coagulation factors has become an important and developing field in cardiovascular research during the last decades.

Thrombus formation is a multistep process that involves a complex but well defined interplay of multiple platelet adhesion/activation receptors, intracellular signaling molecules and coagulation factors. The major players and mechanisms in these processes are, however, only partially known and characterized. In the current thesis, several mechanisms underlying thrombus formation in hemostasis and thrombosis were assessed using different approaches such as specific protein blockage, immunodepletion or genetic deficiency in mice. In particular, the role of the GPIbα-vWF interaction, the platelet activating receptors GPVI and CLEC-2 as well as the intracellular signaling proteins PLD1 and RhoA for platelet function and *in vivo* thrombus formation were investigated. The presented results revealed that these proteins are critical for thrombus formation but differently regulate thrombus initiation, propagation and stabilization. Additionally, the data provided further evidence for the recently raised possibility that pathological thrombus formation and hemostasis may involve partially distinct mechanisms. Moreover, the functional characterization of the newly generated FXIIa inhibitor rHA-Infestin-4, presented in the last part of this study revealed that this inhibitor may serve as a promising pharmacological agent that abolishes occlusive thrombus formation without affecting hemostasis.

Consequently, although data gained from studies using murine thrombosis models cannot directly be transferred to the human situation, the new findings presented here may serve as the basis for the development of a novel generation of antithrombotic agents and strategies for effective therapy of thromboembolic diseases with a good safety profile.

5.1 Studies on the functional role of the GPIbα-vWF interaction and downstream signaling in shear-dependent thrombus formation

5.1.1 The GPIbα-vWF interaction is essential for *in vivo* thrombus stabilization at high shear

Under conditions of arteriolar shear, the initial tethering of flowing platelets to the exposed ECM at sites of vascular injury is mediated by the interaction of the platelet receptor GPIbα with vWF immobilized on collagen. This commonly accepted knowledge has been gained during the last decades from numerous *in vitro* studies using flow chamber assays but also from intensive *in vivo* analyses of arterial thrombus formation in mice deficient in functional GPIbα[43,44,189]. Since mice lacking GPIbα[27] or GPIbβ[28] displayed a severe bleeding diathesis accompanied by a marked macrothrombocytopenia phenotypically resembling the symptoms of human BSS, these mice were not suitable for investigating the role of GPIb in thrombosis. This limitation was, however, overcome by the generation of transgenic mice expressing a mutated form of GPIbα in which the extracellular domain was replaced by the α-subunit of the human IL-4 receptor[207]. As a consequence, these mice revealed dysfunctional GPIbα but nearly normal platelet counts[207]. Bergmeier *et al.* demonstrated that these mice were profoundly protected from $FeCl_3$-induced arterial thrombus formation in mesenteric arterioles as platelets virtually failed to adhere to the injured vessel wall[43]. Furthermore, they showed that platelets with mutated GPIbα were unable to incorporate into a growing thrombus of wild-type platelets in the same injury model[43]. These data provided the first *in vivo* evidence that GPIbα is essential for platelet adhesion and thrombus propagation at sites of vascular lesions. This could also be confirmed in another vascular bed by Konstantinides *et al.* challenging the same mice in a $FeCl_3$-induced carotid injury model[44]. Similarly, Jain *et al.* reported defective thrombus formation after $FeCl_3$-dependent injury of carotid arteries in mice carrying a genetically modified C-terminus of GPIbα, a mutation that disabled binding of the downstream signaling molecule 14-3-3ξ[189]. The observed phenotype of these mice was not as pronounced as in mutant mice lacking the functional extracellular domain of GPIbα[43], which indicated that GPIbα signaling through 14-3-3ξ is less important for arterial thrombus formation than binding of GPIbα to its ligand(s). However, previous thrombosis studies in vWF-deficient mice by Denis *et al.*[172] and Ni *et al.*[174], using the same experimental conditions, demonstrated that the main GPIbα ligand is less important for arterial thrombus formation than the receptor itself. In both studies, initial aggregate formation was indeed delayed but not absent in vWF-deficient mice, and also further thrombus progression occurred. This suggests that GPIbα binding to other ligand(s) in addition to vWF might mediate platelet adhesion and consequent thrombus formation in the applied injury models.

According to the impressive *in vivo* data of GPIbα mutant mice, the receptor has been proposed as a promising target for powerful antithrombotic therapy[43].

To test, whether this proposal first of all holds true for mice, GPIbα was targeted *in vivo* and the effect on pathological thrombus formation was assessed in a $FeCl_3$-induced injury model which was comparable to that used in the above mentioned studies. To do so, GPIbα was functionally inhibited in mice by treatment with non-cytotoxic Fab fragments of the monoclonal antibody p0p/B that specifically block the vWF-binding site on the extracellular domain of GPIbα[183]. These Fab fragments had previously been tested in another murine thrombosis model of ligation-induced endothelial damage in the carotid artery where completely inhibited platelet adhesion to the injured vessel wall was observed[42]. In the current thesis, anti-GPIbα Fab fragment treatment significantly delayed initial aggregate formation but, in line with data obtained in *vWF*$^{-/-}$ mice[175], did not abrogate subsequent thrombus growth in $FeCl_3$-injured mesenteric arterioles (Figure 5A,B). These data further supported the notion that vWF-binding to GPIbα contributes to, but is not essential for the initial adhesion of platelets to the exposed ECM at the wound site. However, an alternative ligand(s) of GPIbα, which may dominantly mediate this process, has not yet been determined. It also remains unclear whether the previously proposed binding partners of GPIbα, thrombospondin-1 and P-selectin, which have been shown to be involved in thrombosis[208,209], may represent likely candidates.

Moreover, in the present study, the GPIbα-vWF interaction rather appeared to be critical for stable platelet-platelet connections in a growing thrombus at very high shear rates as revealed by the continuous release of individual platelets from the thrombus surface when it reached a size that nearly occluded the artery (Figure 5B,C). Consequently, thrombus formation arrested at this stage, allowing blood to pass through a small open channel and thus preventing vessel occlusion in 89% of the p0p/B Fab fragment-treated mice. The thromboprotective effect observed in these animals partially exceeded that reported for *vWF*$^{-/-}$ mice as only 50% of these animals were protected from stable vessel occlusion[175]. However, the overall characteristics of thrombus formation were quite similar between both groups of mice. These findings strongly indicate that the $FeCl_3$-injury model in our hands provides reliable results that are well comparable to those obtained by other groups and hence confirmed the suitability of this thrombosis model as a valid method in the laboratory for further analysis of thrombus formation in mice. The minimal discrepancies between the two studies might be due to slightly different injury procedures which may cause variable severities of the vascular lesion and subsequently different degrees of platelet activation. Furthermore, the data in the present study provided direct proof that vWF-mediated cross-linking of platelets via GPIbα represents the main mechanism for platelet recruitment to a growing thrombus at very high shear rates[22,43]. The interaction of vWF bound to GPIbα on a

circulating platelet with activated integrin αIIbβ3 on the thrombus surface may also account for that process. However, the latter possibility seems rather unlikely as there is increasing evidence that under conditions of extremely high shear, thrombus propagation requires GPIbα and vWF but occurs independently of platelet activation and thereby also of activated integrin αIIbβ3[21-23]. Whether vWF binding to GPIbα is sufficient to mediate stable platelet-platelet cohesion in a growing thrombus or, according to its high "off-rate", is only crucial for the initial tethering of new platelets from the circulation to the thrombus surface, remains still to be determined. The interaction of GPIbα with other ligands might also be responsible for the final step of firm platelet adhesion, such as plasma fibronectin which has previously been shown to be involved in platelet recruitment into a developing thrombus[210,211].

Nevertheless, the results of the p0p/B Fab fragment-treated mice analyzed in a mechanical injury model of the abdominal aorta also supported the importance of the GPIbα-vWF interaction for stable thrombus expansion. Similar to the data of the $FeCl_3$-induced injury, initial thrombus formation was unaltered in animals challenged in this model, but subsequent thrombus progression was virtually abolished when it reached a size that occluded up to 50% of the vessel (as estimated from to the blood flow measurements, Figure 6A,B). Accordingly, one may assume that also under these experimental conditions platelets failed to incooperate into the growing thrombus when the GPIbα-vWF interaction was blocked. These findings are in line with previous studies reporting that maximal thrombus size in a model of laser-induced thrombosis was decreased in mice lacking vWF[212] and that maintenance of open channels after vascular injury prevented vessel occlusion in pigs suffering from von Willebrand's disease[213].

Taken together, the GPIbα-vWF interaction appears to be essential for thrombus progression independently of the applied injury model. Thus, the respective binding site might serve as a novel target for effective antithrombotic therapy (Figure 40). This approach may, however, be accompanied by unwanted bleeding complications as p0p/B Fab fragment treatment severely prolonged tail bleeding times in mice (Figure 6C). However, the hemostatic defect was clearly less pronounced as compared to mice treated with integrin αIIbβ3 blocking Fab fragments[45]. Similarly prolonged bleeding times have previously been observed in our group by Kleinschnitz *et al.* using the same p0p/B Fab fragments[45] and by Denis *et al.* who studied hemostasis in *vWF*$^{-/-}$ mice[173]. Although bleeding time experiments in mice do not directly correlate with possible clinically relevant hemorrhages[214], one may assume that therapeutic targeting of GPIbα might be associated with an increased bleeding tendency. It remains, however, questionable to which extent these anticipated complications would occur in humans. Two independent studies, for example, showed that GPIbα blockage by Fab fragments of monoclonal antibodies, similar to that used in the present study, efficiently

prevented arterial thrombosis in baboons, but at the same time only mildly prolonged skin bleeding times[215,216].

The proposal that GPIbα blockage of the vWF-binding site may represent an attractive antithrombotic concept is also supported by the finding of Kleinschnitz *et al*. that treatment with p0p/B Fab fragments dramatically protected mice from ischemic brain infarction[45]. Importantly, both prophylactic and therapeutic administration of the Fab fragments equally prevented lesion progression and ameliorated the neurological outcome after experimentally induced stroke in the animals. GPIbα targeting was, notably, not associated with an increase in intracranial hemorrhage[45]. In line with these findings, similar data were obtained with *vWF*$^{-/-}$ mice[46].

In summary, the results of the present study show that vWF binding to GPIbα is an essential mechanism for the incorporation of flowing platelets into a growing thrombus after $FeCl_3$- and mechanically induced vascular injury in mice. Furthermore, the data provide clear evidence that blocking of the GPIbα-vWF interaction by Fab fragments virtually mirrors the antithrombotic phenotype of mice lacking vWF. Based on these findings and those discussed above, targeting of the vWF interaction site of GPIbα might be an attractive therapeutic strategy whereas Fab fragments of an anti-GPIbα antibody may serve as a potential therapeutic agent for the prophylaxis and treatment of acute cardio- and cerebrovascular diseases.

5.1.2 PLD1 mediates αIIbβ3 integrin activation under high shear and is critical for pathological thrombus formation but dispensable for hemostasis

As discussed above, GPIbα was suggested as an attractive pharmacological target for antithrombotic therapy. This proposal may, however, similarly be applied to downstream signaling effectors of GPIbα, particularly as mice lacking the GPIbα-binding site for 14-3-3ξ[189] have also been described to display clearly decreased *in vivo* thrombus formation. According to the data presented here, the intracellular signaling protein PLD1 may represent one potential candidate molecule. It could be shown that PLD1 is required for efficient αIIbβ3 integrin activation in a GPIbα-dependent manner under high shear flow conditions and consequently important for stable thrombus formation *in vitro* and *in vivo*. The finding that genetic PLD1 deficiency in mice resulted in impaired thrombus stabilization in models of arterial thrombosis and protection from ischemic brain infarction for the first time identified this enzyme as a fundamental player in pathological thrombus formation.

Studies with inhibitor indirectly blocking PLD activity in human platelets have previously suggested a role of this enzyme for platelet activation and degranulation[191] This was particularly proposed upon PAR1 stimulation[63], a process which has later also been

supposed to trigger PLD-dependent Rap1 activation[64]. However, all these studies made use of a partially insufficient approach by repressing the production of PA, the major downstream messenger of PLD. Due to the lack of alternative methods at that time, the primary alcohol butanol-1 was used to divert PLD activity towards the generation of phosphatidylbutanol instead of the physiologically active PA. Subsequently drawn conclusions about PLD- and PA-dependent functions may have been influenced by the fact that butanol-1 only incompletely prevents PA generation and that it has in addition to phosphatidylbutanol several off-target effects on cell activity[217]. This rather limited the reliability of the respective data. Moreover, this method did not allow discriminations between possibly different roles of the individual PLD isoforms in platelet function.

In the present study, using a knockout approach, these limitations were circumvented. It was demonstrated for the first time that PLD1 and PA are involved in integrin αIIbβ3 inside-out activation after stimulation of G protein- as well as ITAM-coupled receptors, whereas the proposed[191] contribution of PLD1 in the process of α or dense granule release could not be confirmed[190]. Furthermore, the enzyme was identified to be critical for GPIbα-mediated stable platelet adhesion under high shear conditions. The exact mechanism how PLD1 becomes activated in platelets and facilitates integrin αIIbβ3 activation is not clear at present. A previous report by Powner *et al*., described related signaling events in neutrophils where PLD- activity is required for talin-binding to the integrin MAC-1 and thereby essential for mediating cell adhesion and migration[218]. It appears possible that similar mechanisms may also be relevant for integrin activation in platelets. Accordingly, one may hypothesize that PLD1 might activate a signaling cascade that is responsible for proper talin-1 binding to the integrin β subunit, which is the final step of integrin activation and essential for platelet adhesion and aggregation. However, further analyses are required to test this assumption and to clarify the interplay of PLD1 with other signaling proteins.

Furthermore, this study demonstrated that thrombus stabilization was severely diminished in *Pld1*$^{-/-}$ mice under high shear flow conditions *in vitro* and also *in vivo*. Interestingly, PLD1 was dispensable for the initial adhesion of platelets to the collagen surface and also for the following process of aggregate and thrombus formation (Figure 7A). However, the enzyme appeared to be critical for sustained platelet-platelet interactions in the growing thrombus under high shear rates as revealed by the release of platelets from the thrombus surface and finally complete disintegration of formed thrombi after a few minutes of perfusion (Figure 7A). The recruitment and attachment of platelets to the thrombogenic matrix is known to be driven by GPIb, GPVI and the integrins α2β1 and αIIbβ3. Interestingly, the presented data indicated that the first layer of *Pld1*$^{-/-}$ platelets is sufficiently activated under the experimental conditions, most probably due to the GPVI-collagen interaction. This mechanism appears to be independent of PLD1-driven integrin activation, allowing the platelets to firmly adhere on

the collagen surface and to initiate aggregate formation. In contrast, activation and stable incorporation of platelets in the upper layers of the thrombus was impaired. This process is known to be mediated by the action of released soluble mediators, namely ADP and TxA_2 as well as by the GPIbα-vWF interaction and the subsequent signaling[20]. In the light of the data in this thesis showing that *Pld1*$^{-/-}$ platelets failed to firmly adhere on a vWF surface at high shear rates (Figure 7B), one may suggest that PLD1 plays an important role in the platelet activation process during thrombus growth particularly under high shear conditions because it mediates signaling events downstream of GPIbα that lead to integrin αIIbβ3 activation.

This process also appeared to be relevant for thrombus formation *in vivo*, as *Pld1*$^{-/-}$ mice displayed severely defective thrombus stabilization in arterial thrombosis models. In line with the results of the *in vitro* flow adhesion assays, the initial thrombus formation after mechanically as well as chemically induced vascular injury was unaltered in *Pld1*$^{-/-}$ mice when compared to wild-type mice (Figure 8A-C) and even subsequent thrombus propagation was nearly comparable between both groups of animals. However, the final step in thrombus growth to fully occlude the vessel or the irreversible stabilization of occlusive thrombi, respectively was completely abolished in *Pld1*$^{-/-}$ mice (Figure 8A-C). As a consequence and irrespective of the applied injury model, almost all vessels of these animals remained open at the end of the observation period, indicating that at very high shear rates, such as those occurring in stenosed arterial vessels, the lack of PLD1 becomes evident. This observation further supports the assumption that the enzyme plays a critical role in GPIbα-mediated αIIbβ3 integrin activation. Moreover, this function may also account for the reduced phosphatidylserine exposure of *Pld*$^{-/-}$ platelets when activated and aggregated on a collagen surface under high shear flow conditions[190], because it has previously been shown that the platelet procoagulant activity is dependent on GPIbα and αIIbβ3 integrin activation[219]. The decreased ability of *Pld1*$^{-/-}$ platelets to stimulate the coagulation process may at least partially contribute to the defective thrombus stabilization seen in these mice.

Very interestingly, although PLD1 deficiency prevented stable vessel occlusion in pathological thrombosis models, it had no effect on normal hemostasis, as bleeding times of *Pld1*$^{-/-}$ mice were unaltered (Figure 8D). This indicated that PLD1 may represent a novel target molecule for potent antithrombotic therapy without causing bleeding complications. This would especially be advantageous for the treatment of acute ischemic stroke, where the risk of *intracranial hemorrhage* (ICH) is the major limitation of current antithrombotic treatments[220-222]. In the previous part of the presented study (5.1), it was described that blockage of the GPIbα-vWF interaction dramatically diminished lesion progression after experimentally induced ischemic stroke, and that this treatment did not induce ICH, although increasing bleeding times in those mice[45]. In accordance with the assumption that PLD1 acts as a signal transducing enzyme downstream of GPIbα, also *Pld1*$^{-/-}$ mice displayed markedly

reduced infarct volumes and a better neurological outcome, which was, similarly to GPIbα inhibition, not accompanied by an increase in intracerebral bleeding[190]. Since in addition PLD1 deficiency did not affected normal hemostasis, the data clearly emphasize that this enzyme or even downstream effectors might be a preferable target for effective and safe prevention or treatment of thromboembolic events. It is Important to note that, despite the proposed contribution of PLD1 to several cellular functions including degranulation, cytoskeletal reorganization, proliferation and migration[49,223], *Pld*$^{-/-}$ mice are viable, healthy and fertile[190]. These findings have meanwhile also been confirmed by others[224] and might be explained by a potential compensatory capacity of the second PLD isoform, PLD2, or additional enzymes that function similarly to PLD1. Nevertheless, according to these observations, a good general safety profile of an anti-PLD1 therapy may be anticipated.

5.2 Studies on the functional role of the (hem)ITAM-coupled receptors GPVI and CLEC-2 in hemostasis and thrombosis

5.2.1 GPVI is a critical mediator of arterial thrombosis upon $FeCl_3$- and mechanically induced vascular injury

During the last years, GPVI has been established as the major platelet activation receptor for collagen and proposed as an attractive antithrombotic target (Figure 40). This is particularly due to the observation that injection of anti-GPVI antibodies (JAQ1-3) into mice induces specific downregulation of the receptor from the surface of circulating platelets, resulting in a long-term antithrombotic protection but rather no or only a minimal hemostatic defect[42,77,82,83,225]. However, contradictory results have been reported about the functional significance of GPVI for pathological thrombus formation in different experimental thrombosis models. For example, previous studies yielded either no role[78,212] or only a minor role[79,85] for GPVI in laser-induced thrombus formation and only one report showed a significant contribution of the receptor to thrombus formation in this model[226]. These observations are likely explained by the fact that platelet activation and aggregation upon laser-injury is largely dependent on thrombin generation. Variations in the severity of the induced lesions may determine to which extent other signaling pathways contribute to thrombus formation under these experimental conditions[79,85,178]. Many controversies also exist about the relative importance of GPVI-mediated platelet adhesion and activation for arterial thrombosis after $FeCl_3$-induced vascular injury. This type of injury model is a widely used and accepted method in the field of thrombosis research as it relatively easy to perform and to standardize. Moreover, it allows variable levels of injury in different vascular beds and it has been reported to trigger the formation of thrombi that are similar in their composition to those appearing in humans[174]. Previous studies provided evidence for a critical role of GPVI in

$FeCl_3$-induced thrombus formation in mice. Massberg *et al*. were the first to show that GPVI-immunodepletion protected mice from $FeCl_3$-induced occlusive thrombus formation in the carotid artery[42]. This was later confirmed by Dubois *et al.* assessing thrombus formation in mesenteric arterioles of FcRγ-chain-deficient mice (which lack GPVI on the platelet surface[227]) after $FeCl_3$ application[78]. In a third report, also Konstantinides *et al.* described that the majority of tested *Gp6*$^{-/-}$ mice revealed abnormal thrombus formation in a model of $FeCl_3$-induced vascular lesions in carotid arteries[44]. However, these data stand in contrast to the observation recently made by Eckly *et al.*[86], who reported that GPVI-immunodepleted mice are not protected from vessel occlusion after $FeCl_3$-induced injury of mesenteric arterioles as well as carotid arteries. In the study presented here, for the first time a comprehensive analysis of the thrombotic response of genetically as well as immunodepleted GPVI-deficient mice upon $FeCl_3$-induced vascular injury in mesenteric arterioles and carotid arteries was performed. It could be clearly demonstrated that the initial thrombus formation in injured mesenteric arterioles was not altered in mice lacking GPVI compared to wild-type mice, whereas thrombus propagation was impaired due to permanent embolization that strongly delayed or abolished vessel occlusion in these mice (Figure 9A,B). Furthermore, this significant contribution of GPVI-mediated signaling in $FeCl_3$-induced thrombosis was also shown to be independent of the targeted vascular bed as similar observations were made in both groups of GPVI-deficient mice after injury of the carotid artery (Figure 9C). These findings are in line with the above discussed data from earlier studies reported by other groups[42,44,78], but are contradictory to the data obtained by Eckly *et al*.[86]. These discrepancies are difficult to explain at present, but they are most likely related to different experimental conditions. The severity of the vascular injury may vary due to the used $FeCl_3$ concentration, the application method via filter paper or liquid drop and accordingly the exposure time of the vessel to the applied chemical. Consequently, the different experimental conditions may cause variable exposure of different thrombogenic proteins and factors to the flowing blood which differently influence platelet activation and aggregation. To at least partially test this assumption in the present study, another $FeCl_3$ concentration and also a different exposure time was used to achieve a more severe vascular injury in the carotid artery. As a result, thrombus formation was indeed less affected but notably still impaired in GPVI-deficient mice when the injury was induced by 15% instead of 10% $FeCl_3$ or by 3 min instead of 1.5 min application time of the saturated filter paper (data not shown). This indicates that GPVI-mediated platelet adhesion and activation is less important for arterial thrombus formation upon severe chemically induced vascular damage, which is in line with previous reports by others suggesting a pivotal role for TF-mediated thrombin generation in the process of thrombus formation under these conditions[228-230]. However, it remains questionable whether such an extreme vascular injury, probably triggering massive platelet activation in a way that

loss of one critical signaling pathway may be compensated by others, mimics the conditions under which thrombotic events are triggered in human disease.

Eckly *et al*. explained their results by providing a new mechanisms underlying thrombus formation after $FeCl_3$-induced injury[86]. In contrast to the hitherto existing assumption that $FeCl_3$ induces strong denudation of endothelial cells and exposure of subendothelial proteins[172,231], the authors showed that in their hands, $FeCl_3$ indeed severely injures the endothelium but without damaging the *internal elastic lamina* (IEL)[86]. As a consequence, Eckly *et al*. hypothesized that only components of the basement membrane are exposed to the blood flow whereas adhesive proteins which activate GPVI, such as collagen type I, are not present at the injury site and thereby do not contribute to thrombus formation in this model. Furthermore, they demonstrated that $FeCl_3$ application also led to the formation of ferric ion-filled spherical bodies sprouting out of the endothelium into the vessel lumen[86]. According to the finding that on the surface of these bud-like structures high amounts of TF were exposed, they suggested that subsequently generated thrombin is the driving force for thrombus formation after $FeCl_3$-induced injury. Consequently, the authors state that this model may not be suitable to assess the role of subendothelial adhesive proteins and their respective platelet receptors in arterial thrombus formation[86]. The results of the present study, however, strongly suggest that $FeCl_3$ induces a type of vascular injury that causes the exposure of subendothelial collagens and other ECM components to the flowing blood and that these significantly contribute to platelet activation and thrombus formation. This is also supported by previous data from Dubois *et al.*, who visualized considerable exposure of collagen type I to the vessel lumen *in vivo* and on sections of cremaster muscles after injury with $FeCl_3$[78]. Moreover, one has to consider that also proteins of the basement membrane such as collagen type IV, despite its known function as a weak affinity ligand for GPVI, and laminin may also be importantly involved in the initiation of thrombus formation. The role of laminin *in vivo* has still to be determined, but it has been described to mediate platelet spreading through integrin $\alpha6\beta1$-dependent activation of GPVI[72]. Recently, it was hypothesized that proteins from the tunica media, involving also collagen type I, may still be exposed[232] even if the IEL is not damaged as it has been shown to be fenestrated[233]. Together, this indicates that further investigations are required to determine the exact mechanisms underlying platelet adhesion and activation at sites of vascular injury after application of $FeCl_3$.

In a second set of thrombosis experiments, *Gp6*$^{-/-}$ and GPVI-immunodepleted mice were analyzed in a model of mechanical injury of the abdominal aorta. Under these conditions, GPVI deficiency resulted in virtually abrogated thrombus formation and efficiently protected mice from vessel occlusion (Figure 10). These results confirm previous findings from our group by Grüner *et al*. demonstrating that GPVI-immunodepletion in mice inhibited thrombus

formation in that model. Thereby, these studies strongly suggest that platelet adhesion and activation after mechanical vascular injury is largely mediated by exposed collagens and possibly other ECM proteins which interact with their respective platelet receptors in a GPVI-dependent manner. Notably, the observed protection of GPVI-deficient mice from arterial thrombosis after injury of the abdominal aorta (Figure 10) exceeds the effect seen in mice with blocked vWF-GPIbα interaction (Figure 6 A,B). Whereas GPVI-deficient mice only showed minimal reduction of the blood flow after vessel injury, p0p/B-treated mice revealed an initial decline of the blood flow within the first minutes similar to that of wild-type mice, which indicates initially unaltered thrombus formation. This suggests a dominant role of GPVI instead of vWF-GPIbα for platelet adhesion and activation at sites of vascular lesions under these experimental conditions. The proposed important role of GPVI for mechanically induced thrombus formation is, however, not supported by Mangin *et al*., who challenged *FcRg*$^{-/-}$ mice in a Folts-like stenosis-injury model[79]. The discrepancies may to a great extent be explained by the different experimental procedures used in the studies. In contrast to the thrombosis model performed in the present study where the abdominal aorta was injured by a single firm compression for 15 sec with a forceps, the model by Mangin *et al*. comprised an induced vessel stenosis of the carotid artery with a suture followed by one or even repetitive sets of 5 crushes with a forceps. Consequently, as indicated above for a severe $FeCl_3$-induced vascular injury, one may speculate that such a massive vascular injury induces extensive activation of different platelet signaling pathways, which are able to promote thrombus formation independently of each other.

Taken together, this study demonstrates that GPVI-mediated platelet adhesion and activation mechanisms are essential for thrombus formation following $FeCl_3$-induced and mechanically induced vascular injury in mice. These findings confirm that the $FeCl_3$ injury model is well suited to study the involvement of ECM components and their respective platelet receptors in thrombus formation. Furthermore, the data provide direct evidence that GPVI-immunodepletion results in a comparable thromboprotective effect as genetic GPVI deficiency in different thrombosis models, which strongly suggests that GPVI targeting by antibodies *in vivo* does not produce significant undesired side effects on platelet function. These findings are particularly important for the potential development of anti-GPVI based antithrombotic agents. Similar to the observation that injection of JAQ1-3 into mice caused specific immunodepletion of GPVI from the platelet surface[77,225], also two patients have been described who suffer from an autoimmune disease where endogenously developed anti-GPVI antibodies lead to the downregulation of this platelet receptor[87,88]. As a consequence, both mice and patients lacking GPVI display abolished platelet responses to collagen and CRP but only a mild bleeding tendency. Based on this correlation between humans and mice and in the light of the presented data, one may speculate that also a “therapeutically”

induced downregulation of GPVI in human platelets by antibody treatment might be successful and may represent a valuable strategy for the therapy of thromboembolic diseases. This concept is currently under investigation in monkeys using human GPVI-specific mouse monoclonal antibodies to downregulate GPVI from the platelet surface[234]. First success has already been achieved in these studies, as a single subcutaneous injection of one of the analyzed antibodies led to a long-term antiplatelet effect due GPVI-immunodepletion without, notably, significant thrombocytopenia[234], a known "side-effect" of anti-GPVI antibody injection into mice[77].

5.2.2 CLEC-2 is important for thrombus stabilization in hemostasis and thrombosis

CLEC-2 has recently been identified as a prominent transmembrane receptor on the platelet surface that exhibits a remarkable activatory potential[9,235]. However, its physiological role in platelet function has been largely unknown. This study provided the first evidence that CLEC-2 is an essential player in thrombus formation during hemostasis and thrombosis.

Anti-CLEC-2 antibody injection into mice led to the irreversible downregulation of the receptor from the surface of circulating platelets and resulted in severely impaired thrombus formation at arteriolar shear *in vitro* and also *in vivo.* Notably, the initial adhesion of CLEC-2 deficient platelets on collagen under high shear flow conditions was unaltered (Figure 12A), which was, however, not surprising as this process is well established to be mediated by the action of GPIb, GPVI and also $\alpha 2\beta 1$ and $\alpha IIb\beta 3$ integrins[7,236]. CLEC-2 dependent signaling rather appears to be important for the stabilization of direct platelet-platelet contacts in the growing thrombus under flow conditions, as indicated by the fact that newly recruited platelets failed to firmly adhere on the surface of collagen-adherent platelets and were permanently released. As a consequence, aggregates of CLEC-2 deficient platelets formed on collagen at high shear covered less surface area and were strongly diminished in their volume compared to aggregates of control platelets (Figure 12B). Comparable to these data, the process also seemed to be relevant for stable thrombus formation in a $FeCl_3$-induced injury model as single platelets were constantly released and also small aggregate fragments frequently embolized from the surface of the growing thrombus in CLEC-2 deficient mice. Consequently, these animals were profoundly protected from arterial vessel occlusion (Figure 13), suggesting that CLEC-2 may represent an interesting target for effective antithrombotic therapy (Figure 40). Contrary to these data, the overall thrombotic response in CLEC-2 deficient mice after mechanical injury of the abdominal aorta was comparable to control mice (Figure 14). Only a tendency towards delayed vessel occlusion was detectable, indicating a rather minor contribution of CLEC-2 mediated signaling in thrombus formation under these experimental conditions. These observations are not easily explainable but the severity of the mechanical injury may be the reason because it results in massive endothelial

denudation followed by rapid thrombus formation within a few minutes in contrast to the characteristics of the $FeCl_3$-induced vascular injury. One may assume that under such conditions, the profound activation of different platelet activation mechanisms, critical for thrombus growth may overcome the defect in CLEC-2 activity. Ideally, to exclude that CLEC-2 function is only relevant for thrombus stabilization in a $FeCl_3$-injury model, CLEC-2 deficient mice should be analyzed in additional thrombosis models such as the $FeCl_3$-injury model on carotid arteries or the laser-injury model.

Interestingly, however, the importance of CLEC-2 for thrombus stabilization *in vitro* and *in vivo* has meanwhile been supported by Suzuki-Inoue *et al.* who used a genetic knockout approach[9]. As a constitutive CLEC-2 knockout is lethal in mice due to impaired organization and separation of lymphatic and blood vessels during embryonic development[99,100], the group generated CLEC-2 deficient chimeric mice by transplanting fetal liver cells from *Clec-2*$^{-/-}$ embryos into irradiated wild-type mice[9]. In line with data of the present study, the authors reported normal adhesion but a significantly reduced thrombus propagation of CLEC-2 deficient platelets on a collagen surface under high shear flow conditions[9]. Furthermore, these CLEC-2 deficient mice displayed virtually abolished aggregate and thrombus formation in a model of laser-induced injury of mesenteric arterioles[9]. The defect was apparent by the frequent release of only loosely attached platelets from the vessel wall or from platelet aggregates which finally prevented vessel occlusion. These findings also emphasize CLEC-2 as a potential antithrombotic target and concurrently reveal that CLEC-2 immunodepletion perfectly reflect the thrombotic phenotype of genetically CLEC-2 deficient mice. However, a recent report by Hughes *et al.* described contradictory results concerning the role of CLEC-2 for thrombus formation *in vitro*[237]. The authors also used chimeric mice lacking functional CLEC-2 and analyzed the ability of the platelets to from aggregates/thrombi on collagen under arteriolar shear rates. Surprisingly, they found no differences between CLEC-2 deficient and wild-type platelets[237]. The reason for these discrepancies between the different studies are not clear at present, particularly because the used experimental conditions (anticoagulants and shear rate) were largely comparable. One possible explanation could be that due to differences in blood sampling, handling or slightly insufficient anticoagulation in the study by Hughes *et al.* the amount of present soluble mediators such as ADP, TxA_2 and thrombin may have been elevated in their samples. This may consequently affect *in vitro* thrombus formation by compensating the CLEC-2 signaling defect. In the present study, it could be shown that under non-anticoagulated conditions or co-infusion of ADP and U46619, CLEC-2 deficient platelets displayed stable thrombi on collagen in the flow chamber system indistinguishable from controls (Figure 12C). However, it remains questionable whether slightly increased levels of soluble platelet agonists may cause such effects. Due to bleeding complications in the CLEC-2 chimeric mice, Hughes *et al.* were unfortunately not able to

challenge these mice in an arterial thrombosis model[237]. Such an analysis would possibly have been helpful to clarify the controversial results about the role of CLEC-2 in thrombus formation at arteriolar shear.

Nevertheless, the present thesis, demonstrated that antibody-induced CLEC-2 deficiency results in defective thrombus growth and stabilization under flow conditions *in vitro* and *in vivo* (Figure 12 and Figure 13). The mechanism underlying CLEC-2 activation and function remains elusive as the only known physiological ligand of the receptor, podoplanin, is mainly expressed on tumor and lymphatic endothelial cells but not found in the vasculature[96,97]. According to the here presented data, one may speculate that the potential ligand(s) of CLEC-2 should circulate in the plasma or may be expressed/immobilized on the surface of activated platelets. It may also be released by platelets or even become exposed to the blood flow at the wound site. In agreement with these assumptions, Suzuki-Inoue *et al.* recently proposed an interesting mechanism for thrombus stabilization involving CLEC-2 itself as a ligand candidate, as they could demonstrate in different *in vitro* analyses that CLEC-2 molecules are able to undergo direct homophilic associations[100]. However, the relative significance of this interaction for thrombus growth and also the mechanisms that regulate a possible switch between different homophilic binding affinities of CLEC-2 on resting and activated platelets remain to be determined.

The described findings that thrombus stabilization and growth of CLEC-2 deficient platelets is profoundly reduced under flow conditions *in vitro* and *in vivo* may explain the thrombus formation defects observed in other mice lacking different intracellular signaling proteins that act in the CLEC-2-induced activation pathway. The thrombus defect observed in CLEC-2 deficient mice was characterized by a continuous release of single platelets and embolization of small thrombus fragments from the surface of the thrombus during its expansion phase. A similar phenotype of defective thrombus formation *in vitro* as well as *in vivo* has been described for mice lacking *stromal interaction molecule 1* (STIM1), a critical regulator of SOCE in platelets[238]. Platelets of STIM1-deficient mice displayed a selective signaling defect in hem(ITAM)-dependent pathways, indicating that this activation axis is not only involved in platelet adhesion/activation on the ECM via GPVI but also to a certain extent in thrombus progression. Based on the presented data one may assume that the latter process is impaired in STIM1-deficient mice, possibly due to defective CLEC-2 signaling. Similarly, the thrombus instability observed in mice lacking essential molecules of the hem(ITAM)-signaling cascade, such as LAT[239] and PLCγ2[178] as well as the reduced thrombus growth of Filamin A-null platelets determined under flow conditions *in vitro*[240] might also be caused by impaired CLEC-2 mediated signal transduction. Accordingly, the massive thrombus formation under flow conditions *in vitro* of platelets from mice carrying a gain-of-function mutation in the *Plcg2*

gene and also the prothrombotic phenotype of these mice *in vivo* is certainly explainable by the enhanced PLCγ2 activity downstream of CLEC-2[241].

Furthermore, in the present study it was shown that CLEC-2 can be specifically targeted and functionally inactivated by the antibody INU1 *in vivo*. Remarkably, CLEC-2 inhibition was not caused by an INU1-dependent blockade of the receptor but rather based on an antibody-induced irreversible downregulation of CLEC-2 from the surface of circulating platelets. This process of *in vivo* receptor depletion has previously been described for GPVI in mice and in humans[77,88]. The complete loss of CLEC-2 from the platelet surface within a few hours after INU1 injection was confirmed by flow cytometric measurements (Figure 11B) and also by immunoprecipitation[182]. Upon injection of 200 µg INU1 per mouse, the receptor was absent for up to 6 days and as a consequence the platelets were completely unresponsive to rhodocytin during this time, whereas all other activation pathways were virtually unaffected (Figure 11C,D). The mechanism underlying this specific CLEC-2 downregulation has not been identified, particularly because this process is not inducible by antibodies *in vitro* and thereby difficult to assess. For GPVI, it has previously been shown that the receptor is downregulated by antibodies mainly through ectodomain shedding but also through internalization/degradation and that these processes are initiated by GPVI downstream signaling events[77,242,243]. Further experiments are required to determine which process accounts for CLEC-2 downregulation; however, as Fab fragments of INU1 cause a comparable effect to the full IgG, the involvement of the Fc part or the dimeric form of the antibody for this action can be excluded[182].

Irrespective of the exact underlying mechanism, INU1 injection caused a specific CLEC-2 deficiency in platelets that profoundly protected the treated mice from occlusive arterial thrombus formation. At the same time, loss of CLEC-2 was associated with variably but overall significantly prolonged bleeding times (Figure 15). The extent of the bleeding was, however, rather mild when compared to the hemostatic defects accompanied with integrin αIIbβ3 [45] or GPIbα (Figure 6C) blockade, as only one third of CLEC-2 deficient mice displayed prolonged bleeding times or could not arrest bleeding within the observation period, respectively. The high variability of the bleeding times also indicates that CLEC-2 deficiency caused a moderate hemostatic defect most likely due to thrombus instability at the wound site on the tail. Based on this assumption, one may speculate that the lack of CLEC-2 activity may be, at least partially, compensated by the action of other platelet agonists, such as ADP, TxA_2 and thrombin which may vary site between individual mice in their levels present at the wound, possibly due to differences in the tail injury. Similar observations in the variability of the tail bleeding times have previously been reported for mice deficient in other activatory receptors, namely P2Y1[244] or the α2A adrenergic receptor[245], indicating that the mentioned soluble mediators are critical for normal hemostasis. Although bleeding times are

not a valid parameter that allows reliable predictions of a potential bleeding risk[214], it is tempting to speculate that an anti-CLEC-2 therapy might be associated with a relatively low risk of hemorrhagic complications. Interestingly, the finding of the present study that antibody-induced CLEC-2 deficiency translates into a slight hemostatic defect contrasts with data from genetically engineered CLEC-2 deficient mice. Suzuki-Inoue *et al.* reported only a mild bleeding tendency for CLEC-2 deficient chimeras which was, however, not statistically significant[100] and Hughes *et al.* described no alterations in the bleeding times of CLEC-2 deficient chimeras[237]. These discrepancies between the studies may be related to different modes of tail tip removal which may, as indicated above, lead to a variable compensation of the CLEC-2 signaling defect by other platelet activation mechanisms. An additional and more likely explanation for the controversial results of the tail bleeding assay could be the different experimental procedures. Whereas the filter paper method was used in the present study, where hemostasis takes place at room temperature and in the presence of air, Suzuki-Inoue *et al.* and Hughes *et al.* determined the bleeding time of the mice in prewarmed saline at 37°C [100,237]. These different external factors appear to strongly influence the process of hemostasis and thereby determine to which extent the lack of CLEC-2 activity becomes evident. In line with this assumption, also preliminary results showed that INU1-induced CLEC-2 depletion in mice did not result in a significant hemostatic defect when bleeding times were determined in saline (Bender, May *et al.* in revision). These results also argue against INU1 treatment-caused unspecific effects that may, in addition to CLEC-2 depletion, further impair platelet function.

In summary, the present study suggested that CLEC-2 is an essential platelet surface receptor for thrombus stabilization *in vitro* and *in vivo* that can be specifically targeted and functionally inactivated *in vivo*. Thus, CLEC-2 can be proposed as a promising target for effective antithrombotic therapy. However, this prediction is at present rather speculative. It has previously been reported that GPVI can be irreversibly immunodepleted from the surface of murine as well as human platelets *in vivo*[77,87,88,225]. Therefore, one may anticipate that, similar to the observations in mice, also anti-CLEC-2 antibody treatment of humans may result in a specific loss of the receptor from circulating platelets. However, patients with an acquired CLEC-2 deficiency due to autoantibody-induced downregulation of the receptor have not been described yet. The identification of such patients might help to clarify whether CLEC-2 receptor clearance can also be initiated in humans and thereby be considered as a potential therapeutic strategy for antithrombotic treatment. Moreover, INU1 injection into mice has been shown to be associated with a transient but marked thrombocytopenia that persisted for approximately 3 days after antibody treatment[182]. Although it has been experimentally proven that a dramatic drop of platelet count does not *per se* cause spontaneous bleeding complications[246], this may certainly increase the bleeding tendency

after injuries and thereby limit the therapeutic use of anti-CLEC-2 antibodies. The relevance of this concern, however, remains to be determined, as the mechanisms of the transient thrombocytopenia and a possible mechanistic link to the receptor depletion are completely unclear at present. Additionally, there is no evidence so far that therapeutically induced CLEC-2 clearance is also combined with a pronounced reduction of the platelet count in humans as it has been described for mice. Furthermore, the recently described observation that CLEC-2 plays an essential role in blood and lymphatic vessel separation by binding to podoplanin exposed on lymphatic endothelial cells during embryonic development[99,100] may also question its suitability as an adequate antithrombotic target. Nevertheless, according to the current state of knowledge, the findings of the present study may serve as the basis for the development of novel antithrombotic agents for the prophylaxis and treatment of ischemic cardiovascular diseases.

5.2.3 Functionally redundancy of GPVI and CLEC-2 during *in vivo* thrombus formation

As described above the (hem)ITAM-bearing receptors GPVI and CLEC-2 play essential roles in arterial thrombus formation but at the same time do not significantly or only moderately affect normal hemostasis, respectively. As a consequence, these findings, together with the observation that the receptors can be functionally inactivated *in vivo* by specific antibodies, suggested that both receptors might be promising antithrombotic targets.

Therefore, it was assessed whether GPVI and CLEC-2 can be simultaneously downregulated in circulation platelets. Furthermore, since these receptors utilize a similar signaling cascade, including the downstream effectors LAT, SLP76 and PLCγ2[73], it was of high interest to analyze a putative redundant function of GPVI and CLEC-2 in the process of *in vivo* thrombus formation.

This issue was addressed by combined treatment of mice with JAQ1 and INU1. Platelets from these animals showed a specific loss of GPVI and CLEC-2 and were concomitantly refractory to the stimulation with CRP and rhodocytin whereas the expression levels of other prominent surface receptors and the activation response to other platelet agonists was largely unaffected (Bender, May *et al.* in revision). These data provided the first evidence that (hem)ITAM-coupled receptors can simultaneously be targeted *in vivo* without provoking additional effects on platelet function.

The induced double-deficiency of GPVI and CLEC-2 had, however, a remarkable effect on arterial thrombus formation after $FeCl_3$-induced vascular injury that clearly exceeded the defects seen in the respective single-deficient mice (Figure 16). The onset of aggregate formation was significantly delayed and subsequent thrombus propagation was severely diminished as the developing thrombus was more fragile and less in size when compared to

thrombi formed in GPVI- and CLEC-2 single-deficient mice. As a consequence, blood flow maintained in all tested double-deficient mice. These findings strongly suggest that GPVI and CLEC-2 exhibit partially redundant functions in both the initiation of aggregate and thrombus formation, a process that has so far been ascribed to the function of GPIb, GPVI, α2β1 and αIIbβ3 integrins[7,236], and the stabilization of arterial thrombi. Accordingly, it is tempting to speculate that a combined antithrombotic therapy targeting both platelet activation receptors might be more beneficial in the prevention or treatment of thromboembolic diseases than the use of a single mode of platelet inhibition. However, in view of the virtually abolished hemostatic function in GPVI/CLEC-2 double-depleted mice (Bender, May *et al.* in revision), and although there is no direct correlation between bleeding time and bleeding risk[214], the clinical use of such a therapeutic approach would likely be limited by the side-effect of hemorrhagic complications.

The hemostatic defect observed in GPVI/CLEC-2 double-depleted mice clearly exceeded the effects seen in mice treated with Fab fragments of the GPIbα blocking antibody p0p/B (Figure 6C) but was less pronounced as compared to mice in which the integrin αIIbβ3 was inhibited by Fab fragments of the JON/A antibody[45]. In line with these findings, it has previously been described that concomitant deficiency of GPVI and integrin α2β1 resulted in severely prolonged bleeding times in contrast to the respective single-deficiency[83]. Similar observations have been made with aspirin-treated GPVI-deficient mice[83], suggesting that simultaneous inhibition of two platelet adhesion/activation receptors or signaling pathways, respectively, can largely impair the hemostatic function of platelets.

The data of the present study may also be relevant for predicting possible complications of an antithrombotic therapy targeting only one (hem)ITAM-coupled receptor. Based on the severe bleeding defect in GPVI/CLEC-2 double-depleted mice, it can be suggested that the therapeutic deletion of one receptor may severely increase the bleeding tendency in patients suffering from genetic or acquired deficiency or bearing a low expression level of the respective other receptor. Although CLEC-2 deficient patient have not been described yet, most probably because CLEC-2 is critically involved in lymphatic vascular development during embryogenesis[99,100], it can be assumed that patients with an acquired loss of CLEC-2, caused by an autoimmune disease, exist. However, as GPVI-deficient patients have already been described, the scenario of massive bleeding complications upon an anti-CLEC-2 therapy in these individuals appears to be the more relevant problem. These hypotheses could also be supported by a murine model where *Gp6*$^{-/-}$ mice were injected with INU1. Pathological thrombus formation after $FeCl_3$-induced vascular injury (Figure 17) as well as normal hemostasis (Bender, May *et al.* in revision) was severely affected in these mice similar to the defects observed in JAQ1 + INU1-treated mice. In accordance with results of the previous sections, these findings also suggested, albeit only partially, that antibody-

induced irreversible depletion of the (hem)ITAM-coupled receptors from the platelet surface phenotypically mirrors the defects in thrombus formation associated with genetic receptor deficiency. Hence, this further supports the assumption that anti-GPVI antibody-treatment does not cause any obvious side-effects on platelet function.

In summary, this part of the study demonstrated that simultaneous *in vivo* targeting of the (hem)ITAM-bearing receptors GPVI and CLEC-2 results in specific receptor downregulation without influencing other signaling pathways. Furthermore, this double receptor-deficiency in mice has been shown to virtually abolish *in vivo* thrombus formation. These observations may have important implications for the development and application of anti-GPVI and/or anti-CLEC-2 antithrombotic agents.

5.3 RhoA is involved in G_{13}-and G_q-mediated platelet activation and essential for *in vivo* thrombus formation

The functional role of RhoA in platelets has previously been addressed in numerous studies using pharmacological inhibitors, however, this study used for the first time a genetic knockout approach (PF-4 Cre/lox P system) to specifically investigate the impact of RhoA deficiency on platelet function *in vitro* and *in vivo*. It was shown that platelet- and megakaryocyte-specific deletion of RhoA resulted in a marked macrothrombocytopenia, a reduced platelet life span and, as expected, abolished platelet shape change and impaired α and dense granule release in response to G_{13} but notably also to G_q stimulation. The presented data in addition demonstrated that RhoA is required for integrin αIIbβ3-dependent clot retraction but is dispensable for cytoskeletal rearrangements during platelet spreading. Importantly, this study is the first to identify an essential role for the GTPase in hemostasis and thrombosis.

The pronounced thrombocytopenia in *RhoA*$^{-/-}$ mice was accompanied by an increased platelet size but largely unaltered platelet morphology (Figure 18B-D). Surprisingly, the platelet life span was only slightly reduced (Figure 19), indicating that an increased platelet turnover did not account for the reduced platelet counts in these animals. Rather, the findings point to a critical involvement of RhoA in megakaryocyte differentiation and/or platelet formation which would stand in contrast to reports by other groups using inhibitors of the RhoA/ROCK pathway in cultured human megakaryocytes[142,247]. Further experiments are required to clarify this aspect.

Multiple studies using pharmacological inhibitors of RhoA or downstream effectors previously suggested RhoA as a central platelet signaling protein that mediates MLC phosphorylation and consequently platelet shape change upon G_{13}-coupled receptor stimulation[105,131-134]. The results of the present thesis clearly confirmed this view as low concentrations of U46619, thrombin or PAR-4 activating peptide failed to trigger platelet shape change in *RhoA*$^{-/-}$

platelets (Figure 22A). These findings are also completely in line with data from a previous report by Moers *et al.,* showing that platelets lacking $G\alpha_{13}$ displayed abolished RhoA activation and shape change under similar experimental conditions[125]. The shape change defect observed in both studies was also associated with impaired phosphorylation of the RhoA effector MLC (Figure 23 and [125]), establishing RhoA-mediated MLC phosphorylation as the primary signaling pathway for platelet shape change downstream of G_{13}. Interestingly, higher doses of U46619, thrombin and PAR-4 activating peptide, which involved signaling via G_q, largely but not fully re-established the capacity of *RhoA*$^{-/-}$ platelets to undergo shape change (Figure 22A). Together with the finding that low concentrations of ADP, a platelet agonist that exclusively binds to G_q- and G_i-coupled receptors, did not induce shape change in RhoA-deficient platelets (Figure 22B), the data indicated that RhoA may also act downstream of G_q. This has previously also been suggested by others analyzing receptor-dependent regulation of RhoA activation in different cell lines. Chikumi *et al.* demonstrated that activated $G\alpha_q$ proteins were able to stimulate endogenous RhoA in HEK-293T cells[248] and Vogt *et al.* reported that RhoA activation occurred in mouse embryonic fibroblasts by receptor agonists via $G_{12/13}$ stimulation but also, albeit with a lower potency, via $G_{q/11}$-mediated signaling[249]. Consistent with this, Moers *et al*. detected some level of RhoA activation and MLC phosphorylation in response to high concentrations of U46619 in platelets lacking $G\alpha_{13}$ and also in wild-type platelets after activation with ADP[126]. Together, this strongly suggests that RhoA activity may also be regulated by $G\alpha_q$-coupled receptors, however the underlying molecular mechanism is entirely unclear so far. The herein presented data at least indicated that the additionally proposed way of RhoA activation occurs independently of the classical G_q-induced signaling cascade via PLCβ stimulation and intracellular Ca^{2+} mobilization (Figure 24). This was also supported by Vogt *et al.* in a cell line study[249], which at the same time proposed the RhoGEF protein LARG as a potential mediator for $G\alpha_q$-dependent RhoA activation. However, whether LARG or other members of the same RhoGEF family, such as p115RhoGEF or PDZ-RhoGEF, as indicated by Chikumi *et al.*[248], provide this signaling link also in platelets remains still to be determined.

The present study further demonstrated that shape change of *RhoA*$^{-/-}$ platelets was abolished in response to low concentrations of CRP and collagen and was still defective at intermediate and high agonist concentrations, particularly for collagen (Figure 22B). These findings are, however, not surprising as previous reports demonstrated that collagen-induced shape change strongly depends on the release/secretion of soluble mediators such as ADP and mainly TxA_2 that act via G_{13}- and G_q- and G_i-coupled receptors and thereby also via RhoA signaling[126,250]. In contrast, marked MLC phosphorylation was detectable in the mutant platelets upon stimulation with high CRP concentrations (Figure 23), indicating that under these experimental conditions GPVI-induced MLC phosphorylation is dominantly regulated

via Ca^{2+}/calmodulin-dependent MLCK activation and independently of RhoA, as previously supposed for human platelets[136]. This signaling pathway appears, however, not to be sufficient to trigger GPVI activation-dependent shape change under the conditions of aggregometry.

Moreover, the data showed that RhoA plays a critical role in α and dense granule release upon G_{13}-mediated signaling but, interestingly, also partially downstream of G_q (Figure 20B and Figure 21), which directly translated into a reduced aggregation response of *RhoA*$^{-/-}$ platelets at intermediate concentrations of U46619 and PAR-4 activating peptide (Figure 22A,C). These findings confirmed previous indications from inhibition studies[136,249] as well as from reports by Moers *et al.*, analyzing $G\alpha_{13}$-deficient and $G\alpha_{13}/G\alpha_q$ double-deficient platelets[125,126]. Notably, in line with observations from the latter studies, thrombin-induced dense granule release and subsequent aggregation was not affected in *RhoA*$^{-/-}$ platelets (Figure 21 and Figure 22A,C), whereas P-selectin exposure, determined by flow cytometry, was strongly reduced after thrombin activation (Figure 20). This suggested that thrombin induces additional, PAR-independent signaling that may compensate for the lack of RhoA under conditions present in highly dense platelet suspension for aggregation measurements but not under conditions of a strongly diluted platelet sample for flow cytometry. However, as indicated by studies in $G\alpha_{13}$-deficient platelets, thrombin-mediated aggregation processes via GPIbα most probably are not involved[125]. Surprisingly, and in contrast to the finding that secretion after stimulation of the hem(ITAM) receptors GPVI and CLEC-2 was unaltered in *RhoA*$^{-/-}$ platelets (Figure 20B and Figure 21), low and intermediate concentrations of CRP and collagen induced an increased aggregation response in these platelets (Figure 22B,C). It is difficult to explain this phenomenon at present, but as GPVI signaling seemed to be unaffected by the absence of RhoA (Figure 24), rather signaling-independent processes might be altered. Accordingly, the increased size of RhoA-deficient platelets and possibly an associated elevated amount of granules might be involved. This may then lead to an increased degranulation response upon the primary GPVI activation signal in comparison to wild-type platelets. However, further analyses, e.g. concerning the number of granules per *RhoA*$^{-/-}$ platelet are indispensable to assess this vague hypothesis. The data of the present study clearly demonstrated that RhoA is essential for the induction of granule release downstream of G_{13}- and G_q-coupled receptors, however the exact underlying mechanism is unclear at present. The process of RhoA-dependent exocytosis has previously been investigated in different cell types and although a direct association of the GTPase with the membrane of secretory granules has been described, the studies indicated that RhoA rather is involved in actin remodeling to negatively instead of positively regulate exocytosis[251]. Thus, it remains to be determined how RhoA induces degranulation in platelets.

Besides granule release, RhoA has also been implicated in integrin αIIbβ3 inside-out activation[124,125,135,195] as well as in outside-in signaling-dependent cytoskeletal reorganizations[139,140]. In the current study, it was found that *RhoA*$^{-/-}$ deficiency resulted in slightly reduced integrin αIIbβ3 activation in response to U46619 co-stimulated with ADP as well as to thrombin and rhodocytin (Figure 20A). Interestingly, these defects clearly exceeded those observed in platelets lacking $G\alpha_{13}$, particularly for thrombin (data not shown and [125]), which further supported the notion that RhoA is required for signal transduction downstream of G_{13}, but also to a certain extent of G_q. However, additional investigations are necessary to determine whether RhoA directly regulates integrin αIIbβ3 activation or whether the reduced level of activated integrin detectable on the platelets surface is a consequence of defective RhoA-dependent degranulation and subsequently reduced integrin exposure from intracellular compartments during platelet activation.

In a recent study, Gong *et al*. proposed a new model for ligand-induced integrin αIIbβ3 outside-in signaling involving a tight and temporally defined regulation of RhoA activity[139]. They suggested that the GTPase is transiently inhibited by c-Src bound to the β3-tail of the integrin during the early phase of platelet spreading whereas in the following it becomes reactivated and allows clot retraction due to calpain-dependent cleavage of the c-Src-integrin interaction[139]. Although the underlying mechanism was not proven in the herein presented study, the results provided clear evidence that RhoA is dispensable for spreading of activated platelets on fibrinogen but essential for clot retraction (Figure 25 and Figure 28). These findings, however, stand in contrast to observations by Leng *et al.*, using C3 exoenzyme to inactivate RhoA[140], which may be explained by a potential limited specificity and efficiency of the inhibitor.

Interestingly, although RhoA is known to be a critical mediator of cytoskeletal reorganizations and consequently contributes to F-actin bundling and stress fiber formation in numerous cell types[106,112,196], the current thesis indicated that RhoA is not required for F-actin assembly in activated platelets and only partially involved in stress fiber formation and proper granule centralization spread platelets (Figure 26 and Figure 27B). These observations reflect findings of an inhibition study with human platelets[140] and are in line with a recent report by Jackson *et al*., describing that RhoA-deficient keratinocytes were perfectly able to form stress fibers and focal adhesions[122]. Likewise, RhoA was dispensable for actomyosin regulation in primary mouse embryonic fibroblasts[252] which may be due to a functional compensation of RhoA-deficiency by RhoB and RhoC. Since RhoA is the only known Rho isoform expressed in platelets, this kind of redundancy appears not to be a likely explanation for the only moderately altered F-actin structures in *RhoA*$^{-/-}$ platelets[253]. However, one may assume that functional redundancies with other members of the Rho GTPase family may be present in platelets, as RhoA, Cdc42, Rac1 and also RhoF mediate cytoskeletal rearrangements

partially via the common downstream effector mDia[254,255]. Further studies, using e.g. double-deficient mouse strains, are required to elaborate this aspect.

In addition, the data of the current study revealed a role of RhoA in the organization of microtubule structures in spread platelets (Figure 27A). However, the underlying mechanism how RhoA may regulate the tubulin cytoskeleton and whether this is a direct signaling effect or indirectly caused by altered actin structures has not yet been identified. A previous study suggested that microtubule coils may be regulated via the Rho/ROCK pathway during platelet shape change[256], but a contribution of RhoA-dependent activation of mDia, as shown for other cell types[257], should also be considered.

Interestingly, the specific signaling defects of *RhoA*$^{-/-}$ platelets detected *in vitro* did not result in impaired thrombus formation on collagen under high shear flow conditions (Figure 29A). This indicated that RhoA-deficient platelets are sufficiently activated via GPVI to allow adhesion to the matrix, a process that functions independently of soluble mediators[126], but also formation of stable thrombi despite the impaired G_{13}/G_q-signaling pathways. These findings are surprising, particularly as $G\alpha_{13}^{-/-}$ platelets have been shown to display defective thrombus formation in a similar perfusion assay[125]. The discrepancies are difficult to explain but slight differences in the methodology of the experiment and/or possible side effects on platelet function by injection of polyinosinic-polycytidylic acid into mice to induce gene deletion (Mx Cre/lox P system) may be involved. However, RhoA deficiency appeared to moderately but significantly impair platelet adhesion to the surface of an expanding aggregate at very high shear rates (Figure 29A). This defect might probably be ascribed to a reduced GPIbα-vWF-dependent platelet-platelet interaction under high shear conditions in the absence of RhoA, as *RhoA*$^{-/-}$ platelets displayed, despite normal adhesion to vWF, a significantly higher rolling velocity on a the matrix as compared to wild-type platelets (Figure 29B). Consistent with these observations, also human platelets have previously been described to exhibit reduced stationary adhesion contacts with vWF under flow when inhibiting the RhoA/ROCK signaling pathway[138].

Importantly, however, RhoA deficiency resulted in clearly impaired thrombus formation *in vivo* and protected mice from irreversible vessel occlusion. Initial thrombus formation was unaltered in *RhoA*$^{-/-}$ mice, whereas thrombus progression in increasingly stenosed vessels or stabilization of occlusive thrombi was strongly diminished in $FeCl_3$-injured mesenteric arterioles due to permanent release of platelets from the thrombus surface and embolization of thrombus fragments (Figure 30). Similar results were obtained in the model of mechanically induced vascular damage of the abdominal aorta (Figure 31). The observed defect in thrombus stabilization was certainly caused by defective platelet incorporate into an expanding thrombus at high shear but mainly due to impaired degranulation-dependent release of soluble mediators. The latter process is known to be of central importance for

thrombus formation under *in vivo* conditions[244,258,259]. It is important to note that the defective thrombus formation in *RhoA*$^{-/-}$ mice was not caused by the decreased platelet counts in these mice, as e.g. conditional knockout mice (PF-4 Cre/lox P system) deficient in Cdc42 even displayed significantly accelerated thrombus formation in the same $FeCl_3$-injury model due to enhanced granule secretion but despite reduced platelet counts of only 50-80% compared to control[107]. Additionally, thrombocytopenic mice that had a reduced platelet count ranging between 30-50% of normal levels showed slightly delayed but, notably, irreversible vessel occlusion after mechanically induced vascular injury of the abdominal aorta (Figure 38). Thrombocytopenia in these mice was experimentally induced by i.v. injection of 2.5 µg of the anti-GPIbα antibody p0p/B 24 h prior to the experiment[183]. Taken together, this strongly suggested that RhoA plays a fundamental role in occlusive thrombus stabilization.

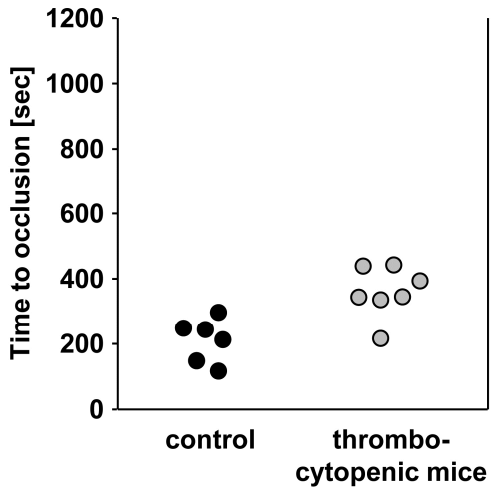

Figure 38. Thrombocytopenic mice display largely unaltered thrombus formation in a mechanical injury model. Mice received either vehicle or 2.5 µg p0p/B antibody 24 h prior to injury to reduce platelet counts to 30-50% of normal levels. The abdominal aorta was injured by tight compression with a forceps and blood flow was monitored using an ultrasonic flow probe. Time to stable vessel occlusion is depicted. One symbol represents one individual.

Furthermore, RhoA deficiency was also associated with a severe increase in bleeding times, indicating that RhoA is also required for thrombus formation during hemostasis (Figure 32). Importantly, *RhoA*$^{-/-}$ mice were profoundly protected from ischemic brain infarction and displayed a better neurological outcome in a model of experimental stroke (Figure 33). Although the bleeding times in these mice were affected, no indications for an increase in ICH, which represents the main complication of current antithrombotic therapy during acute stroke, were detectable. This finding is in line with the previous observation that an increase in bleeding times does not necessarily correlate with an increase in bleeding risk[214].

According to these data, it is tempting to speculate that RhoA may represent a potential target molecule for effective therapy of thromboembolic diseases. However, serious problems of such a therapy may arise from the ubiquitous expression of RhoA and its central role in many cellular functions such as cell contraction, adhesion, migration and cytokinesis[109]. Additionally, the fact that RhoA is located within the cell would further complicate targeting of this GTPase.

In summary, the presented study revealed selective, yet important roles for RhoA in platelet function *in vitro* and *in vivo*. It was shown that RhoA is critical for platelet shape change and efficient α and dense granule release downstream of G_{13} and G_q. In addition, RhoA appeared to be essential for integrin-mediated clot retraction, but not for actomyosin rearrangements and spreading of activated platelets. Furthermore, this study identified RhoA as a crucial mediator of stable thrombus formation during hemostasis and thrombosis.

5.4 The FXIIa inhibitor rHA-Infestin-4 is a potent antithrombotic agent without causing bleeding side effects

In the present study, the suitability of FXII/FXIIa as a novel potential target for antithrombotic therapy (Figure 40) was assessed by characterizing the newly developed FXIIa inhibitor rHA-Infestin-4 and testing its antithrombotic potential in animal models of thrombosis and ischemic stroke. Generation, production and initial characterization of rHA-Infestin-4 were performed by CSL Behring (Marburg, Germany) and served as the basis for this part of the thesis. Our collaboration partners at CSL Behring cloned the above described 7 kDa FXIIa inhibitor Infestin-4 from the hematophagus insect *Triatoma infestans*, extended by an $(His)_6$-tag and determined the pharmacokinetic characteristics of the resulting $(His)_6$-Infestin-4 after i.v. application of 20 mg/kg body weight (2.7 µmol/kg) of the protein into mice. Unfortunately, these measurements revealed that $(His)_6$-Infestin-4 lead to a very low recovery of only 8% of the protein in mice and a short half-life of 0.3 h (Figure 39A) which excluded the application of $(His)_6$-Infestin-4 for further studies employing a reasonable efficient treatment schedule. To circumvent this limitation, CSL Behring generated the rHA-Infestin-4 fusion protein to enhance the bioavailability. SDS-PAGE analysis confirmed the successful generation of the protein with the expected molecular weight of 73 kDa and a purity of approximately 95% (Figure 39B). Pharmacokinetic analysis of rHA-Infestin-4 demonstrated a high recovery of 92% and a half-life of 4.6 h after i. v. injection (2.7 µmol/kg) (Figure 39A).

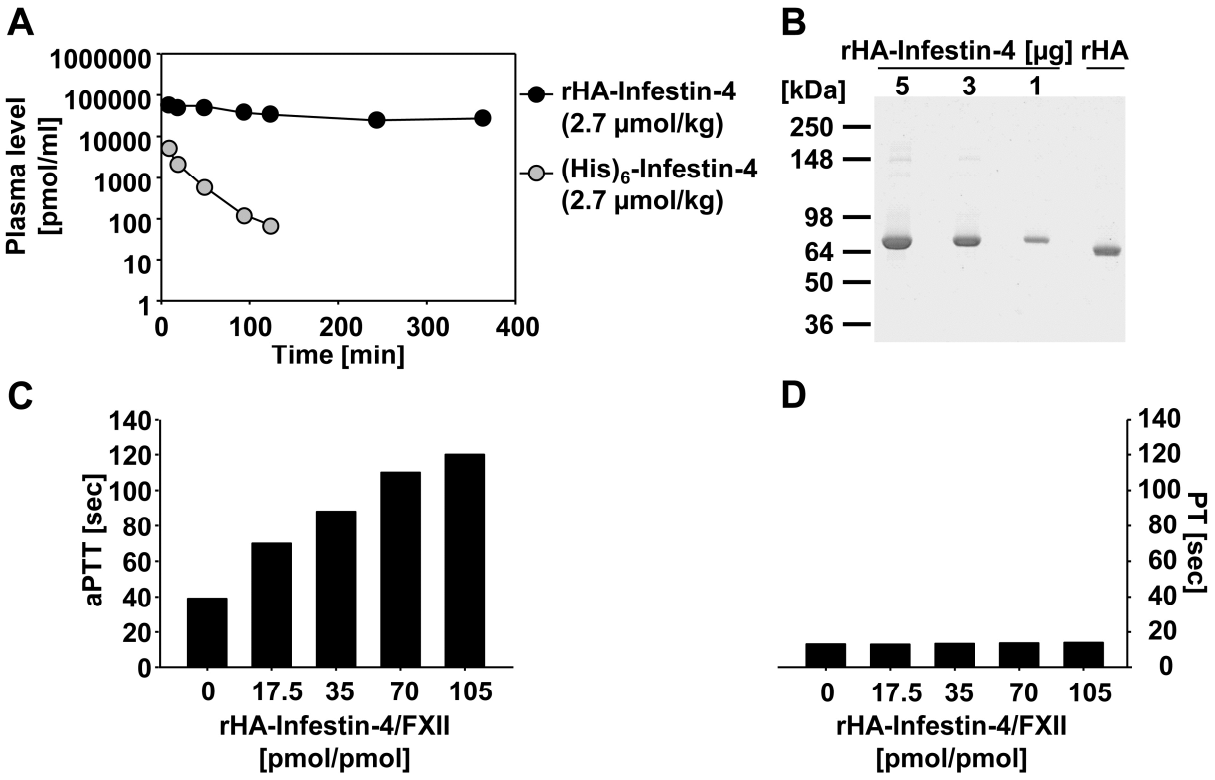

Figure 39. Pharmacokinetic analysis and *in vitro* coagulation. A, Infestin-4 plasma levels in mice at different time points after either rHA-Infestin-4 or $(His)_6$-Infestin-4 injection. Representative measurements from at least 10 individuals are shown. B, SDS-PAGE of purified rHA-Infestin-4 and rHA. C,D, Activated partial thromboplastin time (aPTT) and prothrombin time (PT) of standard human plasma after 2 min incubation with rHA-Infestin-4 at the indicated concentrations. Representative data of 4 independent measurements are illustrated. rHA=recombinant human albumin. (Hagedorn *et al*., *Circulation*, 2010)[202].

The initial *in vitro* characterization of rHA-Infestin-4 by CSL Behring revealed that the protein specifically inhibited the intrinsic coagulation pathway while leaving the extrinsic pathway completely unaffected as rHA-Infestin-4 prolonged aPTT in a dose-dependent manner in SHP without influencing PT (Figure 39C,D). Similar observations were made with mouse and rat plasma[202].

These data together with the results of the herein presented study clearly showed that rHA-Infestin-4 specifically inhibited FXIIa *in vitro* and *in vivo* irrespectively of the analyzed species and induces potent protection of mice and rats from thrombotic events without any detectable effects on hemostasis. Immediately after injection, rHA-Infestin-4 abolished platelet aggregation and thrombus formation at sites of vascular injury (Figure 34A,C), demonstrating rapid and highly efficient inhibition of FXIIa. This strong inhibitory effect was reversible and gradually declined probably when rHA-Infestin-4 was metabolized and cleared from the circulation, as small but unstable thrombi (diameter: ~10 µm) were formed upon vessel injury when rHA-Infestin-4 was administered ~100 min prior to injury. This effect of rHA-Infestin-4 on arterial thrombus formation was confirmed in two different arterial beds, small mesenteric arterioles as well as the carotid artery (Figure 34A-D) and found to be similar in mice and

rats. This indicates that the inhibitor might be effective in different species, including humans, as it very potently inhibits human α/βFXIIa *in vitro* (Table 2). The antithrombotic activity of rHA-Infestin-4 was also evident in a transient cerebral ischemia model where mice displayed profound protection from neurological damage (Figure 37A-C). Furthermore, rHA-Infestin-4 moderately inhibited fibrinolysis as indicated by a reduced D-Dimer concentration in clotted rHA-Infestin-4 spiked plasma. The underlying mechanism is not clear at present, but inhibition of plasmin, as determined in a chromogenic assay (Table 3), may at least partially account for this effect. However, this inhibition does certainly not explain the effective antithrombotic potency of the inhibitor. Whether the antifibrinolytic effect of the inhibitor has any relevance *in vivo* has yet to be determined. Together, these results indicate that rHA-Infestin-4 might be effective in the prophylaxis and treatment of thromboembolic diseases.

Unexpectedly, the marked protection of rHA-Infestin-4 treated mice from arterial thrombosis and ischemic stroke exceeded the effects previously found in FXII-deficient mice[169,170]. Notably, it could be shown that rHA-Infestin-4 did not abrogate the residual thrombotic activity in FXII-deficient mice which excludes an additional albeit subordinated influence of rHA-Infestin-4 on other proteins relevant in thrombus formation. Based on these findings, one may rather hypothesize that the genetic loss of FXII in the mutant mice leads to compensatory upregulation of alternative mechanisms that account for the residual thrombotic activity (Figure 36). Remarkably, the temporary and efficient inhibition of FXIIa *in vivo* was not associated with excessive bleeding (Figure 35), even under conditions of major surgery, in accordance with observations in FXII-deficient mice and humans[169,260]. These findings support the intriguing hypothesis that hemostasis and thrombosis are two mechanistically different processes[169,203] and establish rHA-Infestin-4 as a promising candidate molecule for highly effective and safe antithrombotic therapy. Such a safe therapy might be particularly advantageous in the treatment of acute stroke, as the conventional therapy to prevent lesion progression and recurrent thromboembolism with platelet aggregation inhibitors and anticoagulants like coumarins and heparins is inheritably associated with an increased risk of ICH[220-222]. Moreover, transient blockade of FXIIa activity may help to bridge the risk of vessel reocclusion after thrombolytic therapy. Lack of a sufficiently effective therapy of acute ischemic stroke makes it one of the leading causes of death and disability worldwide[261,262].

The potential use of rHA-Infestin-4 as an antithrombotic agent in clinical practice may to a great extent be influenced by its relatively short *in vivo* half-life (Figure 39A), its corresponding time-dependent antithrombotic effect (Figure 34A,B) as well as its protein size and partially heterologous origin. These properties suggest that rHA-Infestin-4 might be a potent drug for short-term therapy of patients at high risk of thromboembolism in acute clinical settings such as vascular and heart surgery[263]. In addition, rHA-Infestin-4 might be

effective in the prevention of secondary infarctions and subsequent stroke progression, which often occurs shortly after transient ischemic attacks or ischemic stroke even after previously successful recanalization[264].

Furthermore, a recent study on hyperglycemia-induced cerebral hematoma expansion in rodents with ICH suggested another, very specialized therapeutic area for FXIIa inhibitors[265]. Primary ICH is an acutely life-threatening disease state often caused by hypertension and represents besides cerebral ischemia the second leading cause of all stroke cases[266]. This is particularly due to the absence of effective treatment options for acute ICH to date. Diabetes or acute hyperglycemia are additional risk factors which can negatively influence the clinical outcome of ICH. *Liu et al.*[265] now described that plasma kallikrein (PK) inhibits platelet aggregation at sites of tissue trauma under high blood glucose concentrations, thereby enhancing hematoma expansion of ICH in diabetic or acute hyperglycemic rats and mice. Accordingly, a PK inhibitor prevented the extension of the hemorrhagic area in the brain after induced ICH in diabetic rats[265]. Assuming that these pathophysiological mechanisms are also valid in humans, specific inhibition of FXIIa by rHA-Infestin-4 and thus subsequent blockage of PK production might be clinically useful to lower the risk of severe ICH in patients with acute hyperglycemia at hospital admission.

However, to directly transfer the here presented results for the development of a suitable therapeutic concept for humans, a set of further studies is still required, especially because the relationship between FXII and pathological clotting in humans is so far not as clear as in rodents. Various studies reported conflicting results about the impact of FXII deficiency on thrombotic events which may lead to different conclusions about the potential safety profile of an anti-FXIIa therapy. While FXII deficiency was once found to be even a risk factor for thromboembolic diseases[267,268], studies on Swiss and Dutch patients did not confirm this correlation[269,270]. Moreover, reduced plasma FXII levels were identified to afford protection from acute coronary syndrome and lower thrombosis risk[271,272], which would match the situation in mice. In contrast, the Study of Myocardial Infarction-Leiden (SMILE) project demonstrated an inverse association between FXII levels and risk of myocardial infarction[273]. The study by *Endler et al.*[274] described similar observations, whereas, the mortality for a small subpopulation of patients with only 1-10% of normal FXII levels was comparable to the mortality for the population median, indicating a clear difference in thrombosis between moderate and severe FXII deficiency. This, however, raised the possibility that nearly abolished FXIIa activity, which can probably be induced by effective and specific FXIIa inhibition, is different from the conditions of hereditarily reduced FXII levels in humans. To make more reliable predictions about the functional relevance of FXIIa-induced thrombotic activity in humans, inhibition studies in higher developed mammalians than rodents will be important. Remarkably, a recent publication already showed that antibody-mediated

inhibition of FXI activation by FXIIa potently reduced platelet-rich thrombus formation in collagen-coated grafts inserted into an arteriovenous shunt in baboons[275]. Thus, the FXIIa/FXI activation axis appears to play a significant role in pathological thrombus growth across a wide range of species, also emphasizing direct FXII/FXIIa inhibition as a very promising therapeutic option for the treatment of thromboembolic diseases in humans.

Besides rHA-Infestin-4 also other FXIIa inhibitors have been described during the last years which confirmed that FXIIa can be well targeted *in vivo*. However, these inhibitors were either not specific, which might cause several undesirable side effects when therapeutically used, and/or they were clearly less effective as compared to rHA-Infestin-4. The recombinant protein Ir-CPI expressed by the tick *Ixodes ricinus* e.g. interacts with different contact phase factors (FXIIa, FXIa, PK) as well as plasmin[276] and the synthetic FXIIa inhibitor D-Pro-Phe-Arg chloromethyl ketone (PCK) has been described to also block the amidolytic activity of PK, plasmin, FXa, and thrombin *in vitro*[277]. PCK has been shown to protect mice from ischemic stroke in a tMCAO model[170] but displayed a prothrombotic effect in a Rose Bengal murine thrombosis model[278]. Recently, also 3-carboxamide-coumarins have been described as a new class of non-peptidic specific FXIIa inhibitors *in vitro*, however, the member COU254 failed to protect mice from acute ischemic stroke[279].

In summary, the study demonstrated that the newly developed selective FXIIa inhibitor rHA-Infestin-4 is highly active in human plasma and profoundly protects mice and rats from pathological thrombus formation while not affecting hemostasis. This indicates that rHA-Infestin-4 might be a powerful, yet safe, agent for prevention and treatment of acute ischemic cardio- and cerebrovascular events.

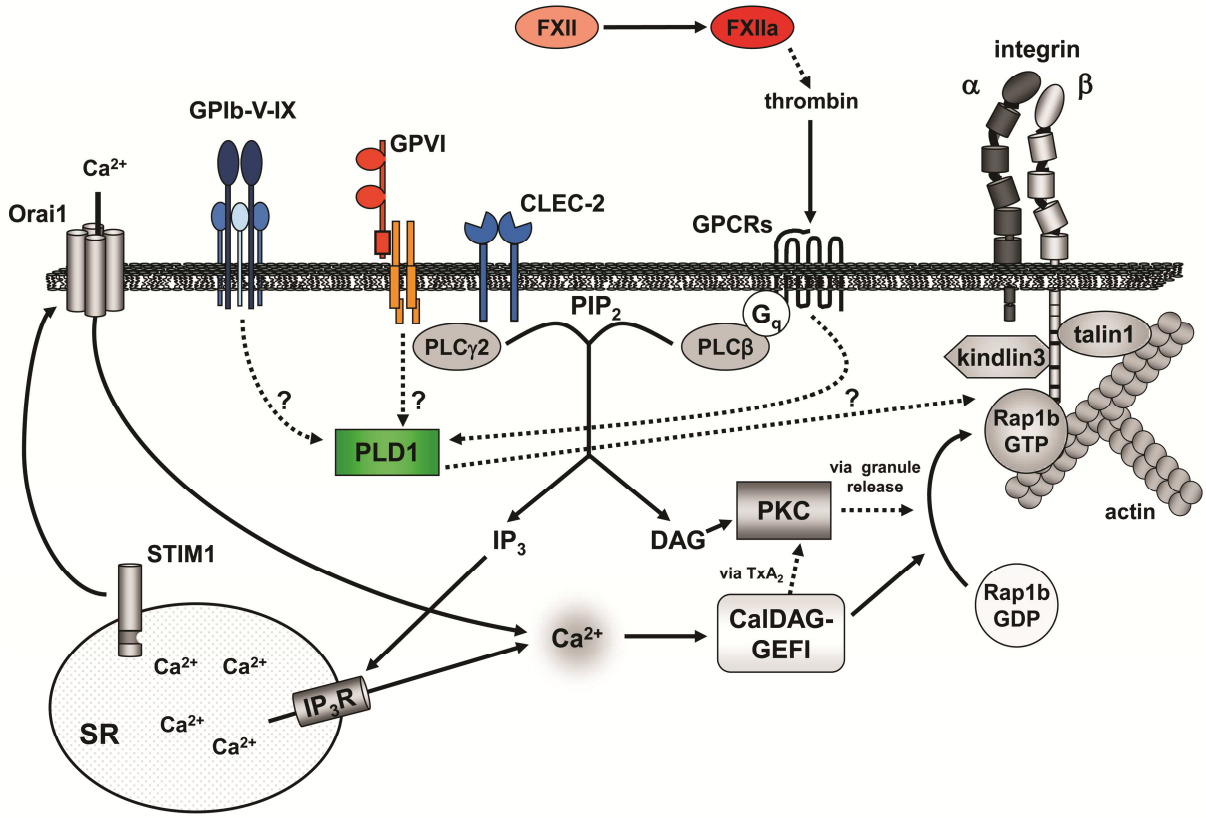

Figure 40. Simplified scheme of platelet receptors and activation pathways required for thrombus formation. Proteins that were analyzed in this study and proposed/tested as promising targets for an effective antithrombotic therapy are highlighted in color. Receptor stimulation leads to the activation of different intracellular signaling molecules and cascades subsequently resulting in the functional upregulation of integrins. PLD1 is activated downstream of different receptors most notably GPIb-V-IX complex and regulates integrin activation, however the defined signaling mechanism remains elusive. Coagulation factor XII contributes to platelet activation via generation of thrombin. (Modified from: Hagedorn *et al., Haemostasiologie*, 2010)[280].

5.5 Concluding remarks and future plans

The presented thesis provides new insights into the complex mechanisms underlying thrombus formation during arterial thrombosis and hemostasis with a special emphasis on the functional roles of the platelet adhesion receptor GPIbα, the (hem)ITAM receptors GPVI and CLEC-2 as well as of the intracellular signaling proteins PLD1 and the Rho GTPase RhoA.

The high incidence of ischemic cardio- and cerebrovascular diseases in industrialized countries together with the limited use of current antithrombotic agents due to bleeding side effects strongly requires alternative therapeutic options. Importantly, some of the data discussed here support the recently raised hypothesis that pathological thrombosis and primary hemostasis may be two mechanistically distinct processes. If this also holds true for humans, it will be possible to target proteins/processes that drive pathological thrombus formation without affecting hemostasis, which would open up new avenues for the development of a novel generation of powerful, yet safe antithrombotic agents.

Additionally, the data point out that genetically engineered mice combined with arterial thrombosis models represent a practical and also a very valuable tool to improve the understanding of *in vivo* thrombus formation and to identify novel targets for therapeutic interventions. This is especially based on the studies of *F12*$^{-/-}$ mice and the consequent generation and functional characterization of rHA-Infestin-4. Furthermore, the development of humanized antibodies and Fab fragments to specifically downregulate or block surface proteins in platelets, respectively, appears to be an attractive pharmacological option for future antithrombotic therapies.

Further experiments are planned in our laboratory to study the role of the second PLD isoform, PLD2, for platelet function and thrombus formation as well as PLD1/PLD2 double-deficient mice to assess potential redundant functions of these enzymes. Moreover, the effects of genetic CLEC-2 deficiency and also of combined GPVI and CLEC-2 deficiency on thrombus formation in pathological thrombosis and hemostasis will be assessed using conditional CLEC-2 knockout mice (a collaboration with S. Watson, University of Birmingham, UK). These investigations will shed new light on the importance of PLD isoforms and (hem)ITAM receptors for platelet function.
In another set of experiments, the impact of RhoA on megakaryocyte maturation and/or platelet formation will be analyzed in detail to clarify the reason for the marked macrothrombocytopenia in RhoA-deficient mice. Further studies will address potential redundancies in platelet and megakaryocyte function of RhoA with the other prominent Rho GTPases, Rac1 and Cdc42, using cell-specific double knockout mice.

6 REFERENCES

1. Italiano JE, Jr., Patel-Hett S, Hartwig JH. Mechanics of proplatelet elaboration. *J Thromb Haemost*. 2007;5 Suppl 1:18-23

2. Junt T, Schulze H, Chen Z, Massberg S, Goerge T, Krueger A, Wagner DD, Graf T, Italiano JE, Jr., Shivdasani RA, von Andrian UH. Dynamic visualization of thrombopoiesis within bone marrow. *Science*. 2007;317:1767-1770

3. Ruggeri ZM. Platelets in atherothrombosis. *Nat Med*. 2002;8:1227-1234

4. Murray CJ, Lopez AD. Mortality by cause for eight regions of the world: Global Burden of Disease Study. *Lancet*. 1997;349:1269-1276

5. Turitto VT, Baumgartner HR. Platelet interaction with subendothelium in flowing rabbit blood: effect of blood shear rate. *Microvasc Res*. 1979;17:38-54

6. Savage B, Almus-Jacobs F, Ruggeri ZM. Specific synergy of multiple substrate-receptor interactions in platelet thrombus formation under flow. *Cell*. 1998;94:657-666

7. Varga-Szabo D, Pleines I, Nieswandt B. Cell adhesion mechanisms in platelets. *Arterioscler Thromb Vasc Biol*. 2008;28:403-412

8. Nieswandt B, Watson SP. Platelet-collagen interaction: is GPVI the central receptor? *Blood*. 2003;102:449-461

9. Suzuki-Inoue K, Fuller GL, Garcia A, Eble JA, Pohlmann S, Inoue O, Gartner TK, Hughan SC, Pearce AC, Laing GD, Theakston RD, Schweighoffer E, Zitzmann N, Morita T, Tybulewicz VL, Ozaki Y, Watson SP. A novel Syk-dependent mechanism of platelet activation by the C-type lectin receptor CLEC-2. *Blood*. 2006;107:542-549

10. Fuller GL, Williams JA, Tomlinson MG, Eble JA, Hanna SL, Pohlmann S, Suzuki-Inoue K, Ozaki Y, Watson SP, Pearce AC. The C-type lectin receptors CLEC-2 and Dectin-1, but not DC-SIGN, signal via a novel YXXL-dependent signaling cascade. *J Biol Chem*. 2007;282:12397-12409

11. Varga-Szabo D, Braun A, Nieswandt B. Calcium signaling in platelets. *J Thromb Haemost*. 2009;7:1057-1066

12. Ren Q, Ye S, Whiteheart SW. The platelet release reaction: just when you thought platelet secretion was simple. *Curr Opin Hematol*. 2008;15:537-541

13. Krishnaswamy S, Nesheim ME, Pryzdial EL, Mann KG. Assembly of prothrombinase complex. *Methods Enzymol*. 1993;222:260-280

14. Fay PJ. Activation of factor VIII and mechanisms of cofactor action. *Blood Rev*. 2004;18:1-15

15. Offermanns S. Activation of platelet function through G protein-coupled receptors. *Circ Res*. 2006;99:1293-1304

16. Wettschureck N, Offermanns S. Rho/Rho-kinase mediated signaling in physiology and pathophysiology. *J Mol Med*. 2002;80:629-638

17. Offermanns S, Toombs CF, Hu YH, Simon MI. Defective platelet activation in G alpha(q)-deficient mice. *Nature*. 1997;389:183-186

18. Clapham DE, Neer EJ. G protein beta gamma subunits. *Annu Rev Pharmacol Toxicol*. 1997;37:167-203

19. Gruner S, Prostredna M, Schulte V, Krieg T, Eckes B, Brakebusch C, Nieswandt B. Multiple integrin-ligand interactions synergize in shear-resistant platelet adhesion at sites of arterial injury in vivo. *Blood*. 2003;102:4021-4027

20. Stegner D, Nieswandt B. Platelet receptor signaling in thrombus formation. *J Mol Med*. 2011;89:109-121

21. Maxwell MJ, Westein E, Nesbitt WS, Giuliano S, Dopheide SM, Jackson SP. Identification of a 2-stage platelet aggregation process mediating shear-dependent thrombus formation. *Blood*. 2007;109:566-576

22. Ruggeri ZM, Orje JN, Habermann R, Federici AB, Reininger AJ. Activation-independent platelet adhesion and aggregation under elevated shear stress. *Blood*. 2006;108:1903-1910

23. Nesbitt WS, Westein E, Tovar-Lopez FJ, Tolouei E, Mitchell A, Fu J, Carberry J, Fouras A, Jackson SP. A shear gradient-dependent platelet aggregation mechanism drives thrombus formation. *Nat Med*. 2009;15:665-673

24. George JN, Nurden AT, Phillips DR. Molecular defects in interactions of platelets with the vessel wall. *N Engl J Med*. 1984;311:1084-1098

25. Berndt MC, Shen Y, Dopheide SM, Gardiner EE, Andrews RK. The vascular biology of the glycoprotein Ib-IX-V complex. *Thromb Haemost*. 2001;86:178-188

26. Lopez JA, Andrews RK, Afshar-Kharghan V, Berndt MC. Bernard-Soulier syndrome. *Blood*. 1998;91:4397-4418

27. Ware J, Russell S, Ruggeri ZM. Generation and rescue of a murine model of platelet dysfunction: the Bernard-Soulier syndrome. *Proc Natl Acad Sci U S A*. 2000;97:2803-2808

28. Kato K, Martinez C, Russell S, Nurden P, Nurden A, Fiering S, Ware J. Genetic deletion of mouse platelet glycoprotein Ibbeta produces a Bernard-Soulier phenotype with increased alpha-granule size. *Blood*. 2004;104:2339-2344

29. Ramakrishnan V, Reeves PS, DeGuzman F, Deshpande U, Ministri-Madrid K, DuBridge RB, Phillips DR. Increased thrombin responsiveness in platelets from mice lacking glycoprotein V. *Proc Natl Acad Sci U S A*. 1999;96:13336-13341

30. Kahn ML, Diacovo TG, Bainton DF, Lanza F, Trejo J, Coughlin SR. Glycoprotein V-deficient platelets have undiminished thrombin responsiveness and Do not exhibit a Bernard-Soulier phenotype. *Blood*. 1999;94:4112-4121

31. Clemetson KJ. A short history of platelet glycoprotein Ib complex. *Thromb Haemost*. 2007;98:63-68

32. Andrews RK, Shen Y, Gardiner EE, Dong JF, Lopez JA, Berndt MC. The glycoprotein Ib-IX-V complex in platelet adhesion and signaling. *Thromb Haemost*. 1999;82:357-364

33. Ozaki Y, Asazuma N, Suzuki-Inoue K, Berndt MC. Platelet GPIb-IX-V-dependent signaling. *J Thromb Haemost*. 2005;3:1745-1751

34. Andrews RK, Harris SJ, McNally T, Berndt MC. Binding of purified 14-3-3 zeta signaling protein to discrete amino acid sequences within the cytoplasmic domain of the platelet membrane glycoprotein Ib-IX-V complex. *Biochemistry*. 1998;37:638-647

35. Andrews RK, Munday AD, Mitchell CA, Berndt MC. Interaction of calmodulin with the cytoplasmic domain of the platelet membrane glycoprotein Ib-IX-V complex. *Blood*. 2001;98:681-687

36. Wu Y, Asazuma N, Satoh K, Yatomi Y, Takafuta T, Berndt MC, Ozaki Y. Interaction between von Willebrand factor and glycoprotein Ib activates Src kinase in human platelets: role of phosphoinositide 3-kinase. *Blood*. 2003;101:3469-3476

37. Sullam PM, Hyun WC, Szollosi J, Dong J, Foss WM, Lopez JA. Physical proximity and functional interplay of the glycoprotein Ib-IX-V complex and the Fc receptor FcgammaRIIA on the platelet plasma membrane. *J Biol Chem*. 1998;273:5331-5336

38. Wu Y, Suzuki-Inoue K, Satoh K, Asazuma N, Yatomi Y, Berndt MC, Ozaki Y. Role of Fc receptor gamma-chain in platelet glycoprotein Ib-mediated signaling. *Blood*. 2001;97:3836-3845

39. Arthur JF, Gardiner EE, Matzaris M, Taylor SG, Wijeyewickrema L, Ozaki Y, Kahn ML, Andrews RK, Berndt MC. Glycoprotein VI is associated with GPIb-IX-V on the membrane of resting and activated platelets. *Thromb Haemost*. 2005;93:716-723

40. Kasirer-Friede A, Cozzi MR, Mazzucato M, De Marco L, Ruggeri ZM, Shattil SJ. Signaling through GP Ib-IX-V activates alpha IIb beta 3 independently of other receptors. *Blood*. 2004;103:3403-3411

41. Kasirer-Friede A, Moran B, Nagrampa-Orje J, Swanson K, Ruggeri ZM, Schraven B, Neel BG, Koretzky G, Shattil SJ. ADAP is required for normal alphaIIbbeta3 activation by VWF/GP Ib-IX-V and other agonists. *Blood*. 2007;109:1018-1025

42. Massberg S, Gawaz M, Gruner S, Schulte V, Konrad I, Zohlnhofer D, Heinzmann U, Nieswandt B. A crucial role of glycoprotein VI for platelet recruitment to the injured arterial wall in vivo. *J Exp Med*. 2003;197:41-49

43. Bergmeier W, Piffath CL, Goerge T, Cifuni SM, Ruggeri ZM, Ware J, Wagner DD. The role of platelet adhesion receptor GPIbalpha far exceeds that of its main ligand, von Willebrand factor, in arterial thrombosis. *Proc Natl Acad Sci U S A*. 2006;103:16900-16905

44. Konstantinides S, Ware J, Marchese P, Almus-Jacobs F, Loskutoff DJ, Ruggeri ZM. Distinct antithrombotic consequences of platelet glycoprotein Ibalpha and VI deficiency in a mouse model of arterial thrombosis. *J Thromb Haemost*. 2006;4:2014-2021

45. Kleinschnitz C, Pozgajova M, Pham M, Bendszus M, Nieswandt B, Stoll G. Targeting platelets in acute experimental stroke: impact of glycoprotein Ib, VI, and IIb/IIIa blockade on infarct size, functional outcome, and intracranial bleeding. *Circulation*. 2007;115:2323-2330

46. Kleinschnitz C, De Meyer SF, Schwarz T, Austinat M, Vanhoorelbeke K, Nieswandt B, Deckmyn H, Stoll G. Deficiency of von Willebrand factor protects mice from ischemic stroke. *Blood*. 2009;113:3600-3603

47. Hammond SM, Altshuller YM, Sung TC, Rudge SA, Rose K, Engebrecht J, Morris AJ, Frohman MA. Human ADP-ribosylation factor-activated phosphatidylcholine-specific

phospholipase D defines a new and highly conserved gene family. *J Biol Chem*. 1995;270:29640-29643

48. Kodaki T, Yamashita S. Cloning, expression, and characterization of a novel phospholipase D complementary DNA from rat brain. *J Biol Chem*. 1997;272:11408-11413

49. McDermott M, Wakelam MJ, Morris AJ. Phospholipase D. *Biochem Cell Biol*. 2004;82:225-253

50. Vorland M, Thorsen VA, Holmsen H. Phospholipase D in platelets and other cells. *Platelets*. 2008;19:582-594

51. Cazzolli R, Shemon AN, Fang MQ, Hughes WE. Phospholipid signalling through phospholipase D and phosphatidic acid. *IUBMB Life*. 2006;58:457-461

52. Exton JH. Phospholipase D-structure, regulation and function. *Rev Physiol Biochem Pharmacol*. 2002;144:1-94

53. Ktistakis NT, Delon C, Manifava M, Wood E, Ganley I, Sugars JM. Phospholipase D1 and potential targets of its hydrolysis product, phosphatidic acid. *Biochem Soc Trans*. 2003;31:94-97

54. Oude Weernink PA, Lopez de Jesus M, Schmidt M. Phospholipase D signaling: orchestration by PIP2 and small GTPases. *Naunyn Schmiedebergs Arch Pharmacol*. 2007;374:399-411

55. Rudge SA, Wakelam MJ. Inter-regulatory dynamics of phospholipase D and the actin cytoskeleton. *Biochim Biophys Acta*. 2009;1791:856-861

56. Stace CL, Ktistakis NT. Phosphatidic acid- and phosphatidylserine-binding proteins. *Biochim Biophys Acta*. 2006;1761:913-926

57. Rubin R. Phosphatidylethanol formation in human platelets: evidence for thrombin-induced activation of phospholipase D. *Biochem Biophys Res Commun*. 1988;156:1090-1096

58. Vorland M, Holmsen H. Phospholipase D in human platelets: presence of isoenzymes and participation of autocrine stimulation during thrombin activation. *Platelets*. 2008;19:211-224

59. Martinson EA, Scheible S, Marx-Grunwitz A, Presek P. Secreted ADP plays a central role in thrombin-induced phospholipase D activation in human platelets. *Thromb Haemost*. 1998;80:976-981

60. Chiang TM. Activation of phospholipase D in human platelets by collagen and thrombin and its relationship to platelet aggregation. *Biochim Biophys Acta*. 1994;1224:147-155

61. Nofer JR, Walter M, Kehrel B, Seedorf U, Assmann G. HDL3 activates phospholipase D in normal but not in glycoprotein IIb/IIIa-deficient platelets. *Biochem Biophys Res Commun*. 1995;207:148-154

62. Coorssen JR. Phospholipase activation and secretion: evidence that PLA2, PLC, and PLD are not essential to exocytosis. *Am J Physiol*. 1996;270:C1153-1163

63. Holinstat M, Voss B, Bilodeau ML, Hamm HE. Protease-activated receptors differentially regulate human platelet activation through a phosphatidic acid-dependent pathway. *Mol Pharmacol*. 2007;71:686-694

64. Holinstat M, Preininger AM, Milne SB, Hudson WJ, Brown HA, Hamm HE. Irreversible platelet activation requires protease-activated receptor 1-mediated signaling to phosphatidylinositol phosphates. *Mol Pharmacol*. 2009;76:301-313

65. Clemetson KJ, Clemetson JM. Platelet collagen receptors. *Thromb Haemost*. 2001;86:189-197

66. Jandrot-Perrus M, Busfield S, Lagrue AH, Xiong X, Debili N, Chickering T, Le Couedic JP, Goodearl A, Dussault B, Fraser C, Vainchenker W, Villeval JL. Cloning, characterization, and functional studies of human and mouse glycoprotein VI: a platelet-specific collagen receptor from the immunoglobulin superfamily. *Blood*. 2000;96:1798-1807

67. Tsuji M, Ezumi Y, Arai M, Takayama H. A novel association of Fc receptor gamma-chain with glycoprotein VI and their co-expression as a collagen receptor in human platelets. *J Biol Chem*. 1997;272:23528-23531

68. Watson SP, Gibbins J. Collagen receptor signalling in platelets: extending the role of the ITAM. *Immunol Today*. 1998;19:260-264

69. Ezumi Y, Shindoh K, Tsuji M, Takayama H. Physical and functional association of the Src family kinases Fyn and Lyn with the collagen receptor glycoprotein VI-Fc receptor gamma chain complex on human platelets. *J Exp Med*. 1998;188:267-276

70. Briddon SJ, Watson SP. Evidence for the involvement of p59fyn and p53/56lyn in collagen receptor signalling in human platelets. *Biochem J*. 1999;338 (Pt 1):203-209

71. Watson SP, Auger JM, McCarty OJ, Pearce AC. GPVI and integrin alphaIIb beta3 signaling in platelets. *J Thromb Haemost*. 2005;3:1752-1762

72. Inoue O, Suzuki-Inoue K, McCarty OJ, Moroi M, Ruggeri ZM, Kunicki TJ, Ozaki Y, Watson SP. Laminin stimulates spreading of platelets through integrin alpha6beta1-dependent activation of GPVI. *Blood*. 2006;107:1405-1412

73. Watson SP, Herbert JM, Pollitt AY. GPVI and CLEC-2 in hemostasis and vascular integrity. *J Thromb Haemost*. 2010;8:1456-1467

74. Morton LF, Hargreaves PG, Farndale RW, Young RD, Barnes MJ. Integrin alpha 2 beta 1-independent activation of platelets by simple collagen-like peptides: collagen tertiary (triple-helical) and quaternary (polymeric) structures are sufficient alone for alpha 2 beta 1-independent platelet reactivity. *Biochem J*. 1995;306 (Pt 2):337-344

75. Polgar J, Clemetson JM, Kehrel BE, Wiedemann M, Magnenat EM, Wells TN, Clemetson KJ. Platelet activation and signal transduction by convulxin, a C-type lectin from Crotalus durissus terrificus (tropical rattlesnake) venom via the p62/GPVI collagen receptor. *J Biol Chem*. 1997;272:13576-13583

76. Jandrot-Perrus M, Lagrue AH, Okuma M, Bon C. Adhesion and activation of human platelets induced by convulxin involve glycoprotein VI and integrin alpha2beta1. *J Biol Chem*. 1997;272:27035-27041

77. Nieswandt B, Schulte V, Bergmeier W, Mokhtari-Nejad R, Rackebrandt K, Cazenave JP, Ohlmann P, Gachet C, Zirngibl H. Long-term antithrombotic protection by in vivo depletion of platelet glycoprotein VI in mice. *J Exp Med*. 2001;193:459-469

78. Dubois C, Panicot-Dubois L, Merrill-Skoloff G, Furie B, Furie BC. Glycoprotein VI-dependent and -independent pathways of thrombus formation in vivo. *Blood*. 2006;107:3902-3906

79. Mangin P, Yap CL, Nonne C, Sturgeon SA, Goncalves I, Yuan Y, Schoenwaelder SM, Wright CE, Lanza F, Jackson SP. Thrombin overcomes the thrombosis defect associated with platelet GPVI/FcRgamma deficiency. *Blood*. 2006;107:4346-4353

80. Kato K, Kanaji T, Russell S, Kunicki TJ, Furihata K, Kanaji S, Marchese P, Reininger A, Ruggeri ZM, Ware J. The contribution of glycoprotein VI to stable platelet adhesion and thrombus formation illustrated by targeted gene deletion. *Blood*. 2003;102:1701-1707

81. Lockyer S, Okuyama K, Begum S, Le S, Sun B, Watanabe T, Matsumoto Y, Yoshitake M, Kambayashi J, Tandon NN. GPVI-deficient mice lack collagen responses and are protected against experimentally induced pulmonary thromboembolism. *Thromb Res*. 2006;118:371-380

82. Schulte V, Reusch HP, Pozgajova M, Varga-Szabo D, Gachet C, Nieswandt B. Two-phase antithrombotic protection after anti-glycoprotein VI treatment in mice. *Arterioscler Thromb Vasc Biol*. 2006;26:1640-1647

83. Gruner S, Prostredna M, Aktas B, Moers A, Schulte V, Krieg T, Offermanns S, Eckes B, Nieswandt B. Anti-glycoprotein VI treatment severely compromises hemostasis in mice with reduced alpha2beta1 levels or concomitant aspirin therapy. *Circulation*. 2004;110:2946-2951

84. Cheli Y, Jensen D, Marchese P, Habart D, Wiltshire T, Cooke M, Fernandez JA, Ware J, Ruggeri ZM, Kunicki TJ. The Modifier of hemostasis (Mh) locus on chromosome 4 controls in vivo hemostasis of Gp6-/- mice. *Blood*. 2008;111:1266-1273

85. Hechler B, Nonne C, Eckly A, Magnenat S, Rinckel JY, Denis CV, Freund M, Cazenave JP, Lanza F, Gachet C. Arterial thrombosis: relevance of a model with two levels of severity assessed by histologic, ultrastructural and functional characterization. *J Thromb Haemost*. 2010;8:173-184

86. Eckly A, Hechler B, Freund M, Zerr M, Cazenave JP, Lanza F, Mangin PH, Gachet C. Mechanisms underlying FeCl(3) -induced arterial thrombosis. *J Thromb Haemost*. 2011;9:779-789

87. Moroi M, Jung SM, Okuma M, Shinmyozu K. A patient with platelets deficient in glycoprotein VI that lack both collagen-induced aggregation and adhesion. *J Clin Invest*. 1989;84:1440-1445

88. Boylan B, Chen H, Rathore V, Paddock C, Salacz M, Friedman KD, Curtis BR, Stapleton M, Newman DK, Kahn ML, Newman PJ. Anti-GPVI-associated ITP: an acquired platelet disorder caused by autoantibody-mediated clearance of the GPVI/FcRgamma-chain complex from the human platelet surface. *Blood*. 2004;104:1350-1355

89. Hermans C, Wittevrongel C, Thys C, Smethurst PA, Van Geet C, Freson K. A compound heterozygous mutation in glycoprotein VI in a patient with a bleeding disorder. *J Thromb Haemost*. 2009;7:1356-1363

90. Dumont B, Lasne D, Rothschild C, Bouabdelli M, Ollivier V, Oudin C, Ajzenberg N, Grandchamp B, Jandrot-Perrus M. Absence of collagen-induced platelet activation caused by compound heterozygous GPVI mutations. *Blood*. 2009;114:1900-1903

91. Colonna M, Samaridis J, Angman L. Molecular characterization of two novel C-type lectin-like receptors, one of which is selectively expressed in human dendritic cells. *Eur J Immunol*. 2000;30:697-704

92. Sobanov Y, Bernreiter A, Derdak S, Mechtcheriakova D, Schweighofer B, Duchler M, Kalthoff F, Hofer E. A novel cluster of lectin-like receptor genes expressed in monocytic, dendritic and endothelial cells maps close to the NK receptor genes in the human NK gene complex. *Eur J Immunol*. 2001;31:3493-3503

93. Kerrigan AM, Dennehy KM, Mourao-Sa D, Faro-Trindade I, Willment JA, Taylor PR, Eble JA, Reis e Sousa C, Brown GD. CLEC-2 is a phagocytic activation receptor expressed on murine peripheral blood neutrophils. *J Immunol*. 2009;182:4150-4157

94. Hughes CE, Pollitt AY, Mori J, Eble JA, Tomlinson MG, Hartwig JH, O'Callaghan CA, Futterer K, Watson SP. CLEC-2 activates Syk through dimerization. *Blood*. 2010;115:2947-2955

95. Chaipan C, Soilleux EJ, Simpson P, Hofmann H, Gramberg T, Marzi A, Geier M, Stewart EA, Eisemann J, Steinkasserer A, Suzuki-Inoue K, Fuller GL, Pearce AC, Watson SP, Hoxie JA, Baribaud F, Pohlmann S. DC-SIGN and CLEC-2 mediate human immunodeficiency virus type 1 capture by platelets. *J Virol*. 2006;80:8951-8960

96. Suzuki-Inoue K, Kato Y, Inoue O, Kaneko MK, Mishima K, Yatomi Y, Yamazaki Y, Narimatsu H, Ozaki Y. Involvement of the snake toxin receptor CLEC-2, in podoplanin-mediated platelet activation, by cancer cells. *J Biol Chem*. 2007;282:25993-26001

97. O'Callaghan CA. Thrombomodulation via CLEC-2 targeting. *Curr Opin Pharmacol*. 2009;9:90-95

98. Uhrin P, Zaujec J, Breuss JM, Olcaydu D, Chrenek P, Stockinger H, Fuertbauer E, Moser M, Haiko P, Fassler R, Alitalo K, Binder BR, Kerjaschki D. Novel function for blood platelets and podoplanin in developmental separation of blood and lymphatic circulation. *Blood*. 2010;115:3997-4005

99. Bertozzi CC, Schmaier AA, Mericko P, Hess PR, Zou Z, Chen M, Chen CY, Xu B, Lu MM, Zhou D, Sebzda E, Santore MT, Merianos DJ, Stadtfeld M, Flake AW, Graf T, Skoda R, Maltzman JS, Koretzky GA, Kahn ML. Platelets regulate lymphatic vascular development through CLEC-2-SLP-76 signaling. *Blood*. 2010;116:661-670

100. Suzuki-Inoue K, Inoue O, Ding G, Nishimura S, Hokamura K, Eto K, Kashiwagi H, Tomiyama Y, Yatomi Y, Umemura K, Shin Y, Hirashima M, Ozaki Y. Essential in vivo roles of the C-type lectin receptor CLEC-2: embryonic/neonatal lethality of CLEC-2-deficient mice by blood/lymphatic misconnections and impaired thrombus formation of CLEC-2-deficient platelets. *J Biol Chem*. 2010;285:24494-24507

101. Hall A. Rho GTPases and the actin cytoskeleton. *Science*. 1998;279:509-514

102. Jaffe AB, Hall A. Rho GTPases: biochemistry and biology. *Annu Rev Cell Dev Biol*. 2005;21:247-269

103. Chang JC, Chang HH, Lin CT, Lo SJ. The integrin alpha6beta1 modulation of PI3K and Cdc42 activities induces dynamic filopodium formation in human platelets. *J Biomed Sci*. 2005;12:881-898

104. McCarty OJ, Larson MK, Auger JM, Kalia N, Atkinson BT, Pearce AC, Ruf S, Henderson RB, Tybulewicz VL, Machesky LM, Watson SP. Rac1 is essential for platelet lamellipodia formation and aggregate stability under flow. *J Biol Chem*. 2005;280:39474-39484

105. Klages B, Brandt U, Simon MI, Schultz G, Offermanns S. Activation of G12/G13 results in shape change and Rho/Rho-kinase-mediated myosin light chain phosphorylation in mouse platelets. *J Cell Biol*. 1999;144:745-754

106. Nachmias VT, Golla R. Vinculin in relation to stress fibers in spread platelets. *Cell Motil Cytoskeleton*. 1991;20:190-202

107. Pleines I, Eckly A, Elvers M, Hagedorn I, Eliautou S, Bender M, Wu X, Lanza F, Gachet C, Brakebusch C, Nieswandt B. Multiple alterations of platelet functions dominated by increased secretion in mice lacking Cdc42 in platelets. *Blood*. 2010;115:3364-3373

108. Pleines I, Elvers M, Strehl A, Pozgajova M, Varga-Szabo D, May F, Chrostek-Grashoff A, Brakebusch C, Nieswandt B. Rac1 is essential for phospholipase C-gamma2 activation in platelets. *Pflugers Arch*. 2009;457:1173-1185

109. Etienne-Manneville S, Hall A. Rho GTPases in cell biology. *Nature*. 2002;420:629-635

110. Ridley AJ, Hall A. The small GTP-binding protein rho regulates the assembly of focal adhesions and actin stress fibers in response to growth factors. *Cell*. 1992;70:389-399

111. Pellegrin S, Mellor H. Actin stress fibres. *J Cell Sci*. 2007;120:3491-3499

112. Burridge K, Chrzanowska-Wodnicka M, Zhong C. Focal adhesion assembly. *Trends Cell Biol*. 1997;7:342-347

113. Fukata Y, Amano M, Kaibuchi K. Rho-Rho-kinase pathway in smooth muscle contraction and cytoskeletal reorganization of non-muscle cells. *Trends Pharmacol Sci*. 2001;22:32-39

114. Sakurada S, Okamoto H, Takuwa N, Sugimoto N, Takuwa Y. Rho activation in excitatory agonist-stimulated vascular smooth muscle. *Am J Physiol Cell Physiol*. 2001;281:C571-578

115. Wojciak-Stothard B, Potempa S, Eichholtz T, Ridley AJ. Rho and Rac but not Cdc42 regulate endothelial cell permeability. *J Cell Sci*. 2001;114:1343-1355

116. Uehata M, Ishizaki T, Satoh H, Ono T, Kawahara T, Morishita T, Tamakawa H, Yamagami K, Inui J, Maekawa M, Narumiya S. Calcium sensitization of smooth muscle mediated by a Rho-associated protein kinase in hypertension. *Nature*. 1997;389:990-994

117. Ghiaur G, Lee A, Bailey J, Cancelas JA, Zheng Y, Williams DA. Inhibition of RhoA GTPase activity enhances hematopoietic stem and progenitor cell proliferation and engraftment. *Blood*. 2006;108:2087-2094

118. del Pozo MA, Vicente-Manzanares M, Tejedor R, Serrador JM, Sanchez-Madrid F. Rho GTPases control migration and polarization of adhesion molecules and cytoskeletal ERM components in T lymphocytes. *Eur J Immunol*. 1999;29:3609-3620

119. Subauste MC, Von Herrath M, Benard V, Chamberlain CE, Chuang TH, Chu K, Bokoch GM, Hahn KM. Rho family proteins modulate rapid apoptosis induced by cytotoxic T lymphocytes and Fas. *J Biol Chem*. 2000;275:9725-9733

120. Xu J, Wang F, Van Keymeulen A, Herzmark P, Straight A, Kelly K, Takuwa Y, Sugimoto N, Mitchison T, Bourne HR. Divergent signals and cytoskeletal assemblies regulate self-organizing polarity in neutrophils. *Cell*. 2003;114:201-214

121. Caron E, Hall A. Identification of two distinct mechanisms of phagocytosis controlled by different Rho GTPases. *Science*. 1998;282:1717-1721

122. Jackson B, Peyrollier K, Pedersen E, Basse A, Karlsson R, Wang Z, Lefever T, Ochsenbein AM, Schmidt G, Aktories K, Stanley A, Quondamatteo F, Ladwein M, Rottner K, van Hengel J, Brakebusch C. RhoA is dispensable for skin development, but crucial for contraction and directed migration of keratinocytes. *Mol Biol Cell*. 2011;22:593-605

123. Morii N, Teru-uchi T, Tominaga T, Kumagai N, Kozaki S, Ushikubi F, Narumiya S. A rho gene product in human blood platelets. II. Effects of the ADP-ribosylation by botulinum C3 ADP-ribosyltransferase on platelet aggregation. *J Biol Chem*. 1992;267:20921-20926

124. Sah VP, Seasholtz TM, Sagi SA, Brown JH. The role of Rho in G protein-coupled receptor signal transduction. *Annu Rev Pharmacol Toxicol*. 2000;40:459-489

125. Moers A, Nieswandt B, Massberg S, Wettschureck N, Gruner S, Konrad I, Schulte V, Aktas B, Gratacap MP, Simon MI, Gawaz M, Offermanns S. G13 is an essential mediator of platelet activation in hemostasis and thrombosis. *Nat Med*. 2003;9:1418-1422

126. Moers A, Wettschureck N, Gruner S, Nieswandt B, Offermanns S. Unresponsiveness of platelets lacking both Galpha(q) and Galpha(13). Implications for collagen-induced platelet activation. *J Biol Chem*. 2004;279:45354-45359

127. Ridley AJ. Rho family proteins: coordinating cell responses. *Trends Cell Biol*. 2001;11:471-477

128. Watanabe N, Madaule P, Reid T, Ishizaki T, Watanabe G, Kakizuka A, Saito Y, Nakao K, Jockusch BM, Narumiya S. p140mDia, a mammalian homolog of Drosophila diaphanous, is a target protein for Rho small GTPase and is a ligand for profilin. *Embo J*. 1997;16:3044-3056

129. van Nieuw Amerongen GP, van Hinsbergh VW. Cytoskeletal effects of rho-like small guanine nucleotide-binding proteins in the vascular system. *Arterioscler Thromb Vasc Biol*. 2001;21:300-311

130. Bauer M, Retzer M, Wilde JI, Maschberger P, Essler M, Aepfelbacher M, Watson SP, Siess W. Dichotomous regulation of myosin phosphorylation and shape change by Rho-kinase and calcium in intact human platelets. *Blood*. 1999;94:1665-1672

131. Paul BZ, Daniel JL, Kunapuli SP. Platelet shape change is mediated by both calcium-dependent and -independent signaling pathways. Role of p160 Rho-associated coiled-

coil-containing protein kinase in platelet shape change. *J Biol Chem*. 1999;274:28293-28300

132. Missy K, Plantavid M, Pacaud P, Viala C, Chap H, Payrastre B. Rho-kinase is involved in the sustained phosphorylation of myosin and the irreversible platelet aggregation induced by PAR1 activating peptide. *Thromb Haemost*. 2001;85:514-520

133. Retzer M, Essler M. Lysophosphatidic acid-induced platelet shape change proceeds via Rho/Rho kinase-mediated myosin light-chain and moesin phosphorylation. *Cell Signal*. 2000;12:645-648

134. Bodie SL, Ford I, Greaves M, Nixon GF. Thrombin-induced activation of RhoA in platelet shape change. *Biochem Biophys Res Commun*. 2001;287:71-76

135. Suzuki Y, Yamamoto M, Wada H, Ito M, Nakano T, Sasaki Y, Narumiya S, Shiku H, Nishikawa M. Agonist-induced regulation of myosin phosphatase activity in human platelets through activation of Rho-kinase. *Blood*. 1999;93:3408-3417

136. Jin J, Mao Y, Thomas D, Kim S, Daniel JL, Kunapuli SP. RhoA downstream of G(q) and G(12/13) pathways regulates protease-activated receptor-mediated dense granule release in platelets. *Biochem Pharmacol*. 2009;77:835-844

137. Huang JS, Dong L, Kozasa T, Le Breton GC. Signaling through G(alpha)13 switch region I is essential for protease-activated receptor 1-mediated human platelet shape change, aggregation, and secretion. *J Biol Chem*. 2007;282:10210-10222

138. Schoenwaelder SM, Hughan SC, Boniface K, Fernando S, Holdsworth M, Thompson PE, Salem HH, Jackson SP. RhoA sustains integrin alpha IIbbeta 3 adhesion contacts under high shear. *J Biol Chem*. 2002;277:14738-14746

139. Gong H, Shen B, Flevaris P, Chow C, Lam SC, Voyno-Yasenetskaya TA, Kozasa T, Du X. G protein subunit Galpha13 binds to integrin alphaIIbbeta3 and mediates integrin "outside-in" signaling. *Science*. 2010;327:340-343

140. Leng L, Kashiwagi H, Ren XD, Shattil SJ. RhoA and the function of platelet integrin alphaIIbbeta3. *Blood*. 1998;91:4206-4215

141. Gao G, Chen L, Dong B, Gu H, Dong H, Pan Y, Gao Y, Chen X. RhoA effector mDia1 is required for PI 3-kinase-dependent actin remodeling and spreading by thrombin in platelets. *Biochem Biophys Res Commun*. 2009;385:439-444

142. Chang Y, Aurade F, Larbret F, Zhang Y, Le Couedic JP, Momeux L, Larghero J, Bertoglio J, Louache F, Cramer E, Vainchenker W, Debili N. Proplatelet formation is regulated by the Rho/ROCK pathway. *Blood*. 2007;109:4229-4236

143. Macfarlane RG. An Enzyme Cascade in the Blood Clotting Mechanism, and Its Function as a Biochemical Amplifier. *Nature*. 1964;202:498-499

144. Davie EW, Ratnoff OD. Waterfall Sequence for Intrinsic Blood Clotting. *Science*. 1964;145:1310-1312

145. Mackman N, Tilley RE, Key NS. Role of the extrinsic pathway of blood coagulation in hemostasis and thrombosis. *Arterioscler Thromb Vasc Biol*. 2007;27:1687-1693

146. McMullen BA, Fujikawa K. Amino acid sequence of the heavy chain of human alpha-factor XIIa (activated Hageman factor). *J Biol Chem*. 1985;260:5328-5341

147. Gailani D, Renne T. Intrinsic pathway of coagulation and arterial thrombosis. *Arterioscler Thromb Vasc Biol*. 2007;27:2507-2513

148. Schmaier AH, Rojkjaer R, Shariat-Madar Z. Activation of the plasma kallikrein/kinin system on cells: a revised hypothesis. *Thromb Haemost*. 1999;82:226-233

149. Ghebrehiwet B, Silverberg M, Kaplan AP. Activation of the classical pathway of complement by Hageman factor fragment. *J Exp Med*. 1981;153:665-676

150. Revak SD, Cochrane CG, Bouma BN, Griffin JH. Surface and fluid phase activities of two forms of activated Hageman factor produced during contact activation of plasma. *J Exp Med*. 1978;147:719-729

151. Kluft C, Dooijewaard G, Emeis JJ. Role of the contact system in fibrinolysis. *Semin Thromb Hemost*. 1987;13:50-68

152. Tanaka A, Suzuki Y, Sugihara K, Kanayama N, Urano T. Inactivation of plasminogen activator inhibitor type 1 by activated factor XII plays a role in the enhancement of fibrinolysis by contact factors in-vitro. *Life Sci*. 2009;85:220-225

153. Braat EA, Dooijewaard G, Rijken DC. Fibrinolytic properties of activated FXII. *Eur J Biochem*. 1999;263:904-911

154. Stavrou E, Schmaier AH. Factor XII: what does it contribute to our understanding of the physiology and pathophysiology of hemostasis & thrombosis. *Thromb Res*. 2010;125:210-215

155. Kannemeier C, Shibamiya A, Nakazawa F, Trusheim H, Ruppert C, Markart P, Song Y, Tzima E, Kennerknecht E, Niepmann M, von Bruehl ML, Sedding D, Massberg S, Gunther A, Engelmann B, Preissner KT. Extracellular RNA constitutes a natural procoagulant cofactor in blood coagulation. *Proc Natl Acad Sci U S A*. 2007;104:6388-6393

156. Maas C, Govers-Riemslag JW, Bouma B, Schiks B, Hazenberg BP, Lokhorst HM, Hammarstrom P, ten Cate H, de Groot PG, Bouma BN, Gebbink MF. Misfolded proteins activate factor XII in humans, leading to kallikrein formation without initiating coagulation. *J Clin Invest*. 2008;118:3208-3218

157. Muller F, Mutch NJ, Schenk WA, Smith SA, Esterl L, Spronk HM, Schmidbauer S, Gahl WA, Morrissey JH, Renne T. Platelet polyphosphates are proinflammatory and procoagulant mediators in vivo. *Cell*. 2009;139:1143-1156

158. van der Meijden PE, Munnix IC, Auger JM, Govers-Riemslag JW, Cosemans JM, Kuijpers MJ, Spronk HM, Watson SP, Renne T, Heemskerk JW. Dual role of collagen in factor XII-dependent thrombus formation. *Blood*. 2009;114:881-890

159. White-Adams TC, Berny MA, Patel IA, Tucker EI, Gailani D, Gruber A, McCarty OJ. Laminin promotes coagulation and thrombus formation in a factor XII-dependent manner. *J Thromb Haemost*. 2010;8:1295-1301

160. Kasthuri RS, Glover SL, Boles J, Mackman N. Tissue factor and tissue factor pathway inhibitor as key regulators of global hemostasis: measurement of their levels in coagulation assays. *Semin Thromb Hemost*. 2010;36:764-771

161. Dahlback B. Blood coagulation and its regulation by anticoagulant pathways: genetic pathogenesis of bleeding and thrombotic diseases. *J Intern Med*. 2005;257:209-223

162. Forbes CD, Pensky J, Ratnoff OD. Inhibition of activated Hageman factor and activated plasma thromboplastin antecedent by purified serum C1 inactivator. *J Lab Clin Med*. 1970;76:809-815

163. Back J, Lang MH, Elgue G, Kalbitz M, Sanchez J, Ekdahl KN, Nilsson B. Distinctive regulation of contact activation by antithrombin and C1-inhibitor on activated platelets and material surfaces. *Biomaterials*. 2009;30:6573-6580

164. Macquarrie JL, Stafford AR, Yau JW, Leslie BA, Vu TT, Fredenburgh JC, Weitz JI. Histidine-rich glycoprotein binds factor XIIa with high affinity and inhibits contact-initiated coagulation. *Blood*. 2011

165. Ratnoff OD, Colopy JE. A familial hemorrhagic trait associated with a deficiency of a clot-promoting fraction of plasma. *J Clin Invest*. 1955;34:602-613

166. Tuddenham EG, Pemberton S, Cooper DN. Inherited factor VII deficiency: genetics and molecular pathology. *Thromb Haemost*. 1995;74:313-321

167. Bugge TH, Xiao Q, Kombrinck KW, Flick MJ, Holmback K, Danton MJ, Colbert MC, Witte DP, Fujikawa K, Davie EW, Degen JL. Fatal embryonic bleeding events in mice lacking tissue factor, the cell-associated initiator of blood coagulation. *Proc Natl Acad Sci U S A*. 1996;93:6258-6263

168. Rosen ED, Chan JC, Idusogie E, Clotman F, Vlasuk G, Luther T, Jalbert LR, Albrecht S, Zhong L, Lissens A, Schoonjans L, Moons L, Collen D, Castellino FJ, Carmeliet P. Mice lacking factor VII develop normally but suffer fatal perinatal bleeding. *Nature*. 1997;390:290-294

169. Renne T, Pozgajova M, Gruner S, Schuh K, Pauer HU, Burfeind P, Gailani D, Nieswandt B. Defective thrombus formation in mice lacking coagulation factor XII. *J Exp Med*. 2005;202:271-281

170. Kleinschnitz C, Stoll G, Bendszus M, Schuh K, Pauer HU, Burfeind P, Renne C, Gailani D, Nieswandt B, Renne T. Targeting coagulation factor XII provides protection from pathological thrombosis in cerebral ischemia without interfering with hemostasis. *J Exp Med*. 2006;203:513-518

171. Nieswandt B, Aktas B, Moers A, Sachs UJ. Platelets in atherothrombosis: lessons from mouse models. *J Thromb Haemost*. 2005;3:1725-1736

172. Kurz KD, Main BW, Sandusky GE. Rat model of arterial thrombosis induced by ferric chloride. *Thromb Res*. 1990;60:269-280

173. Denis C, Methia N, Frenette PS, Rayburn H, Ullman-Cullere M, Hynes RO, Wagner DD. A mouse model of severe von Willebrand disease: defects in hemostasis and thrombosis. *Proc Natl Acad Sci U S A*. 1998;95:9524-9529

174. Farrehi PM, Ozaki CK, Carmeliet P, Fay WP. Regulation of arterial thrombolysis by plasminogen activator inhibitor-1 in mice. *Circulation*. 1998;97:1002-1008

175. Ni H, Denis CV, Subbarao S, Degen JL, Sato TN, Hynes RO, Wagner DD. Persistence of platelet thrombus formation in arterioles of mice lacking both von Willebrand factor and fibrinogen. *J Clin Invest*. 2000;106:385-392

176. Kikuchi S, Umemura K, Kondo K, Saniabadi AR, Nakashima M. Photochemically induced endothelial injury in the mouse as a screening model for inhibitors of vascular intimal thickening. *Arterioscler Thromb Vasc Biol*. 1998;18:1069-1078

177. Falati S, Gross P, Merrill-Skoloff G, Furie BC, Furie B. Real-time in vivo imaging of platelets, tissue factor and fibrin during arterial thrombus formation in the mouse. *Nat Med*. 2002;8:1175-1181

178. Nonne C, Lenain N, Hechler B, Mangin P, Cazenave JP, Gachet C, Lanza F. Importance of platelet phospholipase Cgamma2 signaling in arterial thrombosis as a function of lesion severity. *Arterioscler Thromb Vasc Biol*. 2005;25:1293-1298

179. Konishi H, Katoh Y, Takaya N, Kashiwakura Y, Itoh S, Ra C, Daida H. Platelets activated by collagen through immunoreceptor tyrosine-based activation motif play pivotal role in initiation and generation of neointimal hyperplasia after vascular injury. *Circulation*. 2002;105:912-916

180. Kuijpers MJ, Gilio K, Reitsma S, Nergiz-Unal R, Prinzen L, Heeneman S, Lutgens E, van Zandvoort MA, Nieswandt B, Egbrink MG, Heemskerk JW. Complementary roles of platelets and coagulation in thrombus formation on plaques acutely ruptured by targeted ultrasound treatment: a novel intravital model. *J Thromb Haemost*. 2009;7:152-161

181. Hechler B, Gachet C. Comparison of two murine models of thrombosis induced by atherosclerotic plaque injury. *Thromb Haemost*. 2011

182. May F, Hagedorn I, Pleines I, Bender M, Vogtle T, Eble J, Elvers M, Nieswandt B. CLEC-2 is an essential platelet-activating receptor in hemostasis and thrombosis. *Blood*. 2009;114:3464-3472

183. Nieswandt B, Bergmeier W, Rackebrandt K, Gessner JE, Zirngibl H. Identification of critical antigen-specific mechanisms in the development of immune thrombocytopenic purpura in mice. *Blood*. 2000;96:2520-2527

184. Bergmeier W, Schulte V, Brockhoff G, Bier U, Zirngibl H, Nieswandt B. Flow cytometric detection of activated mouse integrin alphaIIbbeta3 with a novel monoclonal antibody. *Cytometry*. 2002;48:80-86

185. Dirnagl U. Bench to bedside: the quest for quality in experimental stroke research. *J Cereb Blood Flow Metab*. 2006;26:1465-1478

186. Clark WM, Lessov NS, Dixon MP, Eckenstein F. Monofilament intraluminal middle cerebral artery occlusion in the mouse. *Neurol Res*. 1997;19:641-648

187. Bederson JB, Pitts LH, Tsuji M, Nishimura MC, Davis RL, Bartkowski H. Rat middle cerebral artery occlusion: evaluation of the model and development of a neurologic examination. *Stroke*. 1986;17:472-476

188. Moran PM, Higgins LS, Cordell B, Moser PC. Age-related learning deficits in transgenic mice expressing the 751-amino acid isoform of human beta-amyloid precursor protein. *Proc Natl Acad Sci U S A*. 1995;92:5341-5345

189. Jain S, Zuka M, Liu J, Russell S, Dent J, Guerrero JA, Forsyth J, Maruszak B, Gartner TK, Felding-Habermann B, Ware J. Platelet glycoprotein Ib alpha supports experimental lung metastasis. *Proc Natl Acad Sci U S A*. 2007;104:9024-9028

190. Elvers M, Stegner D, Hagedorn I, Kleinschnitz C, Braun A, Kuijpers ME, Boesl M, Chen Q, Heemskerk JW, Stoll G, Frohman MA, Nieswandt B. Impaired alpha(IIb)beta(3) integrin activation and shear-dependent thrombus formation in mice lacking phospholipase D1. *Sci Signal*. 2010;3:ra1

191. Martinson EA, Scheible S, Greinacher A, Presek P. Platelet phospholipase D is activated by protein kinase C via an integrin alpha IIb beta 3-independent mechanism. *Biochem J*. 1995;310 (Pt 2):623-628

192. Li Z, Delaney MK, O'Brien KA, Du X. Signaling during platelet adhesion and activation. *Arterioscler Thromb Vasc Biol*. 2010;30:2341-2349

193. Bender M, Hagedorn I, Nieswandt B. Genetic and antibody-induced GPVI deficiency equally protect mice from mechanically and FeCl(3) -induced thrombosis. *J Thromb Haemost*. 2011

194. Tiedt R, Schomber T, Hao-Shen H, Skoda RC. Pf4-Cre transgenic mice allow the generation of lineage-restricted gene knockouts for studying megakaryocyte and platelet function in vivo. *Blood*. 2007;109:1503-1506

195. Dorsam RT, Kim S, Jin J, Kunapuli SP. Coordinated signaling through both G12/13 and G(i) pathways is sufficient to activate GPIIb/IIIa in human platelets. *J Biol Chem*. 2002;277:47588-47595

196. Savage B, Shattil SJ, Ruggeri ZM. Modulation of platelet function through adhesion receptors. A dual role for glycoprotein IIb-IIIa (integrin alpha IIb beta 3) mediated by fibrinogen and glycoprotein Ib-von Willebrand factor. *J Biol Chem*. 1992;267:11300-11306

197. Morgenstern E, Ruf A, Patscheke H. Ultrastructure of the interaction between human platelets and polymerizing fibrin within the first minutes of clot formation. *Blood Coagul Fibrinolysis*. 1990;1:543-546

198. Stoll G, Kleinschnitz C, Nieswandt B. Combating innate inflammation: a new paradigm for acute treatment of stroke? *Ann N Y Acad Sci*. 2010;1207:149-154

199. Zhang ZG, Zhang L, Tsang W, Goussev A, Powers C, Ho KL, Morris D, Smyth SS, Coller BS, Chopp M. Dynamic platelet accumulation at the site of the occluded middle cerebral artery and in downstream microvessels is associated with loss of microvascular integrity after embolic middle cerebral artery occlusion. *Brain Res*. 2001;912:181-194

200. Campos IT, Amino R, Sampaio CA, Auerswald EA, Friedrich T, Lemaire HG, Schenkman S, Tanaka AS. Infestin, a thrombin inhibitor presents in Triatoma infestans midgut, a Chagas' disease vector: gene cloning, expression and characterization of the inhibitor. *Insect Biochem Mol Biol*. 2002;32:991-997

201. Campos IT, Tanaka-Azevedo AM, Tanaka AS. Identification and characterization of a novel factor XIIa inhibitor in the hematophagous insect, Triatoma infestans (Hemiptera: Reduviidae). *FEBS Lett*. 2004;577:512-516

202. Hagedorn I, Schmidbauer S, Pleines I, Kleinschnitz C, Kronthaler U, Stoll G, Dickneite G, Nieswandt B. Factor XIIa inhibitor recombinant human albumin Infestin-4 abolishes occlusive arterial thrombus formation without affecting bleeding. *Circulation*. 2010;121:1510-1517

203. Stoll G, Kleinschnitz C, Nieswandt B. Molecular mechanisms of thrombus formation in ischemic stroke: novel insights and targets for treatment. *Blood*. 2008;112:3555-3562

204. Choudhri TF, Hoh BL, Zerwes HG, Prestigiacomo CJ, Kim SC, Connolly ES, Jr., Kottirsch G, Pinsky DJ. Reduced microvascular thrombosis and improved outcome in acute murine stroke by inhibiting GP IIb/IIIa receptor-mediated platelet aggregation. *J Clin Invest*. 1998;102:1301-1310

205. Michelson AD. Antiplatelet therapies for the treatment of cardiovascular disease. *Nat Rev Drug Discov*. 2010;9:154-169

206. Mackman N. Triggers, targets and treatments for thrombosis. *Nature*. 2008;451:914-918

207. Kanaji T, Russell S, Ware J. Amelioration of the macrothrombocytopenia associated with the murine Bernard-Soulier syndrome. *Blood*. 2002;100:2102-2107

208. Bonnefoy A, Daenens K, Feys HB, De Vos R, Vandervoort P, Vermylen J, Lawler J, Hoylaerts MF. Thrombospondin-1 controls vascular platelet recruitment and thrombus adherence in mice by protecting (sub)endothelial VWF from cleavage by ADAMTS13. *Blood*. 2006;107:955-964

209. Cambien B, Wagner DD. A new role in hemostasis for the adhesion receptor P-selectin. *Trends Mol Med*. 2004;10:179-186

210. Ni H, Yuen PS, Papalia JM, Trevithick JE, Sakai T, Fassler R, Hynes RO, Wagner DD. Plasma fibronectin promotes thrombus growth and stability in injured arterioles. *Proc Natl Acad Sci U S A*. 2003;100:2415-2419

211. Matuskova J, Chauhan AK, Cambien B, Astrof S, Dole VS, Piffath CL, Hynes RO, Wagner DD. Decreased plasma fibronectin leads to delayed thrombus growth in injured arterioles. *Arterioscler Thromb Vasc Biol*. 2006;26:1391-1396

212. Dubois C, Panicot-Dubois L, Gainor JF, Furie BC, Furie B. Thrombin-initiated platelet activation in vivo is vWF independent during thrombus formation in a laser injury model. *J Clin Invest*. 2007;117:953-960

213. Sawada Y, Fass DN, Katzmann JA, Bahn RC, Bowie EJ. Hemostatic plug formation in normal and von Willebrand pigs: the effect of the administration of cryoprecipitate and a monoclonal antibody to Willebrand factor. *Blood*. 1986;67:1229-1239

214. Rodgers RP, Levin J. A critical reappraisal of the bleeding time. *Semin Thromb Hemost*. 1990;16:1-20

215. Cauwenberghs N, Meiring M, Vauterin S, van Wyk V, Lamprecht S, Roodt JP, Novak L, Harsfalvi J, Deckmyn H, Kotze HF. Antithrombotic effect of platelet glycoprotein Ib-blocking monoclonal antibody Fab fragments in nonhuman primates. *Arterioscler Thromb Vasc Biol*. 2000;20:1347-1353

216. Fontayne A, Meiring M, Lamprecht S, Roodt J, Demarsin E, Barbeaux P, Deckmyn H. The humanized anti-glycoprotein Ib monoclonal antibody h6B4-Fab is a potent and safe antithrombotic in a high shear arterial thrombosis model in baboons. *Thromb Haemost*. 2008;100:670-677

217. Su W, Yeku O, Olepu S, Genna A, Park JS, Ren H, Du G, Gelb MH, Morris AJ, Frohman MA. 5-Fluoro-2-indolyl des-chlorohalopemide (FIPI), a phospholipase D

pharmacological inhibitor that alters cell spreading and inhibits chemotaxis. *Mol Pharmacol*. 2009;75:437-446

218. Powner DJ, Pettitt TR, Anderson R, Nash GB, Wakelam MJ. Stable adhesion and migration of human neutrophils requires phospholipase D-mediated activation of the integrin CD11b/CD18. *Mol Immunol*. 2007;44:3211-3221

219. Kuijpers MJ, Schulte V, Oury C, Lindhout T, Broers J, Hoylaerts MF, Nieswandt B, Heemskerk JW. Facilitating roles of murine platelet glycoprotein Ib and alphaIIbbeta3 in phosphatidylserine exposure during vWF-collagen-induced thrombus formation. *J Physiol*. 2004;558:403-415

220. Adams RJ, Albers G, Alberts MJ, Benavente O, Furie K, Goldstein LB, Gorelick P, Halperin J, Harbaugh R, Johnston SC, Katzan I, Kelly-Hayes M, Kenton EJ, Marks M, Sacco RL, Schwamm LH. Update to the AHA/ASA recommendations for the prevention of stroke in patients with stroke and transient ischemic attack. *Stroke*. 2008;39:1647-1652

221. Paciaroni M, Agnelli G, Micheli S, Caso V. Efficacy and safety of anticoagulant treatment in acute cardioembolic stroke: a meta-analysis of randomized controlled trials. *Stroke*. 2007;38:423-430

222. Camerlingo M, Salvi P, Belloni G, Gamba T, Cesana BM, Mamoli A. Intravenous heparin started within the first 3 hours after onset of symptoms as a treatment for acute nonlacunar hemispheric cerebral infarctions. *Stroke*. 2005;36:2415-2420

223. Huang P, Frohman MA. The potential for phospholipase D as a new therapeutic target. *Expert Opin Ther Targets*. 2007;11:707-716

224. Dall'Armi C, Hurtado-Lorenzo A, Tian H, Morel E, Nezu A, Chan RB, Yu WH, Robinson KS, Yeku O, Small SA, Duff K, Frohman MA, Wenk MR, Yamamoto A, Di Paolo G. The phospholipase D1 pathway modulates macroautophagy. *Nat Commun*. 2010;1:142

225. Schulte V, Rabie T, Prostredna M, Aktas B, Gruner S, Nieswandt B. Targeting of the collagen-binding site on glycoprotein VI is not essential for in vivo depletion of the receptor. *Blood*. 2003;101:3948-3952

226. Kalia N, Auger JM, Atkinson B, Watson SP. Critical role of FcR gamma-chain, LAT, PLCgamma2 and thrombin in arteriolar thrombus formation upon mild, laser-induced endothelial injury in vivo. *Microcirculation*. 2008;15:325-335

227. Nieswandt B, Bergmeier W, Schulte V, Rackebrandt K, Gessner JE, Zirngibl H. Expression and function of the mouse collagen receptor glycoprotein VI is strictly dependent on its association with the FcRgamma chain. *J Biol Chem*. 2000;275:23998-24002

228. Marsh Lyle E, Lewis SD, Lehman ED, Gardell SJ, Motzel SL, Lynch JJ, Jr. Assessment of thrombin inhibitor efficacy in a novel rabbit model of simultaneous arterial and venous thrombosis. *Thromb Haemost*. 1998;79:656-662

229. Pinel C, Wice SM, Hiebert LM. Orally administered heparins prevent arterial thrombosis in a rat model. *Thromb Haemost*. 2004;91:919-926

230. Wang X, Cheng Q, Xu L, Feuerstein GZ, Hsu MY, Smith PL, Seiffert DA, Schumacher WA, Ogletree ML, Gailani D. Effects of factor IX or factor XI deficiency on ferric chloride-induced carotid artery occlusion in mice. *J Thromb Haemost*. 2005;3:695-702

231. Tseng MT, Dozier A, Haribabu B, Graham UM. Transendothelial migration of ferric ion in FeCl3 injured murine common carotid artery. *Thromb Res*. 2006;118:275-280

232. Brill A. A ride with ferric chloride. *J Thromb Haemost*. 2011;9:776-778

233. Wong LC, Langille BL. Developmental remodeling of the internal elastic lamina of rabbit arteries: effect of blood flow. *Circ Res*. 1996;78:799-805

234. Takayama H, Hosaka Y, Nakayama K, Shirakawa K, Naitoh K, Matsusue T, Shinozaki M, Honda M, Yatagai Y, Kawahara T, Hirose J, Yokoyama T, Kurihara M, Furusako S. A novel antiplatelet antibody therapy that induces cAMP-dependent endocytosis of the GPVI/Fc receptor gamma-chain complex. *J Clin Invest*. 2008;118:1785-1795

235. Bergmeier W, Bouvard D, Eble JA, Mokhtari-Nejad R, Schulte V, Zirngibl H, Brakebusch C, Fassler R, Nieswandt B. Rhodocytin (aggretin) activates platelets lacking alpha(2)beta(1) integrin, glycoprotein VI, and the ligand-binding domain of glycoprotein Ibalpha. *J Biol Chem*. 2001;276:25121-25126

236. Ruggeri ZM, Mendolicchio GL. Adhesion mechanisms in platelet function. *Circ Res*. 2007;100:1673-1685

237. Hughes CE, Navarro-Nunez L, Finney BA, Mourao-Sa D, Pollitt AY, Watson SP. CLEC-2 is not required for platelet aggregation at arteriolar shear. *J Thromb Haemost*. 2010;8:2328-2332

238. Varga-Szabo D, Braun A, Kleinschnitz C, Bender M, Pleines I, Pham M, Renne T, Stoll G, Nieswandt B. The calcium sensor STIM1 is an essential mediator of arterial thrombosis and ischemic brain infarction. *J Exp Med*. 2008;205:1583-1591

239. Judd BA, Myung PS, Obergfell A, Myers EE, Cheng AM, Watson SP, Pear WS, Allman D, Shattil SJ, Koretzky GA. Differential requirement for LAT and SLP-76 in GPVI versus T cell receptor signaling. *J Exp Med*. 2002;195:705-717

240. Falet H, Pollitt AY, Begonja AJ, Weber SE, Duerschmied D, Wagner DD, Watson SP, Hartwig JH. A novel interaction between FlnA and Syk regulates platelet ITAM-mediated receptor signaling and function. *J Exp Med*. 2010;207:1967-1979

241. Elvers M, Pozgaj R, Pleines I, May F, Kuijpers MJ, Heemskerk JM, Yu P, Nieswandt B. Platelet hyperreactivity and a prothrombotic phenotype in mice with a gain-of-function mutation in phospholipase Cgamma2. *J Thromb Haemost*. 2010;8:1353-1363

242. Bender M, Hofmann S, Stegner D, Chalaris A, Bosl M, Braun A, Scheller J, Rose-John S, Nieswandt B. Differentially regulated GPVI ectodomain shedding by multiple platelet-expressed proteinases. *Blood*. 2010;116:3347-3355

243. Rabie T, Varga-Szabo D, Bender M, Pozgaj R, Lanza F, Saito T, Watson SP, Nieswandt B. Diverging signaling events control the pathway of GPVI down-regulation in vivo. *Blood*. 2007;110:529-535

244. Leon C, Hechler B, Freund M, Eckly A, Vial C, Ohlmann P, Dierich A, LeMeur M, Cazenave JP, Gachet C. Defective platelet aggregation and increased resistance to thrombosis in purinergic P2Y(1) receptor-null mice. *J Clin Invest*. 1999;104:1731-1737

245. Pozgajova M, Sachs UJ, Hein L, Nieswandt B. Reduced thrombus stability in mice lacking the alpha2A-adrenergic receptor. *Blood*. 2006;108:510-514

246. Goerge T, Ho-Tin-Noe B, Carbo C, Benarafa C, Remold-O'Donnell E, Zhao BQ, Cifuni SM, Wagner DD. Inflammation induces hemorrhage in thrombocytopenia. *Blood*. 2008;111:4958-4964

247. Lordier L, Jalil A, Aurade F, Larbret F, Larghero J, Debili N, Vainchenker W, Chang Y. Megakaryocyte endomitosis is a failure of late cytokinesis related to defects in the contractile ring and Rho/Rock signaling. *Blood*. 2008;112:3164-3174

248. Chikumi H, Vazquez-Prado J, Servitja JM, Miyazaki H, Gutkind JS. Potent activation of RhoA by Galpha q and Gq-coupled receptors. *J Biol Chem*. 2002;277:27130-27134

249. Vogt S, Grosse R, Schultz G, Offermanns S. Receptor-dependent RhoA activation in G12/G13-deficient cells: genetic evidence for an involvement of Gq/G11. *J Biol Chem*. 2003;278:28743-28749

250. Nieswandt B, Schulte V, Zywietz A, Gratacap MP, Offermanns S. Costimulation of Gi- and G12/G13-mediated signaling pathways induces integrin alpha IIbbeta 3 activation in platelets. *J Biol Chem*. 2002;277:39493-39498

251. Ory S, Gasman S. Rho GTPases and exocytosis: what are the molecular links? *Semin Cell Dev Biol*. 2011;22:27-32

252. Melendez J, Stengel K, Zhou X, Chauhan BK, Debidda M, Andreassen P, Lang RA, Zheng Y. RhoA GTPase is dispensable for actomyosin regulation but is essential for mitosis in primary mouse embryonic fibroblasts. *J Biol Chem*. 2011;286:15132-15137

253. Nemoto Y, Namba T, Teru-uchi T, Ushikubi F, Morii N, Narumiya S. A rho gene product in human blood platelets. I. Identification of the platelet substrate for botulinum C3 ADP-ribosyltransferase as rhoA protein. *J Biol Chem*. 1992;267:20916-20920

254. Heasman SJ, Ridley AJ. Mammalian Rho GTPases: new insights into their functions from in vivo studies. *Nat Rev Mol Cell Biol*. 2008;9:690-701

255. Gad AK, Aspenstrom P. Rif proteins take to the RhoD: Rho GTPases at the crossroads of actin dynamics and membrane trafficking. *Cell Signal*. 2010;22:183-189

256. Paul BZ, Kim S, Dangelmaier C, Nagaswami C, Jin J, Hartwig JH, Weisel JW, Daniel JL, Kunapuli SP. Dynamic regulation of microtubule coils in ADP-induced platelet shape change by p160ROCK (Rho-kinase). *Platelets*. 2003;14:159-169

257. Watanabe T, Noritake J, Kaibuchi K. Regulation of microtubules in cell migration. *Trends Cell Biol*. 2005;15:76-83

258. Andre P, Delaney SM, LaRocca T, Vincent D, DeGuzman F, Jurek M, Koller B, Phillips DR, Conley PB. P2Y12 regulates platelet adhesion/activation, thrombus growth, and thrombus stability in injured arteries. *J Clin Invest*. 2003;112:398-406

259. Konopatskaya O, Gilio K, Harper MT, Zhao Y, Cosemans JM, Karim ZA, Whiteheart SW, Molkentin JD, Verkade P, Watson SP, Heemskerk JW, Poole AW. PKCalpha regulates platelet granule secretion and thrombus formation in mice. *J Clin Invest*. 2009;119:399-407

260. Lammle B, Wuillemin WA, Huber I, Krauskopf M, Zurcher C, Pflugshaupt R, Furlan M. Thromboembolism and bleeding tendency in congenital factor XII deficiency--a study on 74 subjects from 14 Swiss families. *Thromb Haemost*. 1991;65:117-121

261. Lopez AD, Mathers CD, Ezzati M, Jamison DT, Murray CJ. Global and regional burden of disease and risk factors, 2001: systematic analysis of population health data. *Lancet*. 2006;367:1747-1757

262. Caro JJ, Huybrechts KF, Duchesne I. Management patterns and costs of acute ischemic stroke : an international study. For the Stroke Economic Analysis Group. *Stroke*. 2000;31:582-590

263. Bendszus M, Stoll G. Silent cerebral ischaemia: hidden fingerprints of invasive medical procedures. *Lancet Neurol*. 2006;5:364-372

264. Heo JH, Lee KY, Kim SH, Kim DI. Immediate reocclusion following a successful thrombolysis in acute stroke: a pilot study. *Neurology*. 2003;60:1684-1687

265. Liu J, Gao BB, Clermont AC, Blair P, Chilcote TJ, Sinha S, Flaumenhaft R, Feener EP. Hyperglycemia-induced cerebral hematoma expansion is mediated by plasma kallikrein. *Nat Med*. 2011;17:206-210

266. Qureshi AI, Mendelow AD, Hanley DF. Intracerebral haemorrhage. *Lancet*. 2009;373:1632-1644

267. Halbmayer WM, Mannhalter C, Feichtinger C, Rubi K, Fischer M. The prevalence of factor XII deficiency in 103 orally anticoagulated outpatients suffering from recurrent venous and/or arterial thromboembolism. *Thromb Haemost*. 1992;68:285-290

268. Bach J, Endler G, Winkelmann BR, Boehm BO, Maerz W, Mannhalter C, Hellstern P. Coagulation factor XII (FXII) activity, activated FXII, distribution of FXII C46T gene polymorphism and coronary risk. *J Thromb Haemost*. 2008;6:291-296

269. Zeerleder S, Schloesser M, Redondo M, Wuillemin WA, Engel W, Furlan M, Lammle B. Reevaluation of the incidence of thromboembolic complications in congenital factor XII deficiency--a study on 73 subjects from 14 Swiss families. *Thromb Haemost*. 1999;82:1240-1246

270. Koster T, Rosendaal FR, Briet E, Vandenbroucke JP. John Hageman's factor and deep-vein thrombosis: Leiden thrombophilia Study. *Br J Haematol*. 1994;87:422-424

271. Zito F, Lowe GD, Rumley A, McMahon AD, Humphries SE. Association of the factor XII 46C>T polymorphism with risk of coronary heart disease (CHD) in the WOSCOPS study. *Atherosclerosis*. 2002;165:153-158

272. Endler G, Mannhalter C, Sunder-Plassmann H, Lalouschek W, Kapiotis S, Exner M, Jordanova N, Meier S, Kunze F, Wagner O, Huber K. Homozygosity for the C-->T polymorphism at nucleotide 46 in the 5' untranslated region of the factor XII gene protects from development of acute coronary syndrome. *Br J Haematol*. 2001;115:1007-1009

273. Doggen CJ, Rosendaal FR, Meijers JC. Levels of intrinsic coagulation factors and the risk of myocardial infarction among men: Opposite and synergistic effects of factors XI and XII. *Blood*. 2006;108:4045-4051

274. Endler G, Marsik C, Jilma B, Schickbauer T, Quehenberger P, Mannhalter C. Evidence of a U-shaped association between factor XII activity and overall survival. *J Thromb Haemost*. 2007;5:1143-1148

275. Cheng Q, Tucker EI, Pine MS, Sisler I, Matafonov A, Sun MF, White-Adams TC, Smith SA, Hanson SR, McCarty OJ, Renne T, Gruber A, Gailani D. A role for factor XIIa-mediated factor XI activation in thrombus formation in vivo. *Blood*. 2010;116:3981-3989

276. Decrem Y, Rath G, Blasioli V, Cauchie P, Robert S, Beaufays J, Frere JM, Feron O, Dogne JM, Dessy C, Vanhamme L, Godfroid E. Ir-CPI, a coagulation contact phase inhibitor from the tick Ixodes ricinus, inhibits thrombus formation without impairing hemostasis. *J Exp Med*. 2009;206:2381-2395

277. Kettner C, Shaw E. Synthesis of peptides of arginine chloromethyl ketone. Selective inactivation of human plasma kallikrein. *Biochemistry*. 1978;17:4778-4784

278. Adams GN, Larusch GA, Stavrou E, Zhou Y, Nieman MT, Jacobs GH, Cui Y, Lu Y, Jain MK, Mahdi F, Shariat-Madar Z, Okada Y, D'Alecy LG, Schmaier AH. Murine prolylcarboxypeptidase depletion induces vascular dysfunction with hypertension and faster arterial thrombosis. *Blood*. 2011;117:3929-3937

279. Kraft P, Schwarz T, Pochet L, Stoll G, Kleinschnitz C. COU254, a specific 3-carboxamide-coumarin inhibitor of coagulation factor XII, does not protect mice from acute ischemic stroke. *Exp Transl Stroke Med*. 2010;2:5

280. Hagedorn I, Vogtle T, Nieswandt B. Arterial thrombus formation. Novel mechanisms and targets Novel mechanisms and targets. *Hamostaseologie*. 2010;30:127-135

7 APPENDIX

Abbreviations

µ	micro
AC	adenylate cyclase
ADAP	adhesion and degranulation promoting adaptor protein
ADP	adenosine diphosphate
aPTT	thromboplastin time
ATP	adenosine trisphosphate
BK	bradikinin
BSA	bovine serum albumin
BSS	Bernard-Soulier syndrome
℃	Degree Celsius
C1 inhibitor	C1 esterase inhibitor
$[Ca^{2+}]_i$	intracellular calcium concentration
CLEC-2	C-type lectin-like receptor 2
CRP	collagen-related peptide
CVX	convulxin
DAG	diacylglycerol
ddH_2O	double-distilled water
DIC	differential interference contrast
ECM	extracellular matrix
ELISA	enzyme-linked immuno absorbance assay
et al.	et alteri
F(VII)a	activated coagulation factor (VII)
F(XII)	coagulation factor (XII)
F-actin	filamentous actin
Fc	Fragment crystallisable
FcR	Fc receptor
$FeCl_3$	Ferric(III)chloride
Fg	fibrinogen
FITC	fluorescein isothiocyanate
g	gram
GAP	GTPase-activating protein
GDI	Guanine nucleotide-dissociation inhibitor
GDP	guanosine diphosphate

GEF	guanine nucleotide exchange factor
GP	glycoprotein
GPCR	G protein-coupled receptor
GTP	guanosine trisphosphate
h	hour(s)
H_2O	water
HIV-1	human immunodeficiency virus type I
HK	high molecular weight kininogen
HRG	Histidine-rich glycoprotein
ICH	intracranial hemorrhage
IEL	internal elastic lamina
IFI	integrated fluorescence intensity
Ig	immunoglobulin
IL	interleukin
IP_3	inositol 1,4,5-triphosphate
ITAM	immunoreceptor tyrosine-based activation motif
kb	kilo base pair
kDa	kilo Dalton
l	liter
LAT	linker for activation of T-cells
M	molar
mDia1	first identified mammalian homologue of *Drosophila diaphanous*
MFI	mean fluorescence intensity
min	minute(s)
MK	megakaryocyte
ml	milliliter
MLC	myosin light chain
MLCK	myosin light chain kinase
MLCP	myosin light chain phosphatase
mm^2	square millimeter
NaCl	sodium chloride
o/n	overnight
PA	phosphatidic acid
PAI-1	plasminogen activator inhibitor-I
PAR	protease-activated receptor
PBS	phosphate buffered saline

PC	phosphatidylcholine
PCK	D-Pro-Phe-Arg chloromethyl ketone
PCR	polymerase chain reaction
PE	phycoerythrin
PF4	platelet factor 4
PI3K	phosphoinositide-3-kinase
PI4P5 kinase	phosphatidylinositol-4-phosphate 5-kinase
PIP_2	phosphatidyinositol-4,5-bisphosphate
PIP_3	phosphatidylinositol-3,4,5-triphosphate
PK	prekallikrein
PKC	proteinkinase C
PL (C)	phospholipase (C)
P-MLC	phosphorylated MLC
ppp	platelet poor plasma
prp	platelet rich plasma
PS	phosphatidylserine
PT	prothrombin time
RC	rhodocytin
ROCK	RhoA-kinase
rpm	rounds per minute
RT	room temperature
SD	standard deviation
SDS	Sodium dodecyl sulfate
SDS-PAGE	Sodium dodecyl sulfate polyacrylamide gel electrophoresis
sec	second(s)
SEM	scanning electron microscopy
SLP-76	Src-homology 2 domain-containing leukocyte-specific phospho-protein of 76 kDa
SOCE	store-operated Ca^{2+} entry
TAE	TRIS acetate EDTA buffer
TE	TRIS EDTA buffer
TEM	transmission electron microscopy
TF	tissue factor
TFPI	tissue factor pathway inhibitor
tMCAO	transient middle cerebral occlusion
tPA	tissue plasminogen activator

TRIS	trishydroxymethylaminomethane
TxA_2	thromboxane A2
U	units
uPA	urokinase plasminogen activator
vWF	von Willebrand factor
wt	wild-type

Acknowledgements

The work presented here was accomplished in the group of Prof. Bernhard Nieswandt at the Department of Experimental Biomedicine, University Hospital and Rudolf Virchow Center, DFG Research Center for Experimental Biomedicine, University of Würzburg.

During the period of my PhD work (January 2008 - June 2011), many people helped and supported me. I would like to thank:

- My supervisor Prof. Bernhard Nieswandt for giving me the opportunity to perform my PhD in his laboratory. I am grateful for his continuous support, his enthusiasm and great ideas during my PhD period. Without this, the work would not have been possible. I specially thank him for introducing me into the scientific community and allowing me to present my work at international conferences, which together enabled me to make new experiences important for my future career.
- Prof. Utz Fischer for helpful discussions throughout my PhD period and for reviewing my thesis.
- Prof. Johan Heemskerk for helpful discussions and advices throughout my PhD period and for reviewing my thesis.
- My colleagues and friends Frauke May, Irina Pleines and Lidija Chakarova for their continuous support in good and bad times during my PhD period and for carefully reading my thesis.
- Juliana Goldmann and Jonas Müller for their technical assistance and genotyping of the genetically modified mice used in this thesis.
- All other members of the lab, who have not been mentioned by name, first of all for the pleasant atmosphere in the group, but also for their helpful discussions and experimental support.
- All external collaboration partners for the trustful cooperation and useful advice as well as for introducing me into new techniques.
- Finally, I would like to specially thank my family: Uli, my parents and my brother Kay for their unfailing patience and support as well as for their continuous encouragement and listening during my life.

Publications

Articles

Hagedorn I[*], Schmidbauer S[*], Pleines I, Kleinschnitz C, Kronthaler U, Stoll G, Dickneite G, Nieswandt B. Factor XIIa inhibitor recombinant human albumin Infestin-4 abolishes occlusive arterial thrombus formation without affecting bleeding. *Circulation.* 2010;121(13):1510-7.
[*] *both authors contributed equally*

Bender M[*], **Hagedorn I**[*], Nieswandt B. Genetic and antibody-induced GPVI deficiency equally protect mice from mechanically and FeCl3-induced thrombosis. *J Throm Haemost.* 2011; 9(7):1423-6. [*] *both authors contributed equally*

Bender M, May F, **Hagedorn I**, Braun A, Nieswandt B. Severely defective hemostasis and arterial thrombus formation in GPVI/CLEC-2 double-depleted mice. *Manuscript in revision*.

Elvers M, Stegner D, **Hagedorn I**, Kleinschnitz C, Braun A, Kuijpers ME, Boesl M, Chen Q, Heemskerk JW, Stoll G, Frohman MA, Nieswandt B. Impaired alpha(IIb)beta(3) integrin activation and shear-dependent thrombus formation in mice lacking phospholipase D1. *Sci Signal.* 2010;3(103).

Pleines I, Eckly A, Elvers M, **Hagedorn I**, Eliautou S, Bender M, Wu X, Lanza F, Gachet C, Brakebusch C, Nieswandt B. Multiple alterations of platelet functions dominated by increased secretion in mice lacking Cdc42 in platelets. *Blood.* 2010;115(16):3364-73.

Kleinschnitz C, Schwab N, Kraft P, **Hagedorn I**, Dreykluft A, Schwarz T, Austinat M, Nieswandt B, Wiendl H, Stoll G. Early detrimental T-cell effects in experimental cerebral ischemia are neither related to adaptive immunity nor thrombus formation. *Blood*. 2010;115(18):3835-42.

May F, **Hagedorn I**, Pleines I, Bender M, Vögtle T, Eble J, Elvers M, Nieswandt B. CLEC-2 is an essential platelet-activating receptor in hemostasis and thrombosis. *Blood*. 2009;114(16):3464-72.

Review

Hagedorn I, Vögtle T, Nieswandt B. Arterial thrombus formation: Novel mechanisms and targets. *Haemostaseologie*. 2010;30(3):127-35.

Oral Presentation

Comparison of genetic and antibody-induced GPVI deficiency in different murine arterial thrombosis models. XXIIIrd Congress of the International Society on Thrombosis and Hemostasis (ISTH), July 2011, Kyoto (Japan). **Accepted for oral presentation.**
Winner of the **Young Investigators Award 2011** (prize money: 500 US$).

rHA-Infestin, a coagulation factor XIIa inhibitor, protects mice from arterial thrombosis and ischemic stroke without impairing hemostasis. XXIInd Congress of the International Society on Thrombosis and Hemostasis (ISTH), July 2009, Boston (MA, USA).
Winner of the **Young Investigators Award 2009** (prize money: 500 US$).

Poster Presentation

FXIIa inhibition protects mice from pathological thrombus formation without impairing hemostasis. The GPCR Dimer Symposium, October 2009, Würzburg (Germany)

The coagulation factor XIIa inhibitor rHA-Infestin-4 protects mice from arterial thrombosis and ischemic stroke without impairing hemostasis. 54. Jahrestagung der Gesellschaft für Thrombose- und Hämostaseforschung (GTH), 1. Joint GTH & NVTH Meeting, Symposium van de Nederlandse Vereniging voor Trombose en Hemostase (NVTH), February 2010, Nürnberg (Germany). Winner of the **Best Poster Award** (prize money: 300 €).

The role of the small GTPase RhoA in platelet function. 5th International Symposium Chiasma, October 2010, Würzburg (Germany)

National Award

Hentschel Preis 2011 conferred by the Hentschel Stiftung „Kampf dem Schlaganfall“ for the work published in *Circulation*: “Factor XIIa inhibitor recombinant human albumin rHA-Infestin-4 abolishes arterial thrombus formation without affecting bleeding” (prize money 4.000 €).

Affidavit

I hereby declare that my thesis entitled “Novel mechanisms underlying arterial thrombus formation: *in vivo* studies in (genetically modified) mice" is the result of my own work. I did not receive any help or support from commercial consultants. All sources and / or materials applied are listed and specified in the thesis.

Furthermore, I verify that this thesis has not yet been submitted as part of another examination process neither in identical nor in similar form.

Würzburg, ……

Date Signature

Eidesstattliche Erklärung

Hiermit erkläre ich an Eides statt, die Dissertation „Neue Mechanismen der arteriellen Thrombusbildung: *in vivo*-Studien in (genetisch veränderten) Mäusen“ eigenhändig, d.h. insbesondere selbständig und ohne Hilfe eines professionellen Promotionsberaters, angefertigt und keine anderen als die von mir angegebenen Quellen und Hilfsmittel verwendet zu haben.

Ich erkläre außerdem, dass die Dissertation weder in gleicher noch in ähnlicher Form bereits in einem anderen Prüfungsverfahren vorgelegen hat.

Würzburg, ……

Datum Unterschrift